

**Molecular Recognition Study of Some Amino
Derivatives of Pyrimidines and Triazines**

Thesis submitted to

University of Pune

For the degree of

Doctor of Philosophy

In

Chemistry

By

Amit Delori

**Division of Organic Chemistry
National Chemical Laboratory
Dr. Homi Bhabha Road
Pune 411 008**

August 2009

DEDICATED TO MY BELOVED PARENTS



Shri. M. L. Delori & Smt. Ramesh Delori



National Chemical Laboratory

Division of Organic Chemistry

Pune – 411008. India

Fax: +91(20) 25902624

Email: vr.pedireddi@ncl.res.in

CERTIFICATE

This is to certify that the work presented in the thesis entitled “**Molecular Recognition Study of Some Amino Derivatives of Pyrimidines and Triazines**” submitted by Amit Delori, was carried out by the candidate at National Chemical Laboratory, Pune, under my supervision. Such materials as obtained from other sources have been duly acknowledged in the thesis.

August 2009

Dr. V. R. Pedireddi
Research Guide
Division of Organic Chemistry
National Chemical Laboratory
Pune 411 008.

CANDIDATE'S DECLARATION

I here by declare that the thesis entitled “**Molecular Recognition Study of Some Amino Derivatives of Pyrimidines and Triazines**” submitted for the degree of Doctor of Philosophy in Chemistry to the University of Pune has not been submitted by me to any other university or institution. This work was carried out at the National Chemical Laboratory, Pune, India.

Amit Delori

National Chemical Laboratory

Pune 411 008.

August 2009

Acknowledgements

With deep sense of gratitude and profound respect, I express my sincere thanks to my mentor, **Dr. V. R. Pedireddi** for his inspiring guidance and constant encouragement throughout my Ph.D. He has been my source of inspiration in many aspects. I not only learnt chemistry from him, but also learnt the attitude, to face the problems and also to resolve them.

It is my privilege to thank Dr. K. N. Ganesh, former Head of the Division of Organic Chemistry, NCL, and currently director, IISER Pune, for his constant support and encouragement during the progress of this work. I take this opportunity to thank Dr. Ganesh pandey, for his continued support as present Head of the Division.

I thank Dr. S. Sivaram, Director NCL, for giving infrastructure facilities and CSIR for financial support. I also thank Dr. B. D. Kulkarni, Deputy Director, for his support and encouragement.

I thank Dr. C. V. V. Sathyanarayana, Dr. P. A. Joy, Dr. Srinivas Hotha, Dr. Ramana, Dr. Alok Sen and Dr. C. G. Suresh for fruitful scientific discussions and support in many aspects.

I am grateful to Dr. Mohan Bhadbhade, Dr. Mrs. Vedavathi Puranik, Dr. Rajesh Gonnade and Dr. Manoj for their assistance in the single crystal X-ray diffraction. I would like to thank Dr. E. Suresh, Bhavnagar and Prof U. P. Singh, IIT Roorkee for their assistance in the collection of X-ray diffraction data.

I am thankful to all the teachers and lecturers, who taught me throughout my career. My sincere thank to Prof S. S. Behl, Prof. Ashok Kumar Sharma, Prof. S. L. Agnish and Prof. Yadav for creating my interest in chemistry during early years of my study in college. I would like to thank my university teachers, Prof Harjit Singh, Prof. T.S. Lobana, Prof. M. S. Hundal, Prof. R. K. Mahajan, Prof. Ishtiaque Ahmad, Prof. Subodh Kumar, Prof. B. S. Randhawa, Dr. Geeta Hundal, Dr. S. S. Chimni, Dr. Manoj Kumar, Dr Parampaul Kaur Banipal, Dr. Palvinder Singh, Dr. Paramjit Kaur and Dr Damanjit Kaur and Dr. Bhartam for further igniting my interest in chemistry through excellent chemistry lectures.

I wish to thank my friendly and cooperative labmates, Prakash, Kapil, Sunil, Seetha, Marivel, Sathya, Manishkumar, Parul, Yogesh, Mayura, Ketaki, Manish, Prince, Nagarajan and Chiranjeevi for their help in various capacities and providing me with an excellent working ambience.

I am very much thankful to NCL, INSA and IUCr for providing me the funding to attend the IUCr-2008 conference, held at Osaka, Japan. I would like to thank Prof. William Jones, University of Cambridge, UK; Prof. Judith Howard, University of Durham, UK; Prof. G. R. Desiraju, IISc, Bangalore, India, Prof. Pinak Chakrabarti, Bose Institute, Calcutta, India; Prof T. N. Guru Rao, IISc, Bangalore, India and Prof. Roland Boese, University of Essen, Germany for giving me valuable suggestions during my poster presentation. I am thankful to *The Crystallographic Society of Japan* for recognizing my work and giving me best poster award at IUCr-2008

I thank all of my university friends Karun, Kapil, Surinder, Jaswinder, Ronny, Harry, Abhishekh, Shivinder, Vaneet, Narinder Singh, Sandeep Singh, Nagendra babu, Rajesh, Dinesh, Kulbir, Parminder, Dharam Paul, Satwinder Singh, Harish, Chauhan, Tnu, Sonali, Ity, Navneet, Bosaki and Mandeep Dhoat for providing me constructive atmosphere which helped me in achieving the goals set in life. I thank D.V. Sanghavi and Pushpesh, who were my room-mates during stay at NCL, my friends Gagan Jyoti, Bhuban Panda, and Merlyn for their company, and for being always with me throughout our association. I would like to thank all my friends in NCL.

I thank my sisters Manju and Ritu, brother-in-law Jatinder and Ajay for their continuous encouragement and my nephews Dhanur, Shubham and nieces Kashish, Shraeya and Garima for their ever smiling faces, which always give freshness and energy to do work. I thank my uncle C. L. Delori, O. P. Delori, Varinder Sehgal and their families and all other relatives for their love and care.

During my Ph.D, I married Loveena, who turned into my best friend. Her encouragement and faith in me always helped me accelerating in my academic carrier. Here I would like to thank GOD for giving me such a good life-partner. I thank my father-in-law, mother-in-law, sister-in-law (Monica) and brother-in-law (Jatinder) for their encouragement.

The blessings and best wishes of my parents keep me active throughout my life. They made me what I am and I owe everything to them. Dedicating this thesis to them is a minor recognition for their invaluable support and encouragement.

I thank all of you once again for your kind support and cooperation.

Table of contents**Chapter 1****Introduction to supramolecular chemistry and its applications**

1.1	Introduction	2
1.2	Supramolecular Chemistry	2
1.3	Molecular Recognition	5
1.4	Intermolecular Interactions	7
1.4.1	Hydrogen Bond	8
1.4.2	Halogen Bond	15
1.5	Self Assembly	19
1.6	Supramolecular Assemblies	20
1.7	Applications of Supramolecular Assemblies	25
1.7.1	Synthesis of New Molecules	26
1.7.2	Pharmaceutical Co-crystallization	29
1.7.3	Applications of Metal-Organic Frameworks	34
1.7.3.1	Gas Storage Properties of Metal-Organic Frameworks	34
1.7.3.2	Separation Properties of Metal-Organic Frameworks	39
1.7.3.3	Catalytic Properties of Metal-Organic Frameworks	40
1.8	Conclusion	42
1.9	References	44

Chapter 2

**Molecular Recognition Studies of 2,4-diamino-6-methyl-1,3,5-triazine
and 2,4-diamino-6-phenyl-1,3,5-triazine with various aliphatic
dicarboxylic acids**

2.1	Introduction	55
2.2	Molecular Adducts of 2,4-Diamino-6-methyl-1,3,5-triazine (DAMT) with Various Aliphatic Dicarboxylic Acids	62
2.2.1	Crystal Structure of 2,4-Diamino-6-methyl-1,3,5-triazine	63
2.2.2	Molecular Complex of DAMT and Oxalic acid	65

2.2.3	Molecular Complex of DAMT and Malonic acid	67
2.2.4	Molecular Complex of DAMT and Succinic acid	69
2.2.5	Molecular Complex of DAMT and Fumaric acid	71
2.2.6	Molecular Complex of DAMT and Acetylenedicarboxylic acid	73
2.2.7	Molecular Complex of DAMT and Glutaric acid	76
2.2.8	Molecular Complex of DAMT and Thiodiglycolic acid	78
2.2.9	Molecular Complex of DAMT and Diglycolic acid	79
2.2.10	Molecular Complex of DAMT and Adipic acid	81
2.2.11	Structural Correlation Between Various Complexes of DAMT with Aliphatic Dicarboxylic Acids.	83
2.2.12	pK _a Towards Specific Host Networks	84
2.2.13	pK _a Towards Specific Hydrogen Bonding Patterns	85
2.3	Molecular Complexes of 2,4-Diamino-6-phenyl-1,3,5-triazine (DAPT) with Various Aliphatic Acids	86
2.3.1	Molecular Complex of DAPT and Malonic acid	89
2.3.2	Molecular Complex of DAPT and Maleic acid	91
2.3.3	Molecular Complex of DAPT and Acetylenedicarboxylic acid	93
2.3.4	Molecular Complex of DAPT and Fumaric acid	95
2.3.5	Molecular Complex of DAPT and Succinic acid	97
2.3.6	Molecular Complex of DAPT and Glutaric acid	99
2.3.7	Molecular Complex of DAPT and Diglycolic acid	100
2.3.8	Molecular Complex of DAPT and Adipic acid	102
2.3.9	Structural Correlation Between Various Complexes Between DAPT and Aliphatic Aicarboxylic Acids.	103
2.4	Conclusions	104
2.5	Experimental Sections	106
2.5.1	Synthesis	106
2.5.2	Crystal Structures Determination	106
2.6	References	116

Chapter 3

Supramolecular assemblies of aminopyrimidines and aminotriazines with aryl and aralkyl carboxylic acids

3.1	Introduction	121
3.2	Molecular Complexes of 2,4-Diamino-6-methyl-1,3,5-triazine (DAMT) with Various Aryl and Aralkyl Carboxylic Acids	128
3.2.1	Molecular Complex of DAMT and Benzoic Acid	129
3.2.2	Molecular Complex of DAMT and Phthalic Acid	130

3.2.3	Molecular Complex of DAMT and Isophthalic Acid	132
3.2.4	Molecular Complex of DAMT and Terephthalic Acid	135
3.2.5	Molecular Complex of DAMT and 1,3-Phenylenediacetic Acid	136
3.3	Molecular complexes of 2,4-Diamino-6-phenyl-1,3,5-triazine (DAPT) with various aryl and aralkyl carboxylic acids	138
3.3.1	Molecular Complex of DAPT and Benzoic Acid	139
3.3.2	Molecular Complex of DAPT and Phthalic Acid	140
3.3.3	Molecular Complex of DAPT and Isophthalic Acid	142
3.3.4	Molecular Complex of DAPT and Terephthalic Acid	144
3.3.5	Molecular Complex of DAPT and 1,3-Phenylenediacetic Acid and 1,4-Phenylenediacetic Acid	146
3.4	Molecular Complexes of 2,4,6-Triaminopyrimidine (TAP) with Various Aryl and Aralkyl Carboxylic Acids	148
3.4.1	Molecular Complex of TAP and Phthalic acid	148
3.4.2	Molecular Complex of TAP and Terephthalic acid	150
3.4.3	Molecular Complex of TAP and 1,3-Phenylenediacetic Acid	151
3.4.4	Molecular Complex of TAP and 1,4-Phenylenediacetic Acid	153
3.5	Conclusion	155
3.6	Experimental Sections	155
3.6.1	Synthesis	155
3.6.2	Crystal Structure Determination	156
3.7	References	163

CHAPTER 4

Supramolecular assemblies of some derivatives of triazines and pyrimidines with 3,5-dinitrobenzoic acid and its derivatives

4.1	Introduction	167
4.2	Molecular Complexes of Melamine and its Derivatives with 3,5-Dinitrobenzoic Acid and its Derivatives	172
4.2.1	Molecular Complexes of Melamine and 3,5-Dinitro- <i>o</i> -toluic Acid	174
4.2.2	Molecular Complexes of Melamine and 3,5-Dinitro- <i>p</i> -toluic Acid	176
4.2.3	Molecular Complexes of DAMT and 3,5-Dinitrobenzoic Acid	178
4.2.4	Molecular Complexes of DAMT with 3,5-Dinitro- <i>o</i> -toluic Acid and 3,5-Dinitro- <i>p</i> -toluic Acid	180
4.2.5	Molecular Complexes of TAP and 3,5-Dinitrobenzoic Acid	181
4.2.6	Molecular Complexes of TAP and 3,5-Dinitro- <i>o</i> -toluic Acid	182
4.3	Structural correlations	183

4.4	Conclusion	185
4.5	Experiment Section	185
4.5.1	Synthesis	185
4.5.2	Crystal Structure Determination	186
4.6	References	191

Abstract

The thesis entitled “Molecular Recognition Study of Some Amino Derivatives of Pyrimidines and Triazines” was carried out to explore the molecular recognition between nitrogen based heterocyclic compounds and carboxylic acids, for the creation of exotic supramolecular assemblies. In this endeavor, supramolecular architectures, in the form of host-guest complexes, helices, interpenetrated networks etc., that have been obtained by co-crystallization of various pyrimidine and triazine containing amines, with aliphatic and aromatic carboxylic acids, are summarized into four chapters. Chapter 1 gives an introduction to supramolecular chemistry and its applications in various materials and pharmaceutical sectors. In Chapter 2, supramolecular architectures formed by the molecular adducts of 2,4-diamino-6-methyl-1,3,5-triazine and 2,4-diamino-6-phenyl-1,3,5-triazine with various aliphatic dicarboxylic acids are discussed. In Chapter 3, the supramolecular assemblies of 2,4-diamino-6-methyl-1,3,5-triazine 2,4-diamino-6-phenyl-1,3,5-triazine and 2,4,6-triaminopyrimidine, with various aryl and aralkyl acids (benzoic, phthalic, isophthalic, terephthalic acids, 1,3-phenylenediacetic acid and 1,4-phenylenediacetic acid) are discussed. Finally in Chapter 4, supramolecular architectures formed by melamine, 2,4-diamino-6-methyl-1,3,5-triazine and 2,4,6-triaminopyrimidine, with some dinitro substituted aromatic acids (3,5-dinitrobenzoic acid, 3,5-dinitro-*o*-toluic acid and 3,5-dinitro-*p*-toluic acid) have been discussed.

Chapter 1

J. M. Lehn, the Nobel Laureate, stated that supramolecular chemistry is the ‘*chemistry beyond the molecules*’, considering the fact that atoms are held together by covalent bonds in molecules, while supermolecules are due to the noncovalent interactions formed between the molecules. In the molecular recognition studies, among the wide range of noncovalent interactions, the hydrogen bonds play a significant role as evident by a vast reports appeared in the literature. Nevertheless, because of the directionality and multipoint recognition features, etc., the other non-covalent bonds such as halogen bonds, π -interactions have also been explored to form a variety of network structures. Such studies are, indeed, not only superb to create supramolecular assemblies of exotic architectures with tailor-made properties, but also to understand functions of several biological processes, such as nucleic acid transcription and translation, enzymatic functions and antibody specificity etc. Recently, the molecular recognition studies have been well considered in pharmaceuticals, under the umbrella of pharmaceutical co-crystallization, providing unprecedented developments in the intellectual property as well as bio aspects of drugs, etc. A detailed discussion of such features of supramolecular chemistry would be presented in Chapter 1.

Chapter 2

Melamine forms an exotic supramolecular assembly with cyanuric acid, in the form of rosette, which served as a representative example to illustrate the efficacy of intermolecular interactions in the formation of robust solid materials. In order to

explore such features with the derivatives of melamine, exploration of co-crystals of 2,4-diamino-6-methyl-1,3,5-triazine, **1**, and 2,4-diamino-6-phenyl-1,3,5-triazine, **2**, with various aliphatic acids has been carried out.

Triazine **1** forms host-guest complexes in all its co-crystals, with various aliphatic dicarboxylic acids, as illustrated in Chart 1.

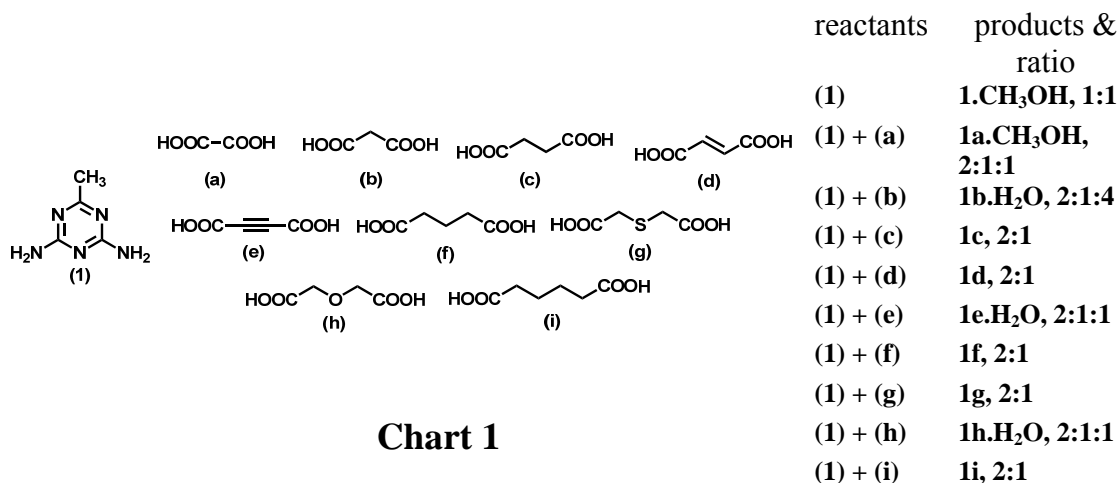


Chart 1

Analysis of the structural data of all the complexes reveals that, depending upon the pK_a of the aliphatic dicarboxylic acids, two types of host-guest complexes were formed, such that if the pK_a of acid is > 3 , the acid molecules act as guests in the host network exclusively formed by the molecules of **1**. However, if the pK_a is < 3.0 , the acids along with triazine **1** constitute a host network, incorporating molecules of solvent of crystallization as guests. The representative examples of host-guest complexes of **1** with acids having $pK_a < 3$ and $pK_a > 3$ are shown in Figure 1 and a detailed account of all the structures is given in this Chapter.

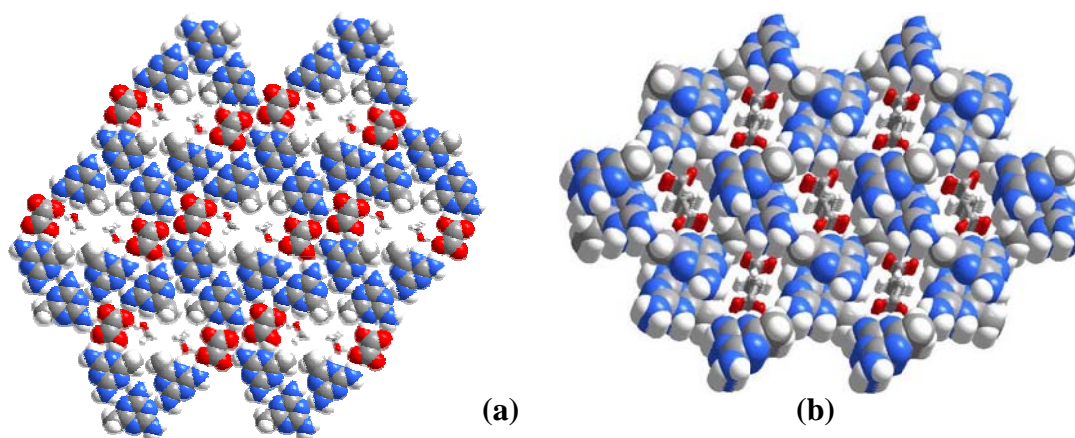
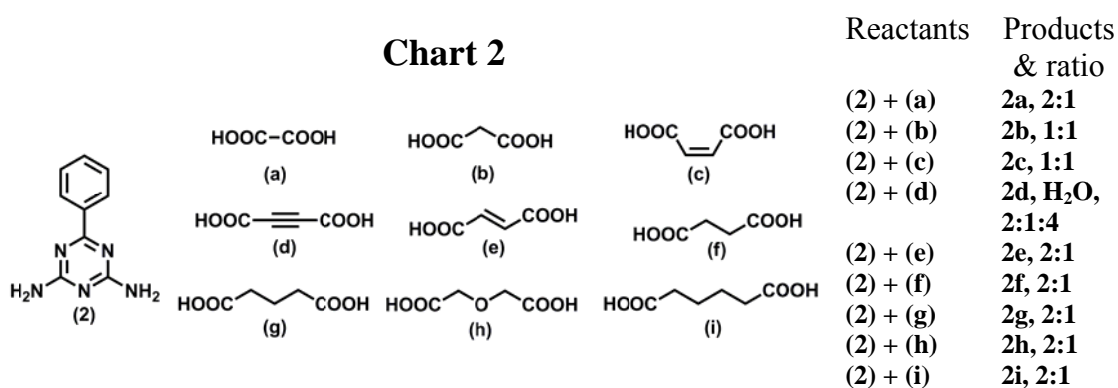


Figure 1. Molecular adduct of 2,4-diamino-6-methyl-1,3,5-triazine with (a) oxalic acid having $pK_a < 3$ and (b) fumaric acid having $pK_a > 3$

However, triazine **2**, an analogue of **1** with the replacement of methyl group by phenyl moiety, did not yield exclusively host-guest assemblies with various aliphatic dicarboxylic acids, illustrated in Chart 2.



The structural features of the co-crystals, thus, obtained with **2** are however, quiet intriguing with a variety of architectures being formed in the form of tapes, cyclic network, helices, host-guest structures, etc. Typical examples of tape and network structures are shown in Figure 2 and the structural features of all other adducts have been discussed in this chapter.

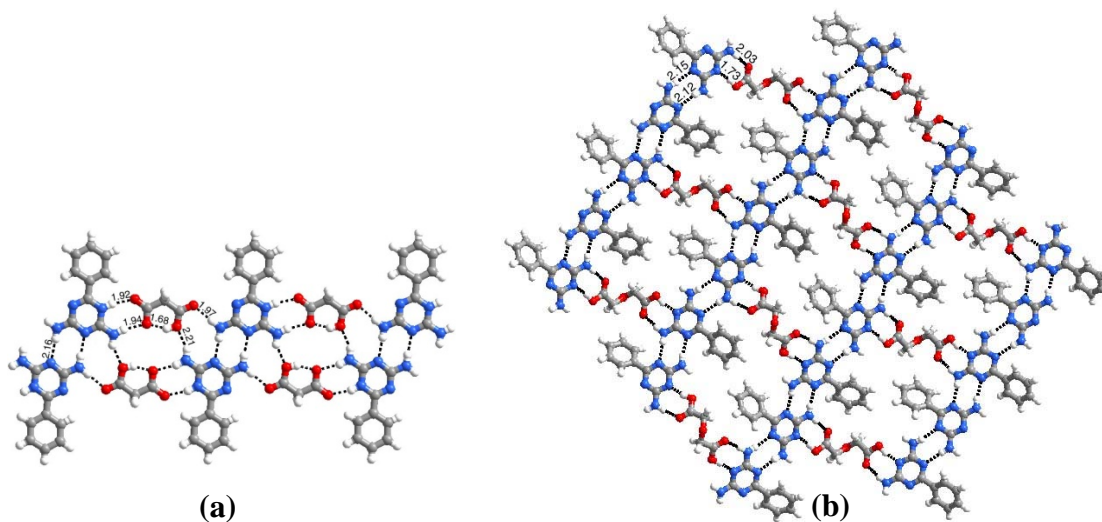


Figure 2. Molecular arrangement in the adducts of **2** with (a) malonic acid and (b) diglycolic acid

Chapter 3

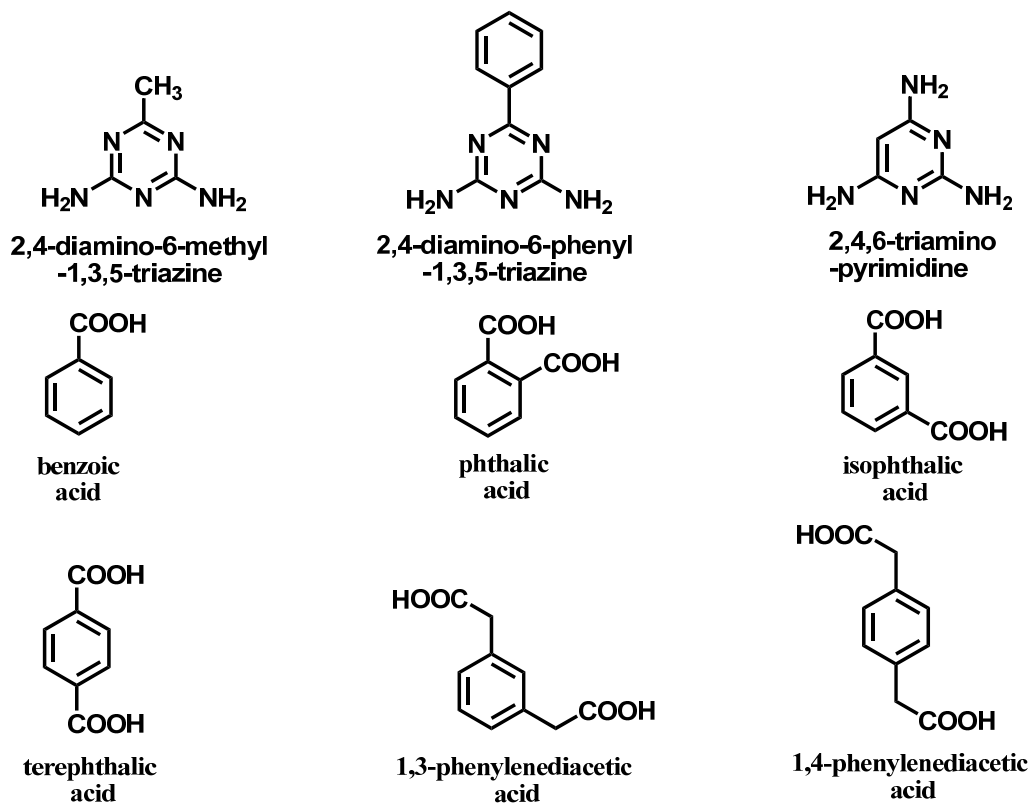


Chart 3

Co-crystallization studies of 2,4-diamino-6-methyl-1,3,5-triazine, 2,4-diamino-6-phenyl-1,3,5-triazine and 2,4,6-triaminopyrimidine has been carried out with various aryl and aralkyl carboxylic acids, as illustrated in Chart 3, have been discussed in Chapter 3.

The adducts have been found to be yielding a variety of supramolecular architectures as illustrated in the representative examples formed by melamine and 2,4-diamino-6-methyl-1,3,5-triazine with isophthalic acid, as shown in Figures 3 and 4, respectively. In the adduct of melamine, a six membered cyclic host is formed by the constituting molecules with cavities of dimensions $8 \times 12 \text{ \AA}^2$, which are being filled by water molecules. It is noteworthy to mention that the incorporation of water molecules in the cavities is facilitated due to the polar nature of the void space because of the protrusion of amino groups into the void space.

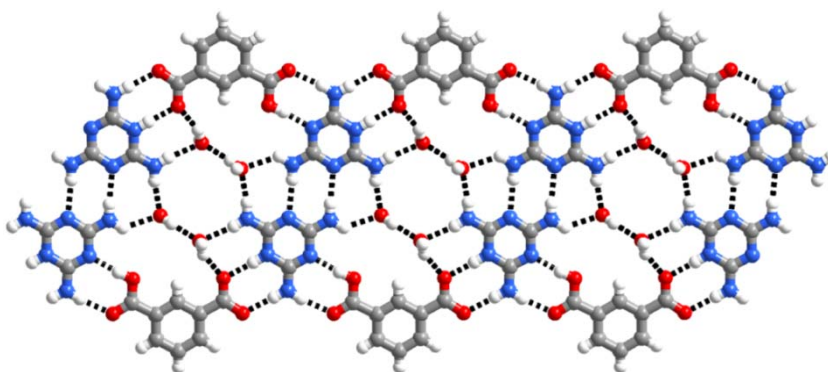


Figure 3. Six member host network observed in the co-crystals of melamine and isophthalic acid, filled by water molecules.

In the adduct of 2,4-diamino-6-methyl-1,3,5-triazine also, an ensemble of six membered cyclic network was observed. However, further aggregation of those

ensembles, establishing interactions by N-H...N hydrogen bonds, yielded void space, being occupied by the molecules of methanol, as shown in Figure 4.

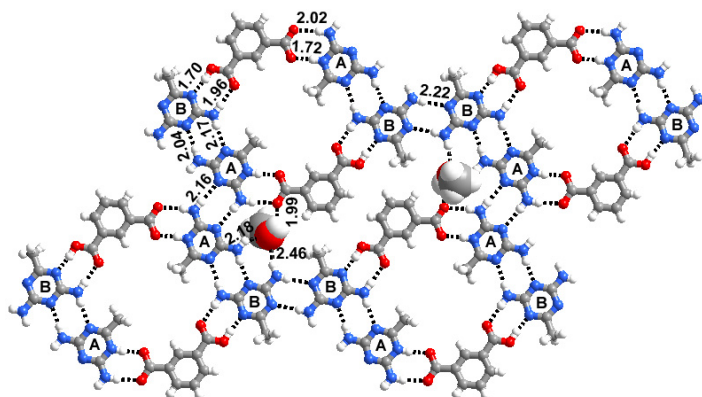


Figure 4. Aggregates of ensembles of six membered cyclic networks, yielding void space, being occupied by methanol molecules.

It is interesting to observe that cavities within the six membered ensembles are non-polar, unlike in the adduct of melamine described above, due to the protrusion of methyl groups from the triazine molecules as well as from the methanol molecules in the adjacent layers, as shown in Figure 5. The detailed discussion of all those structures is given in this Chapter 3.

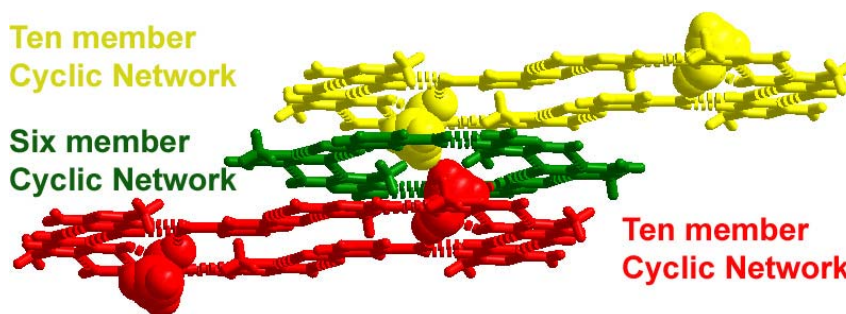
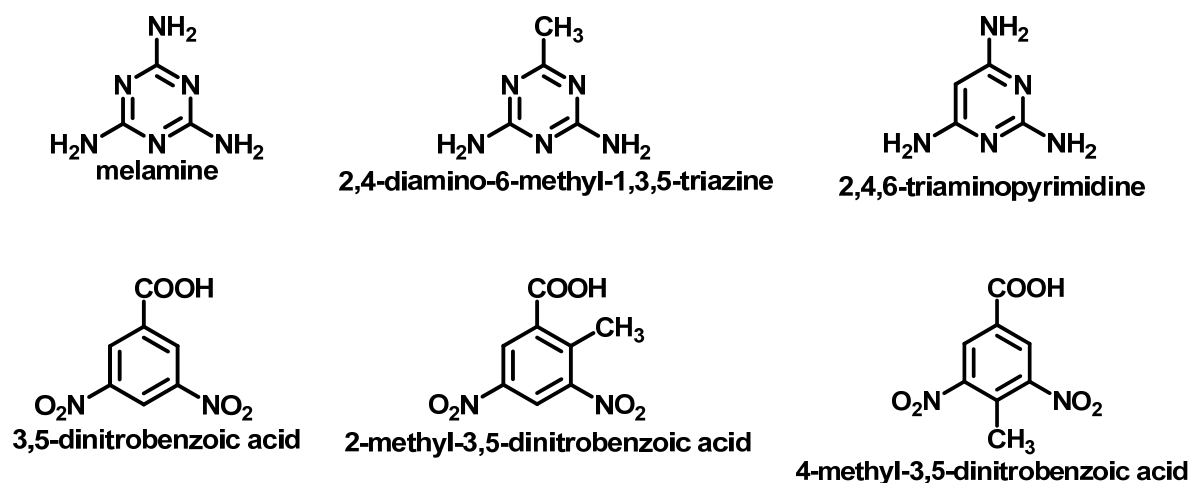


Figure 5. Methyl groups of methanol molecules, in the ten member cyclic network, protruding into the six member cyclic network

Chapter 4

It is well known from the literature that while $-\text{COOH}$ shows affinity to form intermolecular interactions with pyridyl nitrogens through $\text{O}-\text{H}\cdots\text{N}$ hydrogen bonds, which was also illustrated through Chapters 2 and 3, amino groups have profound tendency to interact with nitro groups through different types of $\text{N}-\text{H}\cdots\text{O}$ hydrogen bonds. Since amino pyrimidines and triazines possess both pyridyl nitrogen atoms as well as amino groups, co-crystallization of such molecules with compounds containing both nitro and carboxylic acid functional groups would be of great advantage, to study the impact of multiple functional groups in the supramolecular synthesis. Thus, co-crystals of melamine, 2,4-diamino-6-methyl-1,3,5-triazine and 2,4,6-triaminopyrimidine with various dinitrobenzoic acids have been prepared.

Chart 4



In most of the structures, quartet ensembles formed through N-H \cdots O hydrogen bond, between the constituents, as illustrated in the typical example of 2,4-diamino-6-methyl-1,3,5-triazine and 3,5-dinitrobenzoic acid, as shown in the Figure 6.

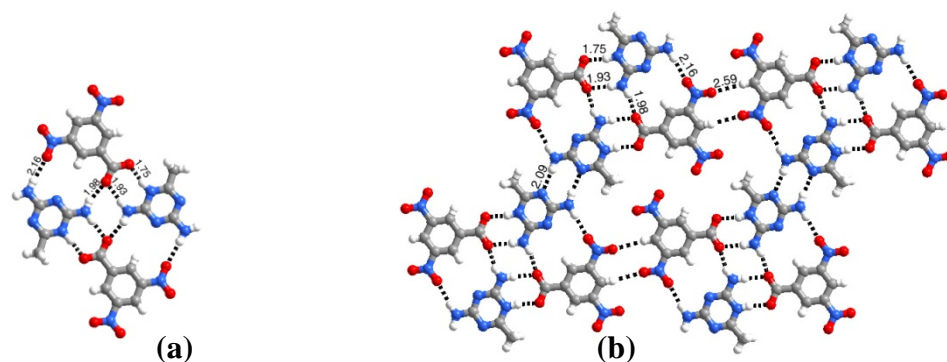
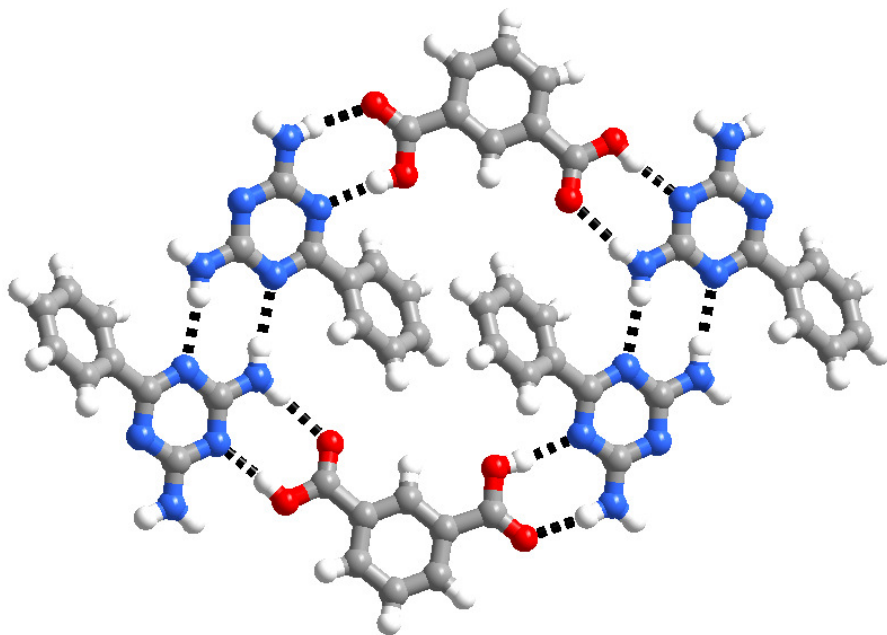


Figure 6. (a) Quartet ensemble observed in the crystal structure of co-crystals of 2,4-diamino-6-methyl-1,3,5-triazine and 3,5-dinitrobenzoic acid (b) Aggregation of adjacent quartet ensembles through N-H \cdots N and C-H \cdots O hydrogen bonds.

References:

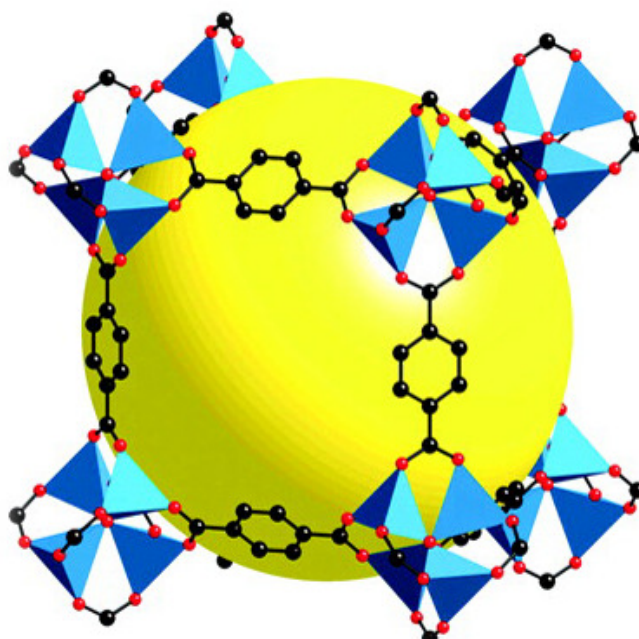
- (1) (a) Lehn, J. M. *Supramolecular Chemistry: Concepts and Perspectives*; VCH: Weinheim, 1995. (b) G. R. Desiraju, T. Steiner *The Weak Hydrogen Bond in Structural Chemistry and Biology*, Oxford University Press, Oxford, 1999. (c) Jones, W. Rao, C. N. R., *Supramolecular Organization and Material Design*, Cambridge University Press.
- (2) Lehn, J. M. *Angew. Chem., Int. Ed.* **1990**, *29*, 1304-1319.
- (3) Pedireddi, V. R.; Chatterjee, S.; Ranganathan, A.; Rao, C. N. R. *J. Am. Chem. Soc.* **1997**, *119*, 10867-10868.
- (4) Delori, A.; Suresh, E.; Pedireddi, V. R. *Chem. Eur. J.* **2008**, *14*, 6967-6977.
- (5) Etter, M. C. *Acc. Chem. Res.* **1990**, *23*, 120-126.

- (6) Dunitz, J. D.; Gavezzotti, A. *Angew. Chem., Int. Ed.* **2005**, *44*, 1766-1787.
- (7) Arora, K. K.; Pedireddi, V. R. *J. Org. Chem.* **2003**, *68*, 9177-9185.
- (8) Perumalla, S. R.; Suresh, E.; Pedireddi, V. R. *Angew. Chem., Int. Ed.* **2005**, *44*, 7752-7757.
- (9) Jetti, R. K. R.; Boese R.; Thakur, T. S.; Vangala, V. R.; Desiraju, G. R. *Chem. Commun.* **2004**, 2526-2527.
- (10) Aakeröy, C. B.; Beatty, A. M.; Helfrich, B. A. *Angew. Chem., Int. Ed.* **2001**, *40*, 3240-3242.
- (11) Steiner, T. *Angew. Chem., Int. Ed.* **2002**, *41*, 48-76.
- (12) MacGillivray, L. R.; Atwood, J. L. *Angew. Chem., Int. Ed.* **1999**, *38*, 1018-1033.
- (13) Moulton, B.; Zaworotko, M. J. *Chem. Rev.* **2001**, *101*, 1629-1658.
- (14) Wuest, J. D. *Chem. Commun.* **2005**, 5830-5837.
- (15) Aakeröy, C. B.; Fasulo, M.; Schultheiss, N.; Desper, J.; Moore, C. J. *Am. Chem. Soc.* **2007**, *129*, 13772-13773.
- (16) Whitesides, G. M.; Mathias, J. P.; Seto, C. T. *Science* **1991**, *254*, 1312-1319.
- (17) Sharma, C. V. K.; Zaworotko, M. J. *Chem. Commun.* **1996**, 2655-2656.
- (18) Walsh, R. D. B.; Bradner, M. W.; Fleischman, S.; Morales, L. A.; Moulton, B.; Rodriguez-Hornedo, N.; Zaworotko, M. J. *Chem. Commun.* **2003**, 186-187.
- (19) Remenar, J. F.; Morissette, S. L.; Peterson, M. L.; Moulton, B.; MacPhee, J. M.; Guzman, H. R.; Almarsson, O. *J. Am. Chem. Soc.* **2003**, *125*, 8456-8457.
- (20) Almarsson, O.; Zaworotko, M. J. *Chem. Commun.* **2004**, 1889-1896.



CHAPTER ONE

INTRODUCTION TO SUPRAMOLECULAR CHEMISTRY AND ITS APPLICATIONS



1.1 Introduction

For many years, chemists have sought to prepare molecules having specific physical and chemical properties for applications in the areas ranging from pharmaceuticals to materials. These properties are not only inherent in the molecules, but also depend on the way in which the molecules interact with each other, by non-covalent interactions, in the solid state, which is broadly defined as self-assembly, is studied as a part of supramolecular chemistry. Nature also use self-assembly strategies, based on non-covalent interactions, such as hydrogen bonds, salt bridges, solvation forces and even metal coordination, in the organization of biological systems like DNA, RNA, proteins etc. Hence, such forces were exploited long before, even the terms “supramolecular chemistry” and “self-assembly” were introduced. In supramolecular assemblies, intermolecular interactions act as supramolecular glue between the molecules in the same way as the covalent bonds connect the atoms in the molecule.

1.2 Supramolecular Chemistry

Beyond molecular chemistry, based on the covalent bond, there lies the field of supramolecular chemistry¹, which aims to gain control over the intermolecular interactions. Supramolecular chemistry was first defined by the Nobel Laureate, J. M. Lehn, as, "*Just as there is a field of molecular chemistry based on the covalent bond, there is a field of supramolecular chemistry, the chemistry of molecular assemblies and of the intermolecular bond.*"² Lehn later eloquently captured the essence of this definition and redefined supramolecular chemistry as "*chemistry beyond the*

molecules"^{3, 1c} or "*chemistry of the non-covalent bond*" considering the fact that supermolecules or supramolecular assemblies are the entities possessing higher complexity than the molecules and are formed by the non-covalent interactions formed between the molecules. Supramolecular chemistry extends from oligomeric supermolecules to the polymeric supramolecular assemblies.⁴ In supramolecular chemistry, various molecules recognize each other if their functional group/groups or shape is complimentary to each other. The term "*Übermoleküle*",⁵ i.e., supermolecules was coined as early as the mid 1930's to describe entities of higher organization, such as dimer of acetic acid. A supermolecule is an organized, complex entity that is created from the association of a few chemical species held together by intermolecular forces. Supramolecular assemblies are the polymolecular entities that result from the spontaneous association of a large undefined number of components. Thus, supramolecular chemistry is a highly interdisciplinary field of science with a focus on the study of hybrid of the chemical, physical and biological features of the chemical species of greater complexity, through the organization utilizing intermolecular non-covalent interactions. Supramolecular chemistry also has a great impact on biotechnology and nanotechnology, which are expected to lead to technological revolutions in near future that will dramatically affect our lifestyles, economy etc., especially towards the development of novel devices. The schematic diagram of supramolecular assemblies formed by hydrogen and co-ordinate bonds are shown in Figure 1.1.⁶ In the domain of supramolecular chemistry, we also study other weak interactions like π - π interactions, van der Waals forces etc.

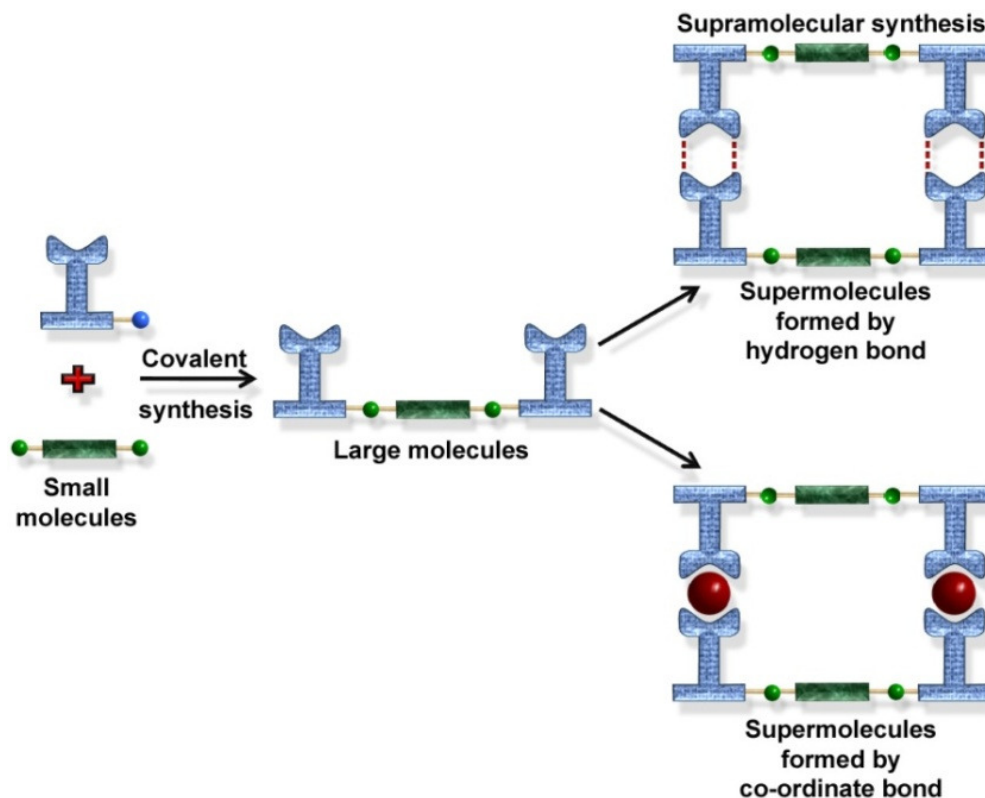


Figure 1.1. Diagram showing the formation of large molecules by covalent synthesis and the formation of supermolecules by hydrogen and co-ordination bonds.

Molecular recognition, intermolecular interactions, and self-assembly are the three keywords that often, one encounter in the discussion of supramolecular-chemistry-governed frontier-research-areas, which are described briefly in the sections to follow.

The concepts of supramolecular chemistry can be realized by correlating it with the jigsaw game. In the jigsaw game there are self-complementary fragments, which can be joined together in only one way (which is energetically most stable) and it leads to a bigger fragment, as illustrated in Figure 1.2. Similarly in the supramolecular chemistry also there are self complementary molecules, which

recognize each other (molecular recognition), by self assembly, utilizing non-covalent forces.⁷

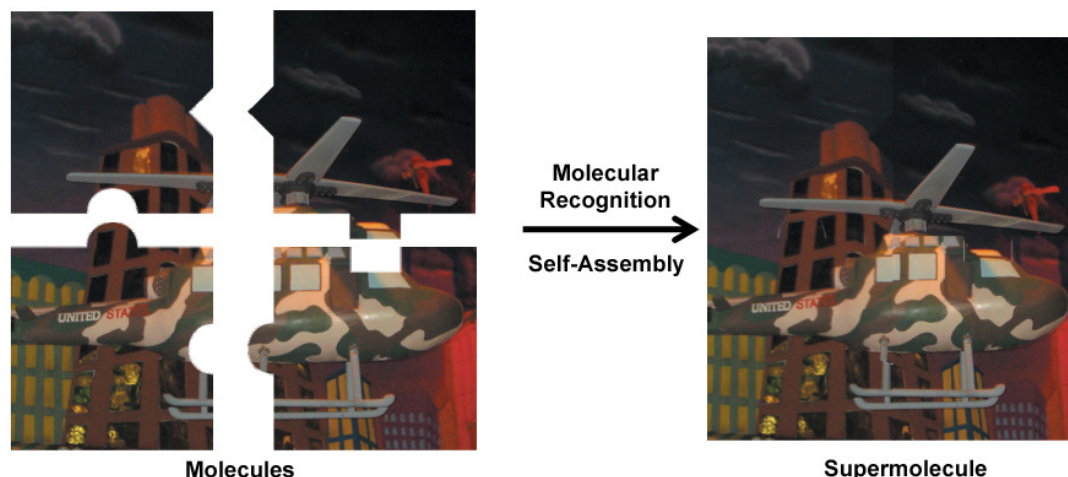


Figure 1.2. Schematic diagram illustrating the processes involved in supramolecular synthesis through utilization of complementary fragments by the correlating it with the jigsaw puzzle.

1.3 Molecular Recognition

The process of interaction between molecules having complimentary functional groups, or shape by its partner is called molecular recognition. “Molecular recognition” in its modern parlance implies that, when two molecules approach each other in a particular way, the potential energy of the pair decreases significantly more than it would for a different manner of approach because of some specific interaction between the molecules.⁸

The importance of molecular recognition first came to light in the middle of the nineteenth century – considerably before the concepts of supramolecular chemistry were established. Emil Fischer proposed “lock and key” principle in 1894 as a mechanism for “molecular recognition”.⁹ This concept proposed that the mechanism

by which an enzyme recognize and interacts with a substrate can be related to a lock and a key system. According to this model, a specific substrate glue to only one receptor, like a key fits into only one lock (See Figure 1.3). So according to the lock and key principle the molecules which are geometrically complimentary to each other, can recognize each other.

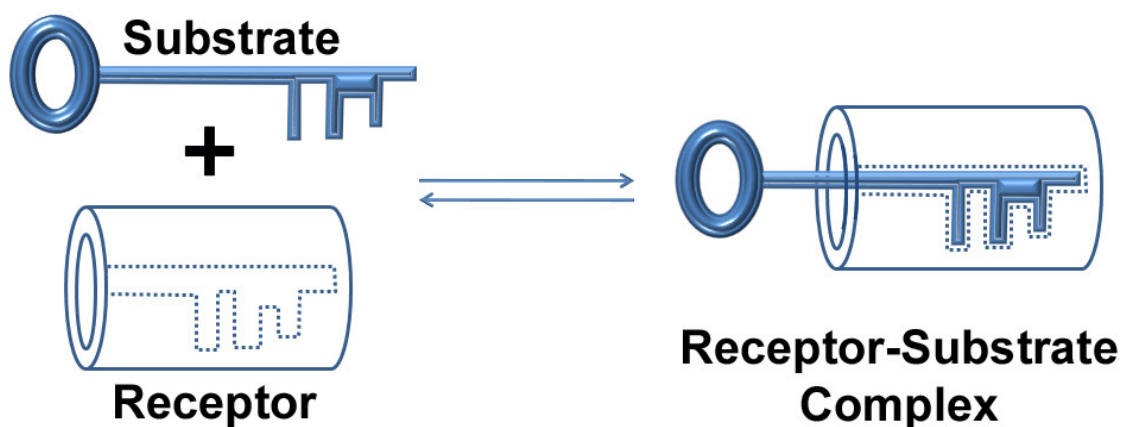


Figure 1.3. Fischer's lock and key mechanism for the molecular recognition.

Binding of substrate to the receptor forms a complex, characterized by its stability (thermodynamic and kinetic) and selectivity. Molecular recognition forms the basis of the highly specific recognition, regulation, etc., that occur in biology, such as substrate binding to the receptor protein, enzymatic reactions, antigen-antibody association, entry of virus into cell, translation and transcription of the genetic code, cellular recognition, and so on. Molecular recognition, thus, implies the read out of information in molecules, leading to the formation of supermolecules or supramolecular assemblies.

The requirements for designing materials with good molecular recognition between substrate and receptor leading to the formation of supermolecule or supramolecular array are—

- 1) Steric (shape and size) complementarity between substrate and receptor
- 2) Interactional complementarity i.e., presence of complementary binding sites in the correct disposition on substrate and receptor.
- 3) Multiple binding sites and strong intermolecular interactions that improves the stability of the complex formed.

In addition to all these factors the medium (solvent) plays an important role through the interaction of solvent molecules with the components of the reaction.

In 1967, Pederson observed that crown ethers show molecular recognition – the first unnatural molecule found to do so. Cram developed this concept to cover a wide range of molecular systems and established a new field of chemistry, host–guest chemistry.¹⁰ In 1978, Lehn attempted to organize these novel findings, highlighting the exotic structural features of ensembles of molecules by proposing a new term “supramolecular chemistry”. The elegance of molecular recognition through small molecules is highlighted with the pioneering work done by Pederson, Cram and Lehn, who were awarded Nobel Prize in 1987.

1.4 Intermolecular Interactions

The interactions between molecules which are not covalent in nature, are called non-covalent interactions. Non-covalent interactions typically include hydrogen bonds, halogen bonds, co-ordinate bonds, π - π interactions, electrostatic interactions, weak van der Waals forces, etc. The non-covalent interactions like the hydrogen bond, halogen bond, co-ordinate bond etc., which are directional in nature can mediate the aggregation of molecules into supermolecules/supramolecular assemblies of predictable topologies, as illustrated in the following sections.

1.4.1 Hydrogen Bond

Hydrogen bond¹¹ is the most widely studied non-covalent interaction in biological and chemical sciences. It plays an important role in maintaining the structure of various biomolecules like DNA, RNA, proteins, etc., and is also responsible for execution of various functions in biology like translation, transcription, cellular recognition, antigen-antibody interaction etc. Hydrogen bonds are sufficiently strong and directional to control and direct the structure of molecules and also form selective binding with other molecules by molecular recognition. Besides this the energy of hydrogen bond is such that it can easily form and break at ambient temperatures, which is the requirement for many biological processes like transcription and translation to take place. Since the strength of hydrogen bond is weak relative to typical covalent bonds, to achieve acceptable stability, therefore molecules in self-assembled aggregates must be joined by many of these weak bonds. Though the hydrogen bonds are feeble, easy to break and sometimes even hard to detect, but in conjunction, they become stronger and lean on each other. This phenomenon, which in scientific terms is called cooperativity,¹² is based on the fact that “1+1 is more than 2”.

Definition of hydrogen bond: Hydrogen bond is a kind of attractive interaction in which a hydrogen atom attached to an highly electronegative atom is attracted to a neighboring electronegative atom (or region of electron excess). Hydrogen bond (H-bond) is represented as a dashed bond between hydrogen and the acceptors (Y), as shown below.

X-H...Y

However, the experimental and theoretical results show that even the hydrogen atoms attached to less electronegative atoms like 'Carbon' atoms in the form of -C-H can be involved in H-bonding interaction.¹³

Stronger the H-bond, shorter is the H...Y distance. H-bonding interaction lead to increase in the X-H distance. As a consequence, a substantial downward frequency shift is observed of X-H peak in IR spectrum of hydrogen bonded systems. Inter and intramolecular hydrogen bonds can be readily distinguished in IR spectroscopy. Generally, the intermolecular hydrogen bonds give rise to broad bands whereas the bands arising from intramolecular hydrogen bonds are sharp and well defined. Intermolecular hydrogen bonds are concentration dependent, whereas intramolecular hydrogen bonds are not. The absorption frequency difference between free and associated molecules is smaller in case of intramolecular hydrogen bonding than in intermolecular association.

Since the formation of X-H...Y bond leads to the deshielding of proton involved in hydrogen bond, so hydrogen bonded protons are shifted downfield in NMR spectrum.

The energy of hydrogen bond is estimated to be in the range of 0.2 to 40 kcal mol⁻¹, and depending upon the strength, the hydrogen bonds are classified into three categories 1) Strong 2) Moderate and 3) Weak. According to system introduced by Jeffrey, hydrogen bonds are called moderate, if the energy is in the range of 4 - 15 kcal mol⁻¹, as observed in water molecules and in carbohydrates¹⁴. Hydrogen bonds with

energies above and below this range are called strong and weak, respectively. Some general properties of these categories are listed in the Table 1.1. However, it must be noted that there are no natural borderlines among these categories, to use in stringent way.

Table 1.1. Properties of strong, moderate and weak hydrogen bonds following the classification of Jeffrey.

X-H...Y	Strong	Moderate	Weak
Interaction type	Quasi-covalent	Mostly electrostatic	Electrostatic/Dispersive
Bond length(Å) H...Y	1.2-1.5	1.5-2.2	> 2.2
Lengthening of X-H	0.08-0.25	0.02-0.08	< 0.02
X...Y(Å)	2.2-2.5	2.5-3.2	> 3.2
Directionality	Strong	Moderate	Weak
Bond Energy (Kcal mol ⁻¹)	15 - 40	4-15	< 4

Unlike moderate and weak hydrogen bonds, strong hydrogen bonds are quasi-covalent in nature and deserve special discussion. If the hydrogen bond is understood as an incipient proton-transfer reaction, a moderate hydrogen bond represents an early stage of such a reaction, while a strong one represents an advanced stage. It may be

noted that from this viewpoint, hydrogen bonds with mainly ionic and little covalent nature are not classified as strong despite high dissociation energies ($-\text{NH}_3^+\cdots\text{Cl}^-$ etc.). Instead, they might be termed ionic interactions with a moderate hydrogen bond formed on top.

A very strong hydrogen bond is generally a manifestation of the complimentary molecules. Depending upon the ΔpK_a (difference in pK_a of the acceptor and donor) either a moderate $\text{X-H}\cdots\text{Y}$ hydrogen bond or an ionic $\text{X}^-\cdots\text{H-Y}^+$ hydrogen bond is formed, both of which are not very covalent. The quasi-covalent situation occurs in a certain critical range of ΔpK_a , the numerical characteristics of which depend on the particular system.¹⁵

Hydrogen-bond modes derived from crystal structures are useful for determining the preferred modes of association of the individual functional groups on complex multifunctional molecules. Hence understanding and analysis of hydrogen bond properties are of great necessity in the studies of supramolecular chemistry. In this respect, graph-set analysis¹⁶ aid in transferring information about molecular recognition properties of molecules from the solid state to solution and mobile phases, and provide a unifying methodology for describing hydrogen-bonded sets of molecules.

Graph set analysis of hydrogen bond motifs in fact simplifies the complex hydrogen bond patterns through specific codes in a systematic process. The method is based on viewing hydrogen bond patterns topologically as if they were intertwined nets with molecules as the nodes and hydrogen bonds as the lines.

Graph set codes are specified using the pattern designator (**G**), its degree (**r**), and the number of donors (**d**) and acceptors (**a**) as shown below.

$$\mathbf{G}_d^a(\mathbf{r})$$

G is a descriptor referring to the pattern of hydrogen bonding. It has four different assignments based on whether hydrogen bonds are inter or intramolecular: **S** (intramolecular), **C** (infinite hydrogen bonding chains), **R** (rings) and **D** (noncyclic dimers and other finite hydrogen bonded sets).

The parameter **r** is the number of atoms in a ring or the repeat length of a chain. For a ring, in an **S** or **R** set, it is defined as the number of atoms in the ring, counted by traversing the ring in one direction, along the shortest chain of covalent and hydrogen bonds until all the atoms in the ring have been counted once. For a chain **C**, the degree is the repeat length of the monomer unit in the chain i.e., the number of atoms encountered by traversing the shortest pathway from the hydrogen atom of one hydrogen bond to the acceptor atom of the next. For **D** motifs, **r** is the number of atoms in the entire length of the hydrogen-bonded set starting with the proton of the first hydrogen bond, proceeding along the shortest pathway, and ending with the acceptor atom in the last hydrogen bond of the set. If there is only one hydrogen bond in the motif, then the **r** for the **D** pattern is 2. Since this pattern occurs so frequently, **r** = 2 is considered the default degree value for a **D** pattern.

The parameters **d** and **a** refer to the number of donors and acceptors used in the hydrogen-bond pattern. When all the molecules in a set are the same, **d** and **a** will be the number of participating donors and acceptors per molecule. When the set is composed of different kinds of molecules, **d** and **a** will be the sum of the participating

donors and acceptors from all the different molecules. The default value for **d** and **a** is 1.

Assigning graph sets to the first-order networks

A first order network, N_1 , is just a sequential listing of the graph sets that corresponds to each motif in the network as shown below.

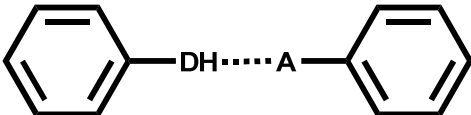
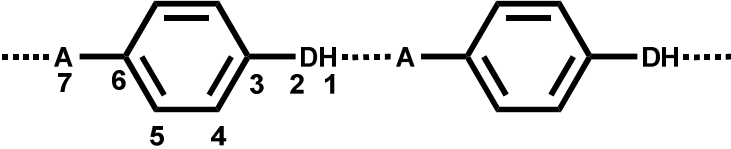
$$N_1 = M_j \cdots M_3 M_2 M_1$$

Here M_1 is the motif containing the highest priority hydrogen bond. The lowest degree pattern is given the highest priority.

Assigning graph sets to the higher-order networks

Higher-order networks arise from the combination of two or more different types of hydrogen bonded motifs. Higher order networks, N_i , are assigned by adding sequentially one new graph set per higher-order network. The lowest degree pattern is given the highest priority, as for motifs and is assigned first, as illustrated in the following examples.

The graph set notation is illustrated further with the help of the following examples

Structure	Graph-set Notation
	D
	C(7)

In some cases H(1) occurs in a ring as well as in a chain. In these cases, the ring may be indicated as a subset, given in brackets.

Structure	Graph-set Notation
	$C_1^2(8)[R_1^2(4)]$

If the hydrogen atom of a single hydrogen bond donor occurs in two of the same rings at the same time, then the graph set assigned to one of the patterns is doubled

Structure	Graph-set Notation
	$2R_1^2(4)$

In the example shown below, since the highest priority hydrogen bond is S(5) and the second highest priority hydrogen bond is S(6), therefore graph set notation for this first order network is $N_1 = S(6)S(5)$. In addition it contains a higher-order network, which arises by the combination of motifs from two different kinds of hydrogen bonds. Higher order networks, N_i , are assigned by adding sequentially one new graph set per higher-order network.

Structure	Graph-set Notation
	$N_1 = S(6)S(5)$ $N_2 = S \frac{1}{2}(9)$

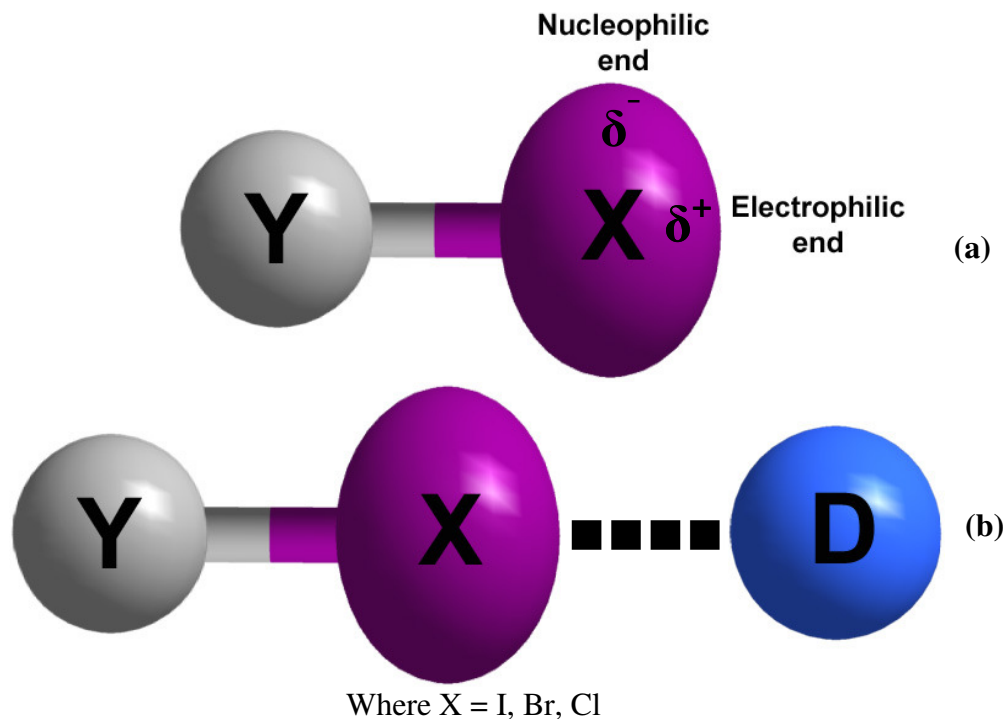
In the example shown below, one kind of hydrogen bond gives rise to a ring and the another kind of hydrogen bond gives rise to chains

Structure	Graph-set Notation
	$N_1 = C(4)R_2^2(8)$ $N_2 = R_4^2(8)$

1.4.2 Halogen Bond

Halogen bonding¹⁷ is a non-covalent interaction, wherein halogen atom functions as an electrophilic species. Halogen bonds (XBs) can be described in general as $D \cdots X-Y$, where X is the electrophilic halogen atom {Lewis acid, halogen bond (XB) donor}, D is the donor of electron density {Lewis base, halogen bond (XB) acceptor} and Y is a carbon, nitrogen or halogen atom as shown below in Figure 1.4 (a) and (b). The halogen bonding arises due to the anisotropic distribution of electron density along the Y-X bond, due to which halogen atom is an electron deficient at the pole and thus forms attractive interaction with the electron donors and this attractive force is called halogen bond. Halogen bond is highly directional interaction and indeed more directional than the hydrogen bond. The consequence of the anisotropic distribution of

electron density around the halogen atom is that the angle between the covalent and non-covalent bonds around the halogen atom in $D\cdots X-Y$ is approximately 180° .



D = N, O, S, Se, Cl, Br, I, Γ , Br^- , Cl^- , F^- and π electron donors etc.

Figure 1.4. (a) Anisotropic distribution of electrons along the Y-X axis. (b) In halogen bonding electrophilic end of X is attracted towards electron rich donor (D).

In agreement with the anisotropic electron density model described above, Cl, Br and I show amphiphilic character. Halogen atoms, thus, function as electron-deficient sites when they form contacts at the pole (electrophilic end), and can also function as electron-rich sites on forming contacts at the equator (nucleophilic end). The term halogen bond addresses the former contacts exclusively. Due to the formation of halogen bonds the $D\cdots X$ distance decreases than the sum of the van der

Waals radii of the involved atoms-the stronger the halogen bond, the shorter the $D\cdots X$ distance. Due to the formation of the halogen bond, indeed, covalent X-Y bond lengthens because of the shift of the electron density from donor D to the antibonding X-Y orbital.

The ability of halogen atoms to interact attractively with electron donors was recognized as early as the 19th century.¹⁸ More than 50 years later, Benesi and Hildebrand reported the first cases of intermolecular donor-acceptor complexes formed from iodine and aromatic hydrocarbons.¹⁹ However, it was Hassel who stressed in his nobel lecture in 1970 the importance of halogen bonding for directing molecular self-assembly phenomena.²⁰ Like hydrogen atoms, halogen atoms are typically located at the periphery of organic molecules and are, thus, ideally positioned to be involved in intermolecular interactions.

As the polarizability of the halogen atoms increases on moving from F to I, so in general the positive potential along the Y-X bond increases on moving from F to I. The electrostatic potential remains negative all around the F atom, whereas an area of positive charge emerges for Cl, Br and I. The magnitude of the positive area increases as the electron-withdrawing effect of the neighboring groups increases. The order $C(sp)-X > C(sp^2)-X > C(sp^3)-X$ is generally followed, and haloalkynes are particularly good XB donors.

Typical organic compounds containing nitrogen atoms especially in heterocyclic compounds, form stronger halogen bonds than do standard oxygen and sulfur compound, but the reverse is true when the pyridine derivatives and the corresponding N-oxides are compared, and is consistent with the electron densities on

the respective donor sites. The relative effectiveness of the oxygen and sulfur atoms as halogen bond acceptor sites typically depends on the nature of the halogen bond donor. The pairings predicted by the hard and soft acids and bases (HSAB) theory are favored, but a general ordering of halogen bond acceptors or donors according to their strength cannot be made. Anions are usually better halogen bond acceptor than neutral species.

Since halogen atoms are much larger and polarizable than hydrogen atoms; thus halogen bonds are more sensitive to steric hinderance than the hydrogen bonds. The strength of the halogen bond can vary in the range 2.4-48 kcal mol⁻¹. The remarkable strength of some halogen bonds allow them to prevail over analogous hydrogen bonds e.g. the formation of intermolecular hydrogen bonds between dissolved species is considerably suppressed if a strong halogen bond donor is added as a co-solute, and in experiments on competitive co-crystal formation, various hydrocarbon derivatives containing two nitrogen atoms prefer to cocrystallize with halogen bond donors rather than hydrogen bond donors as shown below (Figure 1.5). In this example, 1,2-*bis*(4-pyridyl)ethane (1a), which forms co-crystals with 1,4-diiidotetrafluorobenzene (2a) and hydroquinone (3a) separately, however, yields only co-crystals with 2a in a competitive co-crystallization experiment of 1a, 2a and 3a. Thus, in this case halogen bonding is more effective than the hydrogen bonding in the formation of supramolecular architectures.²¹

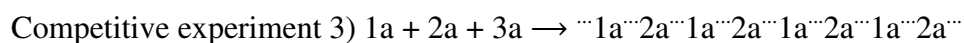
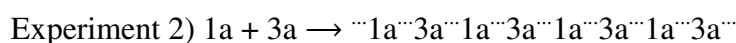
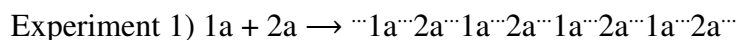
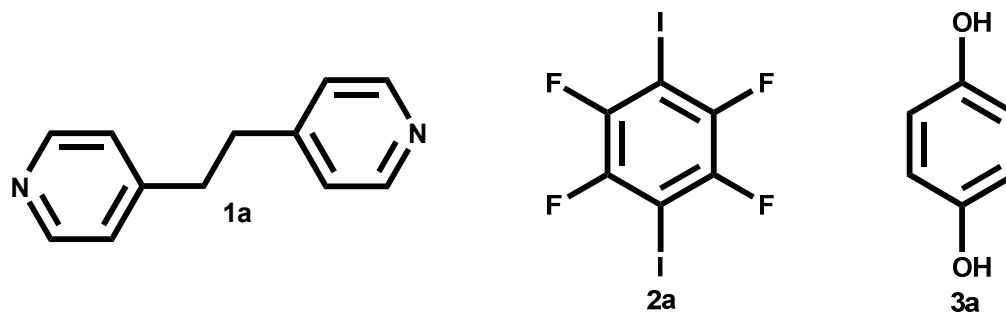


Figure 1.5. In experiment 1 and 2, 1a formed co-crystals with 2a and 3a respectively and in experiment 3 upon dissolving 1a, 2a and 3a in equimolar ratios, 1a formed co-crystal with 2a only.

1.5 Self Assembly

Self-assembly²² is the spontaneous aggregation of molecules under equilibrium conditions into stable, structurally well-defined entities. The process of self assembly proceeds through the noncovalent interactions formed between the complimentary subunits (functional groups) of molecules and the structure and properties of the resultant assemblies are determined by the nature and positioning of the subunits. Molecular self-assembly is ubiquitous in biological systems and underlies the formation of a wide variety of complex biological structures like DNA, RNA and proteins.

Understanding self-assembly and the associated noncovalent interactions are central concern in structural biochemistry and it is now widely used in the formation of supramolecular assemblies having complex structures and architectures through ensembling of several organic molecules. In supramolecular chemistry, simple

building blocks are programmed with the suitably positioned binding sites and they spontaneously assemble to give desired complex structures. During the process of self assembly, there is a large decrease in entropy, therefore, these interactions between molecules must be more favorable energetically than competing interactions with solvents and must be able to overwhelm the entropic advantage of disintegration of the ordered aggregate into a disorder or dissociated state.

1.6 Supramolecular Assemblies

The design of molecular building units that can self-assemble into well-defined architectures in the solid state is a contemporary challenge in supramolecular chemistry. Molecules recognize each other by various molecular recognition patterns and it ultimately leads to the formation of assemblies of higher complexity i.e. either supermolecules or supramolecular assemblies. The formation of a crystal is the perfect example of solid state molecular recognition.²³ Understanding of these various molecular recognition patterns is very important and this leads to the design of solid state structures of fundamental and practical importance. Some of the intermolecular hydrogen bonding patterns, which are involved in the construction of various supermolecules/supramolecular assemblies are listed in Figure 1.6.²⁴

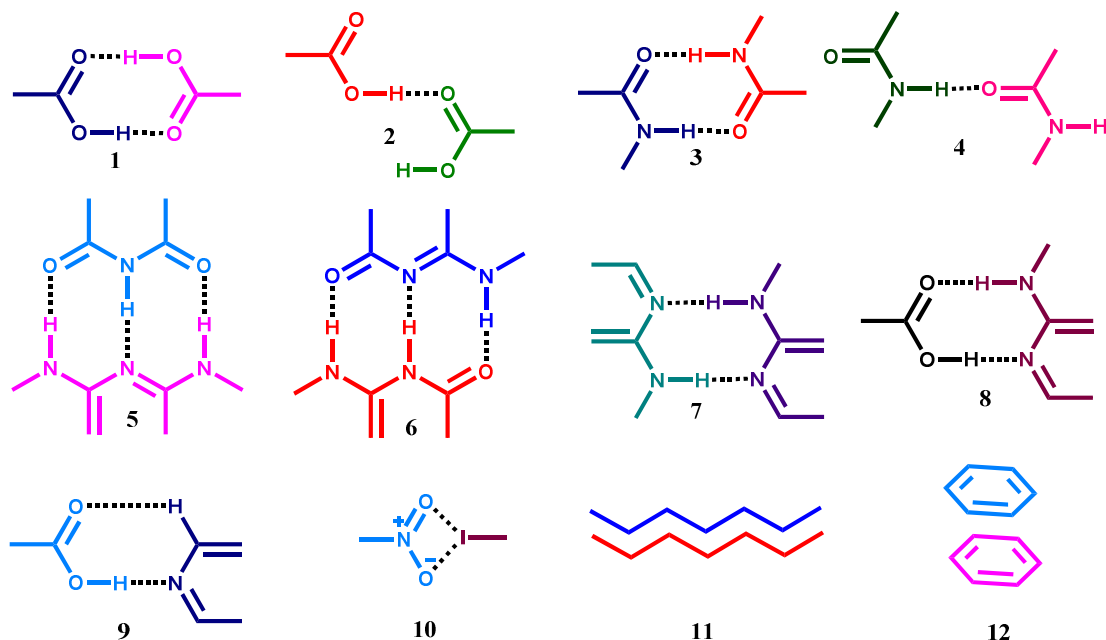


Figure 1.6. Various intermolecular recognition patterns observed in supramolecular assemblies

In the crystal structure of trimesic acid (TMA)²⁵, reported by Marsh and Duchamp, the molecules of trimesic acid recognize each other by the formation of carboxylic acid dimers, and it leads to the creation of a cavity having dimensions $14.5 \times 14.5 \text{ \AA}^2$. Such structures with large voids, in general, get stabilize by either guest inclusion or interpenetration, in crystal lattices. In this case, the molecules of trimesic acid undergo 4-Fold interpenetration to attain a close pack structure, as shown in the Figure 1.7.

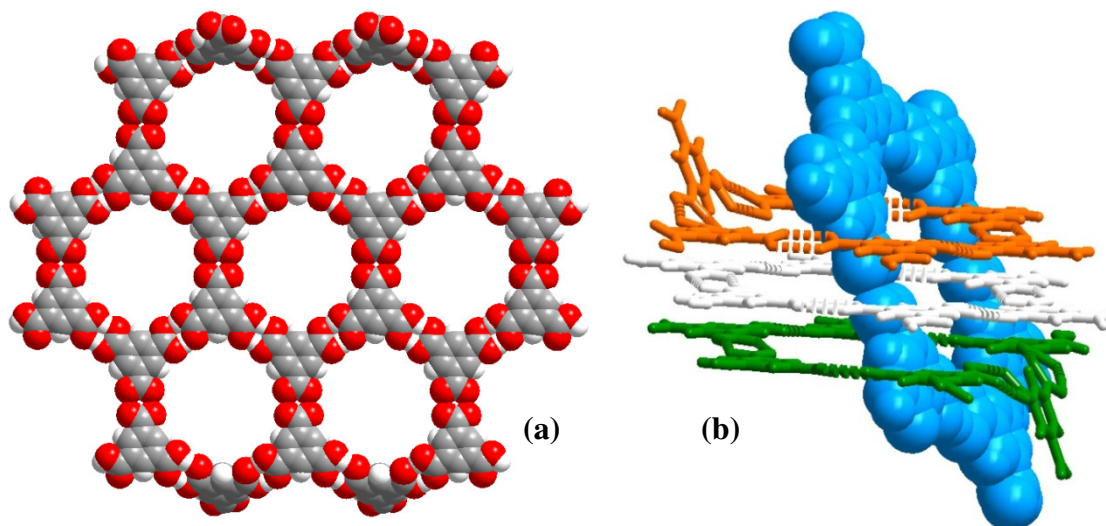


Figure 1.7. (a) Honeycomb network, having cavity of dimensions, $14.5 \times 14.5 \text{ \AA}^2$, observed in the crystal structure of trimesic acid. (b) 4-Fold interpenetration observed in three-dimensional arrangement of the trimesic acid.

In contrast, crystallization of TMA with pyrene from ethanol,²⁶ as reported by Zimmermann and co-workers gave a cyclic host of dimensions $18.5 \times 13 \text{ \AA}^2$, which is filled by the pyrene and ethanol as guest molecules. (See Figure 1.8)

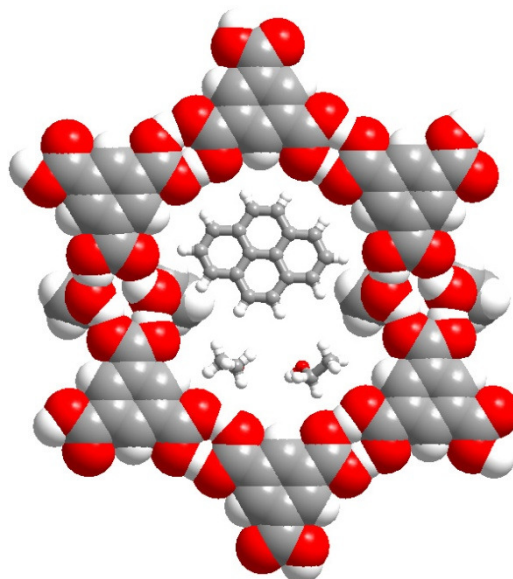


Figure 1.8. Host-Guest network formed by the molecules of TMA and pyrene from ethanol.

Similarly in the experiments of Coppens and co-workers, co-crystallization of TMA and 1,3,5-tri(4-pyridyl)-2,4,6-triazine (TPT), in pyrene solution gave a host network having large cavities of dimensions $22 \times 16 \text{ \AA}^2$, which are being filled by the pyrene as guests,²⁷ as shown in Figure 1.9.

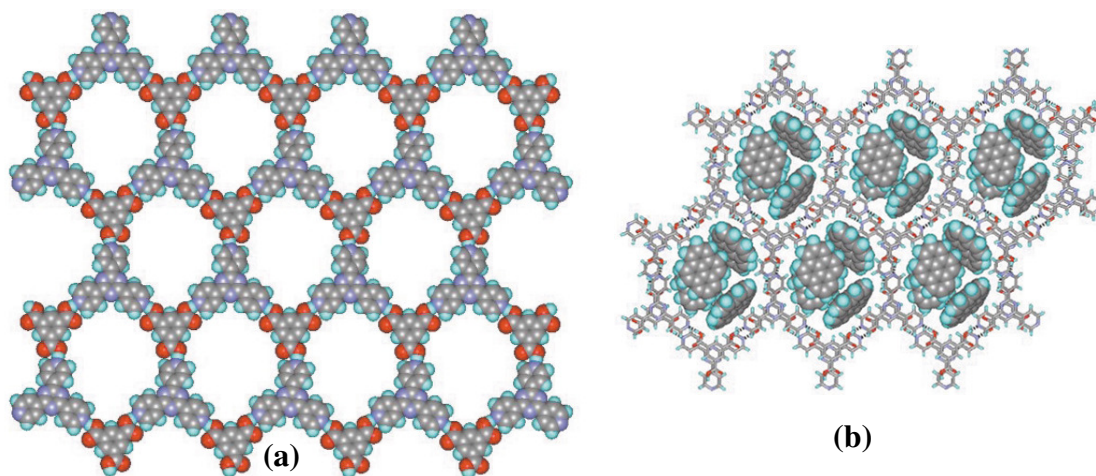


Figure 1.9. Honeycomb framework formed by an adduct of TMA and TPT (a) without pyrene and (b) with pyrene molecules.

Rao and co-workers utilized multipoint recognition between melamine and trithiocyanuric acid to form a rosette network. In the network, three molecules, each of melamine and trithiocyanuric acid are held together by 18 hydrogen bonds to form the rigid network,²⁸ as shown in the Figure 1.10.

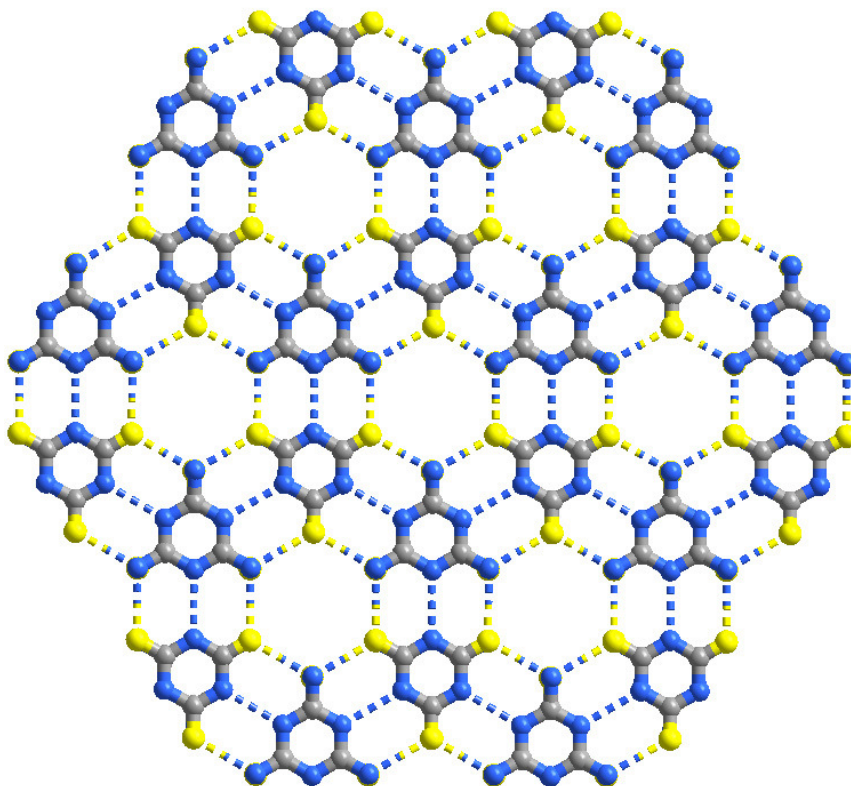


Figure 1.10. Rosette network observed in the adduct of melamine and trithiocyanuric acid through N-H \cdots S and N-H \cdots N hydrogen bonds.

Mak and co-workers reported a multicomponent rosette network by co-crystallizing guanidinium carbonate, tetra-*n*-propyl ammonium hydroxide and boric acid. Packing diagram, as shown in Figure 1.11, highlights the formation of charged layered structure. While the anionic layers, comprise of the guanidinium, carbonate and boric acid form the rosette network, the cationic layers are formed by tetra-*n*-propyl ammonium cations.²⁹

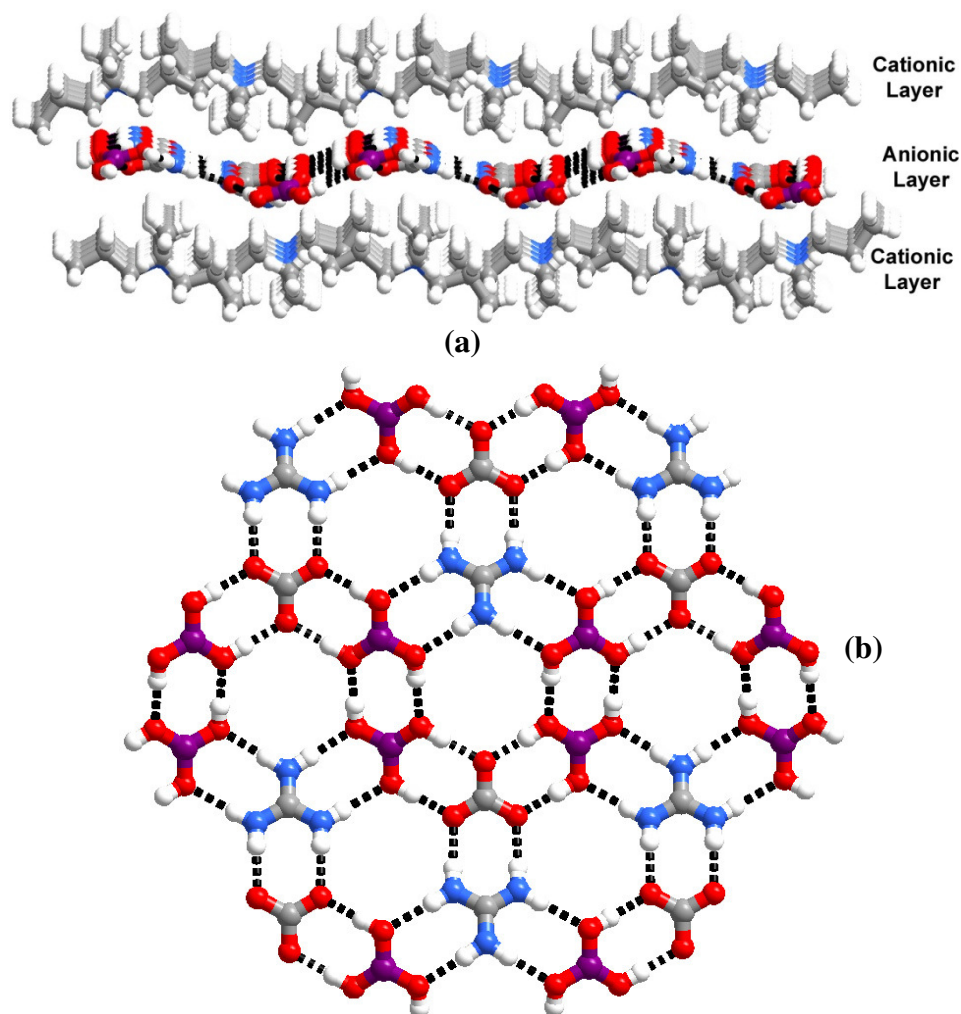


Figure 1.11. (a) Packing of cationic and anionic layers alternatively and (b) rosette network observed in the anionic layer as noted in the crystal structure of tetra-*n*-propylammonium guanidinium carbonate bis(boric acid).

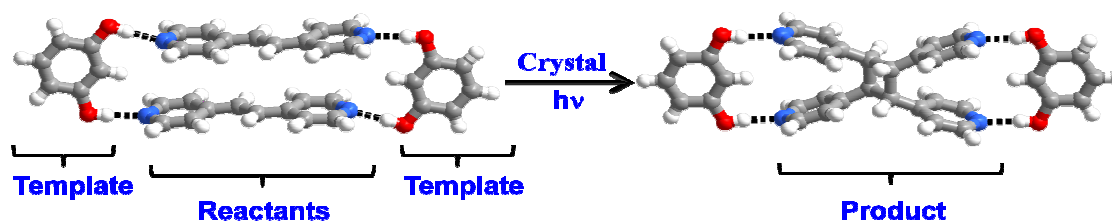
1.7 Applications of Supramolecular Assemblies

Supramolecular assemblies show a lot of applications in various fields varying from synthesis of molecules, pharmaceuticals, catalysis, separation to gas adsorption. The details of some of these are given in the following sections.

1.7.1 Synthesis of New Molecules

Carbon-carbon bond formation lies at the heart of organic synthetic chemistry. Such reactions are used to construct molecules of remarkable complexity. Primary goals in the synthesis of molecules is to obtain possible high yields, limited byproducts, and minimal waste. Novel methods and means of procedures are always on continuous search to develop improved ways to control the formation of covalent bonds. In this process, one of the elegant process of C-C bond formation is based on topochemical principles for [2+2] photoreactions in the solid state, as described by Schmidt and co-workers through a number of crystallographic investigations. According to this principle, for photodimerization to occur in the solid state, olefinic bonds should be parallel and separated by $< 4.2 \text{ \AA}$ in the solid state structure.³⁰ Since then chemists have strived to design molecules that will predictably crystallize to allow such reactions to occur. Such an approach to synthesis lead to the formation of covalent bonds ‘at will’ in solids to facilitate the high yield, solvent-free synthesis of molecules

MacGillivray and co-workers forwarded novel methodology to achieve controlled [2+2] photodimerization reaction,³¹ involving a linear template, based on 1,3-dihydroxybenzene (resorcinol), by enforcing topochemical alignment of olefins in the solid state, creating a template through supramolecular aggregation as demonstrated in the co-crystals of 1,3-dihydroxybenzene (resorcinol) and 1,2-*bis*(4-pyridyl)ethene.³²



Co-crystallization of resorcinol with 1,2-*bis*(4-pyridyl)ethene yielded a four component assembly, 2(4,4'-*bpe*).2(resorcinol), in which the olefins of the complex are arranged in parallel fashion, separated by ~ 4 Å. On photoirradiation, a [2+2] photodimerization reaction took place, yielding *rctt*-tetrakis(4-pyridyl)cyclobutane (tpcb) in 100% yield.

By the similar template directed synthesis [n]-ladderanes³³ were synthesized by most economical and high yields. [n]-ladderane is a molecule that consists of n edge-sharing cyclobutane rings (where $n \geq 2$) that define a molecular equivalent of a macroscopic ladder, as shown in Figure 1.12.

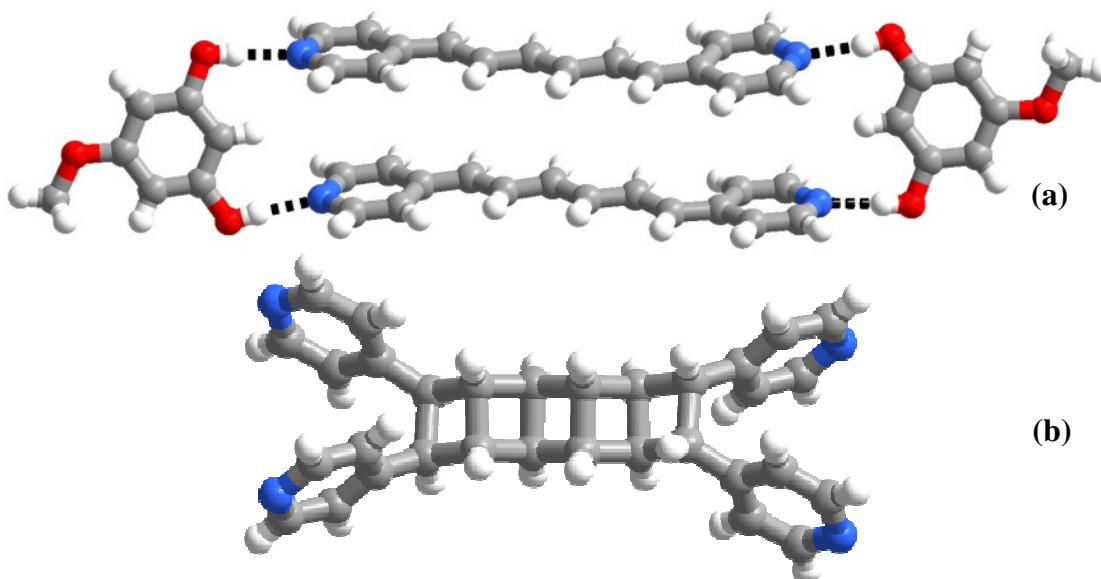


Figure 1.12. a) Co-crystal formed between 5-methoxyresorcinol and 1,6-*bis*(4-pyridyl)hexatriene and b) ladderane formed on irradiating the co-crystal.

Christian Wolf and co-workers utilized pairwise hydrogen bond dimeric interactions between -COOH group of fumaric acid and aza-donor group of 1,8-dipyridylnaphthalene to form a tetrameric assembly stabilized by eight hydrogen bonds.³⁴ The rigid spatial arrangement of the cofacial pyridyl rings in the template forces two adjacent dicarboxylic acids into close proximity with an intermolecular distance of less than 4.0 Å. Photoirradiation of the crystal resulted in stereoselective conversion of fumaric acid to *cis*, *trans*, *cis*-cyclobutanetetracarboxylic acid in 100% yield as shown in Figure 1.13.

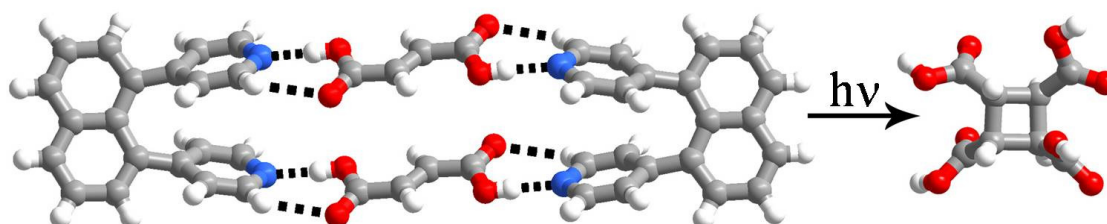


Figure 1.13. Formation of *cis*-cyclobutanetetracarboxylic acid by photodimerization reaction.

Jones and co-workers used polyfunctional templates for the synthesis of [2+2] photodimerized product. On irradiating the co-crystal of 1,2,4,5-benzenetetracarboxylic acid and 1,2-*bis*(4-pyridyl)ethene, in which the adjacent molecules of aza-donor moieties satisfy the criteria of [2+2] photodimerization, the photodimerized product *rcit*-tetrakis(4-pyridyl)cyclobutane (**tpcb**) was obtained in 100% yield.³⁵ Further, irradiated sample upon co-crystallization from DMSO gave a structure with a porous host network, as shown in Figure 1.14 (a) and (b), with the voids being filled by the guest molecules of DMSO and water.

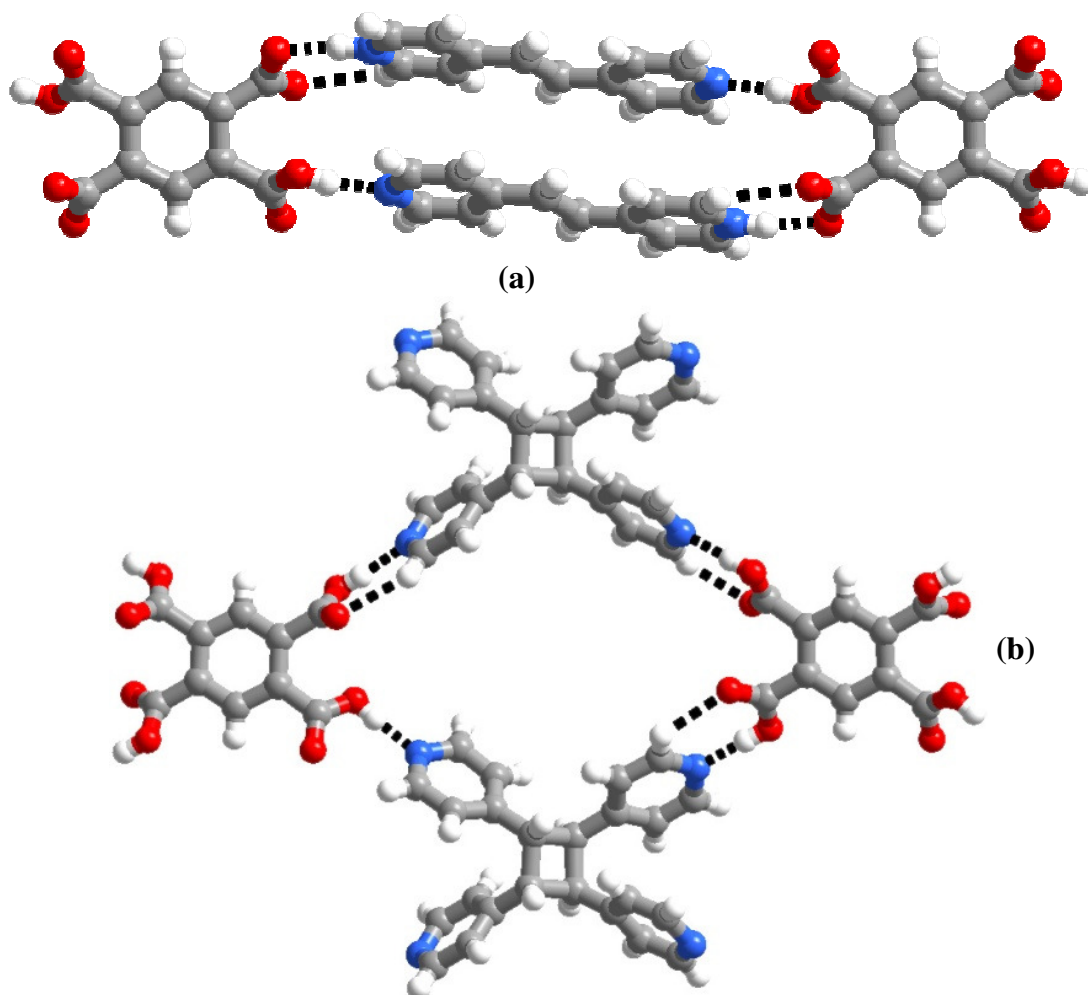


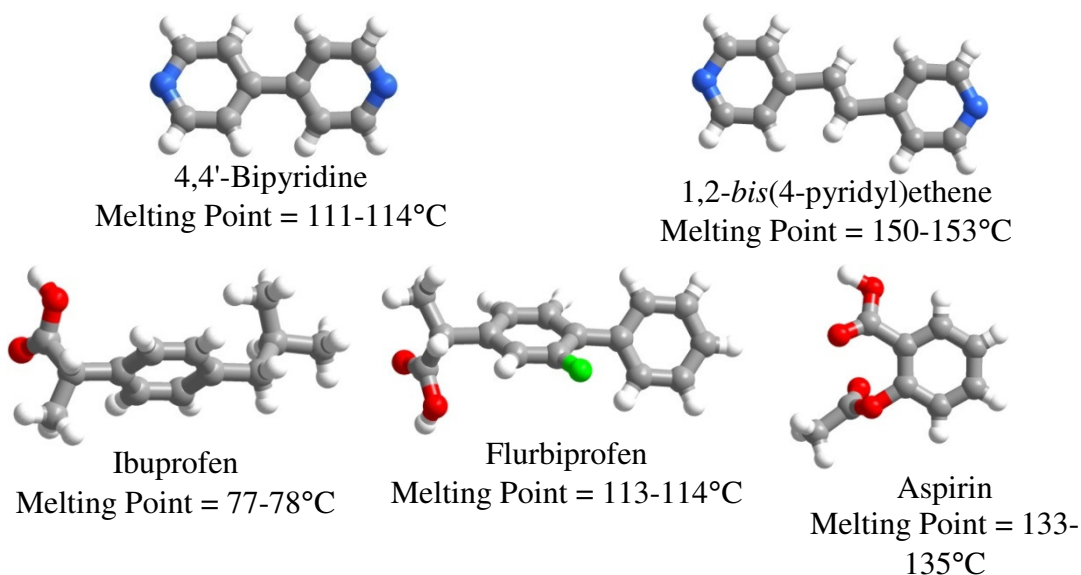
Figure 1.14. (a) Co-crystal formed between 1,2,4,5-benzenetetracarboxylic acid and 4,4'-bipyridine ethene (b) Porous network formed by the irradiation of co-crystal of 1,2,4,5-benzenetetracarboxylic acid and 1,2-*bis*(4-pyridyl)ethene (solvent molecules are removed for clarity)

1.7.2 Pharmaceutical Co-crystallization

The field of supramolecular chemistry enables the design of crystalline molecular complexes or co-crystals, using robust and reliable intermolecular interactions in the form of discrete motifs or patterns. Co-crystallization represents a viable means of enhancing the physical properties of co-crystallizing ligands like their

stability, solubility, melting point etc., which have been well placed into the realm of pharmaceuticals, especially to modify the bioproperties of drug molecules. The challenges within pharmaceutical arena provide a unique opportunity to showcase the power and utility of supramolecular chemistry to solve the real-world problems. Thus, pharmaceutical co-crystallization,³⁶ wherein, one of the ligand is an active pharmaceutical ingredient (API), has demonstrated increased bioavailability through enhanced solubility or stability of drugs etc., which are otherwise sensitive to external parameters like moisture, pressure etc. Some of the elegant contributions from various research groups are illustrated in the following section.

Zaworotko and co-workers co-crystallized 4,4'-bipyridine with ibuprofen, flurbiprofen and aspirin, as well as and 1,2-bis(4-pyridyl)ethene with flurbiprofen, involving dimeric interaction between carboxylic acid functional group and aza-donors.³⁷ In all the co-crystals the drug molecules and the aza-donor compounds co-crystallized in 2:1 ratio, respectively, as shown in Figure 1.15.



Highlight of this study is lowering of melting point of the drug, which is achieved in the example of aspirin and 4,4'-bipyridine.

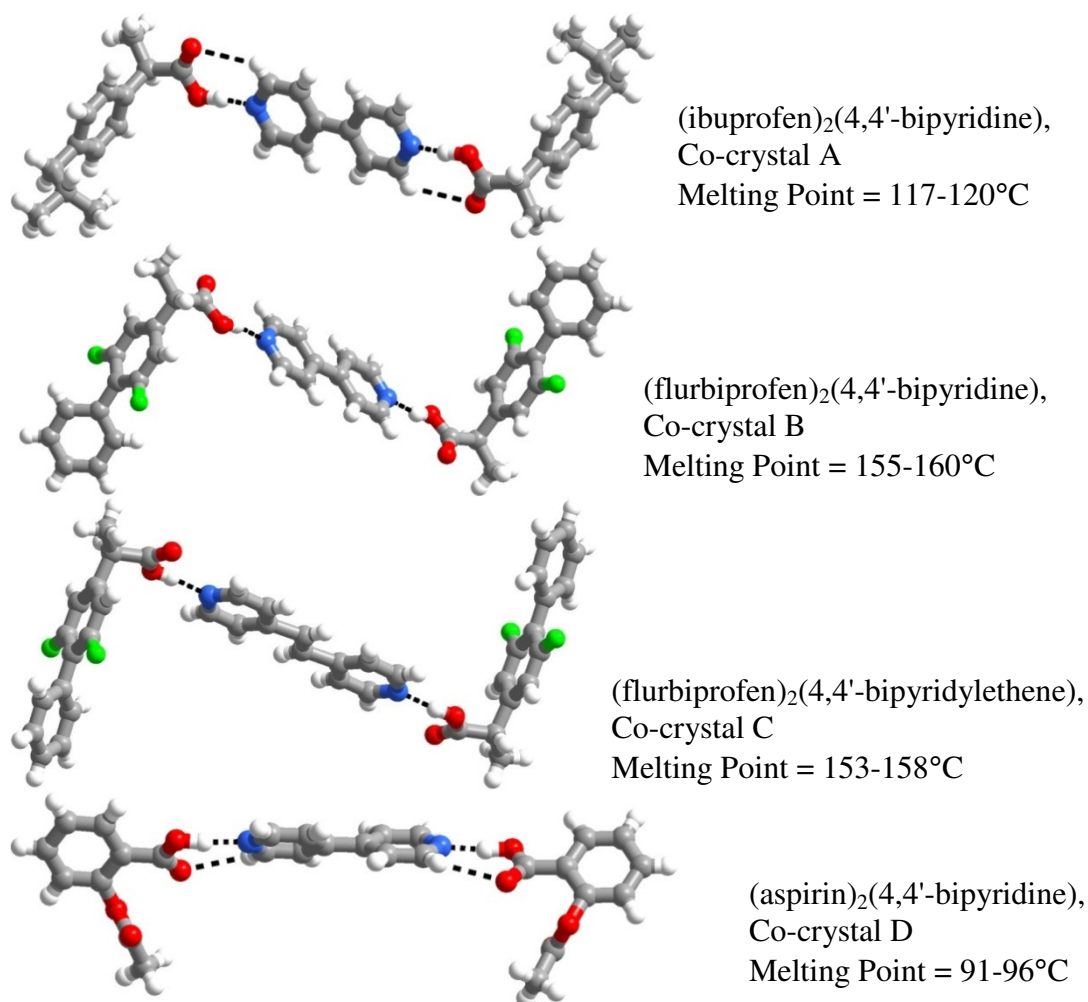


Figure 1.15. Pharmaceutical co-crystals formed between the drug molecules and 4,4'-bipyridine and 1,2-*bis*(4-pyridyl)ethene.

Caffeine is known to exhibit instability with respect to humidity. Jones and co-workers, have prepared co-crystals, A{Caffeine/Oxalic acid (2:1)}, B{Caffeine/malonic acid (2:1)} and D{Caffeine/maleic acid (1:1)}

Material	Condition	Observed Relative Humidity Stability*			
	(%RH)	1 day	3 days	1 week	7 weeks
Caffeine	0	✓	✓	✓	✓
	43	✓	✓	✓	✓
	75	✓	✓	✓	✓
	98	✗	✗	✗	✗
A {Caffeine/Oxalic acid (2:1)}	0	✓	✓	✓	✓
	43	✓	✓	✓	✓
	75	✓	✓	✓	✓
	98	✓	✓	✓	✓
B {Caffeine/malonic acid (2:1)}	0	✓	✓	✓	✓
	43	✓	✓	✓	✓
	75	✓	✓	✓	✓
	98	✓	✓	✓	✗
C {Caffeine/maleic acid (2:1)}	0	✓	✓	✓	✓
	43	✓	✓	✓	✓
	75	✓	✓	✓	✓
	98	✗	✗	✗	✗
D {Caffeine/maleic acid (1:1)}	0	✓	✓	✓	✓
	43	✓	✓	✓	✓
	75	✓	✓	✓	✓
	98	✗	✗	✗	✗
E {Caffeine/glutaric acid (1:1) Form I}	0	✓	✓	✓	✓
	43	✓	✗	✗	✗
	75	✗	✗	✗	✗
	98	✗	✗	✗	✗
F {Caffeine/glutaric acid (1:1) Form II}	0	✓	✓	✓	✓
	43	✓	✓	✓	✓
	75	✓	✓	✓	✓
	98	✓	✓	✗	✗

*Note: The symbol ✓ indicates that the crystalline material was stable at that condition and time point. The symbol ✗ indicates that the crystalline material exhibited physical instability at that time point: Caffeine converted to caffeine hydrate, co-crystals B, C, D and F dissociated into molecular components; and the co-crystal E was observed in some instances to convert to polymorph F before dissociating.

Chart 1

They also compared the stabilities of caffeine with the co-crystals they formed and also some other already known co-crystals like C{Caffeine/maleic acid (2:1)}, E{Caffeine/glutaric acid (1:1) Form I}, F{Caffeine/glutaric acid (1:1) Form II} and the results obtained are as summarized in Chart 1.³⁸

From the results so obtained, it is clear that the co-crystals A, B and F are more stable to the moisture as compared to caffeine itself.

Itraconazole is an extremely water-insoluble antifungal drug that is marketed in the amorphous form (Sporanox capsule) to achieve the required oral bioavailability. Remenar and co-workers made co-crystals of itraconazole with fumaric acid, succinic acid, L-malic acid, L-tartaric acid, D-tartaric acid and D, L-tartaric acid and a typical co-crystal formed between itraconazole and succinic acid in 2:1 ratio, is shown in Figure 1.16.³⁹

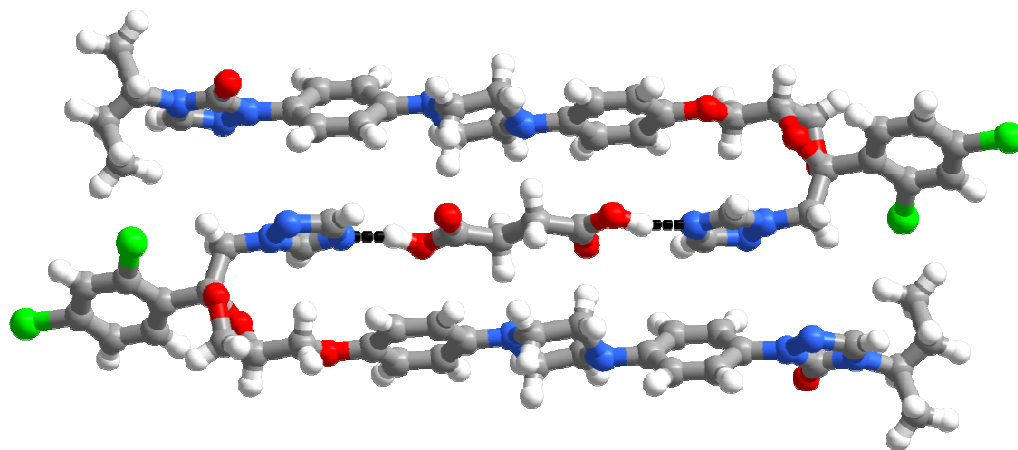
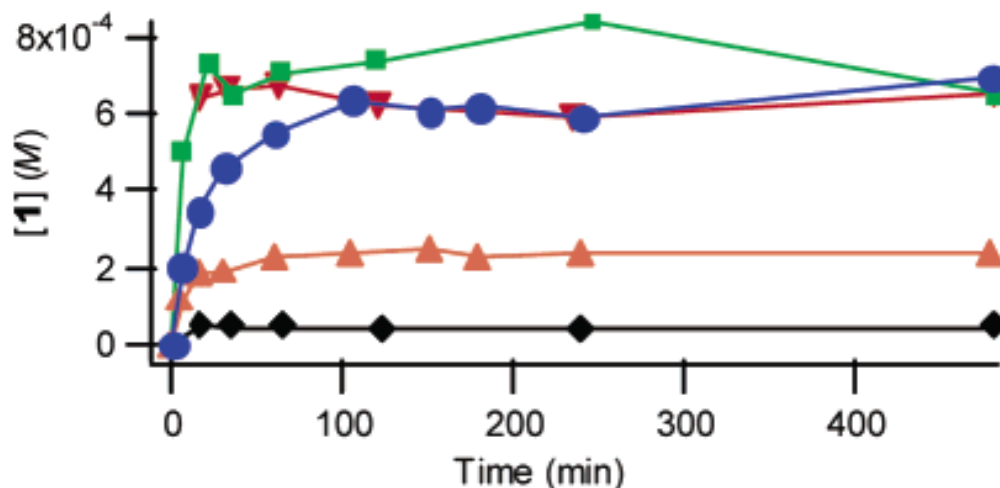


Figure 1.16. Co-crystal formed between itraconazole and succinic acid

The comparison of dissolution studies of amorphous marketed form (Sporanox bead) and crystalline form of itraconazole with co-crystals of itraconazole with succinic acid, L-malic acid, and L-tartaric acid in 0.1N HCl, showed that the co-crystals achieve and sustain from 4- to 20-fold higher concentrations than the

crystalline form of itraconazole. The dissolution profile of co-crystals is more similar to amorphous form than that of crystalline form of itraconazole, as shown below.



Dissolution profile of 0.1 N HCl at 25° C for amorphous form of itraconazole (Sporanox beads (■), itraconazole and L-malic acid co-crystal (▼), itraconazole and L-tartaric acid co-crystal (●), itraconazole and succinic acid co-crystal (▲) and crystalline form of itraconazole 1(◆).

1.7.3 Applications of Metal-Organic Frameworks

Open metal organic frameworks⁴⁰ are widely used as materials for applications in gas storage, separation, catalysis and molecular recognition. Compared to conventionally used microporous inorganic materials like zeolites etc., they can be designed rationally and their pores can be functionalized selectively for various applications.

1.7.3.1 Metal Organic Frameworks as Gas Storage Materials

Porous metal organic frameworks can be used as materials for the gas storage, especially, the hydrogen gas adsorbed in metal organic frameworks has potential

application as alternative fuel for running motor vehicles.⁴¹ Hydrogen is an ideal fuel for running automobiles, as the chemical energy released on its oxidation (33.9 kcal kg⁻¹) is approximately three times larger than the other chemical fuels (for example, the equivalent value for liquid hydrocarbons is 11.2 kcal kg⁻¹). The other advantage of hydrogen is that, it is a green fuel, as the exhaust gas evolved is only water vapors, when burnt with oxygen. But the only problem for running the vehicles on hydrogen gas is its storage.

One of the first metal–organic frameworks investigated for hydrogen storage was the cubic carboxylate-based framework Zn₄O(BDC)₃, also known as MOF-5 or IRMOF-1.⁴² Yaghi and co-workers made use of metal-carboxylate cluster chemistry to form this open metal-organic frameworks. They made MOF-5 by the diffusion of triethylamine into a solution of zinc(II) nitrate and terephthalic acid in DMF/chlorobenzene.

In MOF-5, four ZnO₄ tetrahedra with a common vertex form a supertetrahedral cluster, each edge of the Zn tetrahedron is then capped by the -CO₂ group, to form octahedral secondary building unit (SBU), having formula Zn₄O(CO₂)₆. The octahedral SBU are joined together by benzene links, forming cubic network in which the vertices are the octahedral SBU and the edges are the benzene struts, as shown in Figure 1.17.

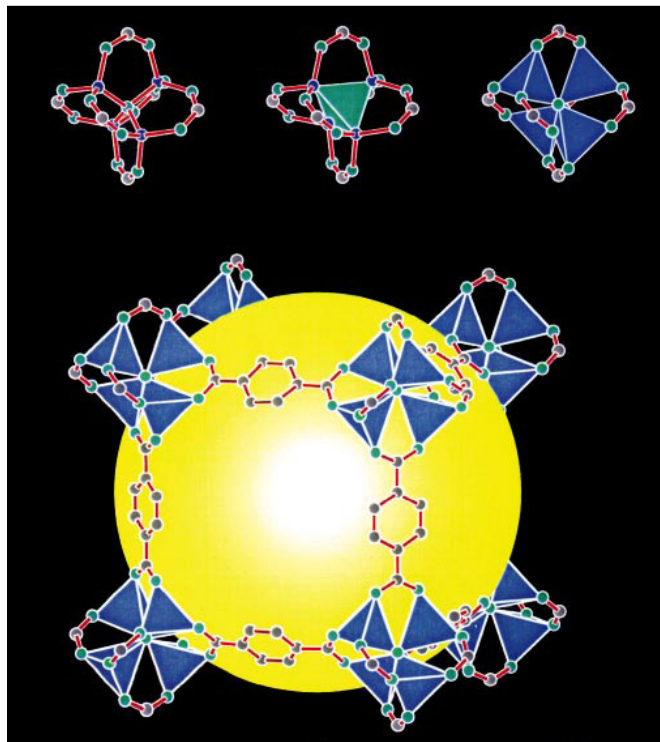


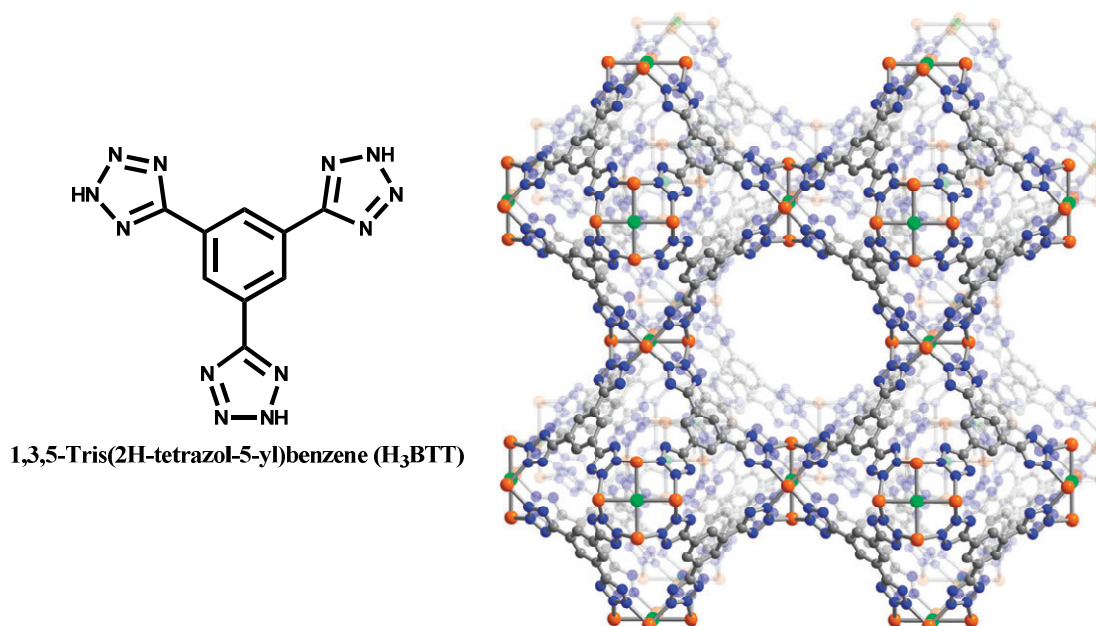
Figure 1.17. Porous network formed by the reaction between terephthalic acid and zinc salt.

In the framework so formed there is a lot of free space and this space is filled by the guest molecules of DMF and C_6H_5Cl . Due to high mobility, the guests can be fully exchanged with chloroform. More significant is that all the chloroform guests can be evacuated from the pores within 3 hours at room temperature and 5×10^{-5} torr, without loss of framework periodicity. They heated the fully desolvated crystals in the air at $300^\circ C$ for 24 hours, which has no effect on either their morphology or crystallinity, which gives a further evidence of the stability of the crystals.

MOF-5 shows different H_2 gas storage properties depending upon the procedure of preparation and handling.⁴³ MOF-5 decomposes in humid air, due to atmospheric water. The best H_2 storage MOF-5 is obtained by minimizing the exposure to water and air. Sample of MOF-5 prepared with exposure of air, adsorbed

5.0 excess wt% H₂, whereas it was 7.1 excess wt% H₂, when MOF-5 was prepared in vacuum.

While Zn₄O(BDC)₃ exhibits excellent hydrogen storage characteristics at 77 K, its performance at 298 K is poor due to the weak interactions with H₂. The framework having open metal coordination sites on its surface can increase the strength of H₂ adsorption, resulting in an improved performance at 298 K. This was first demonstrated in Mn₃[(Mn₄Cl)₃(BTT)₈]₂, prepared by Long and co-workers,⁴⁴ which contains open Mn²⁺ coordination sites, as shown in Figure 1.18. This framework exhibits a volumetric storage capacity of 60 g L⁻¹ at 90 bar and 77 K, despite having a BET surface area of just 2100 m² g⁻¹. Most notably, however, at 90 bar and 298 K, a capacity of 12.1 g L⁻¹ was observed. This is 77% greater than the density of the compressed H₂ gas, under these conditions.



1,3,5-Tris(2H-tetrazol-5-yl)benzene (H₃BTT)

Figure 1.18. Formation of Mn₃[(Mn₄Cl)₃(BTT)₈]₂, having open Mn²⁺ coordination sites

One of the challenges in the field of supramolecular chemistry is the design and synthesis of chemical structures with exceptionally high surface area. In this regard, MOF-177 $\{Zn_4O(1,3,5\text{-benzenetribenzoate})_2\}$, is a representative example for metal-organic framework with a large surface area,⁴⁵ estimated at $4,500\text{m}^2\text{g}^{-1}$. Block shaped crystals of MOF-177 were produced by heating a mixture of H_3BTB and $Zn(NO_3)_2 \cdot 6H_2O$ in *N,N*-diethylformamide (DEF) to 100°C . The crystals were formulated by elemental analysis as $Zn_4O(BTB)_2 \cdot (DEF)_{15} \cdot (H_2O)_3$. On heating this sample, solvent guest molecules leave between $50\text{-}100^\circ\text{C}$, yielding a remarkable three dimensional open framework of composition $Zn_4O(BTB)_2$, as shown in Figure 1.19.

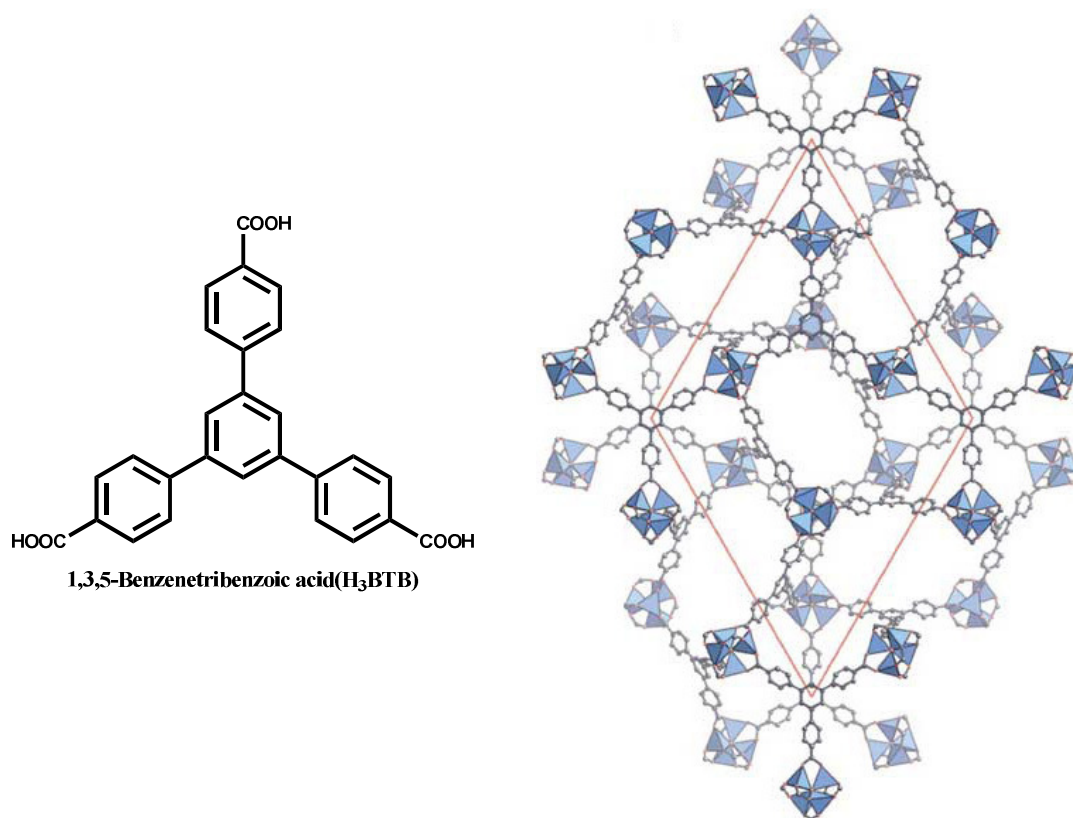


Figure 1.19. Metal organic framework formed between 1,3,5-benzenetribenzoic acid and zinc having high surface area

Hydrogen isotherms up to 90 bar at 77K for MOF-177 show saturation uptake of H₂ between 70 and 80 bar, giving H₂ uptake of 7.5 wt%. Although gravimetric capacity is often a major target for research in H₂ storage materials, there are practical limitations associated with the tank volume required to house the sorbent which makes volumetric capacity just as critical a parameter to consider. So conversion of the gravimetric data to the volumetric data units(g H₂/L), using the crystal density of MOF-177 = 0.477gcm⁻³, H₂ uptake of 32g/L is obtained, which is well within the realm of the 2010 DOE target of 45g/L.

1.7.3.2 Application of Metal Organic Framework in Separation of Molecules

Metal organic frameworks can be utilized for the separation of molecules, as shown by Jing Li et al. They prepared open metal framework of general formula [Cu(4,4'-(hexafluoroisopropylidene)bis(benzoate))(4,4'-(hexafluoroisopropylidene)bis(benzoic acid)_{0.5}], having irregular-shaped micro-channels with alternating large cages and small entrances that connect these cages, as shown in Figure 1.20(a). This network exhibits unique adsorption properties as it adsorbs propane and butane rapidly, but does not adsorb pentane or higher normal or branched hydrocarbons. Thus, the microchannels are unique in being able to separate normal C₂, C₃ and *n*-C₄ olefins and alkanes from all branched alkanes and all normal hydrocarbons above C₄ as shown in Figure 1.20(b).

The unusual property is attributed to a narrowing of channel at intervals of 7.3Å, which is just greater than the length of *n*-C₄ (approximately 6.9 Å), and just less

than the length of $n\text{-C}_5$ (approximately 8.1 Å). The diameter of the neck is approximately 3.2 Å. This neck is large enough for the passage of normal alkanes but small enough for branched alkanes.⁴⁶

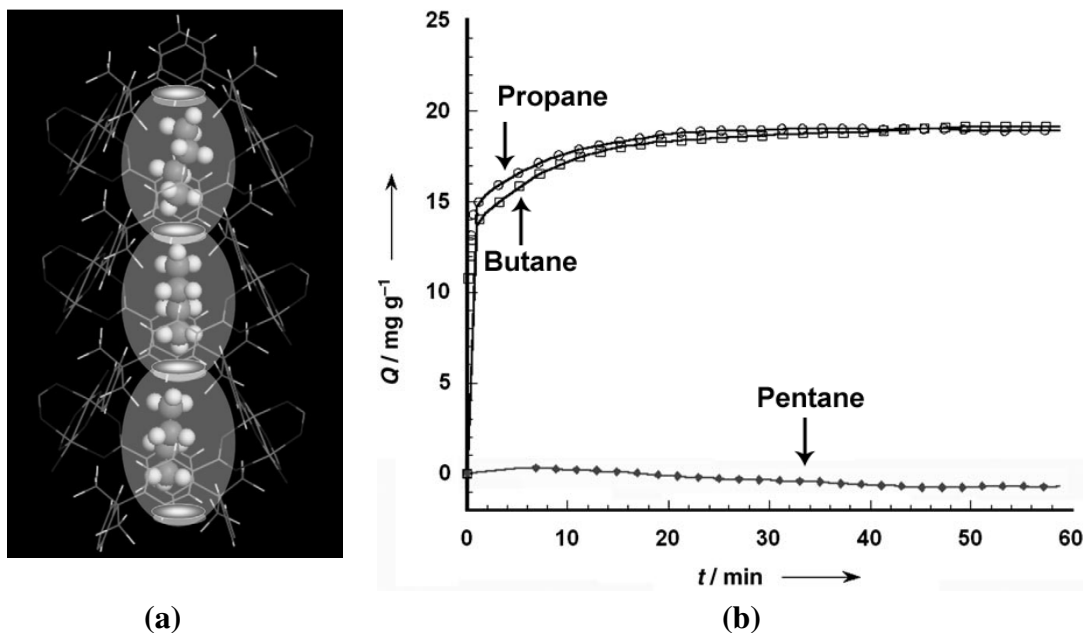


Figure 1.20. (a) Arrangement of butane molecules in the microchannels of the open frame network, with one molecule per cage. (b) Adsorption of propane, butane and pentane at 90°C and 650 torr, as a function of time. Q is the weight of the hydrocarbon molecules adsorbed in the adsorbent

1.7.3.3 Catalytic properties of metal organic frameworks

Metal organic frameworks can catalyze the reactions. In a typical example, Fujita and co-workers showed that a co-ordination network prepared with $\text{Cd}(\text{NO}_3)_2$ and 4,4'-bipyridine, of composition $\{[\text{Cd}(4,4'\text{-bpy})_2(\text{H}_2\text{O})_2](\text{NO}_3)_2 \cdot 4\text{H}_2\text{O}\}_n$, catalyze cyanosilylation of imines under heterogeneous conditions,⁴⁷ as shown in Figures 1.21(a) and (b).

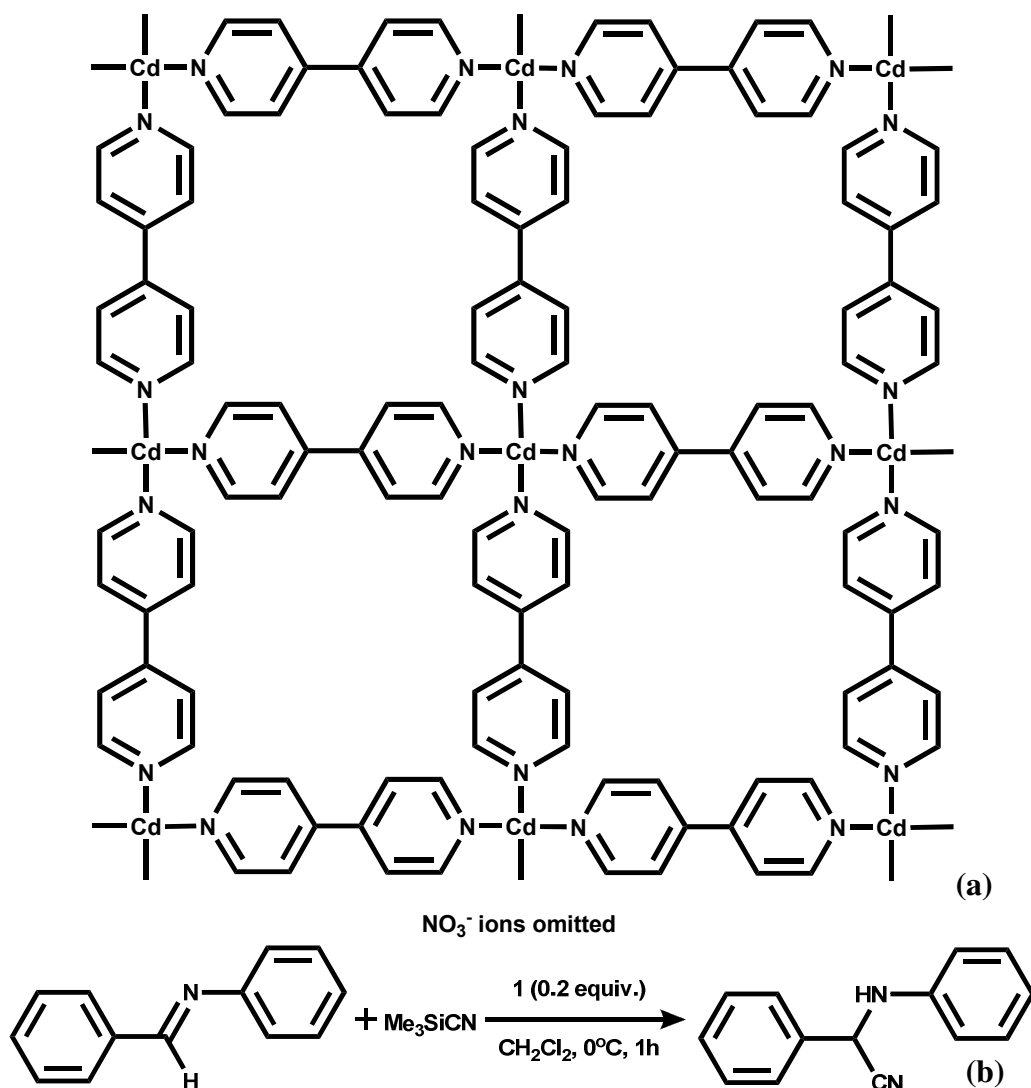


Figure 1.21. (a) Grid network formed by cocrystallizing Cd(NO₃)₂ and 4,4'-bpy of composition $\{[\text{Cd}(4,4'\text{-bpy})_2(\text{H}_2\text{O})_2](\text{NO}_3)_2 \cdot 4\text{H}_2\text{O}\}_n$. (b) catalysed reaction cyanosilylation of imines, under heterogeneous conditions.

Heterogeneous catalytic process is demonstrated by NMR of relatively slow cyanosilylation of CF₃ substituted imine, as shown in Figure 1.22. The solid line in the graph (Figure 1.22 (b) shows progress of the reaction in the presence of catalyst. In a controlled experiment, filtration of this catalyst at any given course of reaction process, retarded the progress of conversion, highlighting the catalytic activity of the

metal-organic framework solid described above, which is represented in dashed and dotted lines, in Figure 1.22 (b).

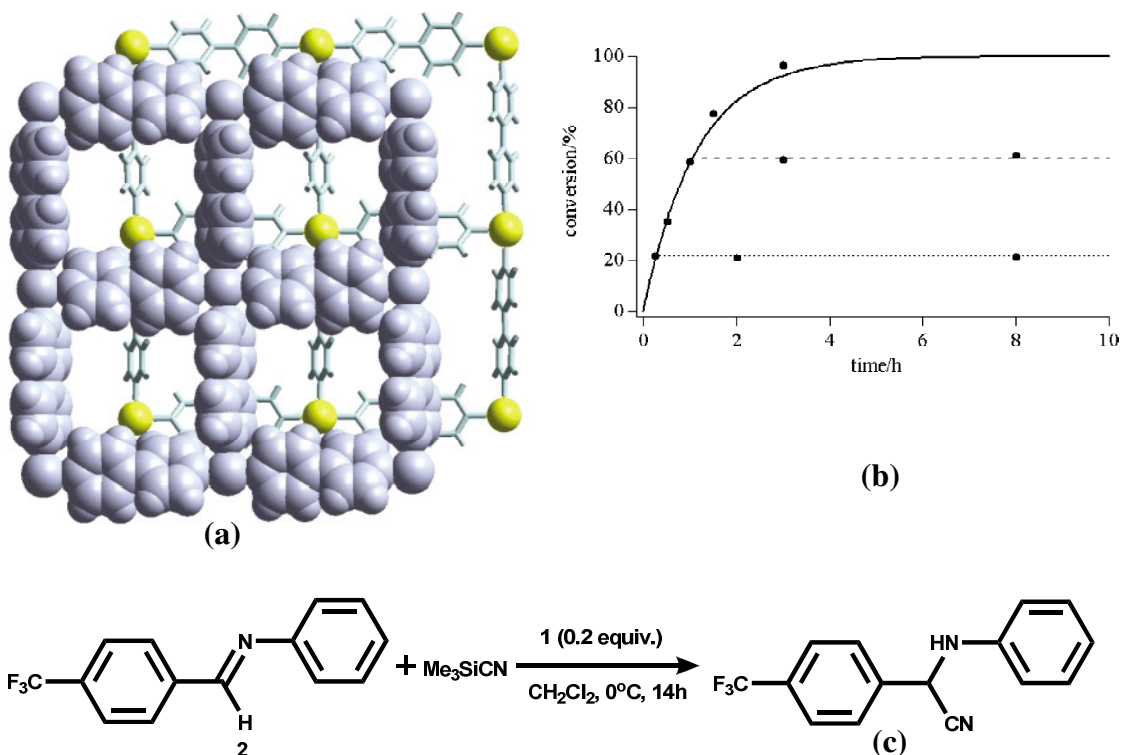


Figure 1.22. (a) Geometrical relationship between the two adjacent layers of **1**. Substrates accommodated in the square cavity of the first layer can interact with Lewis acidic Cd(II) center of the second layer. (b) The conversion of the cyanosilylation of CF₃-substituted imine determined by NMR: dot and dashed lines indicate the conversion after filtration of solid at 0.25 and 1 h, respectively and the reaction is shown in the Figure (c)

1.8 Conclusion

The architectures formed by supramolecular assemblies utilizing non-covalent interactions are not only fascinating, but also have a lot of applications. Non-covalent interactions, molecular recognition and self-assembly are the three keywords that have to be considered for understanding the principles of supramolecular chemistry and

were described briefly in the chapter. Design and synthesis of various supermolecular assemblies utilizing various kind of hydrogen bonding recognition patterns are discussed by taking examples from the literature. In the penultimate section, applications of various supramolecular assemblies in synthesis, pharmaceutical co-crystallization, gas storage, separation and catalysis were discussed. Thus supramolecular chemistry not only give us powerful tool to control the physical properties of materials like their solubility, stability and melting point etc., but also make new functional materials for applications like seperation, catalysis and gas storage etc. Considering the effective utilization of supramolecular assemblies based on this discussion presented in the previous sections, supramolecular assemblies of organic molecules alone, with distinct geometry and tailor-made properties are still not as versatile as metal-organic networks. Keeping this in view and also taken into account the robustness of the assemblies obtained with triazine based systems like melamine, supramolecular synthesis of acid-base complex has been designed to develop robust assemblies with exotic architectures. In this regard, several triazine derivatives and numerous carboxylic acids (aliphatic as well as aromatic) have been employed for the preparation of targeted assemblies. The obtained adducts were analyzed by single crystal X-ray diffraction methods and the exotic structural features for the evaluation in possible applications, are described in the following Chapters.

1.9 References

- (1) (a) Lehn, J. M. *Angew. Chem., Int. Ed.* **1990**, 29, 1304-1319. (b) Whitesides, G. M.; Simanek, E. E.; Mathias, J. P.; Seto, C. T.; Chin, D. N.; Mammen, M.; Gordon, D. M. *Acc. Chem. Res.* **1995**, 28, 37-44. (c) Lehn, J. M. *Supramolecular Chemistry: Concepts and Perspectives*; VCH: Weinheim, 1995. (d) Atwood, J. L.; Davies, J. E. D.; MacNicol, D. D.; Vogtle, F.; Lehn, J.-M. *Comprehensive Supramolecular Chemistry*; Eds.; Pergamon: Oxford, 1996; Vol 6. (e) Wuest, J. D. *Chem. Commun.* **2005**, 5830-5837. (f) Whitesides, G. M.; Mathias, J. P.; Seto, C. T. *Science* **1991**, 254, 1312-1319. (g) MacNicol, D. D.; Toda, F.; Bishop, R. *Comprehensive Supramolecular Chemistry, Solid-State Supramolecular Chemistry: Crystal Engineering*; Eds.; Pergamon: New York, 1996; Vol. 6. (h) Vögtle, F. *Supramolecular Chemistry*, Wiley, Chichester, 1991. (i) Schneider, H.-J.; Dürr, H.; *Frontiers in Supramolecular Organic Chemistry and Photochemistry*, VCH, New York, 1991. (j) Hosseini, M. W. *Acc. Chem. Res.* **2005**, 38, 313-323. (k) Braga, D. *Chem. Commun.* **2003**, 9, 2751-2754. (l) Hollingsworth, M. D. *Science* **2002**, 295, 2410-2413. (m) Moulton, B.; Zaworotko, M. J. *Chem. Rev.* **2001**, 101, 1629-1658. (n) Brammer, L. *Chem. Soc. Rev.* **2004**, 33, 476-487.
- (2) Lehn, J. M. *Pure Appl. Chem.* **1978**, 50, 871-892.
- (3) Lehn, J. M. *Chemistry* **1987**, 444-491.
- (4) Fyfe, M. C. T.; Stoddart, J. F. *Acc. Chem. Res.* **1997**, 30, 393-401.
- (5) (a) Pfeiffer, R. "Organische Molekülverbindungen", Stuttgart, 1927. (b) Wolf, K.L.; Frahm, F. Harms, H. *Phys. Chem. Abt.* **1937**, B36, 17. (b) Wolf, K. L.; Wolff, R. *Angew. Chem., Int. Ed.* **1949**, 61, 191-201.

- (6) (a) Kalsani, V.; Schmittel, M. *Functional, Discrete, Nanoscale Supramolecular Assemblies*; Springer-Verlag Berlin Heidelberg, 2005. (b) Dance, I. *New J. Chem.* **2003**, 27, 1-2.
- (7) Albrecht, M. *Naturwissenschaften* **2007**, 94, 951-966.
- (8) (a) Dunitz, J. D.; Gavezzotti, A. *Angew. Chem., Int. Ed.* **2005**, 44, 1766-1787. (b) Lehn, J. M. *Angew. Chem., Int. Ed.* **1988**, 27, 89-112. (c) Tullio, A. D.; Reale, S.; Angelis, F. D. *J. Mass Spectrom.* **2005**, 40, 845- 865. (d) Fan, E.; Vicent, C.; Geib, S. J.; Hamilton, A. D. *Chem. Mater.* **1994**, 6, 1113-1117. (e) Crowley, J. D.; Bosnich, B. *Eur. J. Inorg. Chem.* **2005**, 2015-2025. (f) Hunter, C. A. *Angew. Chem. Int. Ed.* **2004**, 43, 5310-5324.
- (9) (a) Fischer, E. *Ber. Dtsch. Chem. Ges.* **1894**, 27, 2985. (b) Eschenmoser, A. *Angew. Chem., Int. Ed.* **1994**, 33, 2363. (c) Lichtenthaler, F. W. *Angew. Chem., Int. Ed.* **1994**, 33, 2364-2374. (d) Koshland, D. E. *Angew. Chem., Int. Ed.* **1994**, 33, 2375-2378.
- (10) (a) Heinz, T.; Rudkevich, D.M.; Rebek, J. *Nature*, **1998**, 394, 764-766. (b) Nassimbeni, L. R. *Acc. Chem. Res.* **2003**, 36, 631-637. (c) Ramamurthy, V.; Eaton, D. F. *Chem. Mater.* **1994**, 6, 1128-1136. (d) Cram, D. J.; Tanner, M. E.; Keipert, S. J.; Knobler, C. B. *J. Am. Chem. Soc.* **1991**, 113, 8909-8916. (e) Rebek, J. *J. Org. Chem.* **2004**, 69, 2651-2660.
- (11) (a) Tecilla, P.; Dixon, R. P.; Slobodkin, G.; Alavi, D. S.; Waldeck, D. H.; Hamilton, A. D. *J. Am. Chem. Soc.* **1990**, 112, 9408-9410. (b) Berkovitch-Yellin, Z.; Leiserowitz, L. *J. Am. Chem. Soc.* **1982**, 104, 4052-4064. (c) Gilli, P.; Pretto, L.; Bertolasi, V.; Gilli, G. *Acc. Chem. Res.* **2009**, 42, 33-44. (d) Howard, J. A. K.;

- Hoy, V. J.; O'Hagan, D.; Smith, G. T. *Tetrahedron* **1996**, *52*, 12613-12622. (e)
Feyereisen, M. W.; Feller, D.; Dixon, D. A. *J. Phy. Chem.* **1996**, *100*, 2993-
2997.(f) Coombes, D. S.; Price, S. L.; Willock, D. J.; Leslie, M. *J. Phy. Chem.*
1996, *100*, 7352-7360. (g) Desiraju, G. R. *Chem. Commun.* **1997**, 1475-1482. (h)
Steiner, T. *Chem. Commun.* **1998**, 411-412.(i) Isaacs, E. D.; Shukla, A.; Platzman,
P. M.; Hamann, D. R.; Barbiellini, B.; Tulk, C. A. *Phys. Rev. Lett.* **1999**, *82*, 600-
603. (j) Hobza, P.; Havlas, Z. *Chem. Rev.* **2000**, *100*, 4253-4264. (k) Desiraju, G.
R. *Acc. Chem. Res.* **1996**, *29*, 441-449. (l) Buckingham, A. D.; Del Bene, J. E.;
McDowell, S. A. C. *Chem. Phys. Lett.* **2008**, *463*, 1-10.
- (12) Prins, L. J.; Reinhoudt, D. N.; Timmerman, P. *Angew. Chem. , Int. Ed.* **2001**, *40*,
2382-2426.
- (13) (a) Taylor, R.; Kennard, O. *J. Am. Chem. Soc.* **1982**, *104*, 5063-5070. (b)
Desiraju, G. R.; Murty, B. N. *Chem. Phys. Lett.* **1987**, *139*, 360-361. (c) Nishio,
M.; Hirota, M. *Tetrahedron* **1989**, *45*, 7201-7245. (d) Nishio, M.; Umezawa, Y.;
Hirota, M.; Takeuchi, Y. *Tetrahedron* **1995**, *51*, 8665-8701. (e) Alkorta, I.;
Maluendes, S. *J. Phy. Chem.* **1995**, *99*, 6457-6460. (f) Wahl, M. C.;
Sundaralingam, M. *TRENDS BIOCHEM. SCI.* **1997**, *22*, 97-102. (g) Malone, J. F.;
Murray, C. M.; Charlton, M. H.; Docherty, R.; Lavery, A. J. *J. Chem. Soc.*
,Faraday Trans. **1997**, *93*, 3429-3436. (h) Braga, D.; Grepioni, F.; Tedesco, E.
Organometallics **1998**, *17*, 2669-2672. (i) Thalladi, V. R.; Weiss, H. C.; Bläser,
D.; Boese, R.; Nangia, A.; Desiraju, G. R. *J. Am. Chem. Soc.* **1998**, *120*, 8702-
8710. (j) Steiner, T. *Chem. Commun.* **1998**, 411-412. (k) Aakeröy, C. B.; Evans, T.
A.; Seddon, K. R.; Pálinkó, I. *New J. Chem.* **1999** , *23*, 145-152. (l) Gu, Y.; Kar,

- T.; Scheiner, S. *J. Am. Chem. Soc.* **1999**, *121*, 9411-9422. (m) Gatti, C.; May, E.; Destro, R.; Cargnoni, F. *J. Phys. Chem. A* **2002**, *106*, 2707-2720.
- (14) (a) G. A. Jeffrey and W. Saenger, *Hydrogen Bonding in Biology and Chemistry* (Springer-Verlag, Berlin, 1991).² (b) G. A. Jeffrey, *An Introduction to Hydrogen Bonding* (Oxford University Press, New York, 1997).
- (15) Bhogala, B. R.; Basavoju, S.; Nangia, A. *CrystEngComm* **2005**, *7*, 551-562.
- (16) (a) Etter, M. C. *Acc. Chem. Res.* **1990**, *23*, 120-126. (b) Etter, M. C.; MacDonald, J. C.; Bernstein, J. *Acta Crystogr.* **1990**, *B46*, 256-262. (c) Bernstein, J.; Etter, M. C.; MacDonald, J. C. *J. Chem. Soc., Perkin Trans.* **1990**, 695-698. (d) Bernstein, J.; Davis, R. E.; Shimoni, L.; Chang, N. L. *Angew. Chem., Int. Ed.* **1995**, *34*, 1555-1573.
- (17) (a) Bent, H. A. *Chem. Rev.* **1968**, *68*, 587-648. (b) Lommerse, J. P. M.; Stone, A. J.; Taylor, R.; Allen, F. H. *J. Am. Chem. Soc.* **1996**, *118*, 3108-3116. (c) Dunitz, J. D.; Taylor, R. *Chem. Eur. J.* **1997**, *3*, 89-98. (d) Sarma, J. A. R. P.; Allen, F. H.; Hoy, V. J.; Howard, J. A. K.; Thaimattam, R.; Biradha, K.; Desiraju, G. R. *Chem. Commun.* **1997**, 101-102. (e) Ranganathan, A.; Pedireddi, V. R. *Tetrahedron Lett.* **1998**, *39*, 1803-1806. (f) Masciocchi, N.; Bergamo, M.; Sironi, A. *Chem. Commun.* **1998**, 1347-1348. (g) Thaimattam, R.; Sharma, C. V. K.; Clearfield, A.; Desiraju, G. R. *Cryst. Growth Des.* **2001**, *1*, 103-106. (h) Walsh, R. B.; Padgett, C. W.; Metrangolo, P.; Resnati, G.; Hanks, T. W.; Pennington, W. T. *Cryst. Growth Des.* **2001**, *1*, 165-175. (i) Metrangolo, P.; Resnati, G. *Chem. Eur. J.* **2001**, *7*, 2511-2519. (j) Domercq, B.; Devic, T.; Fourmigué, M.; uban-Senzier, P.; Canadell, E. *J. Mater. Chem.* **2001**, *11*, 1570-1575. (k) Messina, M. T.;

- Metrangolo, P.; Panzeri, W.; Pilati, T.; Resnati, G. *Tetrahedron* **2001**, *57*, 8543-8550. (l) Bond, A. D.; Griffiths, J.; Rawson, J. M.; Hulliger, J. *Chem. Commun.* **2001**, 2488-2489. (m) Lindeman, S. V.; Hecht, J.; Kochi, J. K. *J. Am. Chem. Soc.* **2003**, *125*, 11597-11606. (n) Forni, A.; Metrangolo, P.; Pilati, T.; Resnati, G. *Cryst. Growth Des.* **2004**, *4*, 291-295. (o) Nguyen, H. L.; Horton, P. N.; Hursthouse, M. B.; Legon, A. C.; Bruce, D. W. *J. Am. Chem. Soc.* **2004**, *126*, 16-17. (p) Caronna, T.; Liantonio, R.; Logothetis, T. A.; Metrangolo, P.; Pilati, T.; Resnati, G. *J. Am. Chem. Soc.* **2004**, *126*, 4500-4501. (q) Metrangolo, P.; Neukirch, H.; Pilati, T.; Resnati, G. *Acc. Chem. Res.* **2005**, *38*, 386-395. (r) Metrangolo, P.; Pilati, T.; Resnati, G. *CrystEngComm* **2006**, *8*, 946-947. (s) Awwadi, F. F.; Willett, R. D.; Peterson, K. A.; Twamley, B. *Chemistry* **2006**, *12*, 8952-8960. (t) Imakubo, T.; Kibune, M.; Yoshino, H.; Shirahata, T.; Yoza, K. *J. Mater. Chem.* **2006**, *16*, 4110-4116. (u) Sun, A.; Lauher, J. W.; Goroff, N. S. *Science* **2006**, *312*, 1030-1034. (v) Liantonio, R.; Metrangolo, P.; Meyer, F.; Pilati, T.; Navarrini, W.; Resnati, G. *Chem. Commun.* **2006**, 1819-1821. (w) Metrangolo, P.; Meyer, F.; Pilati, T.; Proserpio, D. M.; Resnati, G. *Chem. Eur. J.* **2007**, *13*, 5765-5772. (x) Metrangolo, P.; Resnati, G.; Pilati, T.; Liantonio, R.; Meyer, F. *J. Polym. Sci., Part A* **2007**, *45*, 1-15. (y) Metrangolo, P.; Meyer, F.; Pilati, T.; Resnati, G.; Terraneo, G. *Angew. Chem., Int. Ed.* **2008**, *47*, 6114-6127.
- (18) (a) Guthrie, F.; *J. Chem. Soc.* **1863**, *16*, 239-244. (b) Seamon, H. W.; Mallet, J. W. *Chem. News.* **1881**, *44*, 188-189.

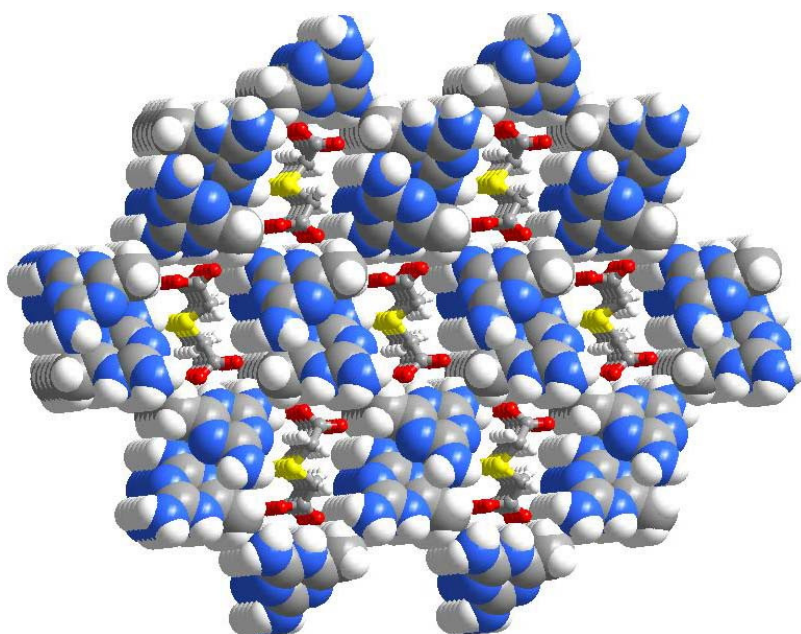
- (19) (a) Benesi, H. A.; Hildebrand, J. H. *J. Am. Chem. Soc.* **1949**, *71*, 2703-2707 (b) Tamres, M.; Yarwood, J.; in *Spectroscopy and Structure of Molecular Complexes* (Ed.: J. Yarwood), Plenum, New York, 1973, pp. 217-301.
- (20) Hassel, O. *Science*, **1970**, *170*, 497-502.
- (21) Corradi, E.; Meille, S. V.; Messina, M. T.; Metrangolo, P.; Resnati, G. *Angew. Chem., Int. Ed.* **2000**, *39*, 1782-1786.
- (22) (a) Philp, D.; Fraser Stoddart, J. *Angew. Chem., Int. Ed.* **1996**, *35*, 1154-1196. (b) Klug, A. *Angew. Chem., Int. Ed.* **1983**, *22*, 565-582.
- (23) Desiraju, G. R. *Angew. Chem., Int. Ed.* **1995**, *34*, 2311-2327.
- (24) Steiner, T. *Angew. Chem., Int. Ed.* **2002**, *41*, 48-76.
- (25) Duchamp, D. J.; Marsh, R. E. *Acta Crystogr.* **B25**, 5-19.
- (26) Kolotuchin, S. V.; Fenlon, E. E.; Wilson, S. R.; Loweth, C. J.; Zimmerman, S. C. *Angew. Chem., Int. Ed.* **1996**, *34*, 2654-2657.
- (27) Ma, B. Q.; Coppens, P. *Chem. Commun.* **2003**, *9*, 2290-2291.
- (28) Ranganathan, A.; Pedireddi, V. R.; Rao, C. N. R. *J. Am. Chem. Soc.* **1999**, *121*, 1752-1753.
- (29) Han, J.; Yau, C. W.; Lam, C. K.; Mak, T. C. W. *J. Am. Chem. Soc.* **2008**, *130*, 10315-10326.
- (30) Schmid, G. M. J. *Pure Appl. Chem.* **1971**, *27*, 647-678.
- (31) (a) Papaefstathiou, G. S.; MacGillivray, L. R. *Org. Lett.* **2001**, *3*, 3835-3837. (b) Papaefstathiou, G. S.; Kipp, A. J.; MacGillivray, L. R. *Chem. Commun.* **2001**, 2462-2463. (c) Varshney, D. B.; Papaefstathiou, G. S.; MacGillivray, L. R. *Chem. Commun.* **2002**, *8*, 1964-1965. (d) Papaefstathiou, G. S.; MacGillivray, L. R.

- Angew. Chem., Int. Ed.* **2002**, *41*, 2070-2073. (e) Friščić, T.; MacGillivray, L. R. *Chem. Commun.* **2003**, *9*, 1306-1307. (f) Papaefstathiou, G. S.; MacGillivray, L. R. *Coord. Chem. Rev.* **2003**, *246*, 169-184. (g) MacGillivray, L. R. *CrystEngComm* **2004**, *6*, 77-78. (h) Friščić, T.; Drab, D. M.; MacGillivray, L. R. *Org. Lett.* **2004**, *6*, 4647-4650. (i) Friščić, T.; MacGillivray, L. R. *Supramol. Chem.* **2005**, *17*, 47-51. (j) Chu, Q.; Swenson, D. C.; MacGillivray, L. R. *Angew. Chem., Int. Ed.* **2005**, *44*, 3569-3572. (k) Friščić, T.; MacGillivray, L. R. *Chem. Commun.* **2005**, 5748-5750. (l) Varshney, D. B.; Gao, X.; Friščić, T.; MacGillivray, L. R. *Angew. Chem., Int. Ed.* **2006**, *45*, 646-650. (m) Friščić, T.; MacGillivray, L. R. *Mol. Cryst. Liq. Cryst.* **2006**, *456*, 155-162. (n) Bucar, D. K.; Papaefstathiou, G. S.; Hamilton, T. D.; Chu, Q. L.; Georgiev, I. G.; MacGillivray, L. R. *Eur. J. Inorg. Chem.* **2007**, 4559-4568. (o) MacGillivray, L. R.; Papaefstathiou, G. S.; Friščić, T.; Hamilton, T. D.; Bucar, D. K.; Chu, Q.; Varshney, D. B.; Georgiev, I. G. *Acc. Chem. Res.* **2008**, *41*, 280-291. (p) Lauher, J. W.; Fowler, F. W.; Goroff, N. S. *Acc. Chem. Res.* **2008**, *41*, 1215-1229. (q) MacGillivray, L. R. *J. Org. Chem.* **2008**, *73*, 3311-3317.
- (32) MacGillivray, L. R.; Reid, J. L.; Ripmeester, J. A. *J. Am. Chem. Soc.* **2000**, *122*, 7817-7818.
- (33) Gao, X.; Friščić, T.; MacGillivray, L. R. *Angew. Chem., Int. Ed.* **2004**, *43*, 232-236.
- (34) Mei, X.; Liu, S.; Wolf, C. *Org. Lett.* **2007**, *9*, 2729-2732.
- (35) Shan, N.; Jones, W. *Tetrahedron Lett.* **2003**, *44*, 3687-3689.

- (36) (a) Caira, M. R.; Nassimbeni, L. R.; Wildervanck, A. F. *J. Chem. Soc., Perkin Trans.* **1995**, 2213-2216. (b) Stanton, M. K.; Bak, A. *Cryst. Growth Des.* **2008**, *8*, 3856-3862. (c) Hörter, D.; Dressman, J. B. *Adv. Drug. Deliv. Rev.* **1997**, *25*, 3-14. (d) Hancock, B. C.; Parks, M. *Pharm. Res.* **2000**, *17*, 397-404. (e) Bettinetti, G.; Caira, M. R.; Callegari, A.; Merli, M.; Sorrenti, M.; Tadini, C. *J. Pharm. Sci.* **2000**, *89*, 478-489. (f) Fleischman, S. G.; Kuduva, S. S.; McMahon, J. A.; Moulton, B.; Bailey Walsh, R. D.; Rodríguez-Hornedo, N.; Zaworotko, M. J. *Cryst. Growth Des.* **2003**, *3*, 909-919. (g) Almarsson, ö.; Hickey, M. B.; Peterson, M. L.; Morissette, S. L.; Soukasene, S.; McNulty, C.; Tawa, M.; MacPhee, J. M.; Remenar, J. F. *Cryst. Growth Des.* **2003**, *3*, 927-933. (h) Remenar, J. F.; MacPhee, J. M.; Larson, B. K.; Tyagi, V. A.; Ho, J. H.; McIlroy, D. A.; Hickey, M. B.; Shaw, P. B.; Almarsson, ö. *Org. Process Res. Dev.* **2003**, *7*, 990-996. (i) Roy, S.; Alexander, K. S.; Riga, A. T.; Chatterjee, K. *J. Pharm. Sci.* **2003**, *92*, 747-759. (j) Almarsson, Ö.; Zaworotko, M. J. *Chem. Commun.* **2004**, *10*, 1889-1896. (k) Morissette, S. L.; Almarsson, Ö.; Peterson, M. L.; Remenar, J. F.; Read, M. J.; Lemmo, A. V.; Ellis, S.; Cima, M. J.; Gardner, C. R. *Adv. Drug. Deliv. Rev.* **2004**, *56*, 275-300. (l) Vishweshwar, P.; McMahon, J. A.; Peterson, M. L.; Hickey, M. B.; Shattock, T. R.; Zaworotko, M. J. *Chem. Commun.* **2005**, 4601-4603. (m) Bis, J. A.; McLaughlin, O. L.; Vishweshwar, P.; Zaworotko, M. J. *Cryst. Growth Des.* **2006**, *6*, 2648-2650. (n) McNamara, D. P.; Childs, S. L.; Giordano, J.; Iarriccio, A.; Cassidy, J.; Shet, M. S.; Mannion, R.; O'Donnell, E.; Park, A. *Pharm. Res.* **2006**, *23*, 1888-1897. (o) Govindarajan, R.; Zinchuk, A.; Hancock, B.; Shalaev, E.; Suryanarayanan, R. *Pharm. Res.* **2006**, *23*, 2454-2468. (p) Friščić, T.; Trask, A.

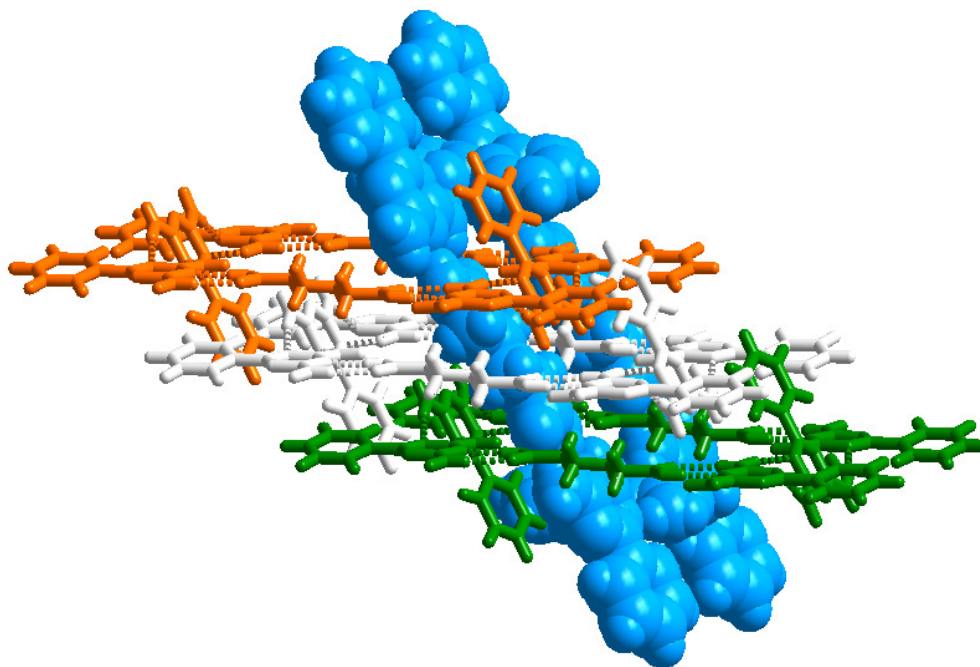
- V.; Jones, W.; Motherwell, W. D. S. *Angew. Chem., Int. Ed.* **2006**, *45*, 7546-7550.
- (q) Vishweshwar, P.; McMahon, J. A.; Bis, J. A.; Zaworotko, M. J. *J. Pharm. Sci.* **2006**, *95*, 499-516. (r) Patel, U.; Haridas, M.; Singh, T. P. *Acta crystallogr.*, **1988** *C44*, 1264-1267. (s) Oswald, I. D. H.; Allan, D. R.; MaGregor, P. A.; Motherwell, W. D.; Parsons, S.; Pulham, C. R. *Acta Crystalgr.*, **2002**, *B58*, 1057-1066. (t) Berge, S. M.; Bighley, L. D.; Monkhouse, D. C. *J. Pharma. Sci.* **1977**, *66*, 1-19. (u) Fleischman, S. G.; Kuduva, S. S.; McMahon, J. A.; Moulton, B.; Bailey Walsh, R. D.; Rodríguez-Hornedo, N.; Zaworotko, M. J. *Cryst. Growth Des.* **2003**, *3*, 909-919. (v) Bhatt, P. M.; Azim, Y.; Thakur, T. S.; Desiraju, G. R. *Cryst. Growth Des.* **2009**, *9*, 951-957. (w) Trask, A. V.; Van De Streek, J.; Motherwell, W. D. S.; Jones, W. *Cryst. Growth Des.* **2005**, *5*, 2233-2241. (x) Haynes, D. A.; Jones, W.; Motherwell, W. D. S. *J. Pharm. Sci.* **2005**, *94*, 2111-2120.
- (37) Bailey Walsh, R. D.; Bradner, M. W.; Fleischman, S.; Morales, L. A.; Moulton, B.; Rodríguez-Hornedo, N.; Zaworotko, M. J. *Chem. Commun.* **2003**, *9*, 186-187.
- (38) Trask, A. V.; Samuel Motherwell, W. D.; Jones, W. *Cryst. Growth Des.* **2005**, *5*, 1013-1021.
- (39) Remenar, J. F.; Morissette, S. L.; Peterson, M. L.; Moulton, B.; MacPhee, J. M.; Guzmán, H. R.; Almarsson, ö. *J. Am. Chem. Soc.* **2003**, *125*, 8456-8457.
- (40) (a) Eddaoudi, M.; Moler, D. B.; Li, H.; Chen, B.; Reineke, T. M.; O'Keeffe, M.; Yaghi, O. M. *Acc. Chem. Res.* **2001**, *34*, 319-330. (b) Yaghi, O. M.; O'Keeffe, M.; Ockwig, N. W.; Chae, H. K.; Eddaoudi, M.; Kim, J. *Nature* **2003**, *423*, 705-714. (c) Fujita, M.; Tominaga, M.; Hori, A.; Therrien, B. *Acc. Chem. Res.* **2005**, *38*, 369-378.

- (41) (a) Rowsell, J. L. C.; Millward, A. R.; Park, K. S.; Yaghi, O. M. *J. Am. Chem. Soc.* **2004**, *126*, 5666-5667. (b) Ward, M. D. *Science* **2003**, *300*, 1104-1105. (c) Schlapbach, L.; Züttel, A. *Nature* **2001**, *414*, 353-358. (d) Chen, B.; Ockwig, N. W.; Millward, A. R.; Contreras, D. S.; Yaghi, O. M. *Angew. Chem., Int. Ed.* **2005**, *44*, 4745-4749. (e) Sudik, A. C.; Millward, A. R.; Ockwig, N. W.; Côté, A. P.; Kim, J.; Yaghi, O. M. *J. Am. Chem. Soc.* **2005**, *127*, 7110-7118. (f) Rowsell, J. L. C.; Yaghi, O. M. *Angew. Chem., Int. Ed.* **2005**, *44*, 4670-4679. (g) Wong-Foy, A. G.; Matzger, A. J.; Yaghi, O. M. *J. Am. Chem. Soc.* **2006**, *128*, 3494-3495.
- (42) Li, H.; Eddaoudi, M.; O'Keeffe, M.; Yaghi, O. M. *Nature* **1999**, *402*, 276-279.
- (43) (a) Rosi, N. L.; Eckert, J.; Eddaoudi, M.; Vodak, D. T.; Kim, J.; O'Keeffe, M.; Yaghi, O. M. *Science* **2003**, *300*, 1127-1129. (b) Rowsell, J. L. C.; Spencer, E. C.; Eckert, J.; Howard, J. A. K.; Yaghi, O. M. *Science* **2005**, *309*, 1350-1354. (c) Rowsell, J. L. C.; Eckert, J.; Yaghi, O. M. *J. Am. Chem. Soc.* **2005**, *127*, 14904-14910. (d) Kaye, S. S.; Dailly, A.; Yaghi, O. M.; Long, J. R. *J. Am. Chem. Soc.* **2007**, *129*, 14176-14177.
- (44) Dincă, M.; Dailly, A.; Liu, Y.; Brown, C. M.; Neumann, D. A.; Long, J. R. *J. Am. Chem. Soc.* **2006**, *128*, 16876-16883.
- (45) Chae, H. K.; Siberio-Pérez, D. Y.; Kim, J.; Go, Y.; Eddaoudi, M.; Matzger, A. J.; O'Keeffe, M.; Yaghi, O. M. *Nature* **2004**, *427*, 523-527.
- (46) Pan, L.; Olson, D. H.; Ciemnomolonski, L. R.; Heady, R.; Li, J. *Angew. Chem., Int. Ed.* **2006**, *45*, 616-619.
- (47) Ohmori, O.; Fujita, M. *Chem. Commun.* **2004**, *10*, 1586-1587.



CHAPTER TWO

MOLECULAR RECOGNITION STUDIES OF 2,4-DIAMINO-6-METHYL-1,3,5-TRIAZINE AND 2,4-DIAMINO-6-PHENYL-1,3,5-TRIAZINE WITH VARIOUS ALIPHATIC DICARBOXYLIC ACIDS



2.1 Introduction

Triazines, like cyanuric acid¹ (1,3,5-triazine-2,4,6-triol), trithiocyanuric acid (1,3,5-triazine-2,4,6-trithiol)², melamine³, and their derivatives, are well studied, due to their ability to form multiple hydrogen bonds, which is well explored in the formation of structures with different types of architectures, varying from linear to crinkled tapes, rosette to host-guest complexes, etc. The proposed infinite, two dimensional rosette network (Figure 2.1a), formed by the complexation of melamine with cyanuric acid, whose crystal structure was revealed by Pedireddi and co-workers⁴, is perhaps the most robust organic supramolecular entity known till date, and also stands as a representative example towards target-oriented supramolecular synthesis. In this complex, the rosette is formed by the aggregation of each of three molecules of melamine and cyanuric acid by 18-hydrogen bonds, as shown in Figure 2.1. This multipoint recognition between the molecules containing complementary functional groups is expected to increase the robustness of the network, thus formed.

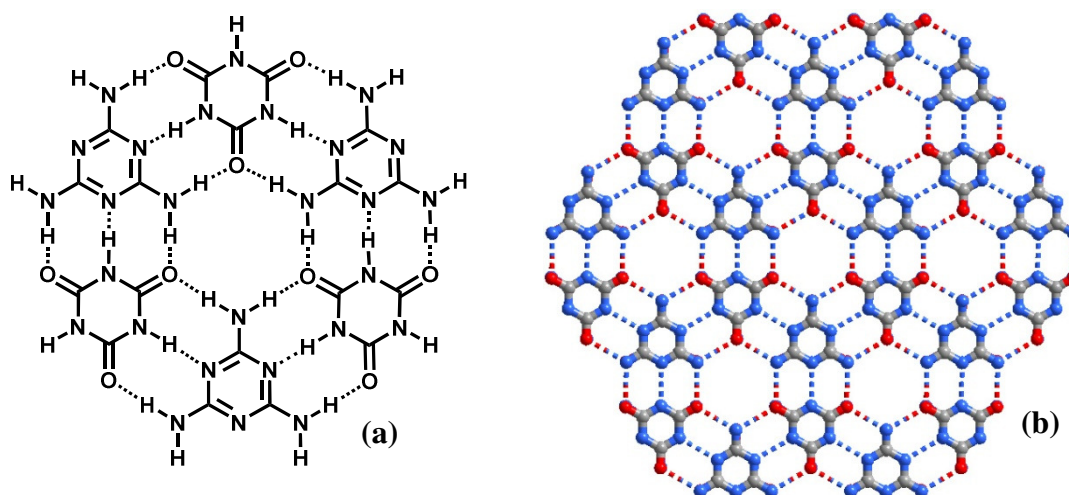


Figure 2.1. (a) Schematic diagram of rosette network observed between melamine and cyanuric acid (b) Arrangement observed in the crystal structure.

In fact many such rosette networks are well documented in the literature⁵. For example, Mascali and co-workers demonstrated the utilization of hydrogen bonding interactions between guanine (G) and cytosine (C) by appropriate functionalization of heterocyclic compound to yield rosette network⁶, by self assembly, as shown in Figure 2.2. Such organization, brought about by non-covalent forces, which are in general difficult to form a covalent perspective, due to the demand of complicated synthetic approaches, as well as economically non-viability.

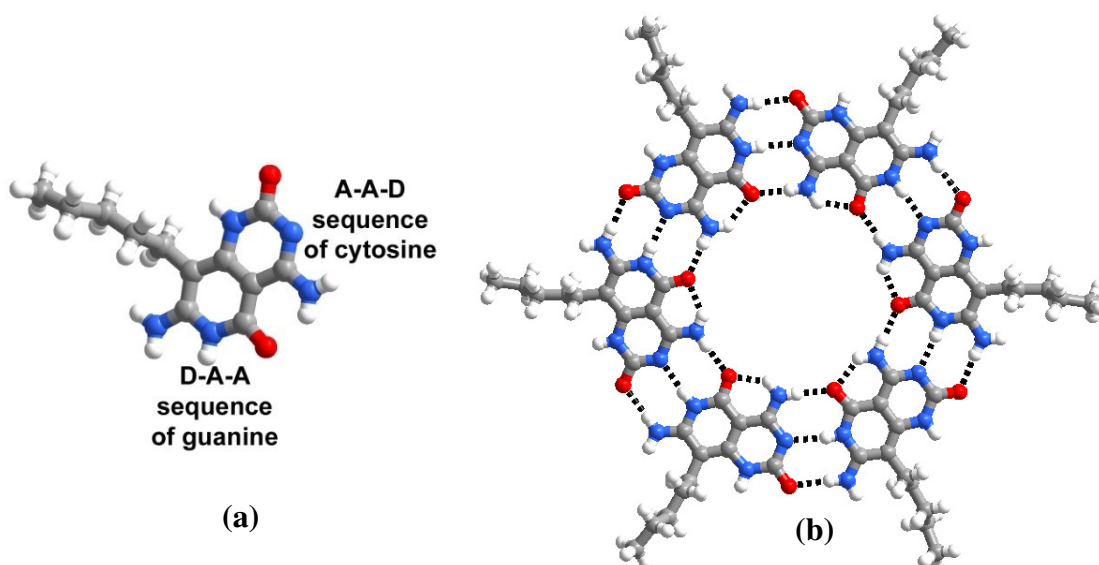


Figure 2.2. (a) Heterocyclic compound having A-A-D sequence of cytosine on one side and D-A-A sequence of guanine on another side (b) Self assembly of molecules leading to the formation of rosette network

In general, formation of different kinds of networks in the solid state structures as mentioned above is attributed to efficient crystal packing, steric hindrance etc. For example, in a typical example of a tape structure, formed between *N,N'*-diphenylmelamine and 5,5-diethylbarbituric acid, the molecules recognize each other by triple hydrogen bond⁷ (Figure 2.3). In this tape, a pair of *N,N'*-diphenylmelamine

and 5,5-diethylbarbituric acid constitute a translational repeat unit. It can be observed that though linear tape is having disadvantage of more steric strain, but it still prevailed due to advantage of close packing, with less void space.

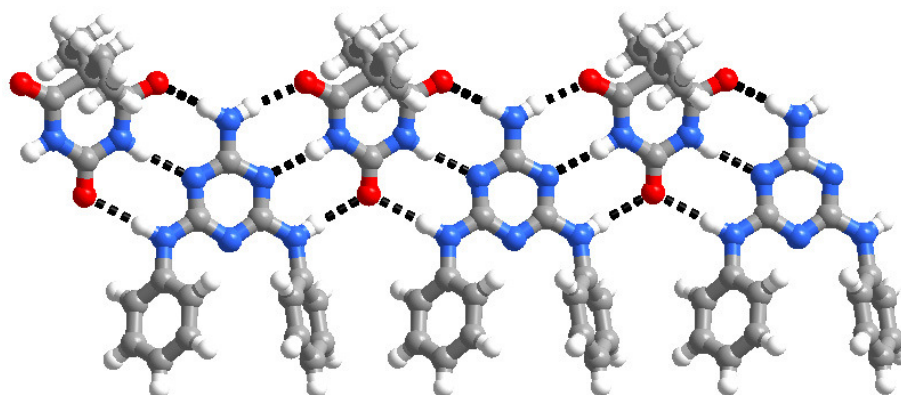


Figure 2.3. Molecular tapes formed between *N,N'*-diphenylmelamine and 5,5-diethylbarbituric acid

However, co-crystallizing *N,N'*-di(*t*-butyl)melamine, with 5,5-diethylbarbituric acid, a crinkled tape is observed⁸, as shown in Figure 2.4.

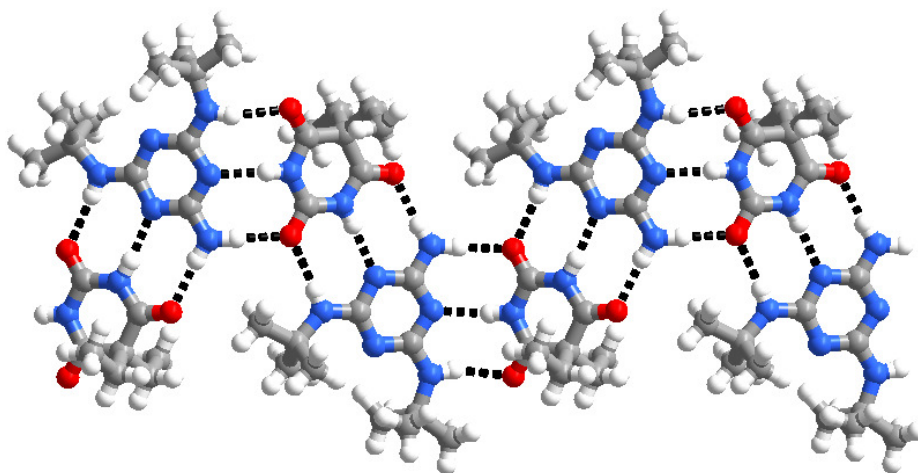


Figure 2.4. Crinkled tape observed between *N,N'*-di(*t*-butyl)melamine and 5,5-diethylbarbituric acid.

This is probably to circumvent the steric hindrance between the *t*-butyl groups on adjacent molecules of *N,N'*-di(*t*-butyl)melamine, which would have arise, if it

forms a linear tape structure, as shown in Figure 2.5. Though in this case, the crinkled tape is having the advantage of lesser steric hindrance, but packing efficiency is less as compared to the linear tape structure shown in Figure 2.3.

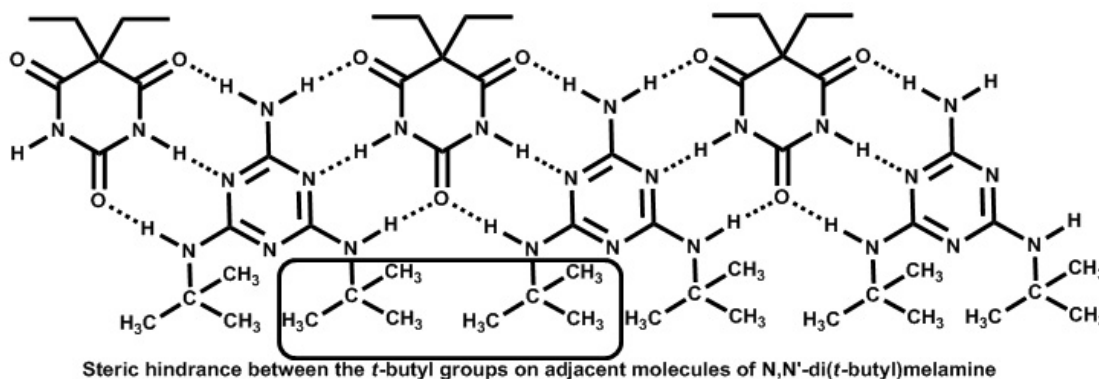


Figure 2.5. Steric hindrance expected in the hypothetical tape.

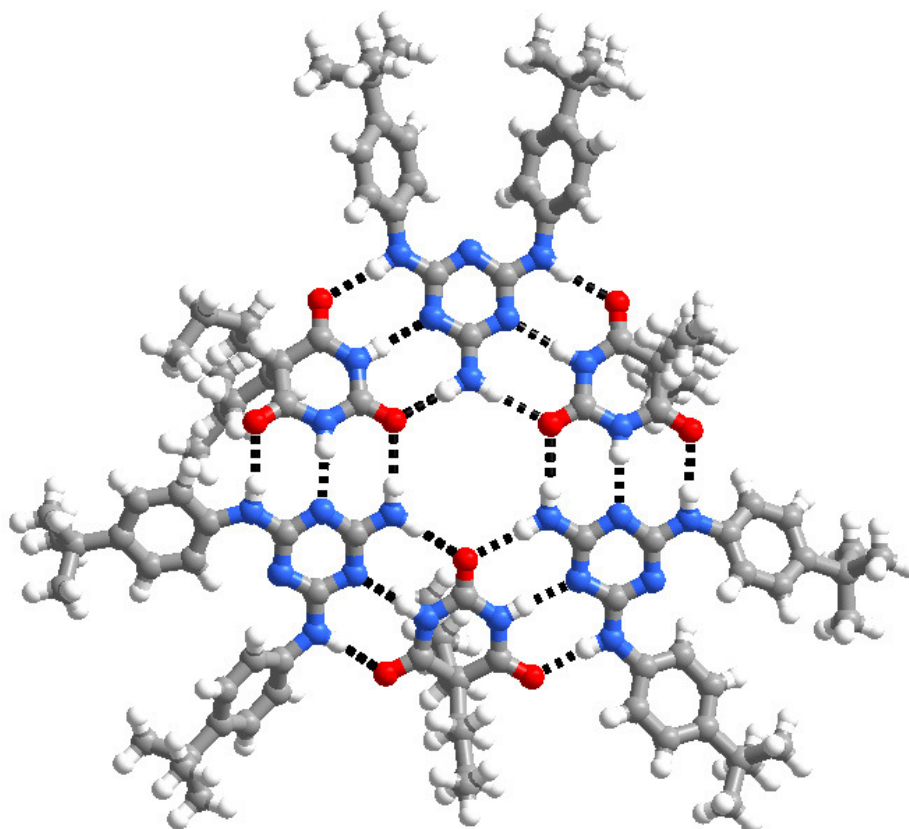


Figure 2.6. Rosette network observed between *N,N'*-bis(4-*t*-butylphenyl)melamine and 5,5-di-*n*-butylbarbituric acid.

On co-crystallizing *N,N'*-bis(4-*t*-butylphenyl)melamine and 5,5-di-*n*-butylbarbituric acid, having bulky groups on both the co-crystallizing ligands, rosette network with least steric hindrance was realized⁹, as shown in Figure 2.6.

Apart from the above discussed self-assembled structures in the form of exotic architectures, another important manifestation of self assembly is formation of host-guest type assemblies. Numerous examples are known in the literature, especially employing symmetrically substituted molecules in the design and synthesis of host-guest assemblies. Among those, representative examples with robust network features are the molecular complexes as formed by trithiocyanuric acid, as reported by Pedireddi and co-workers.

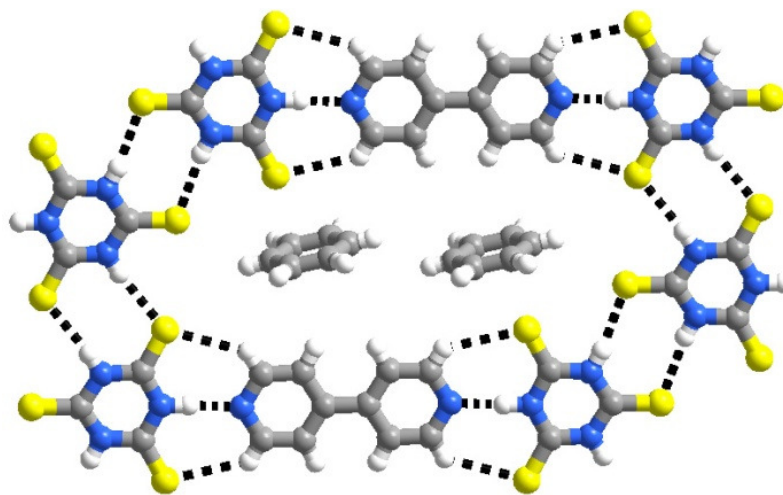


Figure 2.7. Interaction between thiocyanuric acid and 4,4'-bipyridine leading to the formation of host arrangement with benzene molecules as guest entities.

Co-crystallization of trithiocyanuric acid and 4,4'-bipyridine in the presence of benzene gave a complex with trithiocyanuric acid glued to spacer molecules, 4,4'-bipyridine by N-H \cdots N, N-H \cdots S and C-H \cdots S hydrogen bonds form host network, with cavities of dimension 10 Å², which are filled by the solvent molecules of

crystallization, benzene¹⁰, as shown in Figure 2.7. The elegance of this assembly is its robustness even after the removal of the guest species by heating. It was shown that the apohost could be filled with different solvent molecules of variable dimensions, for example *o*-, *m*-, *p*-xylene, anthracene, etc.

In general, molecular recognition studies mediated by intermolecular interactions, it was observed that, prior to recognition, proton exchange takes place, especially, in acid-base mediated assemblies, which was not of serious concern in the early concepts of supramolecular synthesis.

However, in recent times, the importance of pharmaceutical co-crystallization in the development of novel formulations in which the state of the molecular complexes, as salt or neutral is very important phenomenon, a considerable effort have been devoted to establish the conditions for the formation of co-crystals in salt form. According to Johnson and Rumon proton transfer will occur from acid to base if the difference in pK_a between the conjugate acid of the base and the carboxylic acid is > 3.75 , which was further illustrated through specific examples, mediated by carboxylic acid...pyridine (O-H...N hydrogen bonds) assemblies by Nangia and co-workers¹¹. However, it should be noted that pK_a values determined from solution may not provide any information about the strength of a hydrogen bond, mainly because, hydrogen bonding is the sharing of hydrogen atom between two electronegative atoms, whereas pK_a defines the ability of the proton to be transferred from an acid to base.

Further, Aakeroy and co-workers showed that pK_a of the constituents play an important role in the design of supramolecular assemblies¹² with more than two

components and used this concept for the formation of tri-component systems. It has been shown that such systems could be prepared based on the analogy that the best hydrogen bond donor (strongest acids) form hydrogen bonds with the best hydrogen bond acceptor (strongest bases) and the second best hydrogen bond donor form hydrogen bonds with the second best hydrogen bond acceptor, as shown in the Figure 2.8.

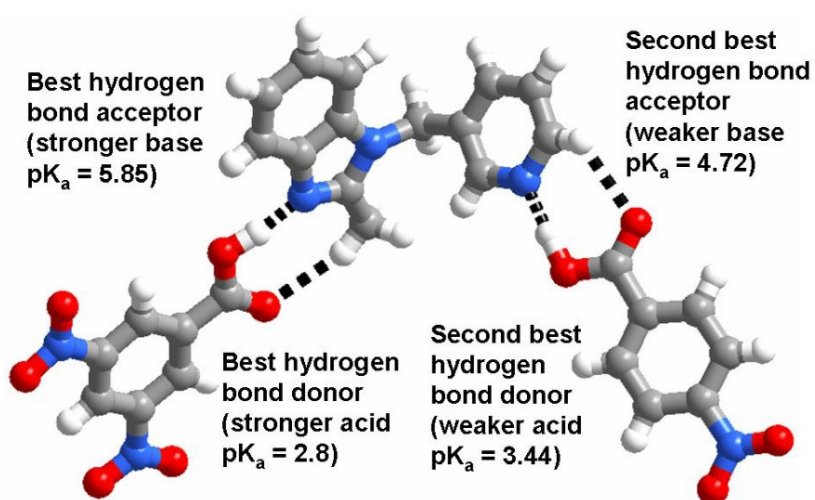


Figure 2.8. Interaction between the best hydrogen bond donor and acceptor as well as the second best hydrogen bond donor and acceptor leading to the formation of tricomponent system.

Nevertheless, the effective significance of pK_a in the supramolecular synthesis has not been well explored, as very limited number of reports are only known in the literature. Further, it is also known that the other physical properties of the co-crystallizing ligands also play a very crucial role in the formation of a specific supramolecular assembly.

Thus, to explore further the combined (mutual) effect of physical properties like geometry, shape, dimensions and pK_a etc. of the co-crystallizing ligands in the

formation of supramolecular assemblies, co-crystallization of some of the melamine derivatives like 2,4-diamino-6-methyl-1,3,5-triazine (**1**) and 2,4-diamino-6-phenyl-1,3,5-triazine (**2**) with various aliphatic dicarboxylic acids, having different shapes, dimensions and pK_a values, has been carried out. The salient features of the co-crystals, thus, obtained are compiled in this chapter.

2.2 Rational Analysis of Molecular Adducts of 2,4-Diamino-6-methyl-1,3,5-triazine with Various Aliphatic Dicarboxylic Acids: pK_a Directed Host-Guest Assemblies

Molecular adducts of 2,4-diamino-6-methyl-1,3,5-triazine, **1**, have been prepared with various aliphatic dicarboxylic acids, which differ by methylene or analogous groups. The molecular complexes, **1a** - **1i**, thus, formed by cocrystallizing **1**, with oxalic; **a**, malonic; **b**, succinic; **c**, fumaric; **d**, acetylene dicarboxylic; **e**, glutaric; **f**, thiodiglycolic; **g**, diglycolic; **h** and adipic acids; **i**, respectively, in a 1:1 ratio, from a methanol solvent, as shown in Chart 1, have been found to be yielding two types of host-guest assemblies with voids/channels in three-dimensional arrangement. The different types of host-guest assemblies¹³ appear to be the resultant of the differences in the acidity of the dicarboxylic acids. It has been observed that acids with $pK_a < 3.0$ yield host network consisting of both **1** and the corresponding acid and the solvent of crystallization or water molecules occupying the void/channel as observed in the adducts **1a**, **1b**, **1e** and **1h**. But, the acids with the $pK_a > 3.0$ occupied the voids created by the host network formed exclusively by the molecules

of **1**, as found in the adducts **1c**, **1d**, **1f**, **1g** and **1i**. Thus, the structural features of 1a-1i are quite intriguing and have been discussed in detail in the following sections.

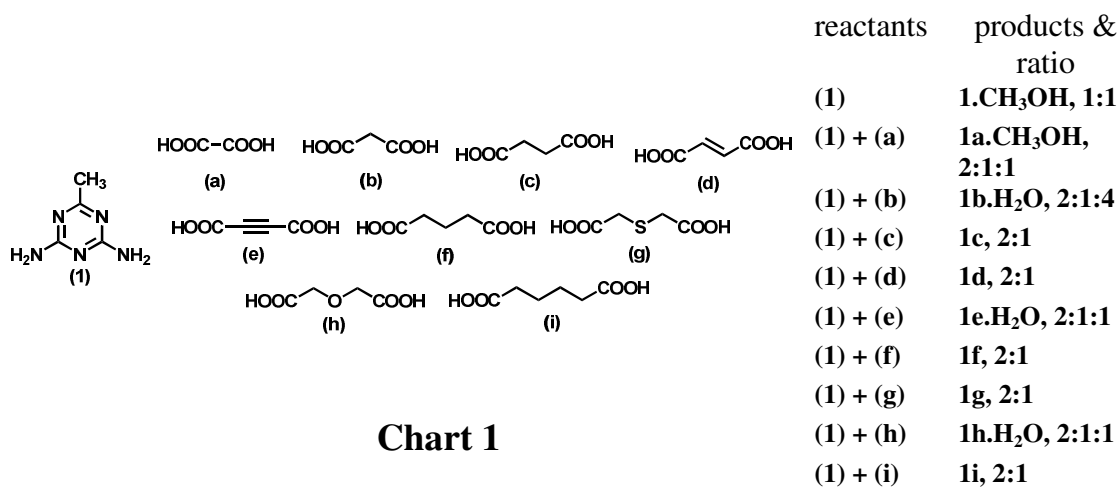


Chart 1

In this process, it was noted that the solid state structure of **1** itself has not been established, hence, structure determination of **1** was also carried out by single crystal X-ray diffraction methods.

2.2.1 Solid state structure of 2,4-diamino-6-methyl-1,3,5-triazine-1

Single crystals of triazine, **1**, were obtained from CH₃OH by slow evaporation process, and structure determination reveals that, **1** crystallizes as methanol solvate, as shown in Figure 2.9(a). Full crystallographic information is given in Table 2.1. Packing of molecules in three-dimensions is quite intriguing with the formation of a host-guest type assembly (Figure 2.9(b)).

In this arrangement, the molecules of **1** self-assemble through N-H···N hydrogen bonds and hydrophobic interactions yielding a host network, with the CH₃OH molecules reside in the channels, thus produced. Around each channel, six molecules of **1** arrange as two triads held together by hydrophobic interactions, while

within each triad the molecules are connected together by two different centrosymmetric N-H \cdots N hydrogen bonded moieties (H \cdots N, 2.12 and 2.16 Å). Complete characteristics of the hydrogen bonds are listed in Tables 2.2. Further, the CH₃OH molecules interact with the host lattice by N-H \cdots O hydrogen bonds (H \cdots O, 2.21 and 2.24 Å, Table 2.2) through -NH₂ groups and O-H \cdots N hydrogen bonds (H \cdots N, 1.97 Å) with pyridyl -N atoms of **1**, as shown in Figure 2.9(c).

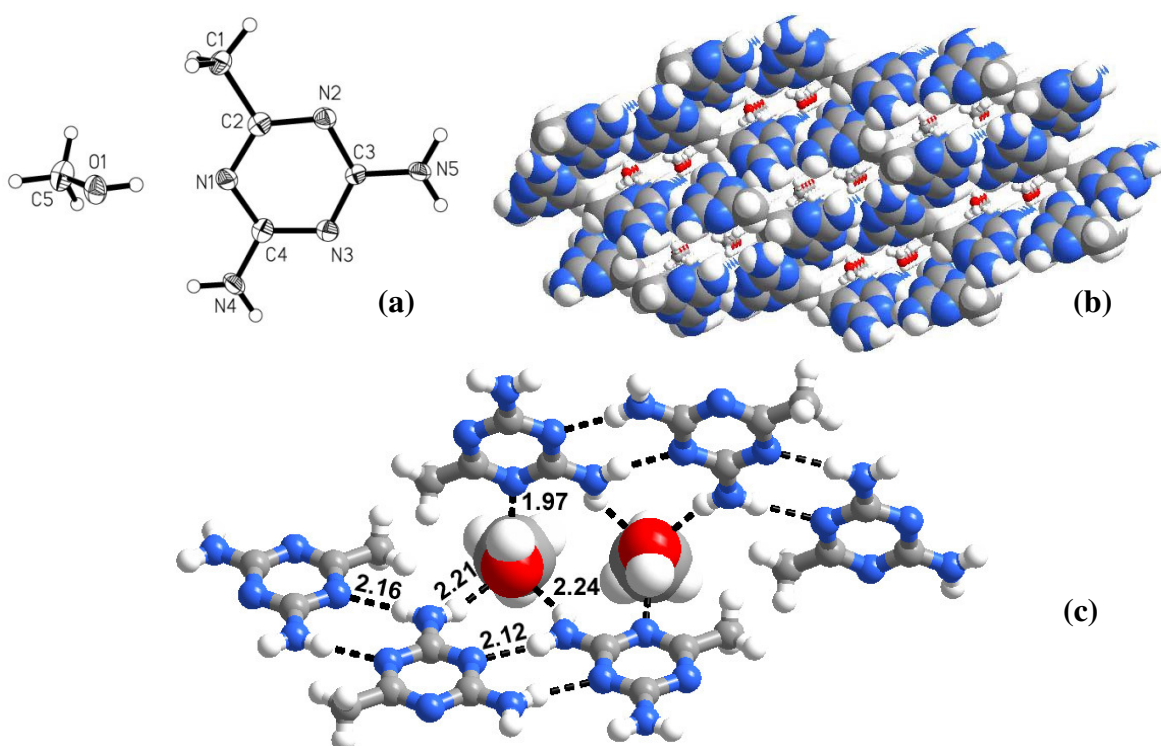


Figure 2.9. (a) ORTEP showing the asymmetric unit contents in the CH₃OH adduct of **1**. (b) Three-dimensional packing arrangement with channels being occupied by CH₃OH molecules. (c) Annotation of interactions between the molecules around a typical channel.

To investigate the stability of the adduct, especially the robustness of the framework formed by **1** in the absence of the guest species, thermal analysis has been carried out. But, it was found that once the CH₃OH molecules are removed, the crystallinity is lost, suggesting the collapse of host-network formed by **1**. However,

guest specific host-lattices are well known in the literature, hence we proceed with co-crystallization experiments of **1** with different acid molecules and the obtained complexes have been analyzed by single crystal X-ray diffraction methods, as described in the following sections.

2.2.2 Molecular adduct between 2,4-diamino-6-methyl-1,3,5-triazine and oxalic acid-1a

Co-crystallization of triazine, **1**, and oxalic acid from CH₃OH, resulted in the formation of a molecular complex, **1a**, in a 2:1 ratio (Table 2.1), along with the solvent of crystallization as shown in Figure 2.10(a). In the three-dimensional packing, the molecules are arranged in the form of stacked sheets as shown in Figure 2.10(b). Arrangement of molecules in a typical sheet is presented in Figure 2.11.

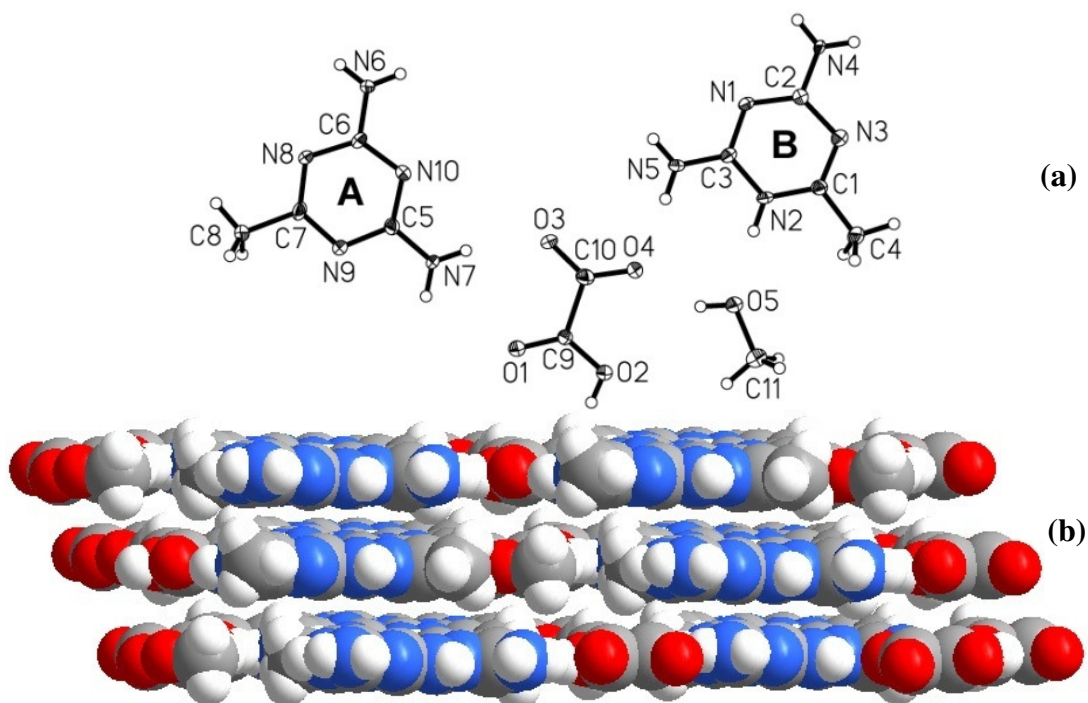


Figure 2.10. (a) ORTEP of the contents of the asymmetric unit in the crystal structure of **1a**. (b) Packing arrangement in the form of stacked sheets.

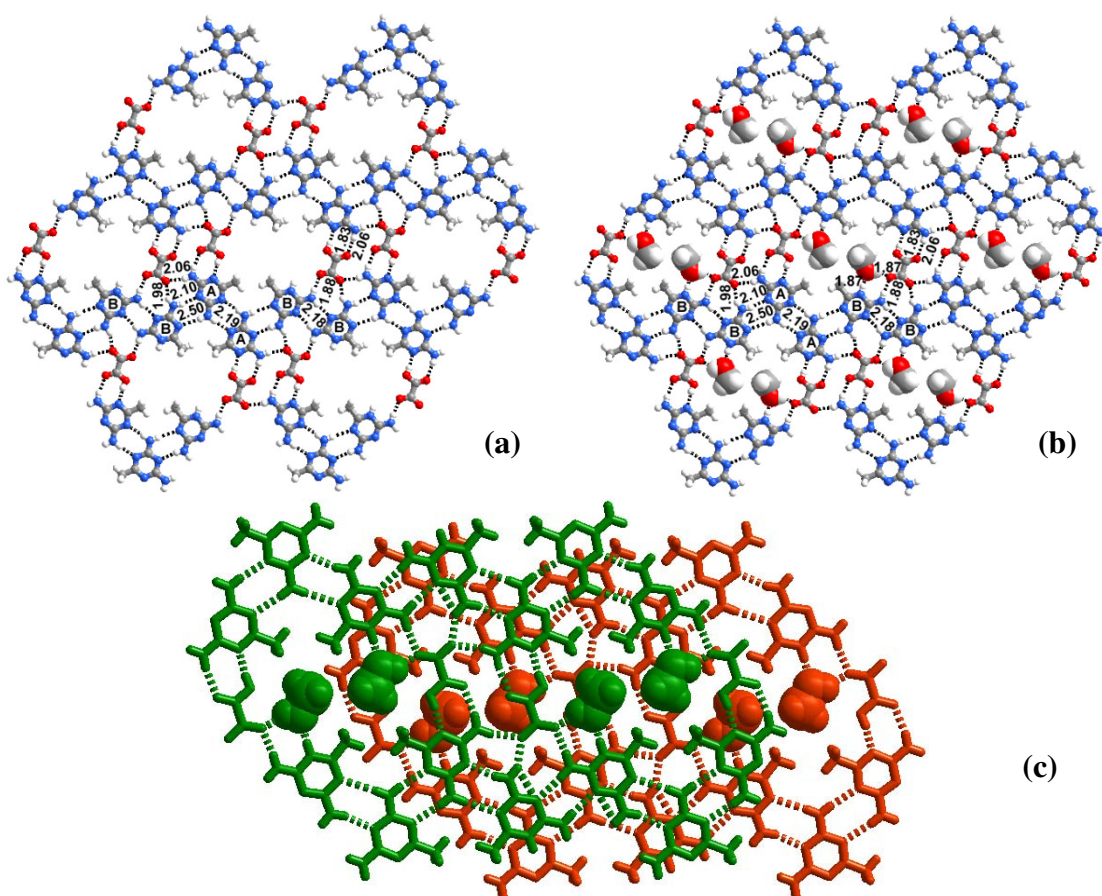


Figure 2.11. (a) Arrangement of molecules in a typical sheet observed in the molecular complex of **1a**, with the cavities being created by the molecules of **1** and oxalic acid. (b) CH₃OH molecules, solvent of crystallization, in the voids observed in the latter drawing. (c) Staggered stacking of adjacent sheets in the crystal structure of **1a**.

In the asymmetric unit of **1a**, the two molecules of **1**, labeled as A and B exist as neutral and charged species respectively. The molecules of A and B interact with the molecules of same kind by the centrosymmetric N-H...N hydrogen bonds by H...N distances of 2.19 and 2.18 Å, respectively, (see Table 2.2) and with each other by the noncentrosymmetric N-H...N hydrogen bonds (H...N distances of 2.10 and 2.50 Å), leading to the formation of a tape, as shown in Figure 2.11(a). The adjacent tapes of triazines are connected together by the molecules of oxalic acid yielding voids (see

Figure 2.11(a)), which are being occupied by solvent of crystallization, CH₃OH (Figure 2.11b). As a result, around each void, six molecules of **1** are arranged as two triads, exactly like in the CH₃OH adduct of **1**, with the only difference being that instead of hydrophobic interactions, in the structure of **1a**, the triads are held together by the oxalic acid molecules. Another important difference between **1** and **1a** is that, in three-dimensional arrangement, the voids did not align in **1a**, unlike in the CH₃OH adduct of **1**, as the adjacent sheets are staggered (see Figure 2.11c). As a consequence of it, channels along a crystallographic axis could not be established in **1a**. Out of the two –COOH groups of oxalic acid, only one is deprotonated. While –COOH form O–H···N (H···N, 1.83 Å) and N–H···O (H···O, 2.06 Å, Table 2.2) pair-wise cyclic hydrogen bonding pattern with the A type molecules of triazine, **1**, the carboxylate group interacts with both A and B type of molecules of **1** by N–H···O[–] hydrogen bonds, by H···O[–] distance 2.06 and 1.88, 1.98 Å (see Table 2.2) respectively.

2.2.3 Molecular adduct between 2,4-diamino-6-methyl-1,3,5-triazine and malonic acid-1b

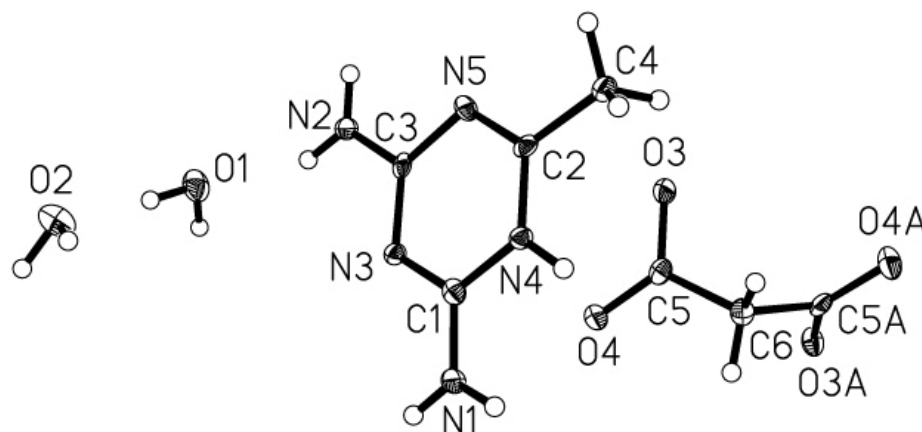


Figure 2.12. ORTEP of asymmetric unit in the crystal structure of **1b**.

Crystals of complex **1b** were obtained from a CH₃OH solution of **1** and malonic acid. The structure determination (Table 2.1) reveals that the asymmetric unit consists of 2:1 ratio of **1** and malonate, respectively, along with water molecules (see Figure 2.12). Comparing **1a** and **1b**, differences in the deprotonation of acids is already apparent with only one of the –COOH being deprotonated in **1a**, while both the –COOH got deprotonated in **1b**, which we discuss in detail in the later sections. In three-dimensional packing, complex **1b** also form a host-guest type assembly with host is being constituted by **1** and malonate molecules, as shown in Figure 2.13, with the channels are being filled by water molecules.

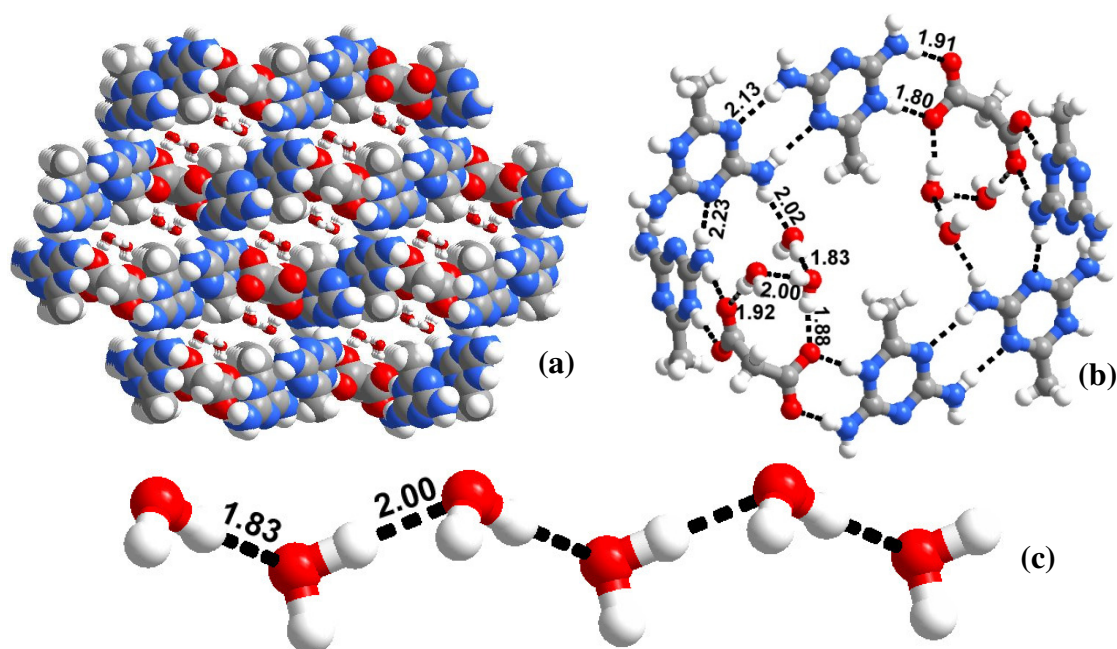


Figure 2.13. (a) Host-guest network observed in complex **1b**, with the channels being filled by water molecules. (b) Recognition pattern between the molecules of **1** and malonate. (c) Interaction between the neighboring water molecules in each channel.

Around each channel, interaction between the molecules of **1** and malonate has a close resemblance to that of **1a**, but differ largely with respect to the interaction

between the molecules of **1**. Although two triads have been noted in **1b** also, as in the CH₃OH adduct of **1** and **1a**, the interaction among the molecules within the triad is quite different. In **1b**, within each triad, molecules of **1** are held together by both dimeric and single N-H \cdots N hydrogen bonds, with the H \cdots N distances of 2.13 and 2.23 Å, respectively (see Table 2.2). Such triads are further held together by malonate molecules through N⁺-H \cdots O⁻ and N-H \cdots O⁻ hydrogen bonds (H \cdots O⁻, 1.80 and 1.91 Å). Water molecules exist in the channels as chains (see Figure 2.13 (c)) formed through O-H \cdots O hydrogen bonds (H \cdots O, 1.83 and 2.00 Å, Table 2.2.), which are in turn connected to the host network through N-H \cdots O (H \cdots O, 2.02 Å) and O-H \cdots O⁻ (H \cdots O⁻, 1.88 and 1.92 Å) hydrogen bonds, with **1** and malonate, respectively, as shown in Figure 2.13(b).

2.2.4 Molecular adduct between 2,4-diamino-6-methyl-1,3,5-triazine and succinic acid-1c

In the structure of complex **1c**, formed between **1** and succinic acid in a 2:1 ratio, no solvent of crystallization or water is present, but succinic acid exists as succinate by deprotonation of both the protons as observed for malonic acid in **1b**. Structure determination parameters obtained from single crystal X-ray diffraction methods are given in Table 2.1. In three-dimensional arrangement, although complex **1c** forms a host-guest type assembly, as shown in Figure 2.14(a), the host is formed entirely by the molecules of **1**, unlike in **1a** and **1b**, and the resultant void space is being occupied by the succinate molecules. Further, detailed analysis of the host network reveals that around each channel, the molecules of **1** exist as dimers, unlike

triads as noted in **1a** and **1b**, with the formation of cyclic N-H \cdots N hydrogen bond dimers with H \cdots N distance of 2.20 Å (see table 2.2), as shown in Figure 2.14(b). These dimers, in turn, interact with succinate molecules by forming N⁺-H \cdots O⁻ and N-H \cdots O⁻ and the corresponding hydrogen bond distances are 1.68 and 1.99 Å, respectively. In addition, a noteworthy feature is the triple-hydrogen bonding pattern between the constituents, consisting of N-H \cdots O⁻ (H \cdots O⁻, 2.05 Å), C-H \cdots N (H \cdots N, 2.64 Å) and N-H \cdots O⁻ (H \cdots O⁻, 2.06 Å) hydrogen bonds (see Figure 2.14(b)).

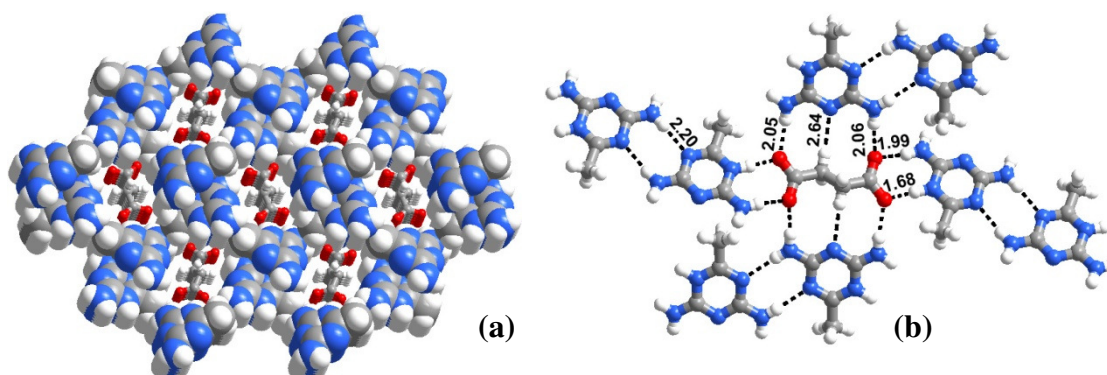


Figure 2.14. (a) Host-guest network observed in complex, **1c**, with the host being formed by the molecules of **1** and succinate molecules occupying the channels, thus created. (b) Arrangement of molecules around each channel with different types of interactions between the molecules of **1** and succinate molecules.

It seems that this type of pattern has evolved due to the complementary distance between the acceptors and donors on **1** and the succinate molecules as the distance, 5.04 Å, between the O atoms at both ends of succinate matches with the distance, 4.63 Å, between the H atoms of -NH₂ groups of **1** involved in the triple hydrogen bond. However, such pattern was not possible in **1a** and **1b** as the corresponding distance between the O atoms in oxalic and malonic acids (2.73/2.65,

3.57 Å, respectively) are not complementary with the distance between the –NH₂ groups on **1**.

Thus, different carbon chain length between the –COOH groups, apparently influencing the nature of the resultant assemblies. To draw further insights into this aspect, complexes of **1** with fumaric acid and acetylenedicarboxylic acid have been prepared, as these two acids having the same number of carbon atoms between the –COOH, as that of succinic acid, expecting formation of isostructural complexes with that of **1c**, and also co-crystallization with glutaric and adipic acids have been carried out as they follow succinic acid in the homologues series, with increased carbon chain length.

2.2.5 Structure of molecular complex of 2,4-diamino-6-methyl-1,3,5-triazine and fumaric acid-1d

Co-crystallization of **1** and fumaric acid in methanol as solvent, a complex, **1d**, in 2:1 ratio is obtained (Table 2.1) and **1d** is isostructural to **1c**, as expected. The packing of molecules in three dimensions is shown in Figure 2.15. The similarity between **1c** and **1d** can be certainly attributed to the similar dimensions of succinic and fumaric acids, even though, the later has different type of hybridization features (sp² in fumaric acid instead sp³ in succinic acid), for the carbons lying in between the –COOH groups. Thus, it highlights the importance of geometrical features of the molecules and position of the complimentary functional groups.

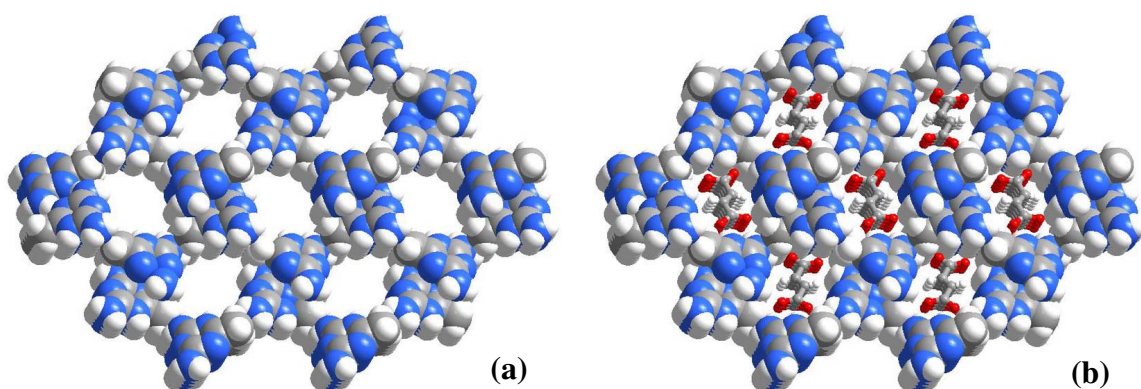


Figure 2.15. a) Host network with channels observed in complex, **1d**. b) Channels filled with fumarate molecules.

In **1d** also, the molecules of **1** exist as dimers with the formation of N-H \cdots N hydrogen bond dimers having H \cdots N distance of 2.24 Å, as found in **1c**. In this case also, both the -COOH groups on the acid molecule are deprotonated and further each acid is surrounded by the four dimers of **1**. These acid molecules, in turn, interact with two dimers of **1** by forming N⁺-H \cdots O⁻ and N-H \cdots O⁻ and the corresponding hydrogen bond distances are 1.78 and 1.99 Å (Table 2.2), respectively. In addition, molecule of dicarboxylic acid forms the triple-hydrogen bonding pattern with two more dimers of **1**, consisting of N-H \cdots O⁻ (H \cdots O⁻, 2.10Å), C-H \cdots N (H \cdots N, 2.68 Å) and N-H \cdots O⁻ (H \cdots O⁻, 2.08 Å) hydrogen bonds (see Figure 2.16), probably due to complementarity of hydrogen bond acceptor sites on the acid, as observed in **1c**, with oxygen atoms at remote ends in fumaric acid are apart by 5.03 Å.

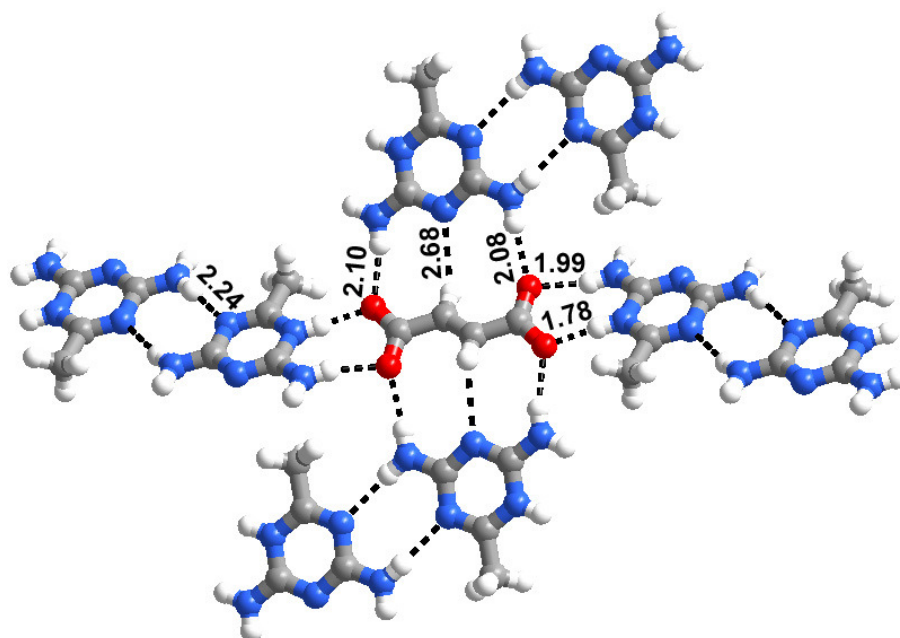


Figure 2.16. Arrangement of molecules around each channel with different types of interactions between the molecules of **1** and fumarate molecules.

2.2.6 Supramolecular structure of complex of 2,4-diamino-6-methyl-1,3,5-triazine and acetylenedicarboxylic acid-**1e**

Co-crystals, **1e**, obtained from a CH₃OH solution of **1** and acetylenedicarboxylic acid has the reactants in a 2:1 ratio in the asymmetric unit (Table 2.1), along with a water molecule, as shown in Figure 2.17(a). In this complex also, carboxylic acid molecules are completely deprotonated as observed in **1b-1d**. Further, complex, **1e**, which is expected to be similar to **1c** and **1d** based on the geometrical considerations of the acid molecules, but adopted a structure similar to **1a**, perhaps, due to the linear geometry of acetylene dicarboxylic acid similar to oxalic acid. Complex **1e**, in three-dimensional arrangement, forms a stacked sheet structure and it is shown in Figure 2.17(b).

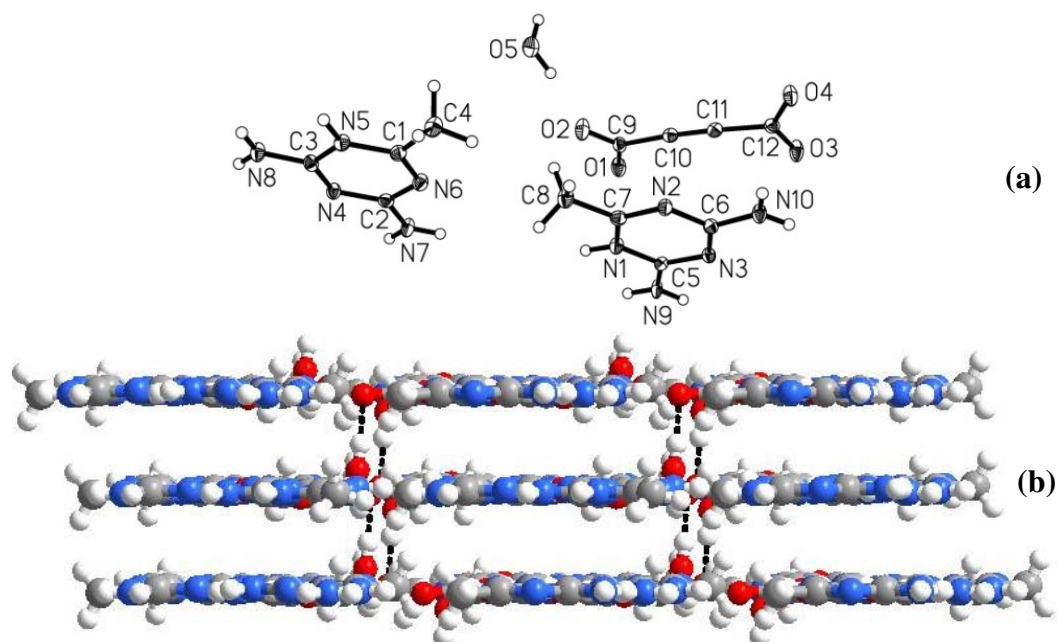


Figure 2.17. (a) Asymmetric unit contents in the crystal structure of complex, **1e**. (b) Stacking of planar sheets in three-dimensional arrangement.

In a typical sheet, the molecules arrange in such a manner that four molecules of **1** and two molecules of acetylenedicarboxylate constitute a six membered host-network, creating cavities, which are being filled by water molecules. Packing analysis, further, reveals the presence of two types of molecules of **1**, labeled as A and B. It has been observed that A type of molecules of **1** interact with the molecules of the same kind by N-H \cdots N hydrogen bond dimers, with H \cdots N distance of 2.17 and 2.18 Å in the form of triads in host network, which extend further to form an infinite tape, as observed in **1a**. However, B type molecules also interact with the molecules of same kind by N-H \cdots N hydrogen bond dimers having H \cdots N distance of 2.17 Å, but constitute only dimers, which do not extend further to form a tape. The molecules of acetylenedicarboxylate interact with the triads formed by the A type molecules of **1**, by

the formation of $\text{N}^+\text{-H}\cdots\text{O}^-$ ($\text{H}\cdots\text{O}^-$, 1.81 Å) and $\text{N-H}\cdots\text{O}^-$ ($\text{H}\cdots\text{O}^-$, 1.99 Å) hydrogen bonds and also with B type molecules of **1**, by $\text{N}^+\text{-H}\cdots\text{O}^-$ ($\text{H}\cdots\text{O}^-$, 1.74 Å) and

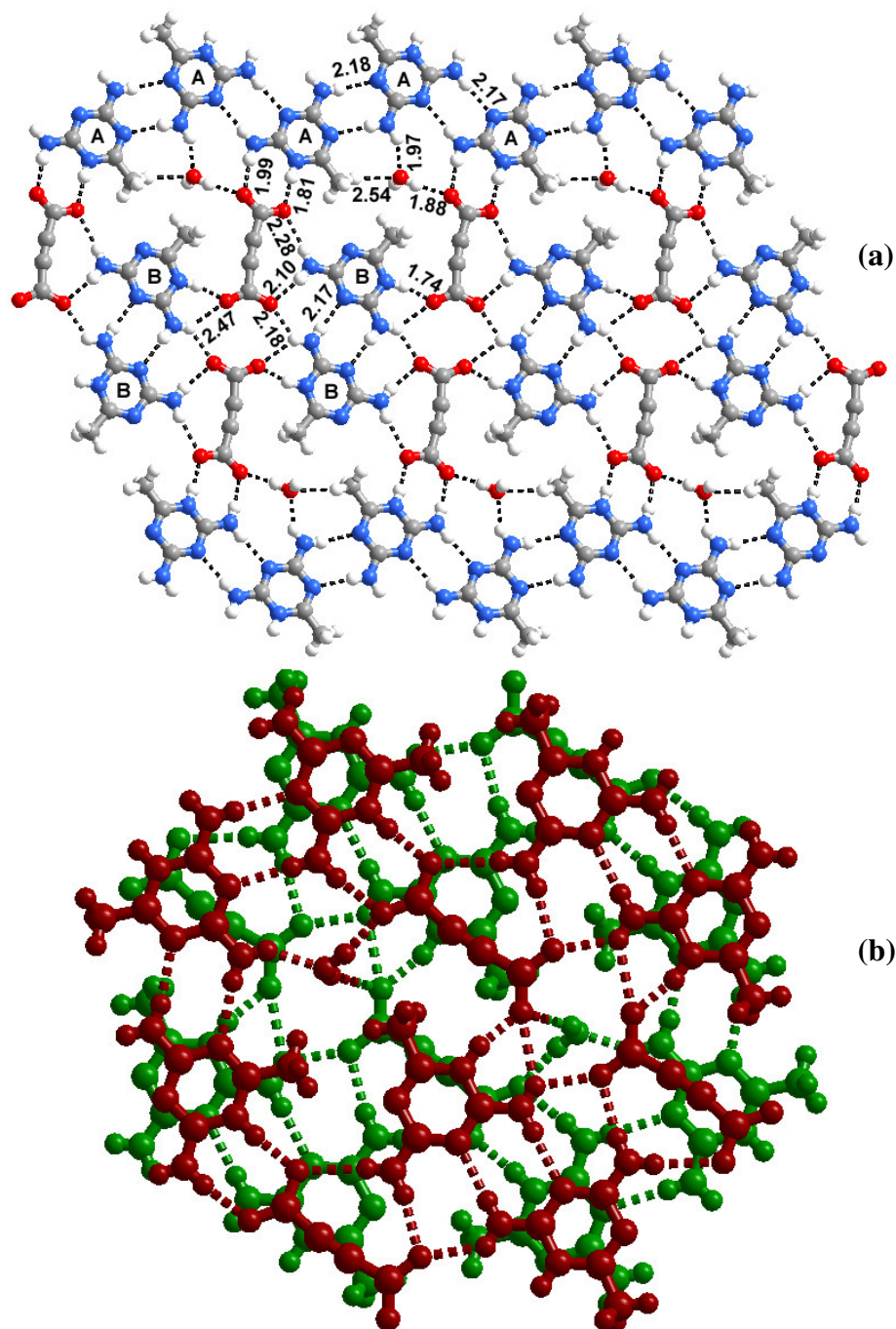


Figure 2.18. (a) Annotation of intermolecular interactions observed within a sheet structure in the complex, **1e**. (b) Overlap of adjacent sheets.

N-H \cdots O $^-$ (H \cdots O $^-$, 2.10, 2.28 Å), to form a six member cyclic host network. The guest molecules (water) interact with the cyclic host by O-H \cdots O $^-$ (H \cdots O $^-$, 1.88 Å), N-H \cdots O (H \cdots O, 1.97 Å) and C-H \cdots O (H \cdots O, 2.54 Å). Such adjacent six membered cyclic host networks interact with each other by the N-H \cdots O $^-$ (H \cdots O $^-$, 2.18 Å) hydrogen bonds and N-H \cdots N hydrogen bond dimers, as shown in Figure 2.18(a). However, around each channel, like in **1a**, the sheets are not aligned along a crystallographic axis; thus, no channels are observed in the three-dimensional arrangement and overlapped adjacent sheets are shown in Figure 2.18(b).

Thus, it appears that geometry of acid molecules also play a critical role in directing the ultimate structure of supramolecular assembly, irrespective of prevalence of complementary distance between the acceptor and donor sites on the co-crystallizing ligands. To evaluate these aspects, further, co-crystallization with other dicarboxylic acids like glutaric and its sulphur and oxygen analogues (thiodiglycolic and diglycolic, respectively) and adipic acid have been carried out. Interestingly, while glutaric, thiodiglycolic and adipic acid form isostructural complexes, similar to **1c** and **1d**, diglycolic gave entirely different structure with very unusual packing, as described below.

2.2.7 Structure of molecular complex of 2,4-diamino-6-methyl-1,3,5-triazine and glutaric acid-1f

Co-crystallization of **1** and glutaric acid from a methanol solution gave a complex, **1f**, in a 2:1 ratio. Single crystal X-ray diffraction analysis reveals that it forms a host-guest type assembly with molecules of **1** yielding a host network, as

shown in Figure 2.19 (a) and also as observed in **1c** and **1d**, while the glutarate occupying the channels, as guest species (see Figure 2.19 (b)).

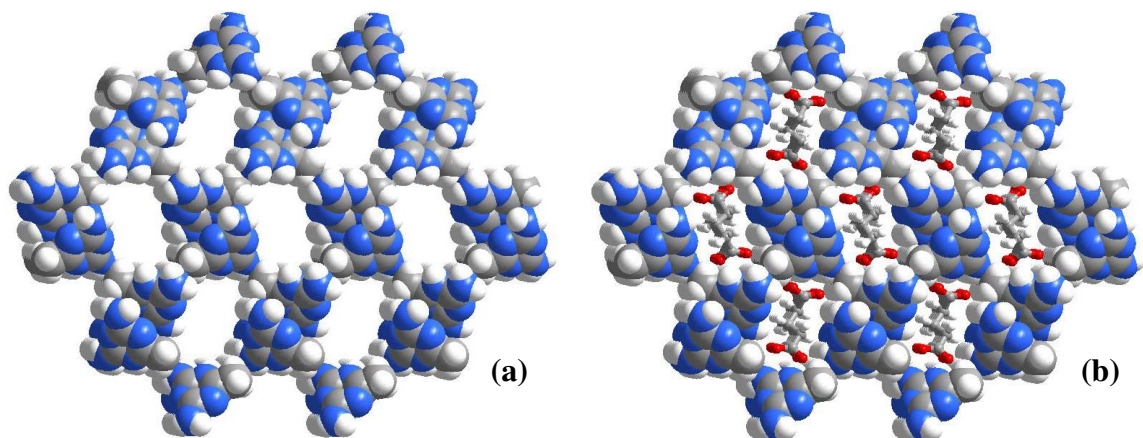


Figure 2.19. (a) Host network observed in **1f**. (b) Glutarate molecules occupying the host network formed, exclusively, by the molecules of **1**.

Further detailed analysis of the host-guest network reveals that in the host network the molecules of **1** exist as N-H \cdots N hydrogen bond dimers, with H \cdots N distance of 2.10 and 2.12 Å. In **1f** also both the carboxylic acid functional groups of acid are deprotonated, as observed in **1c** and **1d**. But in this case, the acid molecules are surrounded by the six dimers of **1**, instead of four as observed in **1c** and **1d**. In particular, it is interesting to note that, in **1f**, acid molecules did not form triple hydrogen bonding pattern observed in **1c** and **1d**, which can be attributed to the increase in chain length of glutaric acid leading to the non-complimentarity between acceptor and donor sites on **1** and acid molecules. In contrast, the carboxylate moieties interact, by single N-H \cdots O $^-$ hydrogen bonds, with H \cdots O $^-$ distances in the range 2.06- 2.34 Å, with four pairs of dimers of **1**, as shown in Figure 2.20.

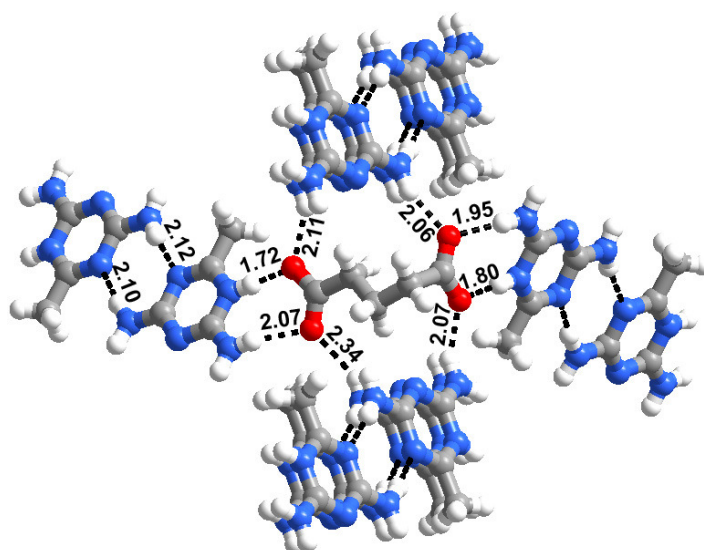


Figure 2.20. Annotation of intermolecular interactions observed in the complex, **1f**.

2.2.8 Molecular adduct between 2,4-diamino-6-methyl-1,3,5-triazine and thiodiglycolic acid-**1g**

Following the similar dimension criteria, complex **1g**, obtained by co-crystallizing **1** and thiodiglycolic acid in 1:1 in methanol solution, gave a 2:1 complex (Table 2.1) between **1** and thiodiglycolic acid, with a host guest network similar to **1c**, **1d** and **1f**, as shown in Figure 2.21

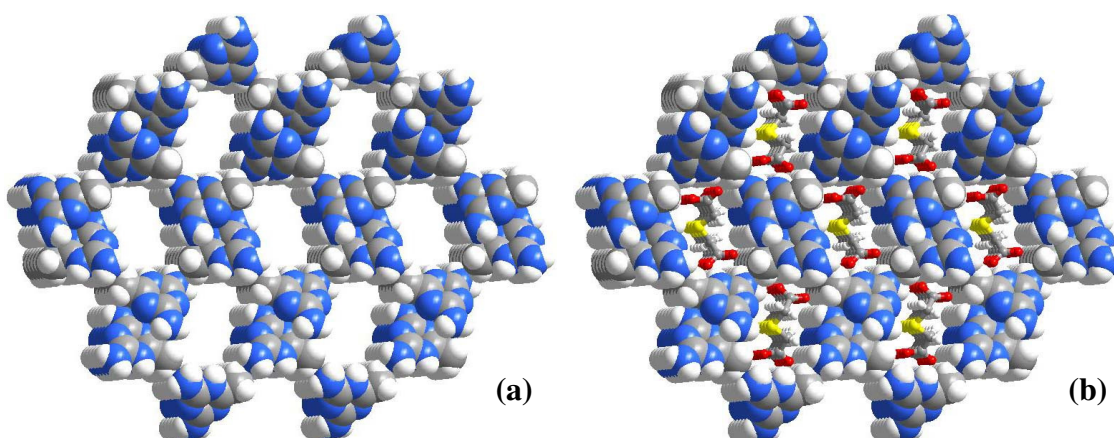


Figure 2.21. (a) Host network observed in **1g**. (b) thioglycolate molecules in the channels of host network formed by the molecules of **1**.

The detailed analysis of **1g** shows that it forms the recognition patterns similar to **1f**. In **1g** also thiodiglycolic acid is completely deprotonated, as observed in **1c**, **1d** and **1f**. The thiodiglycolate molecules interact with **1** through cyclic network as well as single hydrogen bonds with dimers of **1**. In the cyclic network, while the $\text{N}^+\text{-H}\cdots\text{O}^-$ and $\text{N-H}\cdots\text{O}^-$ hydrogen bond, have distances in the range 1.76-2.02 Å (see Table 2.2), in the single $\text{N-H}\cdots\text{O}^-$ hydrogen bond the corresponding $\text{H}\cdots\text{O}^-$ hydrogen bond distances are found to be in the range of 2.04- 2.62 Å, as shown in Figure 2.22.

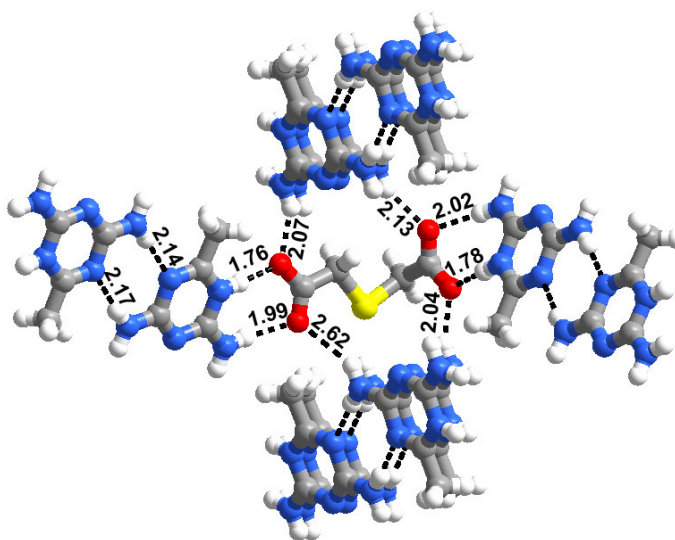


Figure 2.22. Annotation of intermolecular interactions observed in the complex, **1g**.

2.2.9 Structure of molecular complex of 2,4-diamino-6-methyl-1,3,5-triazine and diglycolic acid-1h

In contrast to thiodiglycolic acid, a 2:1 adduct (Table 2.1) of **1** and diglycolic acid, form entirely different supramolecular assembly than the complexes studied so far, irrespective of similarities in dimensions among glutaric, thiodiglycolic and diglycolic acids, But, it has close resemblance to the complex, **1b** with a host-guest network, in three dimensional packing, as shown in Figure 2.23 (b).

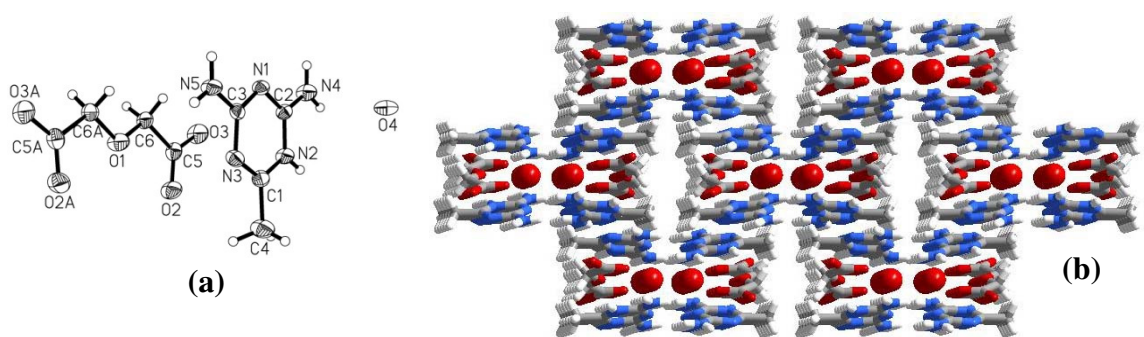


Figure 2.23. (a) Asymmetric unit contents in the crystal structure of **1h**. (b) Packing of molecules in the three-dimensional arrangement.

However, in **1h** also both the carboxylic groups are deprotonated, as observed in complexes **1b-1g**. Further, detailed analysis of the exact nature of interaction among the molecules, reveals an exotic triple helix structure, as shown in Figure 2.24(a).

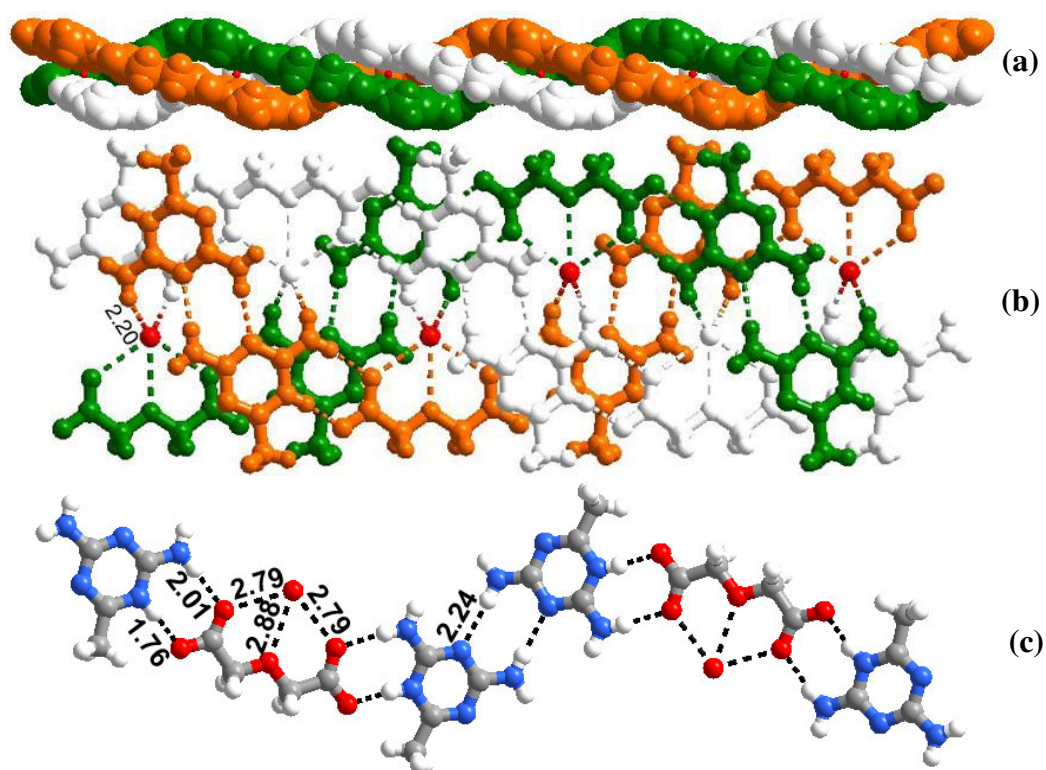


Figure 2.24. (a) Triplet helix observed in the structure of complex, **1h**. (b) Interaction among the helices in the triplet helix. (c) Interactions among the molecules within a helix.

Intermolecular interactions between the helices, in the triple helix, and within each helix are shown in Figures 2.24 (b) and (c) respectively. The helix is formed by sandwiching of diglycolate molecules between the dimers of **1**. The diglycolate molecules form dimeric $\text{N}^+\text{-H}\cdots\text{O}^-$ and $\text{N-H}\cdots\text{O}^-$ hydrogen bond with $\text{H}\cdots\text{O}^-$ distances of 1.76 and 2.01 Å, respectively, with the molecules of **1** (see Figure 2.24(c)). Further, molecules of **1** exist as dimers through $\text{N-H}\cdots\text{N}$ hydrogen bonds having $\text{H}\cdots\text{N}$ distance of 2.24 Å and different helices interact with each other through water molecules.

2.2.10 Analysis of complex of 2,4-diamino-6-methyl-1,3,5-triazine and adipic acid-1i

Crystals obtained from a CH_3OH solution of **1** and adipic acid, are found to be a molecular complex of the components in a 2:1 ratio (Table 2.1). In complex **1i** also, the three-dimensional arrangement highlights the formation of host-guest assembly with the molecules of **1** serving as host and adipic acid molecules as guest, occupying the channels created by **1** (Figure 2.25).

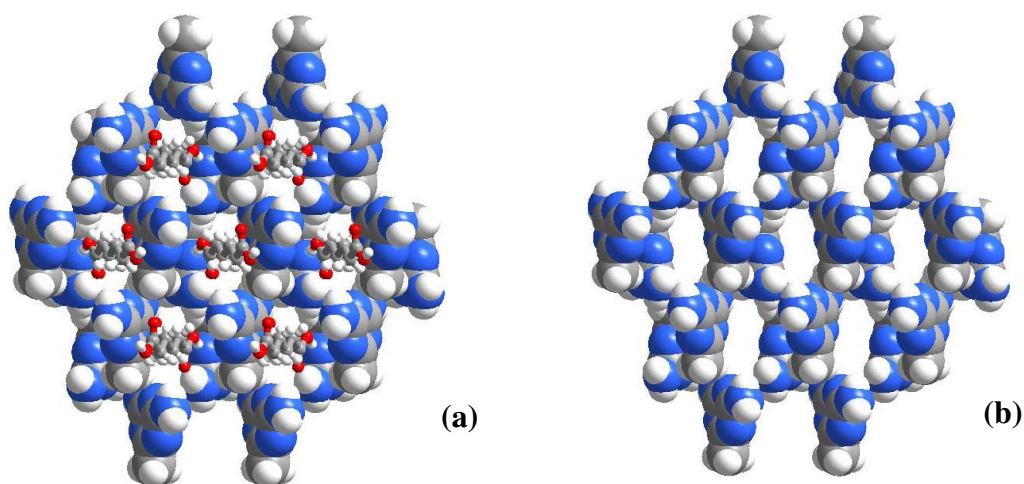


Figure 2.25. (a) Three-dimensional packing of molecules in the complex, **1i**. (b) Clear visualization of channels without the guest acid molecules.

Though the three dimensional packing of **1i** is similar to **1c**, **1d**, **1f** and **1g**, but, the recognition pattern between **1** and acid is through neutral species as adipic acid molecules are not deprotonated, in contrast to what is observed in the molecular complexes **1a-1h**. However, the recognition pattern is similar to **1f** and **1g**, and each adipic acid is surrounded by dimers of **1** formed by the N-H \cdots N hydrogen bonds with H \cdots N distance of 2.09 Å. The molecules of adipic acid interact with two dimers of **1** by O-H \cdots N and N-H \cdots O hydrogen bond dimers by H \cdots N and H \cdots O distances of 1.68 and 2.10 Å, respectively, and with four dimers of **1** by single N-H \cdots O hydrogen bonds (Figure 2.26) having H \cdots O distance of 2.21 and 2.26 Å (Table 2.2).

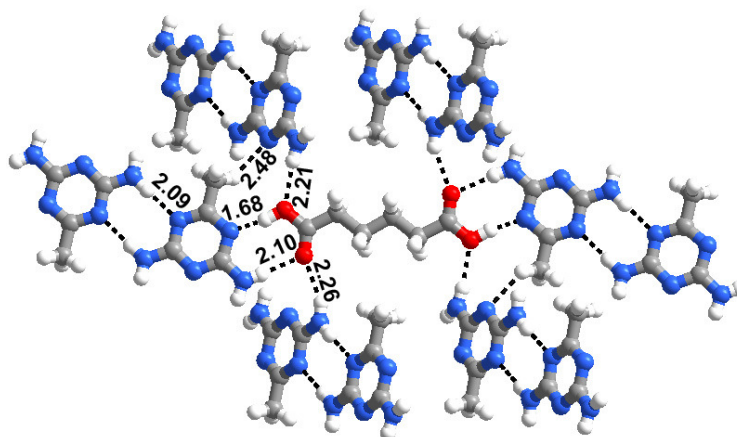


Figure 2.26. Ensemble of molecules with the annotation of intermolecular interactions between **1** and adipic acid

It is interesting to see that this is the first example in this series, wherein a dicarboxylic acid did not undergo proton transfer. This suggests that in addition to the complimentary recognition abilities such as size, shape, position, etc., additional features like pK_a must be playing a significant role starting from the recognition pattern to the ultimate topological arrangements. Hence, a study of correlation of the

structures **1a** - **1i** along with the CH₃OH adduct of **1** has been considered to deduce common features that directed the obtained structural motifs.

2.2.11 Structural correlations among 1a - 1i

Comparison of all the structures **1a** - **1i**, highlights the ability of **1** to form host network in the presence of variety of aliphatic dicarboxylic acids. However, the host network is able to create only voids in two dimensional arrangement in **1a** and **1e**, but it constituted channels in the remaining structures, **1b** - **1d**, **1f** - **1i** and CH₃OH adduct of **1**. A striking feature of these host-guest assemblies is that while in **1a**, **1b**, **1e** and **1h**, the host network is formed by both **1** and corresponding acid/carboxylate molecules (with the voids/channels are being filled by either solvent of crystallization or water molecules), in **1c**, **1d**, **1f**, **1g** and **1i**, the host network is formed by the molecules of **1** and the carboxylate/acid moieties reside in the channels as guests. As we visualize the progress of structures from **1a** → **1i**, the dicarboxylic acids in this series are in the ascending order of increased methylene groups or analogues, but the observed variations in the host-guest types did not bear any direct correlation with such property. Although majority of diacids in this study did convert to dicarboxylates, oxalic acid in **1a** exists as monocarboxylate while adipic acid in **1i** remain intact. These differences indeed are quite intriguing as such anomalies could not be explained by mere structural considerations with high degree of consistency and accuracy. Thus, we looked upon the other physical properties like pK_a which is, in general, the fundamental property that influences the conversion of an acid to a

carboxylate. The analysis has provided vital information and high correlation between the pK_a and the observed structural variations.

Table 2.3. pK_a values of **1** and dicarboxylic acids **a - i**

compound	complex	pK_a	ΔpK_a
2,4-diamino-6-methyl-1,3,5-triazine		4.63	-
oxalic acid	1a	1.23	3.40
acetylenedicarboxylic acid	1e	1.73	2.90
diglycolic acid	1h	2.79	1.84
malonic acid	1b	2.83	1.80
fumaric acid	1d	3.02	1.61
thiodiglycolic acid	1g	3.32	1.31
succinic acid	1c	4.19	0.44
glutaric acid	1f	4.33	0.30
adipic acid	1i	4.42	0.21

2.2.12 pK_a towards specific host networks

pK_a values obtained from different sources are listed in Table 2.3. By considering the ascending order of pK_a values, it is apparent that in this homologues series of dicarboxylic acids, acids with low pK_a values (oxalic, 1.23 and malonic, 2.83) did form host guest complexes by interacting with **1**, yielding host network. However, the acids with high pK_a values (succinic, 4.19, glutaric, 4.34 and adipic, 4.42) have yielded host-guest systems wherein acids remain as guests in the host network created by **1**. The other dicarboxylic acids, fumaric, acetylene, thiodiglycolic and diglycolic also fall into one of these categories correlating with their pK_a values. For example, complexes, **1d** and **1g** corresponding to fumaric and thiodiglycolic acids, respectively, which have pK_a values 3.02 and 3.32, formed complexes similar to **1c** and **1i** while complexes of acetylene and diglycolic (**1e** and **1h**) did form complexes of

hosts like **1a** and **1b**. Thus, taken into consideration of all the acids in this study, it is evident that acids with $pK_a < 3.0$ preferentially gave binary component hosts, while other acids with $pK_a > 3.0$ directed the mono host assemblies. Although further micro analysis for the causes of such variations could not be established, this information perhaps may elude for further systematic studies to appreciate the importance of physical and chemical properties of the co-crystallizing agents for the creation of desired supramolecular assemblies.

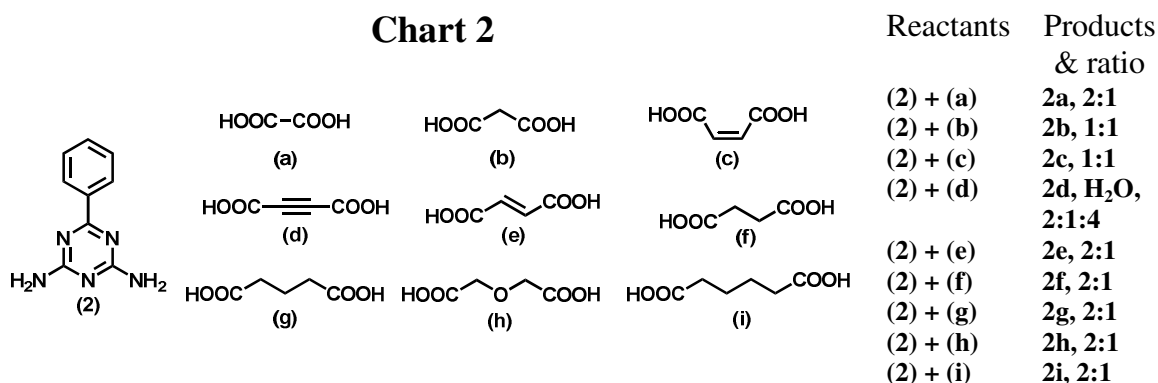
2.2.13 pK_a towards specific hydrogen bonding patterns

Another important anomaly in the complexes **1a** - **1i** is the conversion of carboxylic acids to carboxylate moiety at random and as a result of it, different types of hydrogen bonding patterns – ionic or neutral were formed. For example, while both the $-COOH$ moieties transform to dicarboxylates in the complexes, **1b** - **1h**, leading to the formation of ionic hydrogen bonds like $N^+-H\cdots O^-$, $N-H\cdots O^-$, $O-H\cdots O^-$ etc., only one of the $-COOH$ converts to carboxylate in **1a** and both the $-COOH$ groups remain intact in **1i**, forming neutral $O-H\cdots N$ and $N-H\cdots O$ hydrogen bonds. It has been viewed that such a transformation is the artifact of the strength of the acidity and basicity features of the reactants in the complex, which can be accounted by the pK_a values. Thus, difference in pK_a between the acid and aza-donor compound should give an indication of proton-transfer which can be related ultimately to the appearance of different types of hydrogen bonding patterns. From the Table 2.3, it is apparent that exact quantitative estimation could not be established but a qualitative range of ΔpK_a provided some light on the process of proton transfer in the complexes **1a** - **1i**. Thus,

–COOH groups in this study are found to be converting to carboxylates, if ΔpK_a is > 0.3 and below which it remained intact (**1i**). However, it is noteworthy to mention that deprotonation occurred for both the –COOH groups, in all the complexes except **1a** and **1i**. In complex **1a**, only one of the –COOH groups of oxalic acid did deprotonate and it could be accounted for the wide difference between pK_{a1} (1.23) and pK_{a2} (4.19) of oxalic acid, in contrast to other acids.

2.3 Molecular Complexes of 2,4-Diamino-6-phenyl-1,3,5-triazine with Various Aliphatic Acids: Ensembles with Voids of Self-Filling to Interpenetrating Networks

An important manifestation of the structural studies of **1a-1i**, described in the earlier section, is the preference of **1** to form, exclusively, host-guest assemblies, in the presence of several aliphatic dicarboxylic acids. Thus, it would be appropriate to study the affinity and systematic variations of such triazines towards yielding host-guest type assemblies with different types of functional groups on the core triazine moiety, for example, replacement of methyl group by various functional groups. In particular, if the peripheral groups are bulky and also have conformational freedom, it would be quite attractive as such groups can also effectively fill the void space without the aid of external guest species, like solvent of crystallization etc. Thus, a study of molecular complexes of 2,4-diamino-6-phenyl-1,3,5-triazine with various aliphatic dicarboxylic acids (Chart 2) has been carried out and the structural features as well as the correlations are discussed in the following sections. Endeavours were initiated with the analysis of solid state structure of **2**, reported by Hoz and co-workers¹⁶.



In the asymmetric unit of **2** there are two crystallographically symmetry independent molecules of **2**, labeled as A and B (Figure 2.27 (a)). The molecules of A and B interact with each other by N-H \cdots N hydrogen bonds, thus yielding linear tapes and the adjacent tapes are held together by N-H \cdots N hydrogen bonds formed between B molecules (Figure 2.27 (b)). Thus the observed network suggests that co-crystallizing ligands can interact with molecules of **2**, either by replacing the molecules of **A**, or by inserting between the molecules of **B**. To explain such features, structural studies on the complexes of **2** have been directed to evaluate the molecular recognition patterns between **2** and the corresponding acids. In this process, it has been noted that a molecular complex of **2** and oxalic acid is already known in the literature. But, discussion of structural features was limited to molecular conformational analysis without any insight about three-dimensional arrangement. Hence, structural analysis of the complex has been carried out as described below.

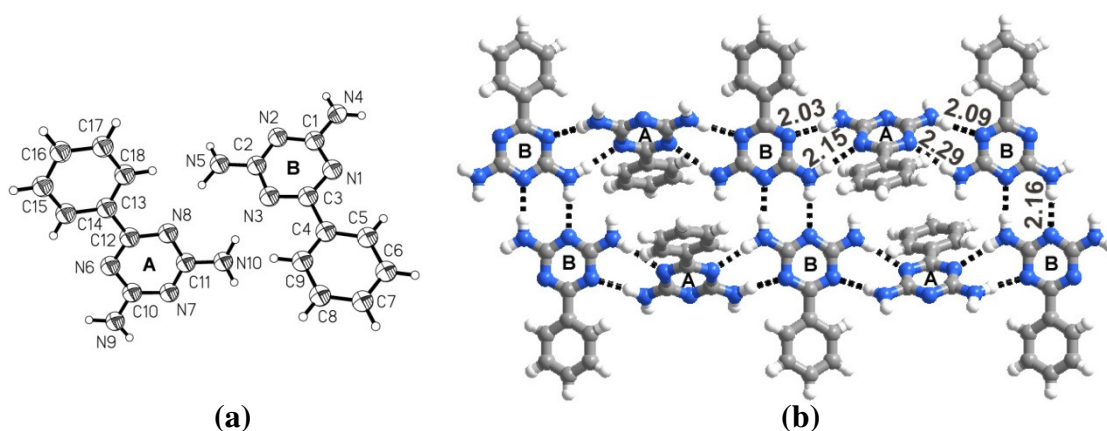


Figure 2.27. (a) ORTEP showing the asymmetric unit of **2**. (b) Annotation of interaction between the molecules of **2**, leading to the formation of six member cyclic network.

Molecular complex of **2** with oxalic acid, reported by Aghabozorg and co-workers forms a network with voids¹⁴, as shown in Figure 2.28 (a). In this structure, the adjacent molecules of **2** interact to form tapes, by N-H \cdots N hydrogen bonds, with H \cdots N distances of 2.09 and 2.64 Å. The molecules of oxalic acid, act as spacers, connect the adjacent tapes of **2** by N⁺-H \cdots O⁻ and N-H \cdots O⁻ hydrogen bond with H \cdots O⁻ distances of 1.83 and 1.84 Å, respectively, as shown in Figure 2.28(a), thus yielding void space of dimensions 10.6 \times 10.8 Å². Although the phenyl groups on **2** are directed towards the void space, but it remains unoccupied as the groups flipped away from the plane of the layers by an angle of 82°. Hence, the large void space, further gets stabilized by undergoing 3-fold interpenetration, as shown in Figure 2.28 (b) and (c). It is apparent that **2** also has ability to form a host-guest network with oxalic acid as observed in **1a** (**1** + oxalic acid) except that voids are being filled through interpenetration rather than by solvent of crystallization. Observing such good

correlation between **1a** and **2a**, study of the complexes of **2** obtained by co-crystallization of it with other dicarboxylic acids has been advanced further.

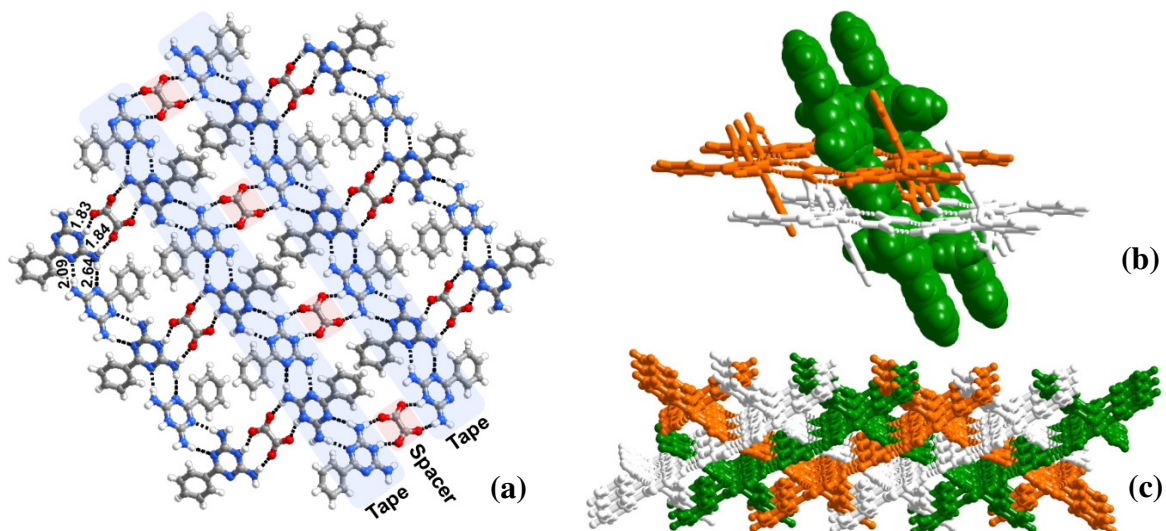


Figure 2.28. (a) Eight member cyclic network, having void space of dimensions $10.6 \times 10.8 \text{ \AA}^2$, formed by the interaction of **2** and oxalic acid. (b) and (c) Network with voids get stabilized by undergoing 3-fold interpenetration¹⁵.

2.3.1 Molecular adduct of 2,4-diamino-6-phenyl-1,3,5-triazine with malonic acid-2b

Co-crystallization of malonic acid and triazine, **2**, from CH_3OH , resulted in the formation of a molecular complex in a 1:1 ratio (Table 2.4), as shown in Figure 2.29.

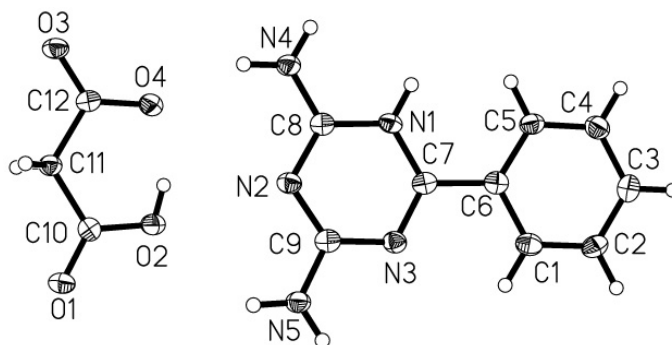


Figure 2.29. ORTEP showing the asymmetric unit of **2b**.

It has been found that only one of the two carboxylic acid groups, on malonic acid, is deprotonated and the proton of the other carboxylic acid functional group is involved in the intramolecular O-H \cdots O $^-$ hydrogen bond, having H \cdots O distance of 1.68 Å (Table 2.5). Further analysis of the structure shows that, molecules of **2** form dimers through a cyclic hydrogen bond pattern of N-H \cdots N hydrogen bonds, with H \cdots N distance of 2.16 Å. Between such dimers, two malonate molecules are sandwiched, as shown in Figure 2.30, constituting a tape structure.

The carboxylate group of the malonate interacts with only one molecule in the dimer of **2**, by a pairwise N $^+$ -H \cdots O $^-$, N-H \cdots O $^-$ hydrogen bonds with H \cdots O $^-$ hydrogen bond distance of 1.92 and 1.94 Å, respectively. However the carboxylic acid group interacts with both the molecules in the dimer of **2**, by N-H \cdots O hydrogen bonds (H \cdots O, 1.97 and 2.21 Å). Complete characteristics of the hydrogen bonds are listed in Table 2.4.

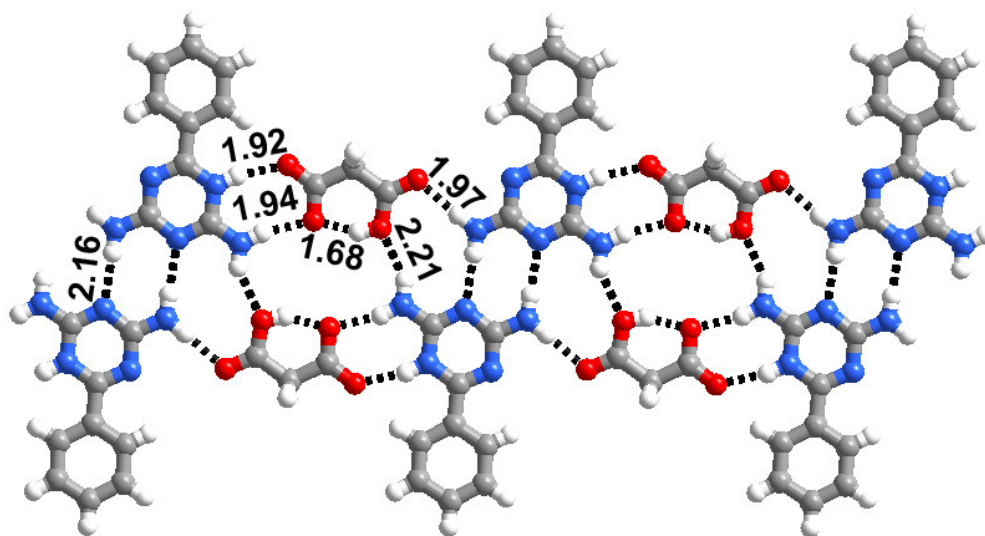


Figure 2.30. Arrangement of molecules of **2** and malonic acid in the co-crystals yielding a tape structure.

In three dimensional arrangement such adjacent tape assemblies, ultimately interact with each other by C-H \cdots O and C-H \cdots O $^-$ hydrogen bonds (H \cdots O and H \cdots O $^-$ distances of 2.58 and 2.73 Å), as shown in Figure 2.31.

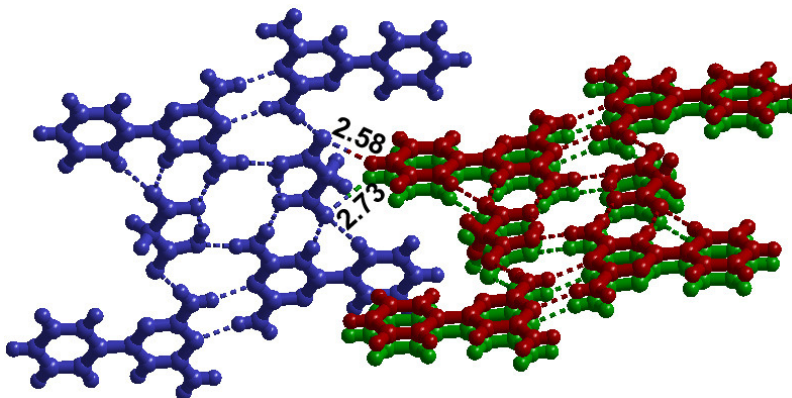


Figure 2.31. Annotation of interactions in three dimensional arrangement of **2b**.

2.3.2 Structure of molecular complex of 2,4-diamino-6-phenyl-1,3,5-triazine and maleic acid-2c

Molecular complex, **2c**, obtained between **2** and maleic acid in 1:1 ratio, from a methanol solution has an asymmetric unit with two symmetry independent molecules of both **2** and **c**. In this complex **2c** also one of the -COOH groups on maleic acid deprotonated and the proton of the other carboxylic acid functional group involved in the intramolecular O-H \cdots O $^-$ hydrogen bond, with H \cdots O $^-$ distance of 1.53 and 1.63 Å (Figure 2.32). Further, molecules of **2** form dimers, through N-H \cdots N hydrogen bonds, which are being separated by maleic acid molecules as shown in Figure 2.32(b). Thus, the carboxylate group of molecules of monodeprotonated maleic acid interacts with only one of the molecules in the dimers formed by **2**, by a pairwise N $^+$ -H \cdots O $^-$ and N-H \cdots O $^-$ hydrogen bonds (H \cdots O $^-$, 1.84, 1.97 and 1.95, 1.98 Å). However, carboxylic acid group on malonic acid interacts with both the molecules of **2** within the dimer, by

N-H \cdots O hydrogen bonds (H \cdots O distance of 2.09, 2.14 and 2.15 Å), as shown in Figure 2.32 (b).

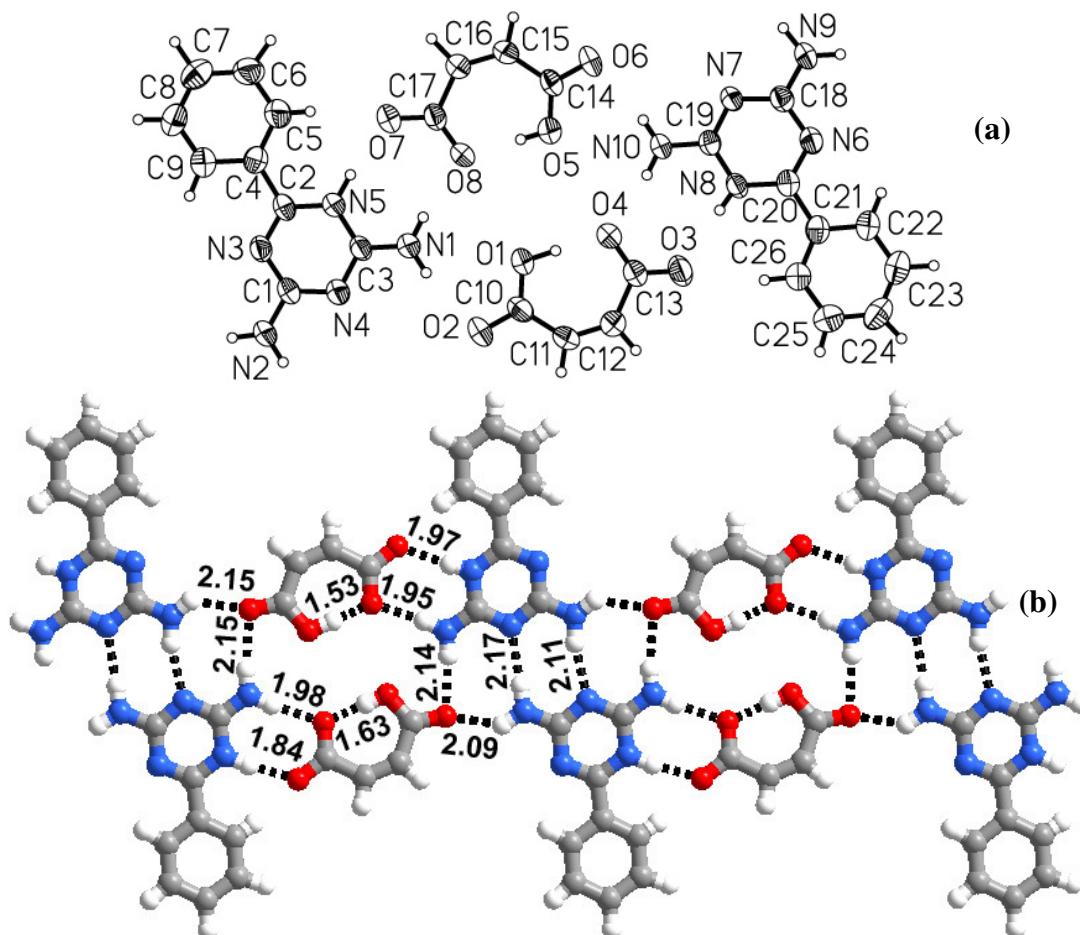


Figure 2.32. (a) ORTEP showing the asymmetric unit of **2c**. (b) Arrangement of molecules of **2** and maleic acid in the co-crystals yielding molecular double tapes.

In three dimensional arrangement, the adjacent tapes interact by C-H \cdots π hydrogen bond, with distances of 2.92 and 3.34 Å to form a crinkled sheet structure, as shown in Figure 2.33. Thus, the similarities between **2b** and **2c** about basic recognition and one-dimensional arrangement may be due to the similar molecular dimensions of malonic and maleic acids, as well as prevalence of intramolecular hydrogen bond.

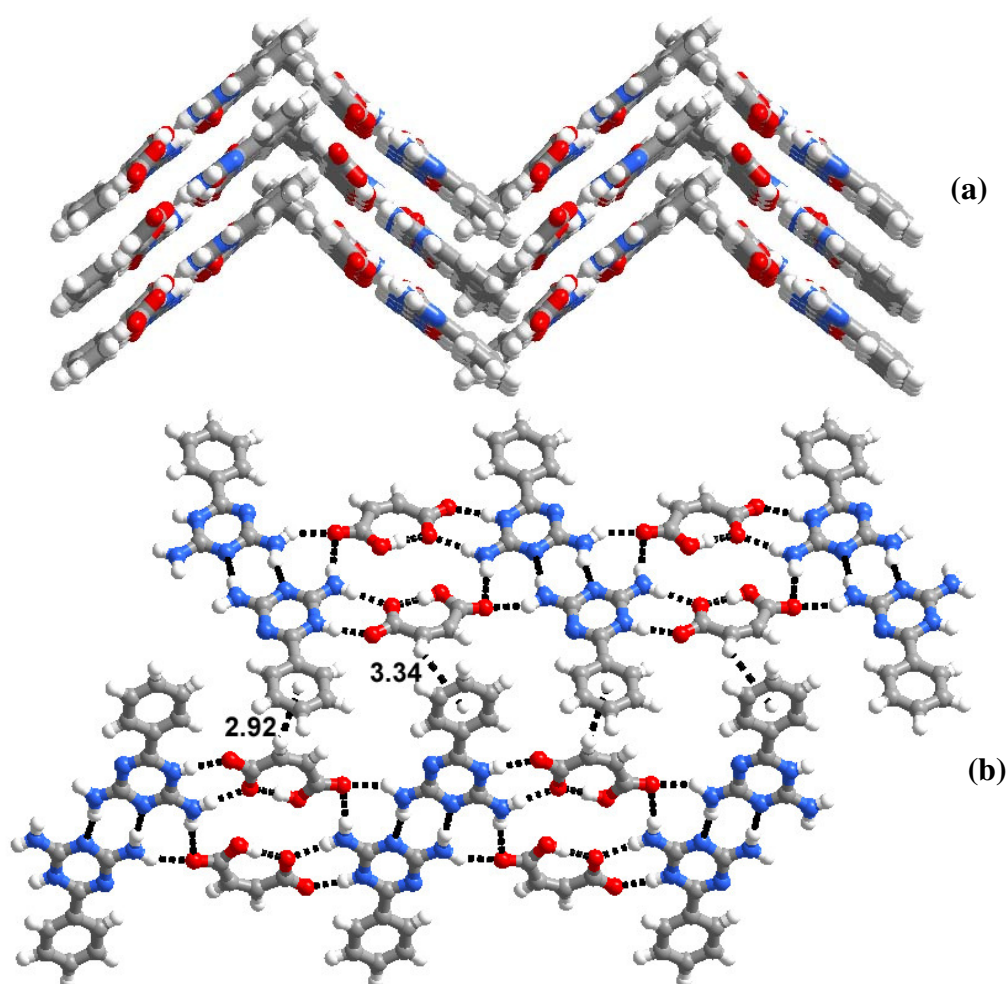


Figure 2.33. (a) Packing diagram, showing the zig-zag sheets (b) Annotation of interactions between the adjacent tapes.

2.3.3 Supramolecular structure of molecular complex of 2,4-diamino-6-phenyl-1,3,5-triazine and acetylene dicarboxylic acid-2d

Co-crystals, **2d**, obtained from a CH_3OH solution of **2** and acetylenedicarboxylic acid have the co-crystallizing ligands in a 2:1 ratio, in the asymmetric unit (Table 2.4), along with water molecules, as shown in Figure 2.34 (a). In **2d** both the carboxylic acid functional groups of acetylene dicarboxylic acid are deprotonated as observed in **2a**, unlike in **2b** and **2c**. In three dimensional

arrangement, the molecules of **2** and acetylenedicarboxylic acid aggregate, yielding channels, with void space of dimensions $8 \times 9 \text{ \AA}^2$, as shown in Figure 2.34 (b), due to the stacking of adjacent sheets held together by the π - π interactions. The channels, thus, created are being filled by water molecules.

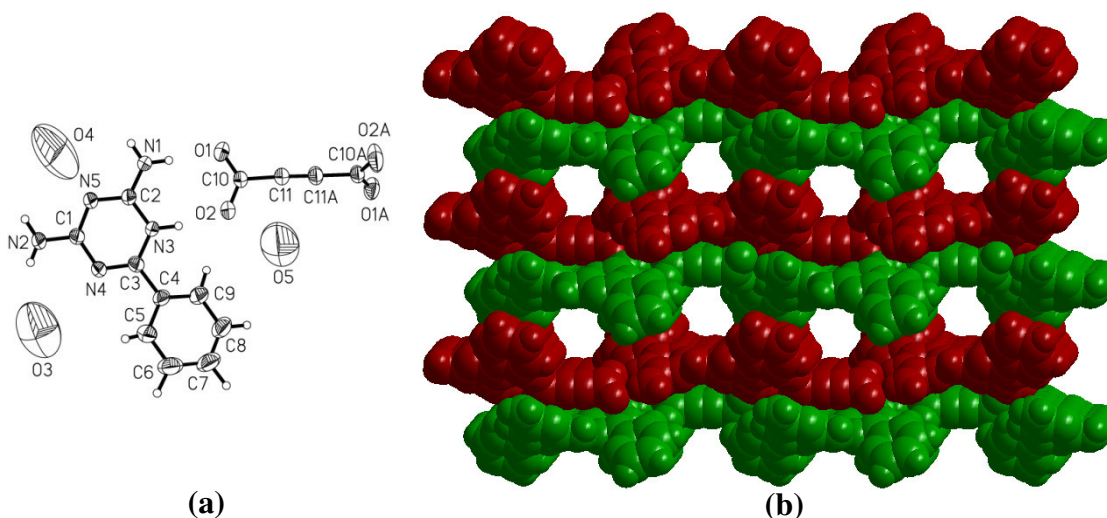


Figure 2.34. (a) ORTEP showing the asymmetric unit of **2c**. (b) Packing diagram showing channels in three dimensions.

Detailed analysis of a typical sheet shows the formation of molecular tapes by **2**, through the two centrosymmetric N-H \cdots N hydrogen bond dimers, with H \cdots N distance of 2.11 and 2.28 \AA . Such tapes are held together by acetylenedicarboxylate by N $^+$ -H \cdots O $^-$ and N-H \cdots O $^-$ hydrogen bonds, with the corresponding hydrogen bond distances being 1.82 and 1.99 \AA , respectively. Such an association created, in principle, a cyclic network, having voids of $17 \times 7 \text{ \AA}^2$ dimensions but part of it is being filled by the bulky phenyl substituent, thus, limiting the dimension to $\sim 7 \times 7 \text{ \AA}^2$, which is being filled by water molecules, as shown in Figure 2.35 (a) and (b).

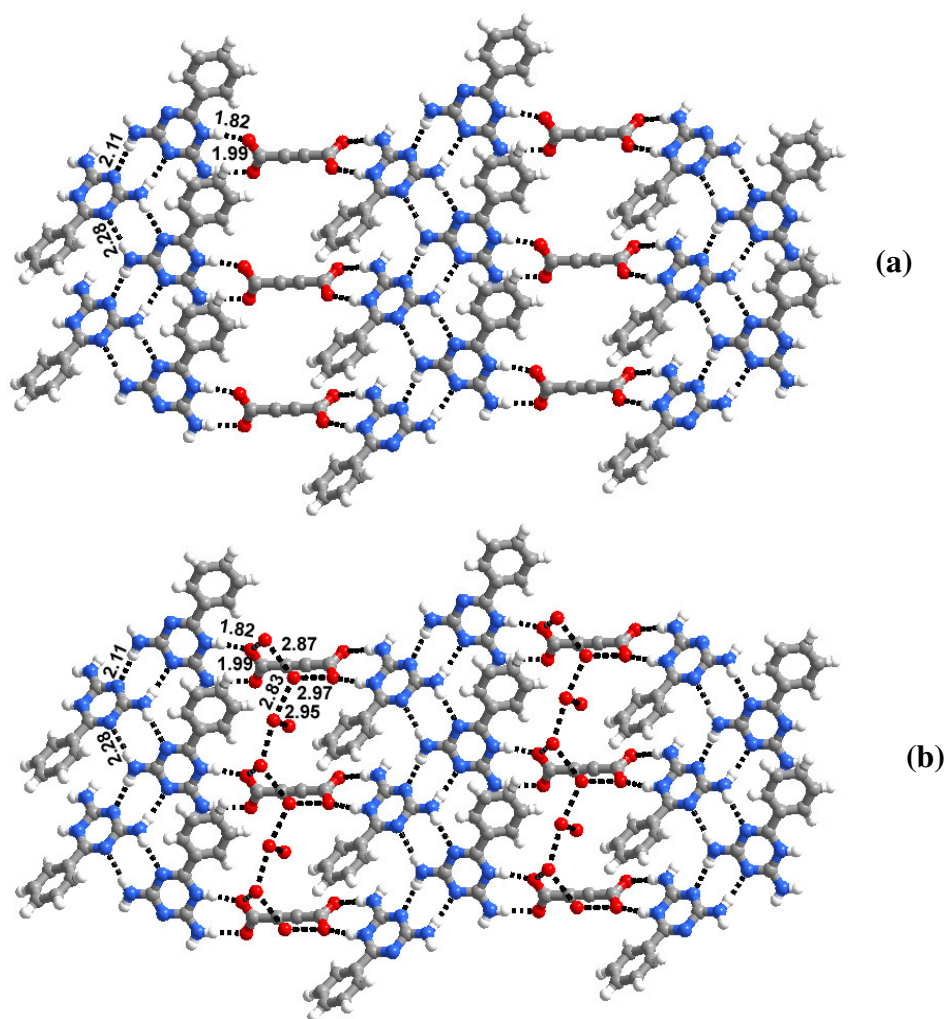


Figure 2.35. Two adjacent tapes joined together by the molecules of acetylene dicarboxylate to form (a) an eight member cyclic network, having void space of dimensions $7 \times 7 \text{ \AA}^2$ (b) water molecules occupying the void space so created.

2.3.4 Molecular adduct of 2,4-diamino-6-phenyl-1,3,5-triazine with fumaric acid-2e

Co-crystallization of fumaric acid and triazine, **2**, from CH_3OH , resulted in the formation of co-crystals, **2e**, in a 2:1 ratio. In contrast to the other complexes discussed above, acid molecules remain intact without undergoing deprotonation. In three dimensions, molecules in **2e** form a layered structure. Detailed analysis of a typical

sheet shows that, molecules of **2** form molecular tapes by two N-H \cdots N hydrogen bond dimers, (H \cdots N distance of 2.14, 2.17 and 2.19 Å), as shown in Figure 2.36. Further these tapes are held together by the molecules of fumaric acid through O-H \cdots N and N-H \cdots O hydrogen bonds (H \cdots N and H \cdots O bond distances 1.64, 1.85; 2.04, 2.10 Å). Such an association created an eight member cyclic network, yielding voids of 12.5 x 11.5 Å² dimension, as shown in Figure 2.36 (c). Thus, **2e** has a similar structure as that of **2a**. However the void space is self filled by the two phenyl rings on **2**, thus, precluding the interpenetration in contrast to the arrangement in **2a**.

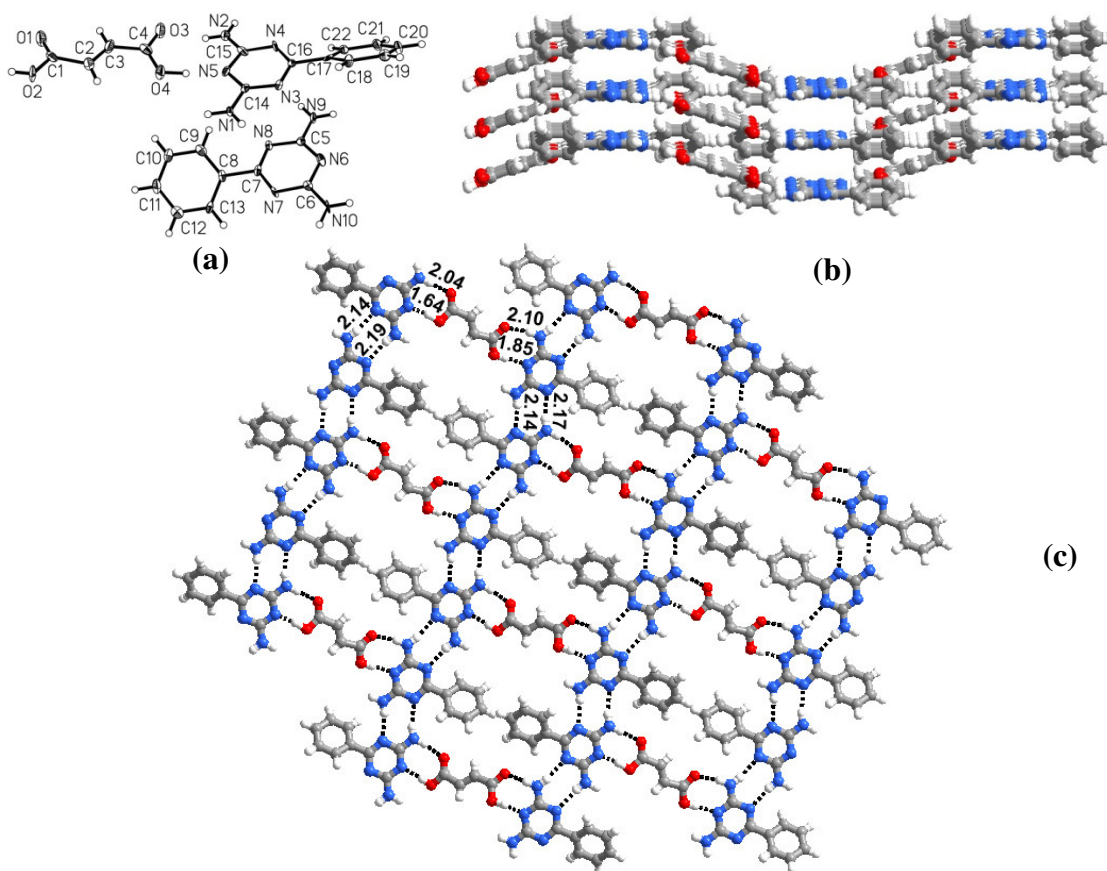


Figure 2.36. (a) ORTEP diagram of the molecular complex **2e** (b) packing diagram showing the presence of layered structure (c) eight membered cyclic network observed in a typical sheet.

2.3.5 Molecular complex of 2,4-diamino-6-phenyl-1,3,5-triazine with succinic acid-2f

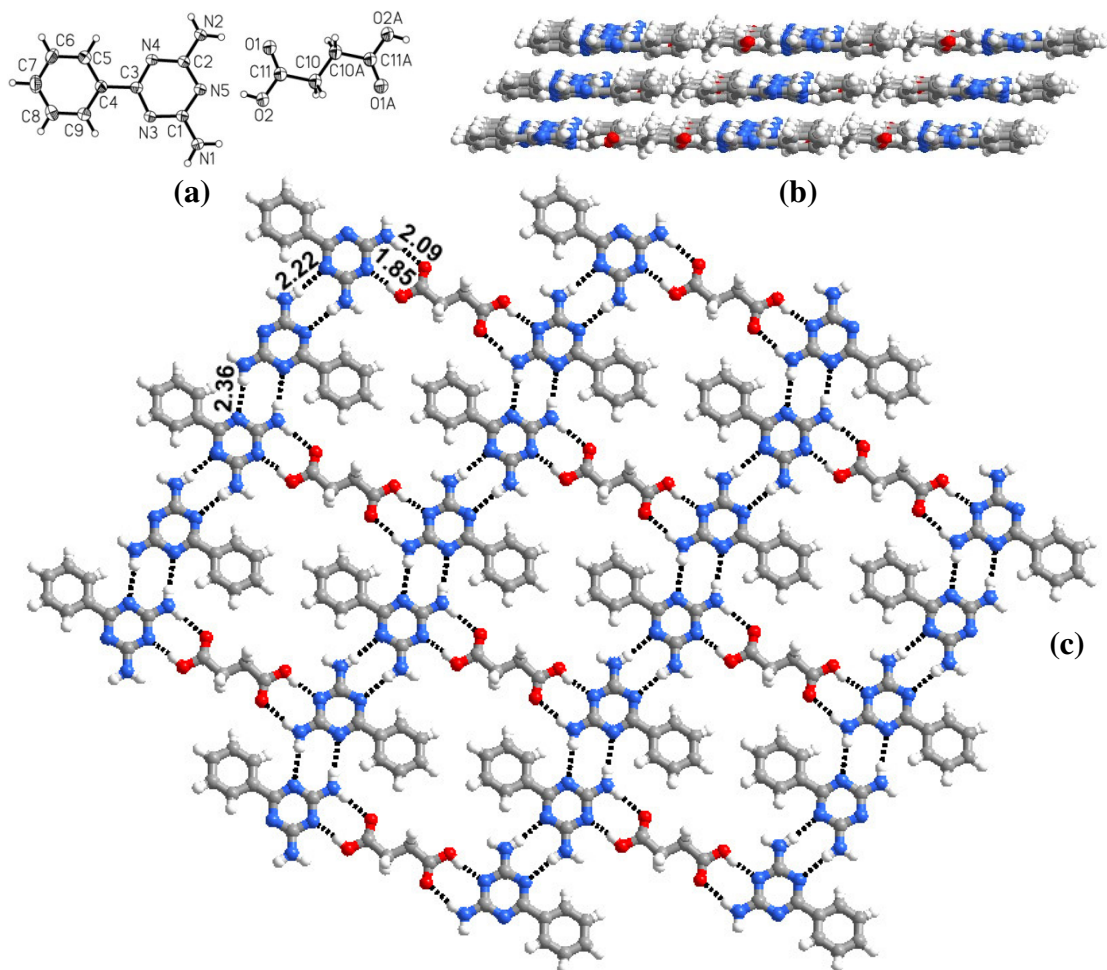


Figure 2.37. (a) ORTEP diagram of the molecular complex **2f** (b) packing diagram showing layers in three-dimensional arrangement. (c) annotation of interactions in a typical sheet.

2:1 co-crystals **2f**, (Table 2.4) obtained between **2** and succinic acid, form a network having topology similar to **2e**. In **2f** also the molecules in the asymmetric unit are neutral, (Figure 2.37 (a)) as observed in **2e** and in contrast to **2b-2d**. In three dimensional arrangement, molecules in the complex **2f**, form a layered structure.

Detailed analysis of a typical sheet shows the formation of cyclic network, as observed in **2e**. Further, it was observed that molecules of **2** form molecular tapes through two centrosymmetric N-H \cdots N hydrogen bond dimers (H \cdots N distance of 2.22 and 2.36 Å). The molecules of succinic acid, as a spacer, hold the two adjacent tapes of **2** by O-H \cdots N and N-H \cdots O hydrogen bonds, with H \cdots N and H \cdots O bond distances 1.85 and 2.09 Å, respectively. Thus voids with dimensions 12.6 x 12 Å² as formed, which are self filled by the two phenyl rings of the molecules of **2**, by protruding into the cavity, as shown in Figure 2.37 (c).

It appears that apart from the chain length, geometry of the molecules also play a significant role in the three-dimensional packing of molecules in the complexes **2a-2f**. Thus, although the maleic acid is also associated with four carbon chain, similar to fumaric and succinic acid, but still its packing is similar to that observed between **2** and malonic acid, probably due to geometrical similarities, in contrast to the networks formed by the linear molecules, acetylene dicarboxylic, fumaric and succinic acids, which formed cyclic networks. To evaluate these aspects further, co-crystallization of **2** with other dicarboxylic acids like glutaric and its oxygen analogue (diglycolic acid), have been carried out. Though diglycolic acid formed a cyclic network, similar to that observed in **2d-2f**, the molecules of glutaric acid form entirely different type of structure, as described below.

2.3.6 Supramolecular structure of 2,4-diamino-6-phenyl-1,3,5-triazine and glutaric Acid-2g

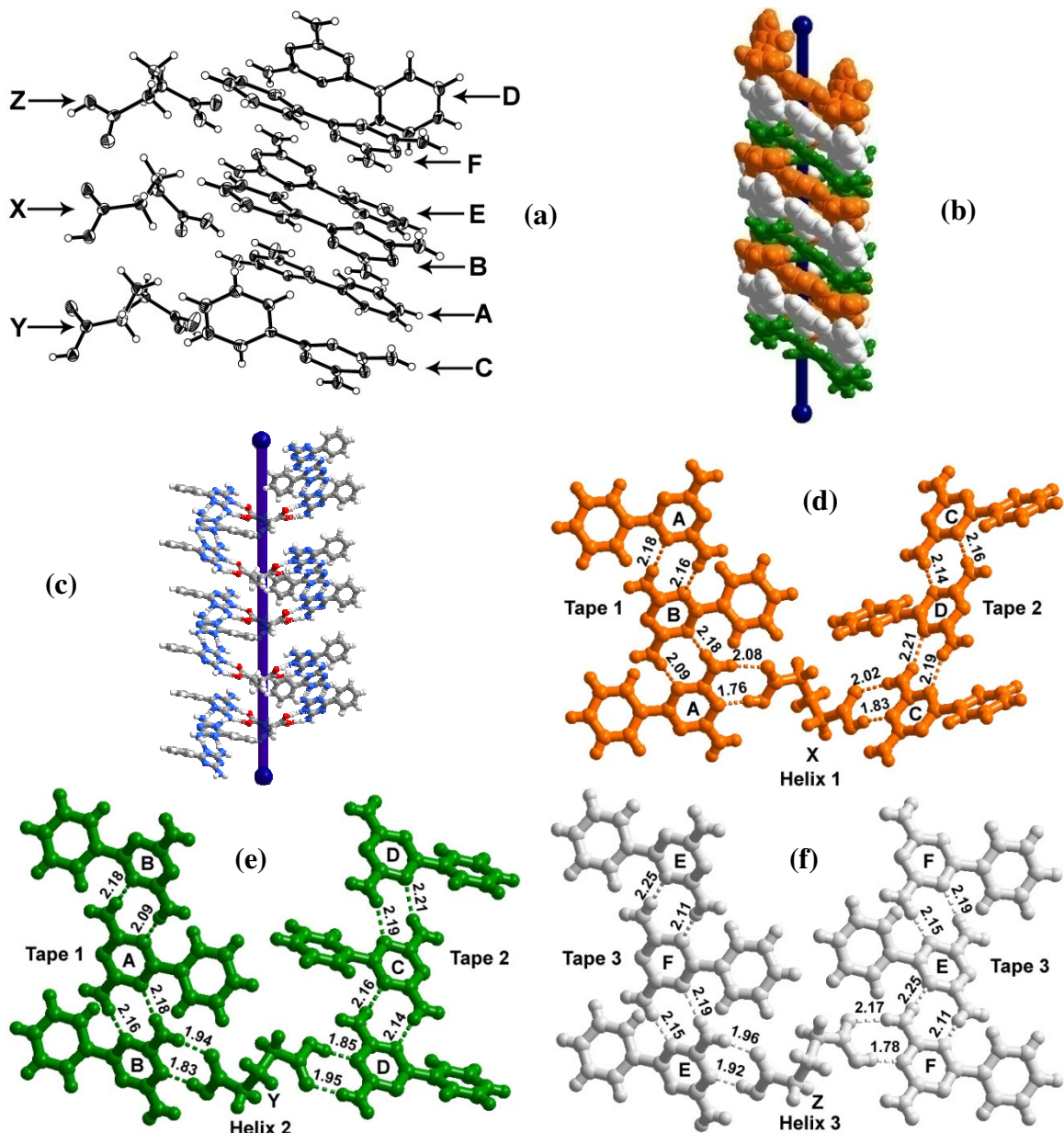


Figure 2.38. (a) ORTEP diagram of the molecular complex **2g** (b) helical arrangement observed in **2g** (c) three helices interweave to form triple helical structure (d)-(f) annotation of interactions observed in three different helices; helix 1 (orange), 2 (green) and 3 (off-white) respectively.

2:1 co-crystals, **2g**, (Table 2.4) obtained from a methanol solution of **2** and glutaric acid has an asymmetric unit with six molecules of **2** (labeled A, B, C, D, E and F) and three glutaric acid molecules (X, Y and Z). Further, all acid molecules remain neutral as observed in **2e** and **2f** (see Figure 2.38 (a)). Detailed analysis of the structure shows that, in the complex **2g**, molecules aggregate to form an exotic triple helix structure, having three different types of helices, labeled as helix 1, 2 and 3, and also each helix is represented in different color, as shown in Figure 2.38 (b).

In **2g**, three different types of molecular tapes of **2** are observed, constituted by each of two symmetry independent molecules, out of six molecules present in the asymmetric unit, through N-H \cdots N hydrogen bonds. The H \cdots N distances are found to be in the range 2.09-2.25 Å (see Table 2.5). The arrangement of these tapes are illustrated in Figure 2.38 (d), (e) and (f). These tapes are further held together by glutaric acid molecules by O-H \cdots N and N-H \cdots O hydrogen bonds, yielding three different helices. The corresponding hydrogen bond distances are listed in Table 2.5. In each helix, one of the three acid molecules interact with tapes of **2** (Figure 2.38 (d), (e) and (f)), in such a manner that two helices are formed due to the adjoining of *heteromeric* tapes, while third helix is the resultant of interaction between the *homomeric* tapes.

2.3.7 Co-crystal of 2,4-diamino-6-phenyl-1,3,5-triazine and diglycolic acid-2h

Co-crystallization of **2** and diglycolic acid, from a methanol solution, in 1:1 ratio yielded good quality single crystals. Structure analysis revealed that it formed a 2:1 molecular adduct **2h**, as shown in Figure 2.39 (a). But, in contrast to the exotic

helical structure observed in **2g**, in three dimensional arrangement, the molecules in the adduct **2h**, form a layered structure (Figure 2.39 (b)).

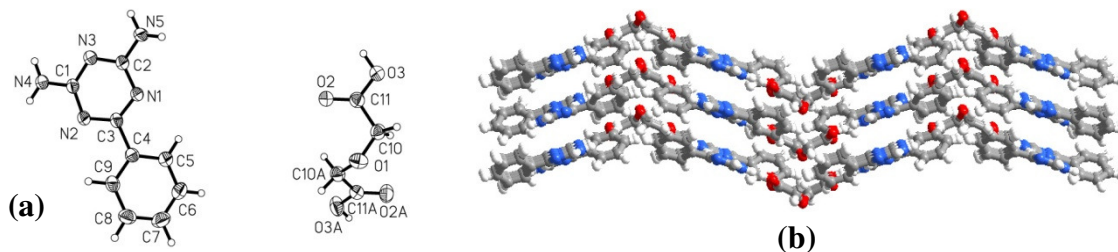


Figure 2.39. (a) ORTEP diagram of the molecular complex, **2h** (b) packing diagram showing the formation of layered structure.

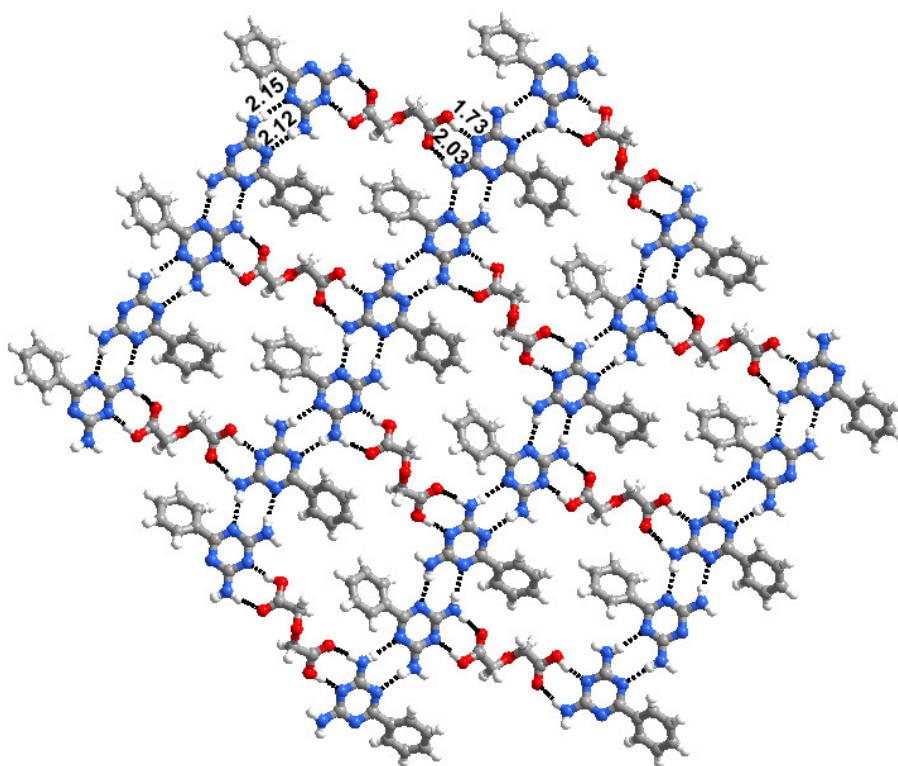


Figure 2.40. Annotation of interactions observed in **2h**.

Detailed analysis of a typical sheet, so obtained, shows that in **2h** also the molecules in the asymmetric unit are neutral as observed in **2e-2g** and aggregate along with **2** yielding an arrangement, which closely resembles **2e** and **2f**. In this structure also, the molecular tapes of **2**, are formed by two centrosymmetric N-H \cdots N hydrogen

bond dimers, with H \cdots N distances of 2.12 and 2.15 Å. The molecules of diglycolic acid act as spacer, joining the two adjacent tapes of **2** by O-H \cdots N and N-H \cdots O hydrogen bonds (H \cdots N and H \cdots O bond distances 1.73 and 2.03 Å). Thus a eight member cyclic entity with void space having dimensions 12.3 \times 11.5 Å is established, which is self-filled by the two phenyl rings of the molecules of **2**, as shown in Figure 2.40.

It is interesting to note that diglycolic acid with five atom chain also has given the void space of similar dimensions as that of four carbon dicarboxylic acids like succinic and fumaric acids. It is mostly due to the similarities in chain length (5.06 Å) with that of other acids (succinic acid, 5.06 Å; fumaric acid 4.90 Å), which is perhaps due to the conformation of diglycolic acid influenced by oxygen hetero atom.

2.3.8 Co-crystal of 2,4-diamino-6-phenyl-1,3,5-triazine and adipic acid-2i

Co-crystallization of **2** with adipic acid (having chain length dimensions much higher than four and five members analogues of the series), gave co-crystals, **2i**, (Table 2.4) in a 2:1 ratio. In this structure also the molecular tapes of **2** are formed by two N-H \cdots N hydrogen bond dimers, having H \cdots N distance of 2.11 and 2.24 Å. The molecules of adipic acid, as spacer, join the two adjacent tapes of **2** by O-H \cdots N and N-H \cdots O hydrogen bonds (H \cdots N and H \cdots O bond distances 1.90 and 2.12 Å), with voids, as observed in **2e**, **2f** and **2h**. However, in complex **2i**, phenyl moieties on **2** are flipped out of plane of the void space, thus, voids of dimensions 12 \times 17 Å² are noted (see Figure 2.41(b)). Such an arrangement around void space was, indeed, observed in **2a**, which ultimately being filled by interpenetration. Interestingly, in **2i** also, the void

space was filled by 4-fold interpenetration in three dimensional arrangement, as shown in Figures 2.41(c) and (d). The flipping of phenyl rings could be interpreted as incommensuration between the volume of phenyl rings and void space.

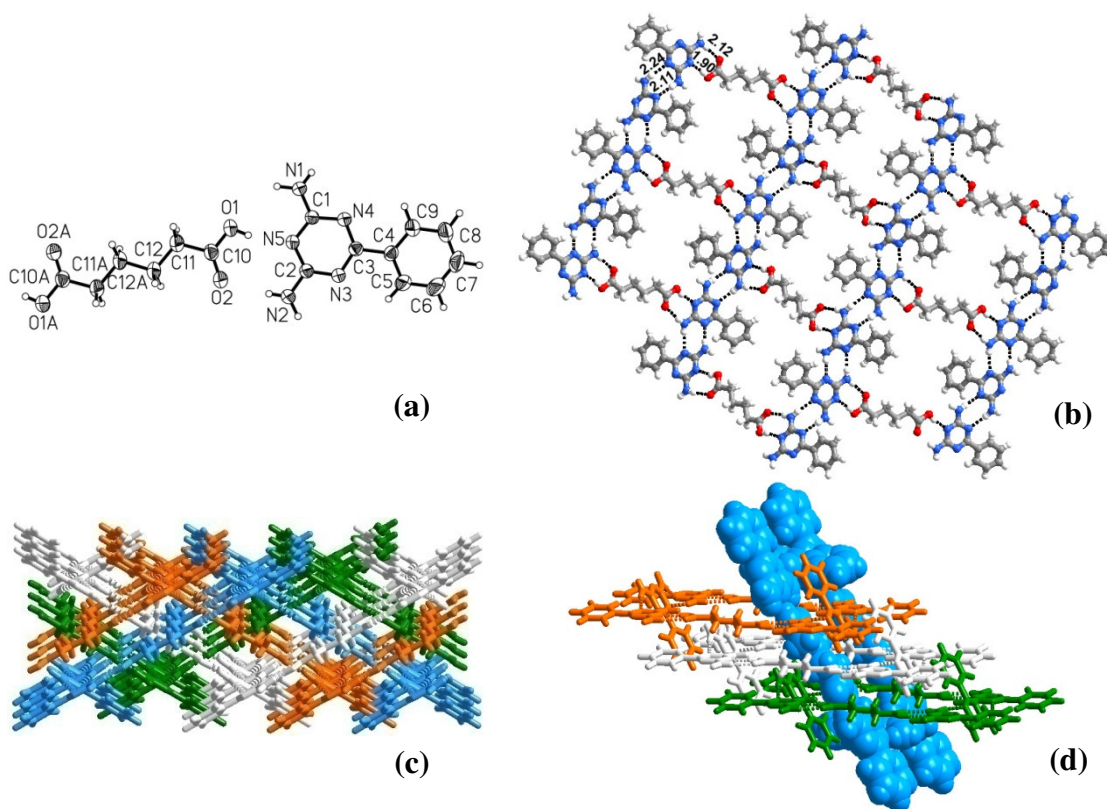


Figure 2.41. (a) ORTEP diagram of the molecular complex **2i** (b) eight member cyclic void of dimensions 12 x 17 Å² observed in **2i**. (c) and (d) 4-fold interpenetrated network observed in **2i**.

2.3.9 Structural correlations among **2a** – **2i**

Organic ensembles formed by 2,4-diamino-6-phenyl-1,3,5-triazine, **2** with various aliphatic dicarboxylic acids have been elucidated as tape structures, which are packed either by effective close packing (**2b**, **2c**) or with void space (**2d-2i**). While in the close-packed structures adjacent dimers of **2** are held together by aliphatic acids, void structures are formed due to the binding of adjacent tapes of **2** by corresponding

acid molecules. It is important to note that, although, in principle, voids are apparent in some complexes, it is been self filled by the available bulky and sticky phenyl moiety, thus, giving an appeal of close-packed arrangement. In case, the void space is not sufficiently able to fit in phenyl moiety, then, the group itself flipped due to conformational flexibility either incorporating solvent of crystallization or water molecules as observed in **2d** (acetylenedicarboxylic acid) or facilitating different levels of interpenetration as observed in **2a** and **2i**. However we could not establish any conclusion for the observed variation with respect to pK_a of the acids, in contrast to the observations made for **1a-1i**. Nevertheless, the study proclaims the ability of triazines for their affinity to interact with aliphatic dicarboxylic acids, yielding predominantly void structures, that are being filled by guest species of either one of the co-crystallizing ligand/solvent of crystallization or by interpenetration.

2.4 Conclusions

Co-crystals **1a - 1i**, have been prepared by crystallization of **1** with various aliphatic dicarboxylic acids (oxalic, malonic, succinic, fumaric, acetylene dicarboxylic, glutaric, thiodiglycolic, diglycolic and adipic acids) from methanol. All the complexes were obtained in a 2:1 ratio of **1** and the corresponding acid in the form of carboxylates, except in **1a** and **1i**. While all the complexes serve as representative examples in the class of host-guest assemblies, two types of host networks were observed and differences are attributed to the variations in the pK_a of the acid molecules under consideration. Host composed of only the molecules of **1** is prevailed (**1c, 1d, 1f, 1g** and **1i**), if the pK_a of the acid is found to be > 3.0 , instead a host

comprising of molecules of **1** and the carboxylate together was observed (**1a**, **1b**, **1e** and **1h**), whenever the pK_a is found to be < 3.0 . Such a relation between the host networks and pK_a has not been established earlier and this revelation may further prompts for an extensive study of numerous other acids and also many other host-guest assemblies which may be of quite useful to apply in different areas like catalysis, separation process etc. In all these complexes, molecules of **1** exist either as triads (**1a**, **1b** and **1e**) or dimers (**1c**, **1d**, **1f** - **1i**) that are exclusively been formed by different types of N-H...N hydrogen bonds. In addition, we have noted that interaction between **1** and the corresponding acid molecules is ionic in nature with the proton transfer from the acid to the molecules of **1** except in **1a** and **1i**. In this regard, we have correlated the observations with the pK_a difference between **1** and the corresponding acids. These observations also perhaps may lead to the development of specific type of hydrogen bonding patterns, ionic, neutral etc. using different types of species, which are useful for the designing of systems with varied physical properties.

Co-crystals of **2** obtained with various aliphatic dicarboxylic acids show the remarkable structural correlation with the structure of **2**. While in complexes **2b** and **2c**, acid molecules interact between adjacent dimers of **2**, forming the six member cyclic networks, in **2d**, **2e**, **2f**, **2h** and **2i**, the acids are as spacers, between the tapes of molecules of **2**. However, in all the complexes, an eight membered cyclic network is prevailed. As the length of the spacer molecule of aliphatic acid is increased, the dimensions of the eight member cyclic void formed by it also increased, but it is self

filled by phenyl moieties except in **2i**. In **2i**, the network formed with void space of 13 x 13 Å², is stabilized by undergoing 4-fold interpenetration.

2.5 Experimental Sections

2.5.1 Synthesis

All the chemicals, reagents and solvents were obtained from commercial suppliers and used without further purification. Spectroscopic-grade solvents were used in all co-crystallization studies. All co-crystals, **1a-1i** and **2b-2i**, were prepared by dissolving the respective reactants in a ratio of 1:1 in methanol and allowing the solvent to evaporate under ambient conditions. In all the cases, single crystals, suitable for X-ray diffraction analysis, were obtained over the period of 3-5 days.

General procedure for the synthesis of complexes, 1a-1i and 2b-2i

In a typical preparation, compound **1** (0.0625 g, 0.5 mmol) and succinic acid (0.0590 g, 0.5 mmol) were dissolved in CH₃OH (20 mL) by gentle warming in a water bath. The resultant solution was evaporated under ambient conditions and with protection from external mechanical disturbances, and within 48 h, good quality, colorless crystals of **1c** were obtained that were suitable for single-crystal X-ray diffraction studies.

2.5.2 Crystal structures determination

Good quality single crystals of , **1a-1i** and **2b-2i**, were carefully selected with the aid of a polarized Leica microscope equipped with CCD camera, and glued to a glass fiber using an adhesive (cyanoacrylate). In all the cases, the crystals were smeared in the adhesive solution to prevent decay of crystals upon exposure to X-rays.

The intensity data were collected on a Bruker single crystal X-ray diffractometer, equipped with an APEX detector, at temperature varying from 133 K to 298 K, see table 2.1 and 2.2. Subsequently, the data were processed using Bruker suite of programmes (SAINT),¹⁶ and the convergence was found to be satisfactory with good R_{int} parameters. The details of the data collection and crystallographic information are given in Table 2.1 and Table 2.2. The structure determination by direct methods and refinements by least-squares methods on F^2 were performed using SHELXTL-PLUS package. The processes were smooth without any complications. All non-hydrogen atoms were refined anisotropically. All the intermolecular interactions were computed using PLATON.¹⁷

Table 2.1. Crystallographic data for **1** and molecular complexes **1a-1i**

	1	1a	1b	1c	1d
Formula	(C ₄ H ₇ N ₅): (C ₁ H ₄ O ₁)	(C ₄ H ₈ N ₅): (C ₄ H ₇ N ₅): (C ₂ H ₁ O ₄): (C ₁ H ₄ O ₁)	2(C ₄ H ₈ N ₅): 1(C ₃ H ₂ O ₄): 4(H ₂ O)	2(C ₄ H ₈ N ₅): 1(C ₄ H ₄ O ₄)	2(C ₄ H ₈ N ₅): C ₄ H ₂ O ₄
Formula Wt.	157.19	372.37	426.42	368.38	366.36
Crystal habit	Blocks	Blocks	Rod-Shaped	Rectangular Blocks	Blocks
Crystal color	Colorless	Colorless	Colorless	Colorless	Colorless
Crystal system	Monoclinic	Triclinic	Monoclinic	Monoclinic	Monoclinic
Space group	<i>C</i> 2/ <i>c</i>	<i>P</i> $\bar{1}$	<i>C</i> 2/ <i>c</i>	<i>P</i> 2 ₁ / <i>n</i>	<i>P</i> 2 ₁ / <i>n</i>
<i>a</i> (Å)	20.857(6)	7.170(3)	22.193(3)	5.390 (1)	5.409 (1)
<i>b</i> (Å)	5.409(2)	9.789(4)	4.598(1)	11.467 (1)	11.634(2)
<i>c</i> (Å)	13.911(4)	12.329(5)	19.397(3)	13.629 (1)	13.556(2)
α (deg)	90.00	81.20 (1)	90.00	90.00	90.00
β (deg)	95.46 (1)	79.76 (1)	103.48 (1)	100.08 (1)	100.57 (1)
γ (deg)	90.00	72.53 (1)	90.00	90.00	90.00
<i>V</i> (Å ³)	1562.3(9)	807.7(6)	1924.8(6)	829.4(2)	838.6(2)
<i>Z</i>	8	2	4	2	2
<i>D</i> _{calc} (g cm ⁻³)	1.337	1.531	1.471	1.475	1.451
<i>T</i> (K)	133(2)	133(2)	273(2)	273(2)	298(2)
λ (Mo-K α)	0.71073	0.71073	0.71073	0.71073	0.71073
μ (mm ⁻¹)	0.100	0.123	0.124	0.115	0.113
2 θ range (deg)	50.52	50.60	50.48	50.48	50.52
Limiting indices	-24 \leq <i>h</i> \leq 22 -6 \leq <i>k</i> \leq 4 -16 \leq <i>l</i> \leq 15	-8 \leq <i>h</i> \leq 8 -11 \leq <i>k</i> \leq 11 -14 \leq <i>l</i> \leq 14	-23 \leq <i>h</i> \leq 26 -5 \leq <i>k</i> \leq 5 -23 \leq <i>l</i> \leq 12	-6 \leq <i>h</i> \leq 6 -13 \leq <i>k</i> \leq 13 -16 \leq <i>l</i> \leq 8	-6 \leq <i>h</i> \leq 6 -13 \leq <i>k</i> \leq 13 -16 \leq <i>l</i> \leq 16
<i>F</i> (000)	672	392	904	388	384
No. of Reflns. Measured	3778	8034	4616	4079	5953
No. Unique Reflns.	1417	2943	1755	1505	1525
No. of Reflns. used	921	2188	1361	1440	1295
No. of Parameters	103	240	157	124	123
GOF on <i>F</i> ²	1.072	1.178	1.142	1.110	1.038
<i>R</i> _{<i>I</i>} [<i>I</i> > 2 σ (<i>I</i>)]	0.0854	0.0926	0.0736	0.0369	0.0408
<i>wR</i> ₂	0.1952	0.2063	0.1482	0.1025	0.1137
Final diff. Fourier map (e ⁻ Å ⁻³) max, min	0.382, -0.345	0.364, -0.385	0.268, -0.282	0.218, -0.198	0.180, -0.203

Table 2.1. Continued.....

	1e	1f	1g	1h	1i
Formula	2(C ₄ H ₈ N ₅): 1(C ₄ O ₄): 1(H ₂ O)	2(C ₄ H ₈ N ₅): 1(C ₅ H ₆ O ₄)	2(C ₄ H ₈ N ₅): 1(C ₄ H ₄ O ₄ S ₁)	2(C ₄ H ₈ N ₅): 1(C ₄ H ₄ O ₅): 1(H ₂ O ₁)	2(C ₄ H ₇ N ₅): 1(C ₆ H ₁₀ O ₄)
Formula Wt.	382.36	382.41	400.44	402.40	396.43
Crystal habit	Rectangular Blocks	Blocks	Rod-Shaped	Rod-Shaped	Rod-Shaped
Crystal color	Colorless	Colorless	Colorless	Colorless	Colorless
Crystal system	Triclinic	Orthorhombic	Orthorhombic	Orthorhombic	Monoclinic
Space group	<i>P</i> $\bar{1}$	<i>Pca</i> 2 ₁	<i>Pca</i> 2 ₁	<i>Fddd</i>	<i>P2</i> ₁ / <i>c</i>
<i>a</i> (Å)	9.368 (1)	30.431(6)	31.408(4)	10.734(2)	10.130(2)
<i>b</i> (Å)	9.909 (1)	5.132 (1)	4.938 (1)	24.449(6)	7.558 (1)
<i>c</i> (Å)	10.807 (1)	11.515(2)	11.596 (1)	27.871(6)	13.244(2)
α (deg)	66.85 (1)	90.00	90.00	90.00	90.00
β (deg)	76.40 (1)	90.00	90.00	90.00	109.71 (1)
γ (deg)	63.14 (1)	90.00	90.00	90.00	90.00
<i>V</i> (Å ³)	820.9(1)	1798.3(6)	1798.5(5)	7314.0(3)	954.6(3)
<i>Z</i>	2	4	4	16	2
<i>D</i> _{calc} (g cm ⁻³)	1.547	1.412	1.479	1.454	1.379
<i>T</i> (K)	273(2)	298(2)	273(2)	273(2)	298(2)
λ (Mo-K α)	0.71073	0.71073	0.71073	0.71073	0.71073
μ (mm ⁻¹)	0.124	0.109	0.224	0.119	0.105
2 θ range(deg)	50.46	50.46	50.48	50.46	50.50
Limiting indices	-11 ≤ <i>h</i> ≤ 11 -11 ≤ <i>k</i> ≤ 11 -12 ≤ <i>l</i> ≤ 12	-35 ≤ <i>h</i> ≤ 36 -6 ≤ <i>k</i> ≤ 6 -9 ≤ <i>l</i> ≤ 13	-28 ≤ <i>h</i> ≤ 37 -5 ≤ <i>k</i> ≤ 5 -13 ≤ <i>l</i> ≤ 13	-12 ≤ <i>h</i> ≤ 10 -29 ≤ <i>k</i> ≤ 25 -33 ≤ <i>l</i> ≤ 30	-12 ≤ <i>h</i> ≤ 10 -8 ≤ <i>k</i> ≤ 9 -15 ≤ <i>l</i> ≤ 15
<i>F</i> (000)	400	808	840	3392	420
No. of Reflns. Measured	6000	8181	8399	8805	4592
No. Unique Reflns	2940	1714	3220	1661	1706
No. of Reflns. used	2603	1539	3078	1310	1492
No. of Parameters	262	286	261	129	164
GOF on F ²	1.193	1.091	1.070	1.171	1.121
<i>R</i> _{<i>I</i>} [<i>I</i> > 2 σ (<i>I</i>)]	0.0582	0.0418	0.0353	0.0898	0.0461
<i>wR</i> ₂	0.1202	0.1005	0.0899	0.1838	0.1246
Final diff. Fourier map (e ⁻ ·Å ⁻³) max, min	0.309, -0.281	0.194, -0.162	0.274, -0.160	0.619, -0.273	0.241, -0.298

Table 2.2. Characteristic hydrogen bond distances (Å) and angles (°) of the **1** and molecular complexes **1a-1i**[#]

Hydrogen Bond, D-H...A	1			1a			1b			1c			1d		
N-H...N	2.12	2.98	173	2.10	2.94	165	2.13	2.99	176	2.20	3.06	175	2.24	3.10	175
	2.16	3.01	175	2.18	3.03	171	2.23	3.02	153						
				2.19	3.04	170									
				2.50	3.36	176									
N-H...O	2.21	3.05	164	2.06	2.91	169	2.02	2.83	157						
	2.24	2.92	136												
N-H...O ⁻				1.88	2.74	174	1.91	2.77	175	1.99	2.80	156	1.99	2.80	157
				1.98	2.75	149				2.05	2.85	156	2.08	2.94	173
				2.06	2.91	166				2.06	2.91	172	2.10	2.91	158
N ⁺ -H...O				1.87	2.73	174									
N ⁺ -H...O ⁻							1.80	2.67	173	1.68	2.64	174	1.78	2.64	176
O-H...N	1.97	2.79	172	1.83	2.64	170									
O-H...O							1.83	2.75	175						
							2.00	2.91	162						
O-H...O ⁻				1.87	2.59	147	1.88	2.79	168						
							1.92	2.76	165						
C-H...N										2.64	3.55	156	2.68	3.45	140
C-H...O ⁻										2.51	3.42	159	2.58	3.51	164

[#] Three columns for each structure represent H...A, D...A distances and D-H...A angle, respectively for a typical hydrogen bond, being represented as D-H...A

Table 2.2. Continued.....

Hydrogen Bond, D-H...A	1e			1f			1g			1h			1i		
N-H...N	2.17	3.03	178	2.10	3.05	172	2.14	3.00	176	2.16	3.01	174	2.09	3.00	176
	2.17	3.03	178	2.12	2.99	172	2.17	3.03	176	2.24	3.09	169			
	2.18	3.04	172												
N-H...O	1.97	2.74	148							2.20	2.92	142	2.10	2.93	173
													2.21	3.07	174
													2.26	3.08	156
N-H...O ⁻	1.99	2.83	169	1.95	2.80	170	1.99	2.81	159	2.01	2.86	171			
	2.10	2.95	171	2.06	2.91	160	2.02	2.88	169						
	2.18	2.81	130	2.07	2.87	154	2.04	2.88	155						
	2.28	3.13	173	2.07	2.88	152	2.07	2.84	149						
	2.47	3.15	137	2.11	2.87	148	2.13	2.94	156						
				2.34	3.03	146	2.62	3.35	144						
N ⁺ -H...O ⁻	1.74	2.67	165	1.72	2.58	176	1.76	2.62	176	1.76	2.61	171			
	1.81	2.71	176	1.80	2.66	178	1.78	2.64	176						
O-H...N													1.68	2.65	171
O-H...O ⁻	1.88	2.74	169												
	2.15	2.88	143												
C-H...N													2.48	3.29	141
C-H...O	2.54	3.48	168												
C-H...O ⁻				2.43	3.34	158	2.48	3.35	150						
							2.49	3.24	135						

Three columns for each structure represent H...A, D...A distances and D-H...A angle, respectively for a typical hydrogen bond, being represented as D-H...A

Table 2.4. Crystallographic data for the molecular complexes **2b-2i**

	2b	2c	2d	2e
Formula	(C ₉ H ₁₀ N ₅): (C ₃ H ₃ O ₄)	2(C ₉ H ₁₀ N ₅): 2(C ₄ H ₃ O ₄)	2(C ₉ H ₁₀ N ₅): (C ₄ O ₄) : 4(H ₂ O)	2(C ₉ H ₉ N ₅): (C ₄ H ₄ O ₄)
Formula Wt.	291.27	606.57	560.54	490.50
Crystal habit	Plate	Blocks	Rod-Shaped	Blocks
Crystal color	Colorless	Colorless	Colorless	Colorless
Crystal system	Monoclinic	Orthorhombic	Monoclinic	Monoclinic
Space group	<i>P2₁/c</i>	<i>Pca2₁</i>	<i>C2/c</i>	<i>P2₁/c</i>
<i>a</i> (Å)	8.314(7)	8.541(2)	7.366 (1)	6.716(4)
<i>b</i> (Å)	5.126 (5)	14.221(3)	20.169 (2)	26.184(2)
<i>c</i> (Å)	29.126(3)	23.174(5)	17.965 (2)	12.511(8)
α (deg)	90.00	90.00	90.00	90.00
β (deg)	93.37(1)	90.00	94.13 (1)	90.29 (1)
γ (deg)	90.00	90.00	90.00	90.00
<i>V</i> (Å ³)	1239.2(2)	2814.8(1)	2662.0(5)	2200.0(2)
<i>Z</i>	4	4	4	4
<i>D_{calc}</i> (g cm ⁻³)	1.561	1.431	1.399	1.481
<i>T</i> (K)	120(2)	298(2)	273(2)	140(2)
λ (Mo-K α)	0.71073	0.71073	0.71073	0.71073
μ (mm ⁻¹)	0.121	0.110	0.109	0.108
2 θ range (deg)	50.00	50.50	50.48	50.78
Limiting indices	-9 \leq h \leq 9 -6 \leq k \leq 4 -34 \leq l \leq 34	-10 \leq h \leq 10 -16 \leq k \leq 17 -27 \leq l \leq 27	-8 \leq h \leq 8 -24 \leq k \leq 24 -21 \leq l \leq 21	-7 \leq h \leq 8 -31 \leq k \leq 31 -14 \leq l \leq 14
<i>F</i> (000)	608	1264	1176	1024
No. of Reflns. Measured	7144	19374	15853	15468
No. Unique Reflns.	2184	5062	2406	3985
No. of Reflns. used	1509	4324	1614	3614
No. of Parameters	191	475	222	321
GOF on F ²	0.985	1.031	1.581	3.699
<i>R_I</i> [<i>I</i> > 2 σ (<i>I</i>)]	0.0429	0.0490	0.0712	0.2018
<i>wR₂</i>	0.0995	0.1201	0.2193	0.5122
Final diff. Fourier map (e ⁻ ·Å ⁻³) max, min	0.214, -0.261	0.180, -0.231	1.114, -0.489	1.221, -1.099

Table 2.4. Continued.....(Crystallographic data for the molecular complexes **2e-2h**)

	2f	2g	2h	2i
Formula	2(C ₉ H ₉ N ₅) : (C ₄ H ₆ O ₄)	2(C ₉ H ₉ N ₅): (C ₅ H ₈ O ₄)	2(C ₉ H ₉ N ₅): (C ₄ H ₆ O ₅)	2(C ₉ H ₉ N ₅): (C ₆ H ₁₀ O ₄)
Formula Wt.	492.51	506.54	508.51	520.56
Crystal habit	Rectangular Blocks	Blocks	Plates	Rectangular Blocks
Crystal color	Colorless	Colorless	Colorless	Colorless
Crystal system	Triclinic	Monoclinic	Orthorhombic	Monoclinic
Space group	<i>P</i> $\bar{1}$	<i>Cc</i>	<i>Pccn</i>	<i>C2/c</i>
<i>a</i> (Å)	6.777 (2)	20.790(8)	12.311(4)	29.848(6)
<i>b</i> (Å)	8.102 (4)	13.308(5)	25.757(8)	7.212 (1)
<i>c</i> (Å)	11.878 (4)	27.702 (1)	7.477(2)	12.098(2)
α (deg)	90.57(2)	90.00	90.00	90.00
β (deg)	101.46 (1)	111.09(1)	90.00	96.13 (1)
γ (deg)	114.53 (1)	90.00	90.00	90.00
<i>V</i> (Å ³)	578.4(4)	7151.0(5)	2370.9(1)	2589.4(8)
<i>Z</i>	1	12	4	4
<i>D</i> _{calc} (g cm ⁻³)	1.414	1.411	1.425	1.335
<i>T</i> (K)	298(2)	120(2)	273(2)	273(2)
λ (Mo-K α)	0.71073	0.71073	0.71073	0.71073
μ (mm ⁻¹)	0.103	0.102	0.106	0.096
2 θ range (deg)	50.50	50.00	50.46	50.48
Limiting indices	-8 ≤ <i>h</i> ≤ 8 -9 ≤ <i>k</i> ≤ 9 -14 ≤ <i>l</i> ≤ 14	-27 ≤ <i>h</i> ≤ 27 -17 ≤ <i>k</i> ≤ 13 -29 ≤ <i>l</i> ≤ 36	-12 ≤ <i>h</i> ≤ 14 -30 ≤ <i>k</i> ≤ 28 -8 ≤ <i>l</i> ≤ 8	-35 ≤ <i>h</i> ≤ 35 -8 ≤ <i>k</i> ≤ 8 -14 ≤ <i>l</i> ≤ 14
<i>F</i> (000)	258	3192	1064	1096
No. of Reflns. Measured	8150	24331	11071	8579
No. Unique Reflns.	2085	8869	2146	2330
No. of Reflns. used	1531	7141	1751	1451
No. of Parameters	209	1006	216	229
GOF on F ²	1.049	1.025	1.125	1.099
<i>R</i> ₁ [<i>I</i> >2 σ (<i>I</i>)]	0.0393	0.0499	0.0564	0.0597
<i>wR</i> ₂	0.1030	0.1089	0.1228	0.1418
Final diff. Fourier map (e ⁻ .Å ⁻³) max, min	0.144, -0.243	0.240, -0.303	0.139, -0.214	0.397, -0.401

Table 2.5. Characteristic hydrogen bond distances (Å) and angles (°) of the **2** and molecular complexes **2b-2i**

D-H...A	2b			2c			2d			2e		
N-H...N	2.16	3.02	166	2.11	3.05	163	2.11	2.99	170	2.14	2.99	166
				2.17	3.07	172	2.28	3.08	165	2.14	2.99	168
										2.17	3.01	166
										2.19	3.04	168
N-H...O	1.97	2.85	176	2.09	2.84	139				2.04	2.82	150
	2.21	2.98	146	2.14	2.99	172				2.10	2.89	153
				2.15	2.87	136						
				2.15	3.00	170						
N-H...O ⁻	1.94	2.81	168	1.95	2.80	170	1.99	2.83	168			
				1.98	2.84	171	2.11	2.91	160			
N ⁺ -H...O ⁻	1.92	2.78	166	1.84	2.77	173	1.82	2.74	169			
				1.97	2.78	172						
O-H...N										1.64	2.68	159
										1.85	2.67	173
O-H...O ⁻	1.68	2.46	155	1.53	2.44	168						
				1.63	2.44	172						
C-H...O	2.58	3.42	147				2.57	3.42	144			
C-H...O ⁻	2.31	3.24	166	2.30	3.16	153	2.36	3.19	137			
	2.73	3.49	138y	2.31	3.10	154						

Table 2.5. Continued.....

D-H...A	2f			2g			2h			2i		
N-H...N	2.22	3.10	166	2.09	2.97	174	2.12	3.01	169	2.11	3.00	178
	2.36	3.21	162	2.11	2.99	174	2.15	3.02	175	2.24	3.15	171
				2.14	3.01	170						
				2.15	3.00	164						
				2.16	3.01	163						
				2.16	3.03	171						
				2.18	3.04	167						
				2.18	3.05	175						
				2.19	3.01	156						
				2.19	3.06	176						
				2.21	3.04	156						
				2.25	3.11	167						
N-H...O	2.09	2.96	173	1.94	2.81	171	2.03	2.92	166	2.12	2.93	172
				1.95	2.82	170				2.37	3.02	124
				1.96	2.84	173						
				2.02	2.89	171						
				2.08	2.94	165						
				2.17	3.03	165						
O-H...N	1.85	2.66	170	1.76	2.59	169	1.73	2.67	170	1.90	2.68	167
				1.78	2.61	167						
				1.83	2.66	169						
				1.83	2.66	170						
				1.85	2.68	173						
				1.92	2.76	172						

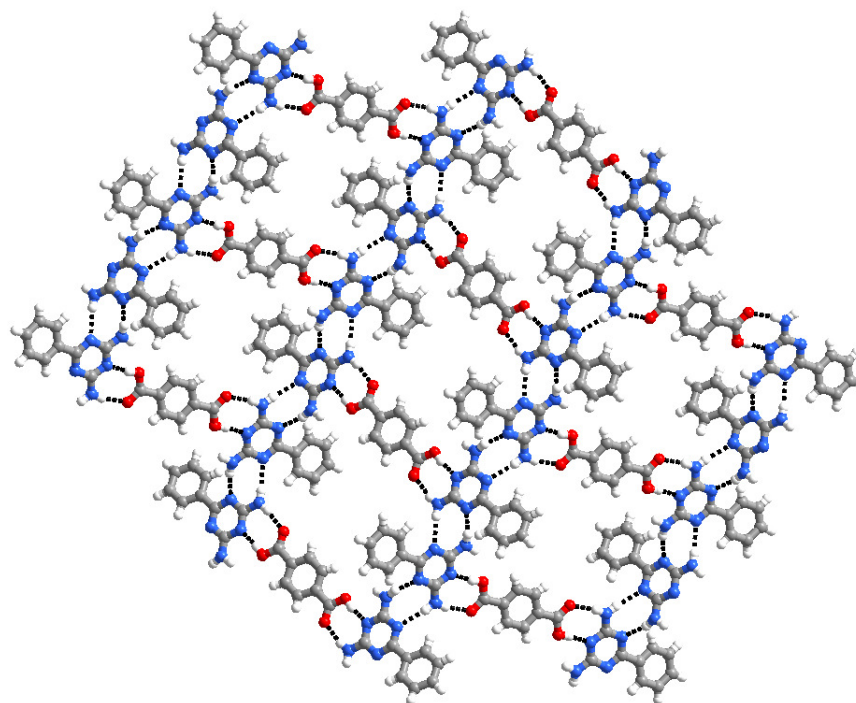
2.6 References

- (1) (a) Whitesides, G. M.; Simanek, E. E.; Mathias, J. P.; Seto, C. T.; Chin, D. N.; Mammen, M.; Gordon, D. M. *Acc. Chem. Res.* **1995**, *28*, 37-44. (b) Seto, C. T.; Whitesides, G. M. *J. Am. Chem. Soc.* **1990**, *112*, 6409-6411. (c) Whitesides, G. M.; Mathias, J. P.; Seto, C. T. *Science* **1991**, *254*, 1312-1319. (d) MacDonald, J. C.; Whitesides, G. M. *Chem. Rev.* **1994**, *94*, 2383-2420. (e) Pedireddi, V. R.; Belhekar, D. *Tetrahedron* **2002**, *58*, 2937-2941. (f) Marivel, S.; Suresh, E.; Pedireddi, V. R. *Tetrahedron Lett.* **2008**, *49*, 3666-3671. (g) Barnett, S. A.; Blake, A. J.; Champness, N. R. *CrystEngComm* **2003**, *5*, 134-136.
- (2) (a) Pedireddi, V. R.; Chatterjee, S.; Ranganathan, A.; Rao, C. N. R. *J. Am. Chem. Soc.* **1997**, *119*, 10867-10868. (b) Ranganathan, A.; Pedireddi, V. R.; Chatterjee, S.; Rao, C. N. R. *J. Mater. Chem.* **1999**, *9*, 2407-2411. (c) Ranganathan, A.; Pedireddi, V. R.; Rao, C. N. R. *J. Am. Chem. Soc.* **1999**, *121*, 1752-1753. (d) Ahn, S.; Prakashreddy, J.; Kariuki, B. M.; Chatterjee, S.; Ranganathan, A.; Pedireddi, V. R.; Rao, C. N. R.; Harris, K. D. M. *Chem. Eur. J.* **2005**, *11*, 2433-2439. (e) Guo, F.; Cheung, E. Y.; Harris, K. D. M.; Pedireddi, V. R. *Cryst. Growth Des.* **2006**, *6*, 846-848. (f) Krepps, M. K.; Parkin, S.; Atwood, D. A. *Cryst. Growth Des.* **2001**, *1*, 291-297.
- (3) (a) Lange, R. F. M.; Beijer, F. H.; Sijbesma, R. P.; Hooft, R. W. W.; Kooijman, H.; Spek, A. L.; Kroon, J.; Meijer, E. W. *Angew. Chem., Int. Ed.* **1997**, *36*, 969-971. (b) Tukada, H.; Mazaki, Y. *Chem. Lett.* **1997**, 411-442. (c) Kulkarni, G. U.; Thomas, R. *Beilstein J. Org. Chem.* **2007**, *17*, 1-4. (d) Lazar, A. N.; Danylyuk, O.; Suwinska, K.; Coleman, A. W. *New J. Chem.* **2006**, *30*, 59-64. (e) Karle, I;

- Gilardi, R. D.; Chandrashekhar Rao.; Muraleedharan, K. M.; Ranganathan, S. J. *Chem. Cryst.* **2006**, *33*, 727-749.
- (4) (a) Whitesides, G. M.; Mathias, J. P.; Seto, C. T. *Science* **1991**, *254*, 1312-1319.
(b) Bielejewska, A.; Marjo, C. E.; Prins, L. J.; Timmerman, P.; Jong, F. D.; Reinhoudt, D. N. *J. Am. Chem. Soc.* **2001**, *123*, 7518-7533. (c) Ranganathan, A.; Pedireddi, V. R.; Rao, C. N. R. *J. Am. Chem. Soc.* **1999**, *121*, 1752-1753.
- (5) (a) Zerkowski, J. A.; Seto, C. T.; Whitesides, G. M. *J. Am. Chem. Soc.* **1992**, *114*, 5473-5475. (b) Mathias, J. P.; Seto, C. T.; Simanek, E. E.; Whitesides, G. M. *J. Am. Chem. Soc.* **1994**, *116*, 1725-1736.
- (6) Mascal, M.; Hext, N. M.; Warmuth, R.; Moore, M. H.; Turkenburg, J. P. *Angew. Chem., Int. Ed.* **1996**, *35*, 2203-2206.
- (7) Zerkowski, J. A.; Seto, C. T.; Wierda, D. A.; Whitesides, G. M. *J. Am. Chem. Soc.* **1990**, *112*, 9025-9026.
- (8) Zerkowski, J. A.; Whitesides, G. M. *J. Am. Chem. Soc.* **1994**, *116*, 4298-4304.
- (9) Hursthouse, M.B.; T.Gelbrich, T.; Platerv. M. J. *Private Communication* **2003**.
- (10) Ranganathan, A.; Pedireddi, V. R.; Chatterjee, S.; Rao, C. N. R. *J. Mater. Chem.* **1999**, *9*, 2407-2411.
- (11) (a) Johnson, S.L.; Rumon, K. A. *J. Phys. Chem.* **1965**, *69*, 74. (b) Lynch, D. E.; McClenaghan, I. *Acta Crystallogr.* **2001**, *57*, 830. (c) Huang, K. -S.; Britton, D.; Etter M. C.; Byrn, S. R. *J. Mater. Chem.* **1997**, *7*, 713 (d) Vishweshwar, P.; Nangia, A.; Lynch, V. M. *J. Org. Chem.* **2002**, *67*, 556 (e) Lynch, D. E.; Jones, G. D. *Acta Crystallogr.* **2004**, *B60*, 748. (f) Bhogala, B. R.; Basavoju, S.; Nangia, A. *CrystEngComm* **2005**, *7*, 551-562.

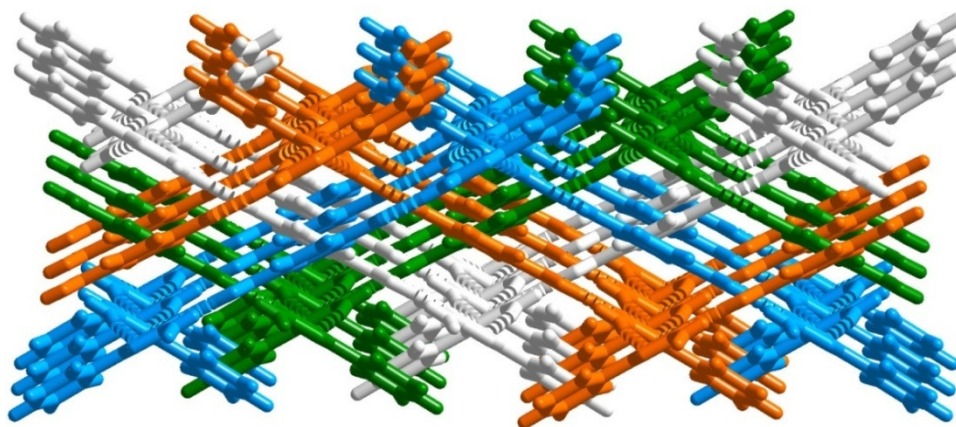
- (12) (a) Aakeröy, C. B.; Desper, J.; Urbina, J. F. *Chem. Commun.* **2005**, 2820-2822. (b) Aakeröy, C. B.; Beatty, A. M.; Helfrich, B. A. *Angew. Chem., Int. Ed.* **2001**, *40*, 3240-3242. (c) Aakeröy, C. B.; Salmon, D. J. *CrystEngComm* **2005**, *7*, 439-448. (d) Aakeröy, C. B.; Beatty, A. M.; Helfrich, B. A.; Nieuwenhuyzen *Cryst. Growth Des.* **2003**, *3*, 159-165.
- (13) (a) MacGillivray, L. R.; Papaefstathiou, G. S.; Friščić, T.; Hamilton, T. D.; Buiar, D. K.; Chu, Q.; Varshney, D. B.; Georgiev, I. G. *Acc. Chem. Res.* **2008**, *41*, 280-291. (b) Fujita, M.; Tominaga, M.; Hori, A.; Therrien, B. *Acc. Chem. Res.* **2005**, *38*, 369-378. (c) Arora, K. K.; Pedireddi, V. R. *J. Org. Chem.* **2003**, *68*, 9177-9185. (d) Kepert, C. J. *Chem. Commun.* **2006**, 695-700. (e) Pedireddi, V. R.; Jones, W.; Chorlton, A. P.; Docherty, R. *Tetrahedron Lett.* **1998**, *39*, 5409-5412. (f) Thaimattam, R.; Xue, F.; Sarma, J. A. R. P.; Mak, T. C. W.; Desiraju, G. R. *J. Am. Chem. Soc.* **2001**, *123*, 4432-4445. (g) Kawano, S.-I.; Fujita, N.; Shinkai, S. *Chem. Commun.* **2003**, 1352-1353.
- (14) Aghabozorg, H.; Ghadermazi, M.; Sadr-jhanlou, E. *Anal.Sci.* **2006**, *22*, x255-x256.
- (15) (a) Batten, S. R.; Robson, R. *Angew. Chem., Int. Ed.* **1998**, *37*, 1461-1494. (b) Maly, K. E.; Gagnon, E.; Maris, T.; Wuest, J. D. *J. Am. Chem. Soc.* **2007**, *129*, 4306-4322. (c) Sauriat-Dorizon, H.; Maris, T.; Wuest, J. D.; Enright, G. D. *J. Org. Chem.* **2003**, *68*, 240-246. (d) Mallinson, P. R.; Smith, G. T.; Wilson, C. C.; Grech, E.; Wozniak, K. *J. Am. Chem. Soc.* **2003**, *125*, 4259-4270. (e) Metrangolo, P.; Meyer, F.; Pilati, T.; Proserpio, D. M.; Resnati, G. *Chem. Eur. J.* **2007**, *13*, 5765-5772.

- (16) (a) Siemens, SMART System, Siemens Analytical X-ray Instrument Inc., Madison, WI (USA), 1995; (b) G. M. Sheldrick, SADABS Siemens Area Detector Absorption Correction Program, University of Gottingen, Gottingen, Germany, 1994; (c) G. M. Sheldrick, SHELXTL-PLUS program for crystal structure solution and refinement, University of Gottingen, Gottingen, Germany.
- (17) A. L. Spek, PLATON, molecular geometry program, University of Utrecht, The Netherlands, 1995.



CHAPTER THREE

SUPRAMOLECULAR ASSEMBLIES OF SOME AMINOTRIAZINES AND 2,4,6-TRIAMINOPYRIMIDINE WITH ARYL AND ARALKYL CARBOXYLIC ACIDS



3.1 Introduction

Aminotriazines are well explored in supramolecular chemistry, due to their tendency to form strong hydrogen bonds by interacting with molecules of same kind or with the molecules containing complimentary functional groups. Wuest and co-workers utilized such ability of aminotriazines to self-assemble through intermolecular interactions, in particularly, by N-H...N hydrogen bonds to prepare numerous exotic architectures.¹ For example, the molecules of 1,2,4,5-tetrakis(4-(2,4-diamino-1,3,5-triazin-6-yl)phenyl)-3,6-diphenylbenzene self-assemble to form rectangular structure with cavities (Figure 3.1), while the molecules of hexakis(4-(2,4-diamino-1,3,5-triazin-6-yl)phenyl)benzene self-assemble to form triangular architecture with voids, as shown in Figure 3.2.

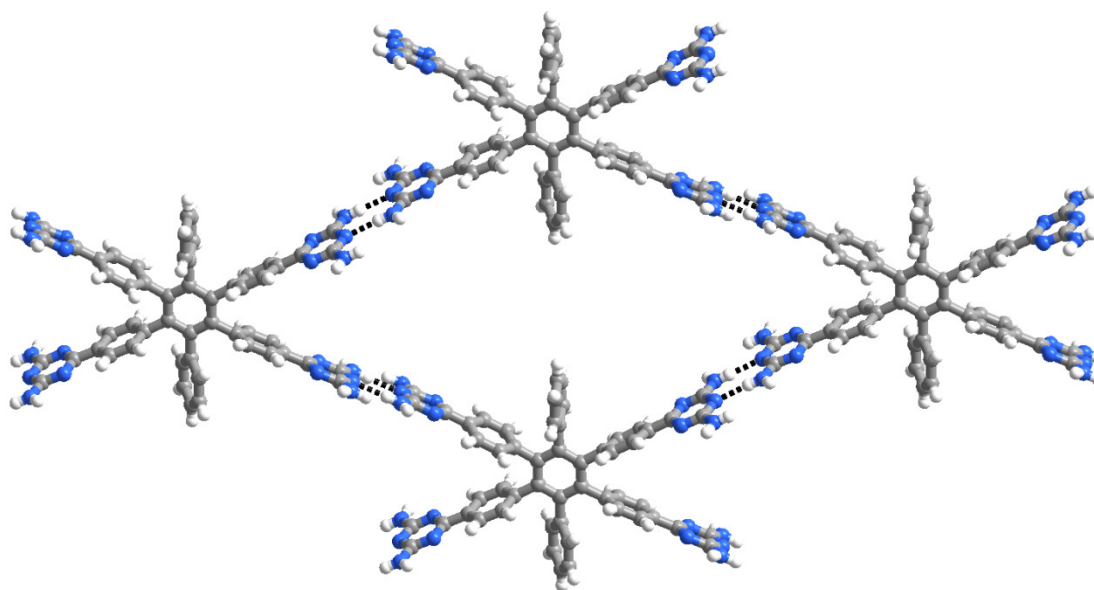


Figure 3.1. Aminotriazine molecules interacting with each other to form a rectangular cavity structure.

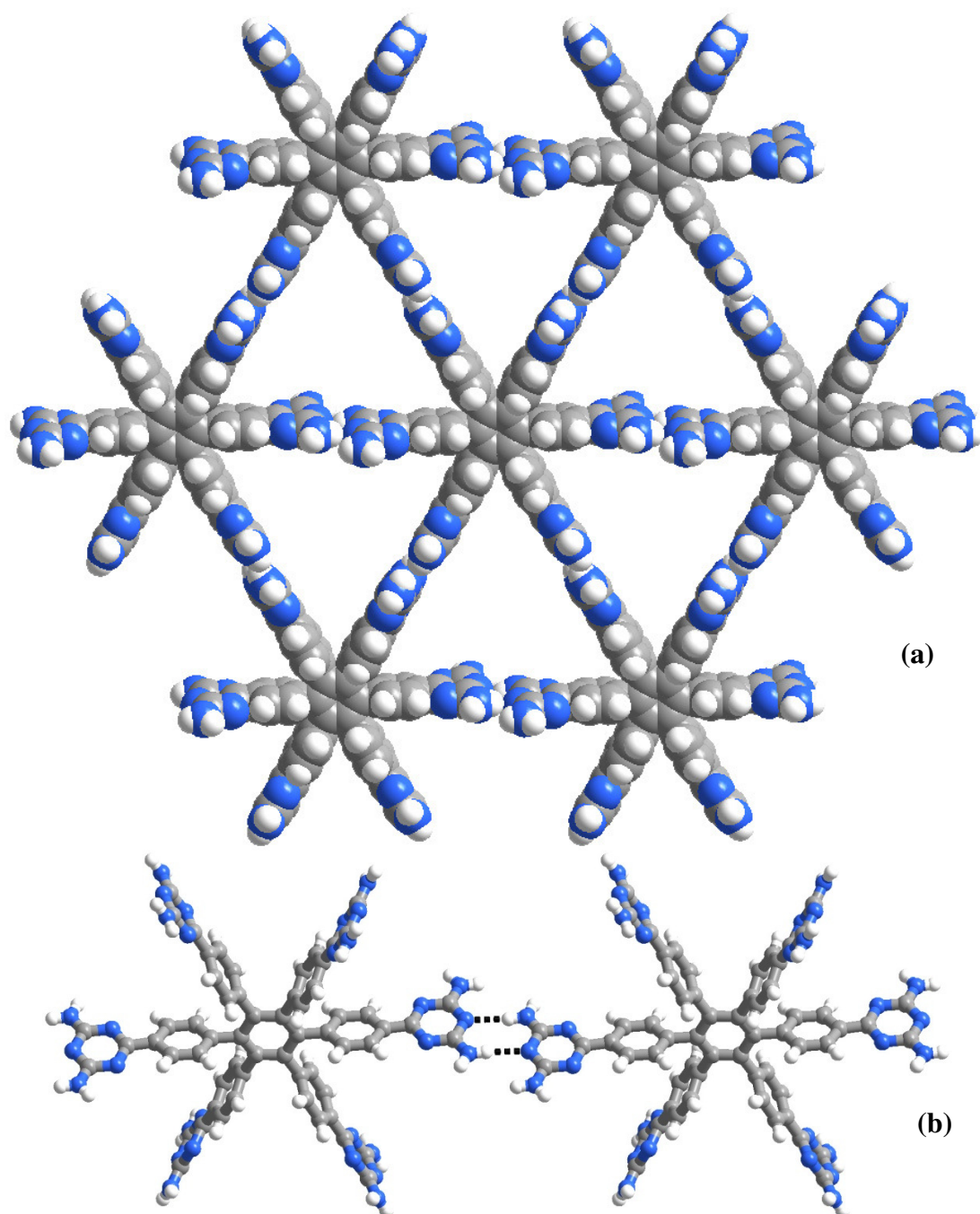
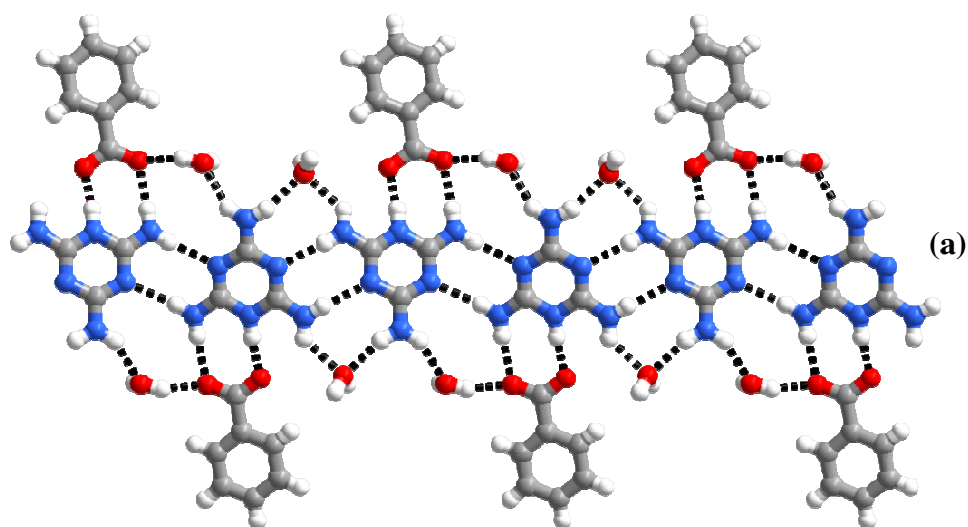


Figure 3.2. (a) Self-assembly of aminotriazine molecules to form a triangular architecture with cavities. (b) Annotation of interaction observed between the molecules of aminotriazines.

Janczak and co-workers reported a molecular complex between melamine and benzoic acid,² utilizing the ability of melamine to form hydrogen bonds with the molecules containing carboxylic acid functional groups. In the crystal structure of complex formed between melamine and benzoic acid, proton transfer takes place from benzoic acid molecules to melamine. The molecules of melaminium interact with each other by N-H \cdots N hydrogen bonds, forming tapes and the molecules of benzoate interact with those tapes by pairwise N⁺-H \cdots O⁻ and N-H \cdots O⁻ hydrogen bonds like pendants, as shown in Figure 3.3(a). Similar structure was observed even in the complex of melamine and phthalic acid as shown in Figure 3.3(b).³



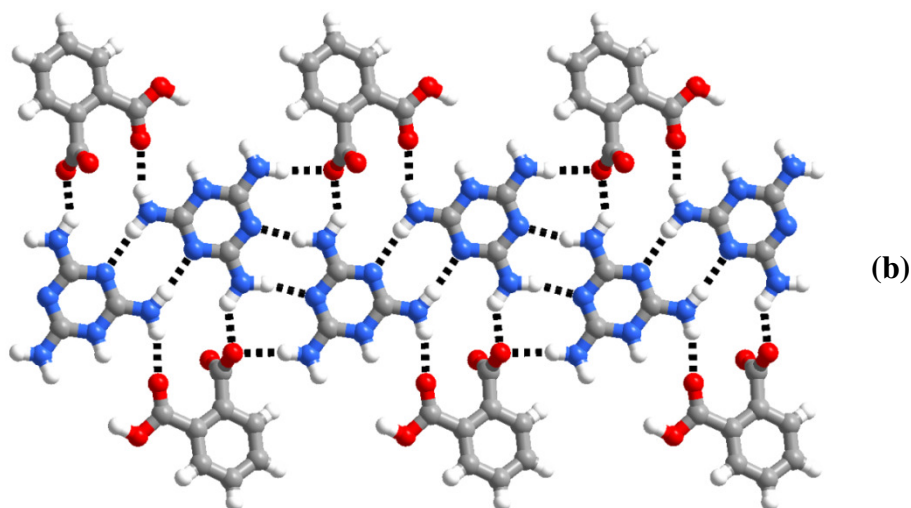


Figure 3.3. Tape structure observed in the complex between (a) Melamine and benzoic acid and (b) Melamine and phthalic acid.

However, in the molecular complex between melamine and isophthalic acid,⁴ melaminium and isophthalate aggregate by pairwise $\text{O-H}\cdots\text{N}$, $\text{N-H}\cdots\text{O}$ and $\text{N}^+-\text{H}\cdots\text{O}^-$, $\text{N-H}\cdots\text{O}^-$ hydrogen bonds, which extends, in two dimensions, forming six member host network, with void space of dimensions $12.5 \times 8.5 \text{ \AA}^2$, which is being filled by water molecules, as shown in Figure 3.4.

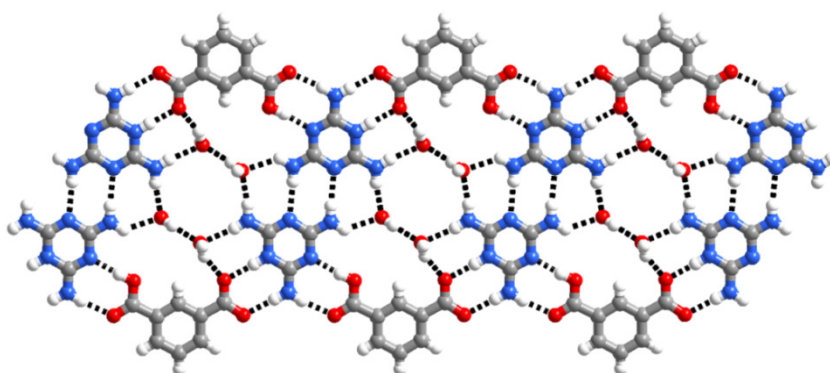


Figure 3.4. Host-guest network formed by melamine and isophthalic acid.

Yao and co-workers reported the formation of a molecular complex between melamine and terephthalic acid,⁵ in which melaminium ions interact with each other as

dimers by N-H \cdots N hydrogen bonds. Such dimers further interact with terephthalate molecules by N⁺-H \cdots O⁻ and N-H \cdots O⁻ hydrogen bonds (see Figure 3.5).

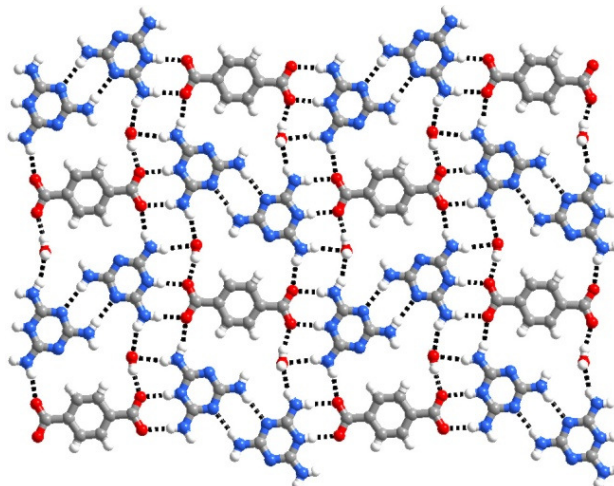


Figure 3.5. Supramolecular network formed by melamine and terephthalic acid

Chen and co-workers reported the host-guest complex formed between melamine and trimesic acid,⁶ which is quite intriguing with the formation of two types of voids. In this complex also proton transfer takes place from the molecules of trimesic acid to the molecules of the melamine. The melaminium ions form dimers, by N-H \cdots N hydrogen bonds, which are being held together by trimesic acid through O-H \cdots N, N-H \cdots O and N⁺-H \cdots O⁻, N-H \cdots O⁻ hydrogen bonds, leading to the formation of a cyclic host network, with void space of $11.0 \times 9.0 \text{ \AA}^2$ dimensions, which is being filled by four water molecules. Further, such ensembles are aggregated in the extended network through O-H \cdots O⁻ hydrogen bonds, thus, creating a network with empty space of $11.9 \times 8.1 \text{ \AA}^2$ dimensions, which is also filled by water molecules, as shown in Figure 3.6.

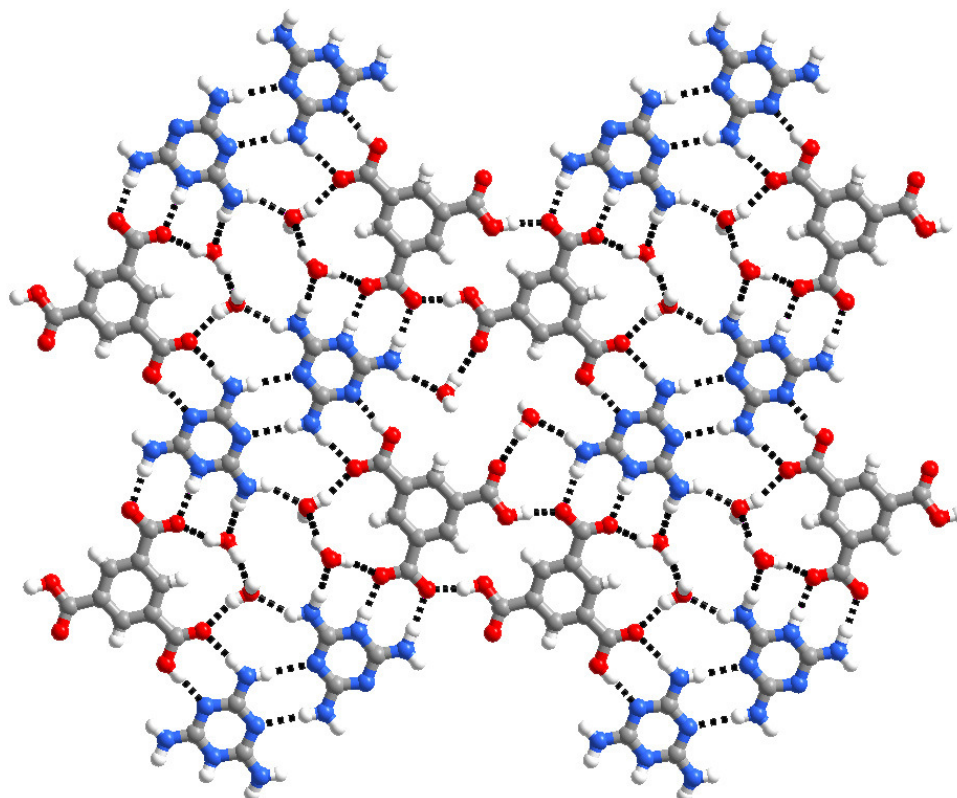


Figure 3.6. Host-guest network formed by melamine and trimesic acid.

Karle and co-workers prepared a molecular complex between melamine and mellitic acid,⁷ in which also melaminium ions in the form of dimers, held together by N-H \cdots N hydrogen bonds, interact with carboxylates, yielding a six member cyclic host network. Such an association creates cavities of $12.0 \times 9.4 \text{ \AA}^2$ dimensions, which are being filled by water molecules (Figure 3.7).

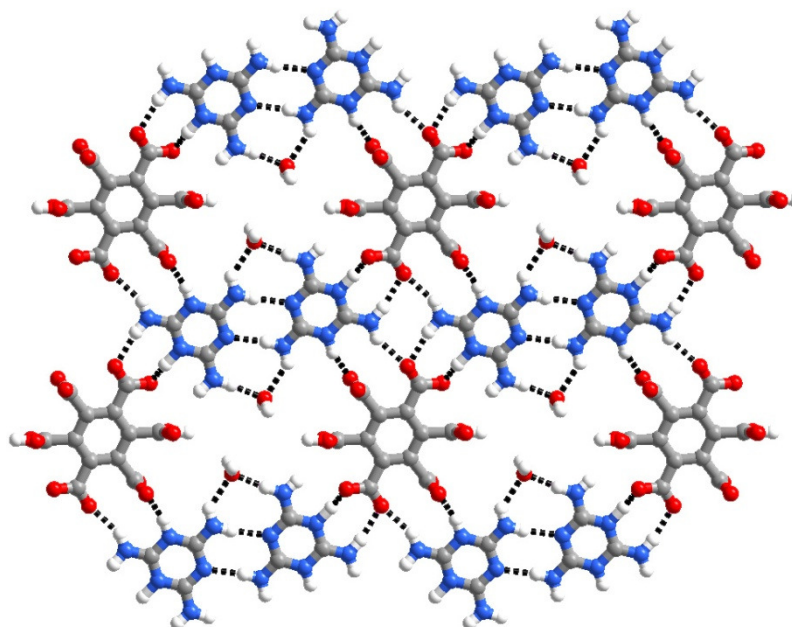


Figure 3.7. Host-guest network formed by melamine and mellitic acid.

In addition to melamine, its geometrical analogue, 2,4,6-triaminopyrimidine is also well utilized in the design of exotic supramolecular architectures. Pedireddi and co-workers reported complexes of 2,4,6-triaminopyrimidine with various aliphatic dicarboxylic acid,⁸ addressing systematic variation in the assemblies with respect to the chain length of aliphatic dicarboxylic acids. In a typical example, formation of a molecular complex between 2,4,6-triaminopyrimidine and thiodiglycolic acid proceeds through proton transfer and establishing interaction between the co-crystallized ligands by both $N^+-H\cdots O^-$ and $N-H\cdots O^-$ hydrogen bonds. Thus, a six membered host network is formed with void space, being filled by solvent of crystallization, methanol, as shown in Figure 3.8.

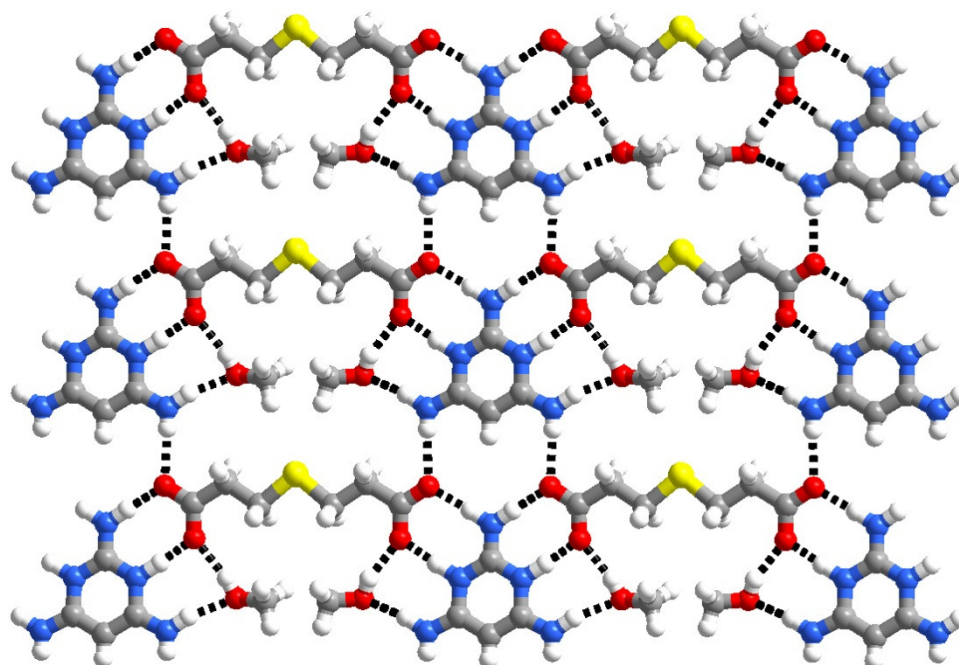


Figure 3.8. Host-guest network formed by triaminopyrimidine and thiodiglycolic acid.

Considering the elegance and systematics in the structures reported in the literature, as described above, it is apparent that numerous structures of aromatic carboxylic acids as co-crystal formers are well explored, in particular, in association with melamine. Thus, taking into account the exotic host-guest structures, reported in the Chapter 1, obtained by co-crystallization of 2,4,-diamino-6-methyl-1,3,5-triazine and 2,4,-diamino-6-phenyl-1,3,5-triazine (geometrical analogues of melamine) with different aliphatic carboxylic acids, a study of supramolecular architecture of those triazines with aryl and arylalkyl carboxylic acids would also be of great significance for through understanding of variations in the nature of intermolecular interactions that may be influenced different substituents like $-\text{CH}_3$, phenyl etc. For this purpose, co-crystallization studies of 2,4,-diamino-6-methyl-1,3,5-triazine and 2,4,-diamino-6-phenyl-1,3,5-triazine with different aromatic acids, as listed in Chart 1, have been

carried out. The structural features of the complexes/adducts/co-crystals would be discussed in the following sections.

Chart 1			Reactants	Products and ratio
<p>2,4-diamino-6-methyl-1,3,5-triazine (1)</p> <p>2,4-diamino-6-phenyl-1,3,5-triazine (2)</p> <p>2,4,6-triamino-pyrimidine (3)</p> <p>benzoic acid (a)</p> <p>phthalic acid (b)</p> <p>isophthalic acid (c)</p> <p>terephthalic acid (d)</p> <p>1,3-phenylenediacetic acid (e)</p> <p>1,4-phenylenediacetic acid (f)</p>			1 + a	1a, 2:2:1H ₂ O
			1 + b	1b, 1:1
			1 + c	1c, 2:1:1CH ₃ OH
			1 + d	1d, 2:1:2 H ₂ O
			1 + e	1e, 1:1
			2 + a	2a, 1:1
			2 + b	2b, 1:1
			2 + c	2c, 1:1
			2 + d	2d, 2:1
			2 + e	2e, 2:1
			2 + f	2f, 2:1
			3 + b	3b, 1:1:2 H ₂ O
			3 + d	3d, 2:1:2H ₂ O
			3 + e	3e, 1:1
			3 + f	3f, 1:1

3.2 Supramolecular assemblies of 2,4-diamino-6-methyl-1,3,5-triazine with aryl and arylalkyl carboxylic acids

Co-crystals of 2,4-diamino-6-methyl-1,3,5-triazine, **1** with various carboxylic acids (see Chart 1) have been prepared, by co-crystallization of the respective complementary compounds, from methanol, at ambient condition, by slow evaporation process. All the complexes, thus, obtained, have been analyzed by single crystal X-ray diffraction method and the structural description is illustrated in the following sections.

3.2.1 Supramolecular assembly of 2,4-diamino-6-methyl-1,3,5-triazine with benzoic acid-1a

Co-crystallization of **1** and benzoic acid gave a complex **1a**, in a 1:1 ratio along with water molecules, (Table 3.1), as shown in the Figure 3.9(a). Asymmetric unit has two symmetry independent molecules each of **1** and benzoic acid, without any proton transfer from the acid to triazine. In three dimensional packing, it forms a layered structure, as shown in Figure 3.9(b)

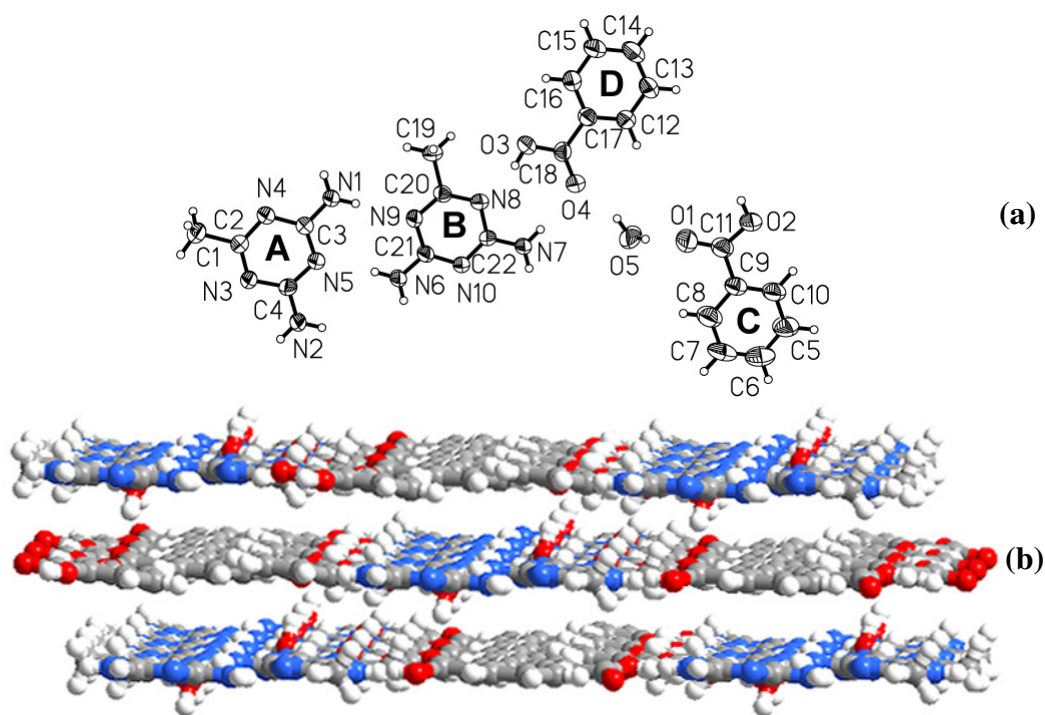


Figure 3.9. (a) ORTEP diagram of the complex **1a**. (b) Layered packing observed in the complex **1a**.

Detailed analysis of a typical layer reveals that, aggregation of discrete tapes leads to the formation of layers. In a typical tape, molecules of triazine **1** are held together by series of N-H \cdots N hydrogen bond patterns, represented in Figure 3.10. Thus, symmetry related molecules (A and B) bound to each other by dimeric N-H \cdots N

hydrogen bonds, with H \cdots N distances of 2.16 and 2.17 Å, yielding dimers of A and B molecules. Such dimers are also further connected to each other by different types of N-H \cdots N hydrogen bonds, with the corresponding distances being 2.11 and 2.12 Å. Such an association ultimately lead to the formation of infinite tapes of molecules of triazines, **1**. Benzoic acid molecules are attached those tapes as pendant moieties, through a pair-wise O-H \cdots N and N-H \cdots O (H \cdots N, 1.79, 1.80 and H \cdots O, 2.06, 2.07 Å) hydrogen bonds, as shown in Figure 3.10. In such an arrangement, water molecules are embedded, connecting to both acid and triazine molecules through O-H \cdots O and N-H \cdots O hydrogen bonds and annotation of these bonds is depicted in Figure 3.10.

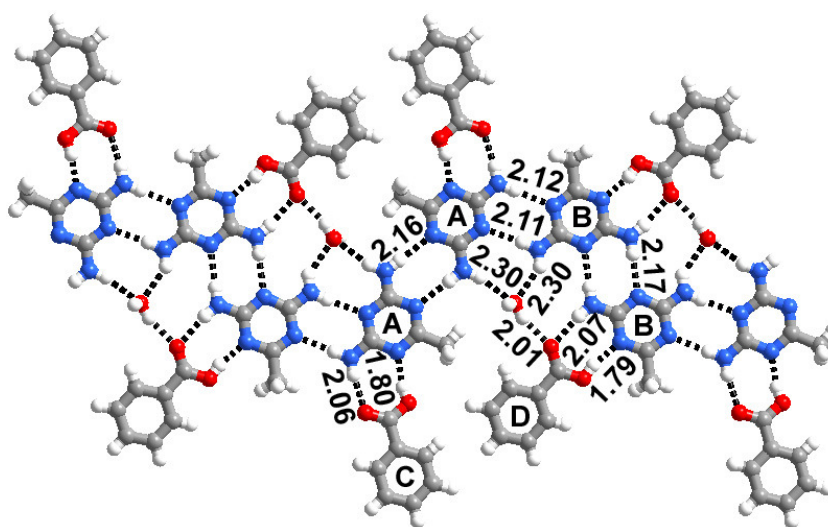


Figure 3.10. Tape structure observed in the complex, **1a**.

3.2.2 Molecular adduct of 2,4-diamino-6-methyl-1,3,5-triazine with phthalic acid-**1b**

Co-crystallization of **1** and phthalic acid from methanol gave a complex, **1b**, in 1:1 ratio of the co-crystallized ligands (Table 3.1), as shown in Figure 3.11(a). In the molecular complex, **1b**, unlike in **1a**, proton transfer takes place from only one of the carboxyl group of phthalic acid to the molecules of **1**, while hydrogen atom on the

second -COOH group is involved in an intramolecular hydrogen bond formation. In the three dimensional packing, molecules in **1b**, form a stacked sheet structure (Figure 3.11(b)).

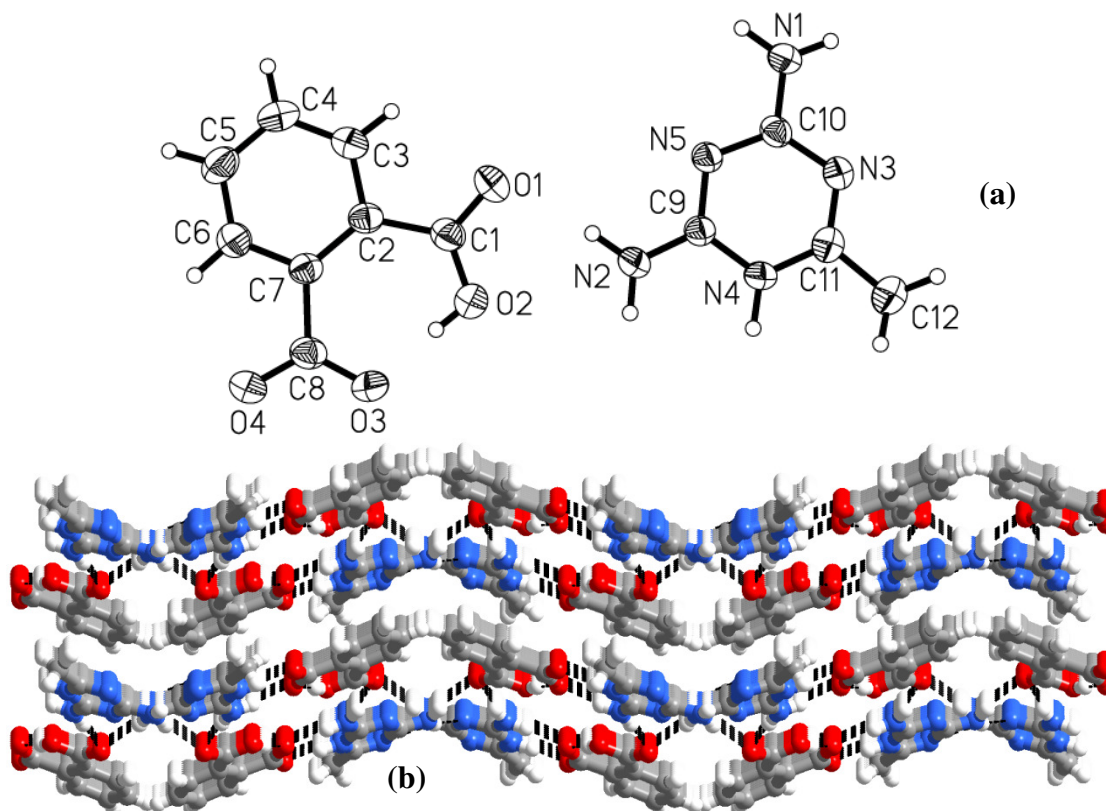


Figure 3.11. (a) ORTEP diagram of the complex **1b**. (b) Packing of layers observed in the complex, **1b**.

The recognition pattern shows that the molecules of **1** and phthalic are held together by $\text{N}^+\text{-H}\cdots\text{O}^-$ and $\text{N-H}\cdots\text{O}^-$ hydrogen bonds ($\text{H}\cdots\text{O}$, 1.71 and 2.00 Å) and such binary components are further connected to each other by $\text{N-H}\cdots\text{O}$ ($\text{H}\cdots\text{O}$, 2.04 Å) hydrogen bonds, yielding tetramers, as shown in Figure 3.12(a). The tetramers, thus, formed interact with neighboring units by $\text{N-H}\cdots\text{N}$ hydrogen bonds ($\text{H}\cdots\text{N}$, 2.11 Å) and

by N-H \cdots O hydrogen bonds (H \cdots O, 2.06 Å, (Table 3.2), yielding a sheet structure, in two dimensional arrangement, as shown in Figures 3.12(b) and (c).

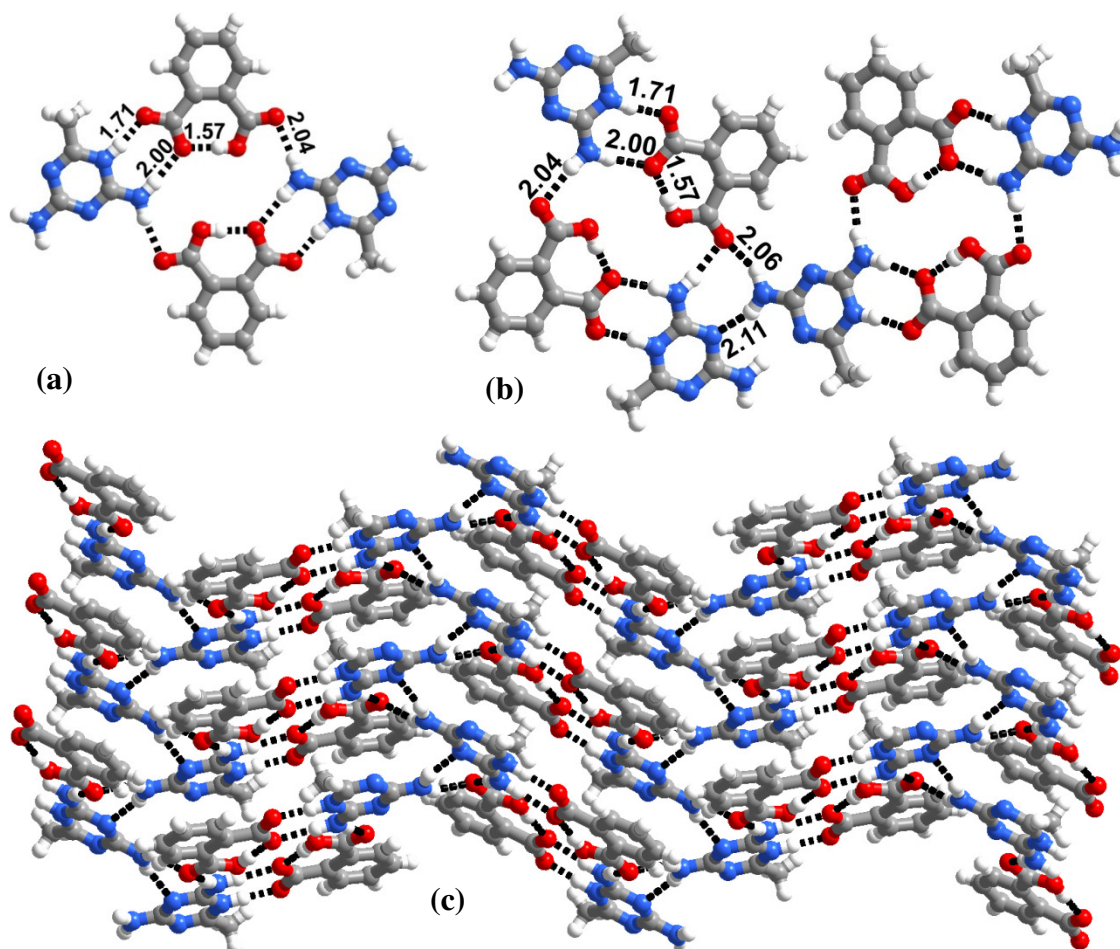


Figure 3.12. (a) Tetramer observed in the complex **1b**. (b) Interaction between the tetramers observed in **1b**. (c) Sheet structure observed in the complex **1b**.

3.2.3 Molecular adducts of 2,4-diamino-6-methyl-1,3,5-triazine with isophthalic acid-1c

Co-crystallization of **1** and isophthalic acid gave a complex, **1c**, in 2:1 ratio, along with solvent of crystallization (Table 3.1). Out of two molecules of **1** (A and B) observed in the asymmetric unit, only A is protonated, as shown in the Figure 3.13(a).

In three dimensional arrangement, molecules pack as stacked layers, as represented in Figure 3.13(b).

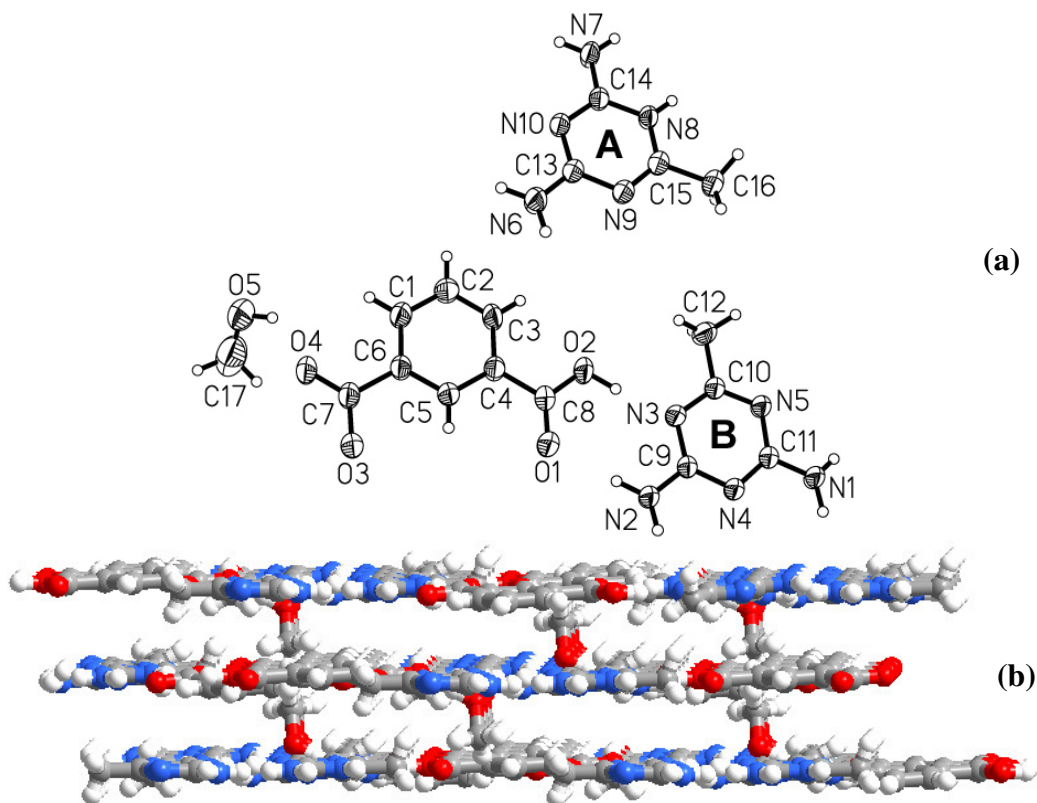
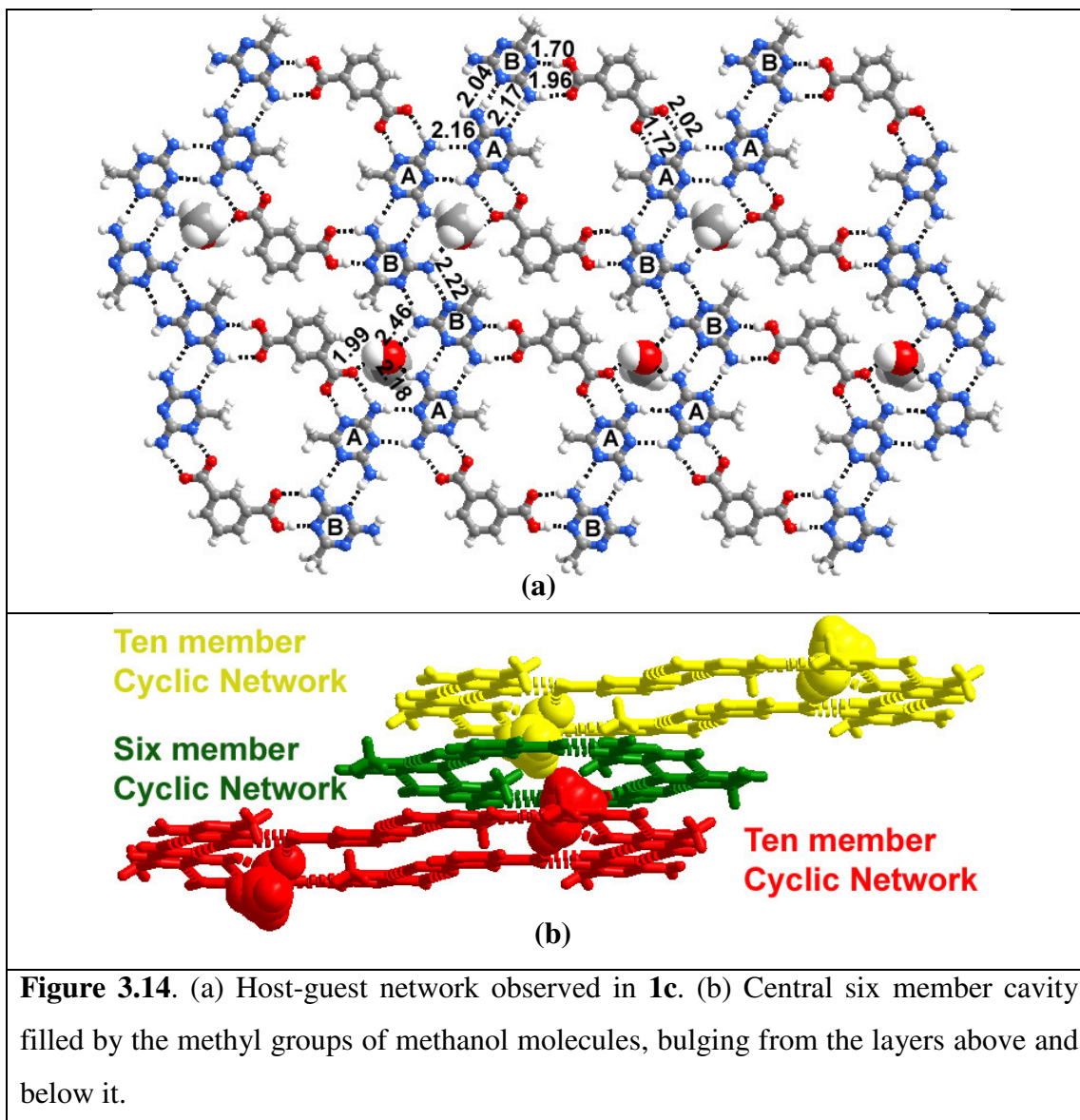


Figure 3.13. (a) ORTEP diagram of the complex **1c**. (b) Layered packing observed in the complex **1c**.

In a typical sheet, the molecules of **1** and the acid recognize each other, constituting a cyclic network with voids. Within a cyclic network, while the two molecules of triazine (A and B) recognize each other by N-H \cdots N hydrogen bonds (H \cdots N, 2.04 and 2.17 Å), isophthalic acid molecules hold two such adjacent dimers by N⁺-H \cdots O⁻, N-H \cdots O⁻ (H \cdots O⁻, 1.72 and 2.02 Å) as well as O-H \cdots N (H \cdots N, 1.70 Å), N-H \cdots O (H \cdots O, 1.96 Å) hydrogen bond dimers, leading to the formation of a six membered cyclic network⁹ with void space of 10.6 × 9.2 Å² dimensions (see Figure 3.14(a)). It is

interesting to note that such huge cavities remain unfilled by any additional molecules within the two-dimensional arrangement.



Further, the hexameric ensembles are extended in two-dimensional arrangement, through N-H \cdots N hydrogen bonds (H \cdots N, 2.16, 2.22 Å), formed between the molecules of exclusively either A or B. Due to such aggregation, a different void space is being created, which is occupied by methanol molecules, with the

establishment of interaction by N-H \cdots O (H \cdots O, 2.18, 2.46 Å) and O-H \cdots O $^-$ hydrogen bonds, (H \cdots O $^-$, 1.99 Å), with the host lattice, as shown in Figure 3.14(a). Full details of the hydrogen bonds are given in Table 3.2. In three dimensional arrangement, the layers are stacked in such a way that the cavities found within hexameric units are being filled by methyl groups, corresponding to methanol molecules, bulging from adjacent layers, as shown in Figure 3.14 (b).

3.2.4 Supramolecular assembly of 2,4-diamino-6-methyl-1,3,5-triazine with terephthalic acid-1d

Co-crystallization of **1** and terephthalic acid gave a complex **1d**, in a 2:1 ratio, along with water molecules. In three dimensional packing, it forms a layered structure, as shown in Figure 3.15.

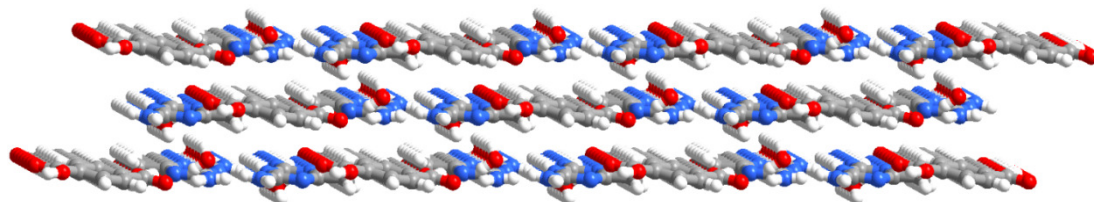


Figure 3.15. Layered packing observed in the complex 1d **1d**.

In a typical layer, the molecules of **1** recognize each other by N-H \cdots N hydrogen bonds (H \cdots N, 2.30 Å), to form *homomeric* dimers. The molecules of terephthalic acid connect the adjacent dimers, like spacers, by a pairwise O-H \cdots N (H \cdots N, 1.65 Å) and N-H \cdots O (H \cdots O, 2.10 Å) hydrogen bonds, yielding an infinite molecular tape, as shown in (Figure 3.16(a)). In the further extension, in two dimensional arrangement, adjacent tapes are connected to each other by water molecules, through N-H \cdots O (H \cdots O, 2.12, 2.13 Å) and O-H \cdots O (H \cdots O, 2.05 Å, Table 3.2) hydrogen bonds, as depicted in Figure 3.16(b).

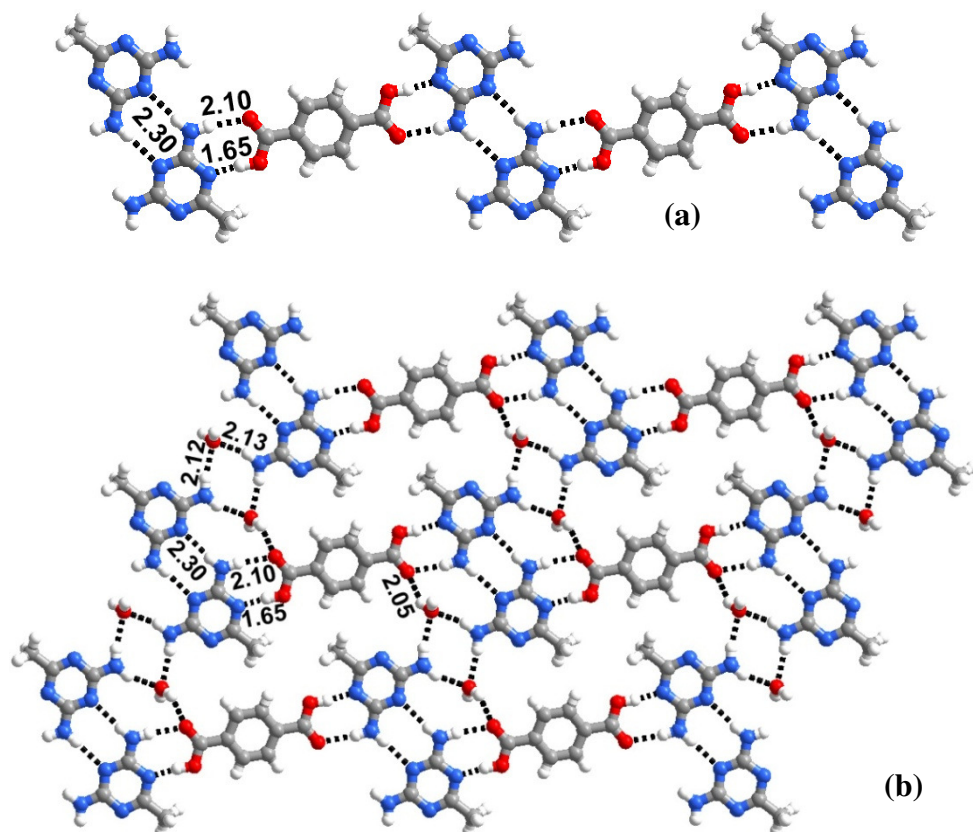
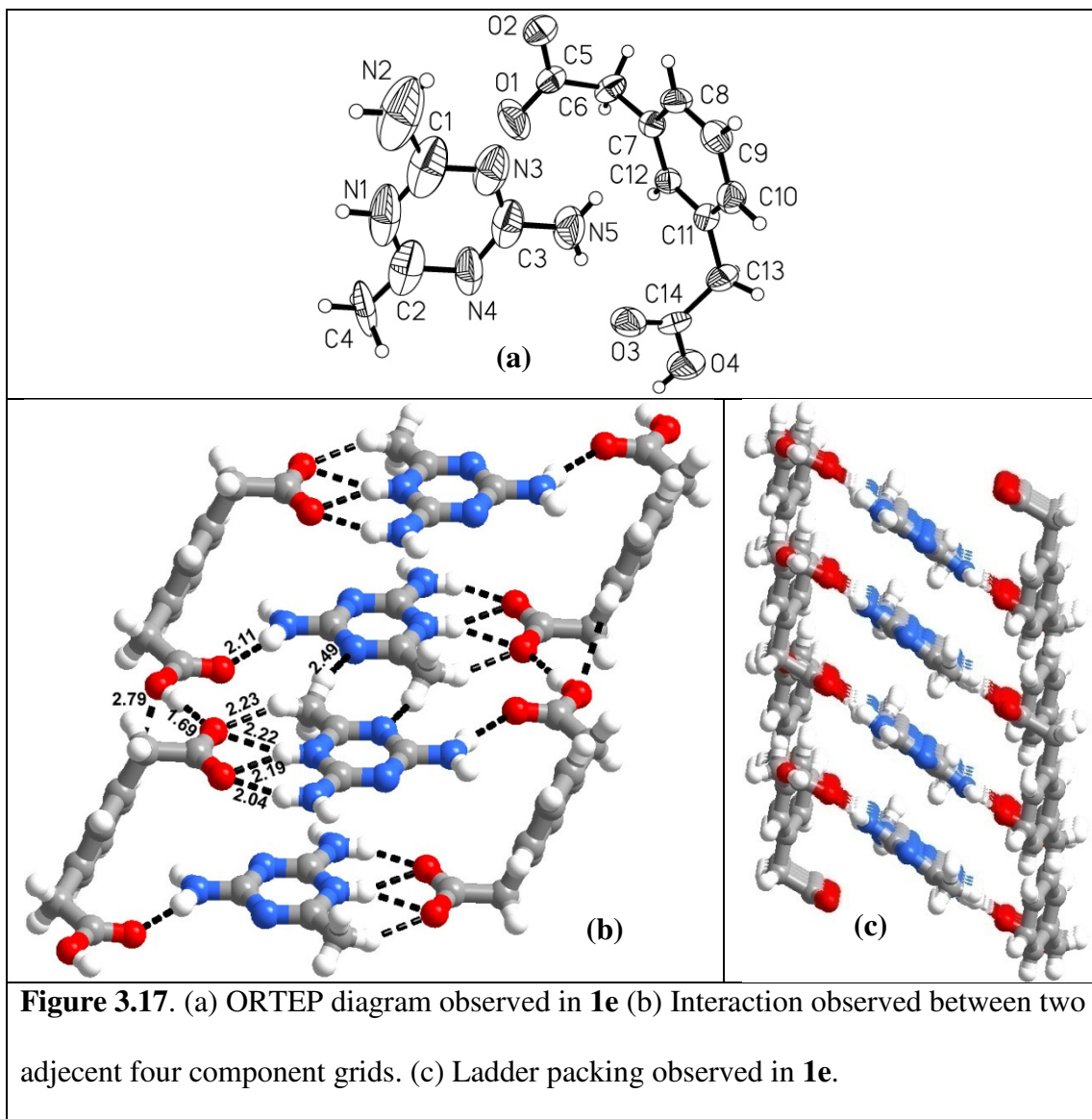


Figure 3.16. (a) Molecules of **1** and terephthalic acid interacting to form molecular tapes (b) Adjacent molecular tapes interacting to form sheet structure.

3.2.5 Supramolecular assemblies of 2,4-diamino-6-methyl-1,3,5-triazine with 1,3-phenylenediacetic acid-1e

Co-crystals, **1e**, obtained from methanol solution of **1** and 1,3-phenylenediacetic acid, has reactants in a 1:1 ratio (Table 3.1), as shown in Figure 3.17(a). In this complex, proton transfer takes place from the molecules of the acid to the triazine, **1**, and further the molecules aggregate as four component grids comprising two molecules of each acid and triazine, **1**.



Within a grid, acid groups establish interaction with the triazine **1**, by $\text{N}^+ \cdots \text{H} \cdots \text{O}^-$ ($\text{H} \cdots \text{O}^-$, 2.19, 2.22 Å), $\text{N}-\text{H} \cdots \text{O}^-$ ($\text{H} \cdots \text{O}^-$, 2.04 Å) hydrogen bonds, as shown in Figure 3.17(b). Such cyclic networks are arranged along a crystallographic direction as blocks, being connected to each other by $\text{O}-\text{H} \cdots \text{O}^-$ ($\text{H} \cdots \text{O}^-$, 1.69 Å) and $\text{C}-\text{H} \cdots \text{N}$ ($\text{H} \cdots \text{N}$, 2.49 Å) hydrogen bonds. (Figure 3.17(b)). In three dimensional arrangement, such blocks are packed, resembling a ladder type network,¹⁰ as shown in Figure 3.17(c),

with rods being formed by the acid molecules, through close packing, while triazines molecules being rungs.

It is apparent from the structural studies of **1a-1e** that replacement of $-\text{NH}_2$ by $-\text{CH}_3$ from melamine to triazine **1**, not only the recognition pattern with corresponding aromatic acids remain almost similar, even the two-dimensional arrangement as well as packing in three-dimensions is also unaltered, as one may find it by comparing **1a-1e** with the corresponding co-crystals of melamine described in the introduction section. It may be perhaps due to the negligible influence of $-\text{CH}_3$ group in the formation of effective hydrogen bonds. To understand further the robustness of structures observed in **1a-1e** even to bulky substituents but no hydrogen bonding sites, further attempts have been directed towards preparation and structural analysis of co-crystals of 2,4-diamino-6-phenyl-1,3,5-triazine with the carboxylic acids listed in Chart 1.

3.3 Supramolecular Assemblies of 2,4-Diamino-6-phenyl-1,3,5-triazine with Aryl and Alkyl Carboxylic Acids



2,4-diamino-6-methyl-1,3,5-triazine (1) **2,4-diamino-6-phenyl-1,3,5-triazine (2)**

2,4-Diamino-6-phenyl-1,3,5-triazine, **2** an analogue of 2,4-diamino-6-methyl-1,3,5-triazine **1** with the replacement of $-\text{CH}_3$ group by phenyl moiety is co-crystallized with various aryl and alkyl carboxylic acids (see, Chart 3.1) from

CH₃OH solvent, under ambient conditions. Single crystals suitable for X-ray diffraction are obtained in all the cases and the details of the molecular complexes **2a-2f** are described in the following sections. Complete crystallographic details are listed in Table 3.1 and characterization of intermolecular interaction are given in Table 3.2.

3.3.1 Supramolecular assemblies of 2,4-diamino-6-phenyl-1,3,5-triazine with benzoic acid-2a

Molecular complex, **2a**, is obtained, in a 1:1 ratio (Table 3.1), upon co-crystallization of 2,4-diamino-6-phenyl-1,3,5-triazine, **2**, and benzoic acid from methanol (Figure 3.18(a)). In three dimensional packing, it forms intermerged bent layers, as shown in Figure 3.18(b).

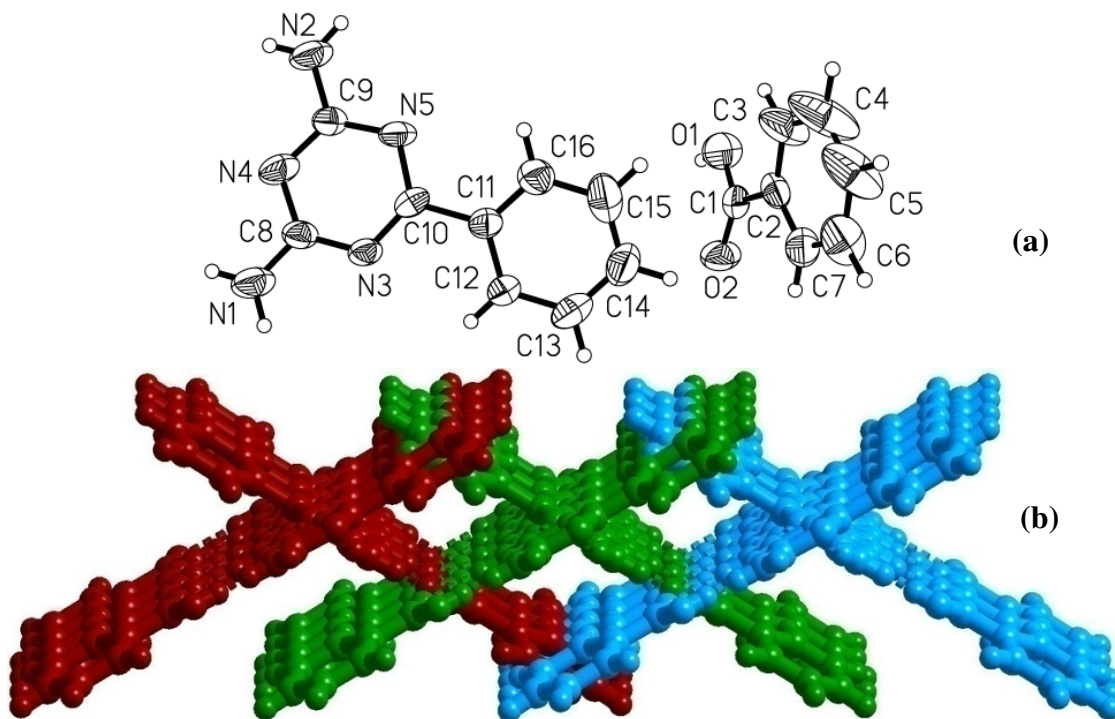


Figure 3.18. (a) ORTEP diagram observed in **2a** (b)Packing diagram observed in **2a**.

Recognition pattern within a typical layer shows the arrangement of molecules in the form of tapes. The adjacent molecules of triazine, **2** recognize each other by N-

H \cdots N hydrogen bonds (H \cdots N, 2.14, 2.31 Å) and form an infinite tape structure. The molecules of benzoic acid interact with the molecular tapes of **2**, like pendants, through a pair-wise hydrogen bonds, O-H \cdots N (H \cdots N, 1.79 Å) and N-H \cdots O (H \cdots O, 2.03 Å, (Table 3.2)), as shown in Figure 3.19. Thus, structures **1a** and **2a** have similar two dimensional arrangement, despite a large variation in the dimensions between the substituents -CH₃ and -phenyl moieties.

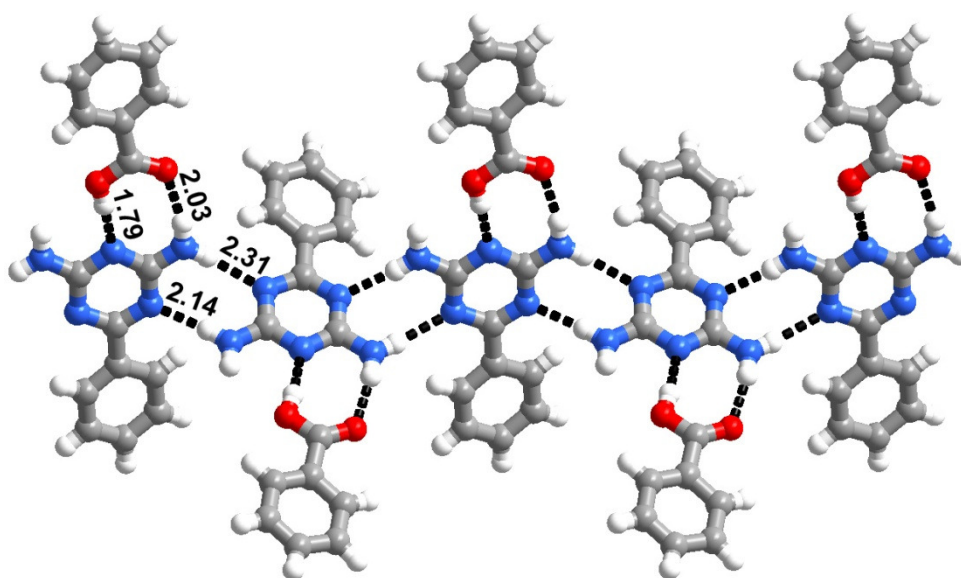


Figure 3.19. Tape network formed in the complex **2a**.

3.3.2 Co-crystals of 2,4-diamino-6-phenyl-1,3,5-triazine with phthalic acid-**2b**

Molecular adduct, **2b**, is obtained, in a 1:1 ratio (Table 3.1), upon co-crystallizing 2,4-diamino-6-phenyl-1,3,5-triazine, **2**, and phthalic acid, from methanol (Figure 3.20(a)). The structure of **2b** has several common features with that of **1b**, with respect to the molecular conformation of the acid as well as recognition features between the triazine **2** and the acid, as mention below. One of the two -COOH groups on phthalic acid is only deprotonated and the proton of the other carboxylic acid

functional group is involved in the intramolecular O-H \cdots O $^-$ hydrogen bond with H \cdots O $^-$ distance of 1.59 Å, as observed in the complex **1b** (formed between triazine, **1** and phthalic acid). In three dimensional packing, a layer structure (Figure 3.20(b)) is realized and a typical layer is formed by the aggregation of discrete molecular tapes.

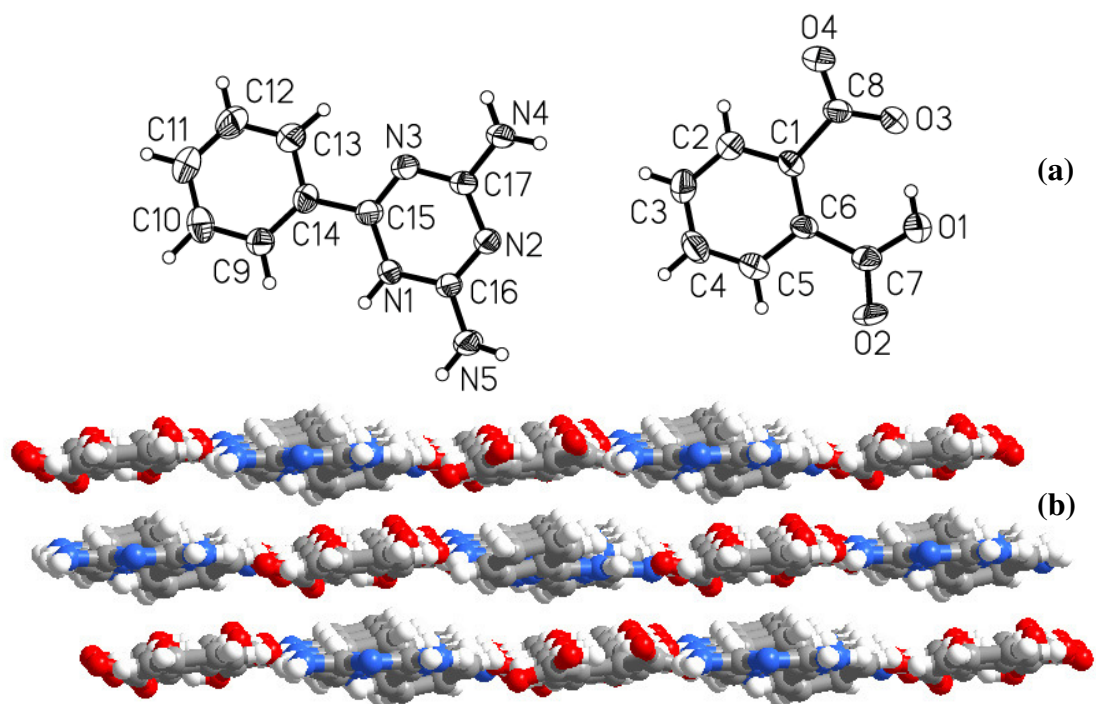


Figure 3.20. (a) ORTEP diagram observed in **2b**. (b) Packing diagram observed in **2b**.

In a typical tape, the molecules of triazine, **2**, exist as discrete dimers held together by N-H \cdots N hydrogen bonds (H \cdots N, 2.15 Å), as depicted in Figure 3.21. The molecules of phthalic acid are sandwiched between such adjacent dimers, establishing interaction through N $^+$ -H \cdots O $^-$ (H \cdots O $^-$, 1.87 Å), N-H \cdots O $^-$ (H \cdots O $^-$, 1.99 Å) as well as N-H \cdots O (H \cdots O, 2.09, 2.28 Å) hydrogen bonds, yielding an infinite tape structure (see Figure 3.21).

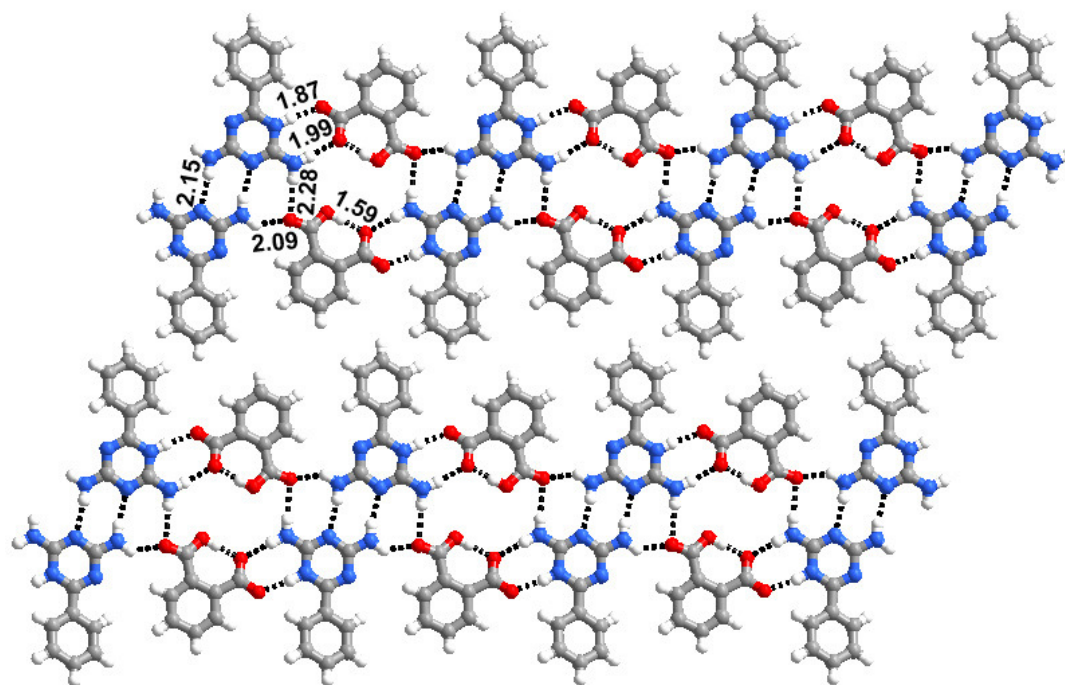


Figure 3.21. Tape network observed in the complex **2b**.

3.3.3 Molecular complex of 2,4-diamino-6-phenyl-1,3,5-triazine with isophthalic acid-**2c**

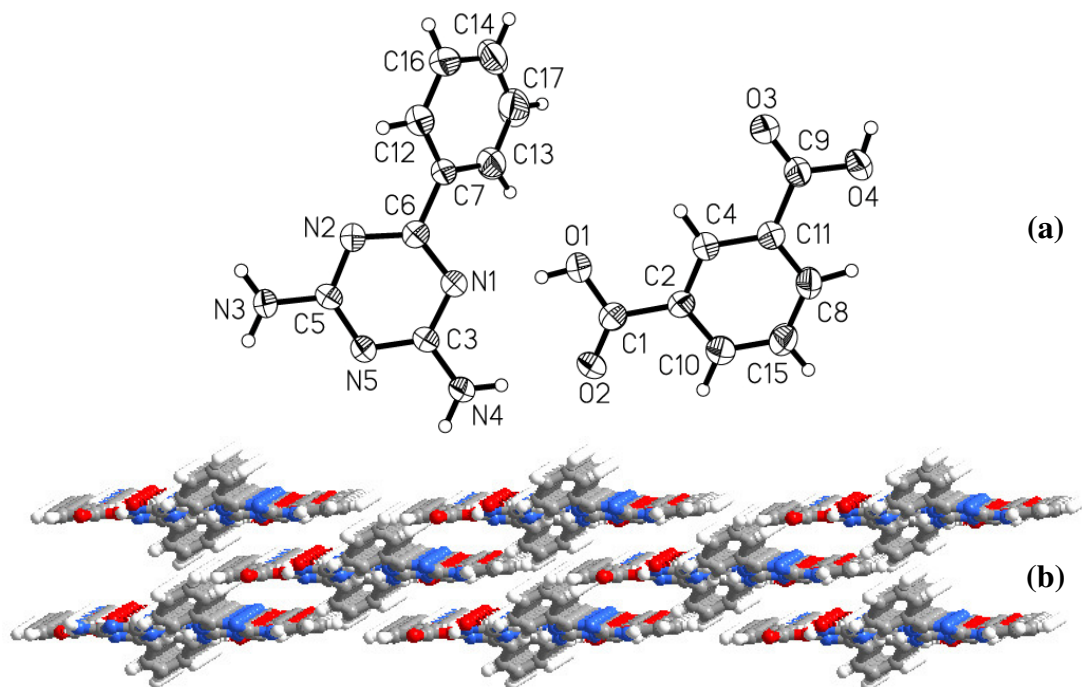
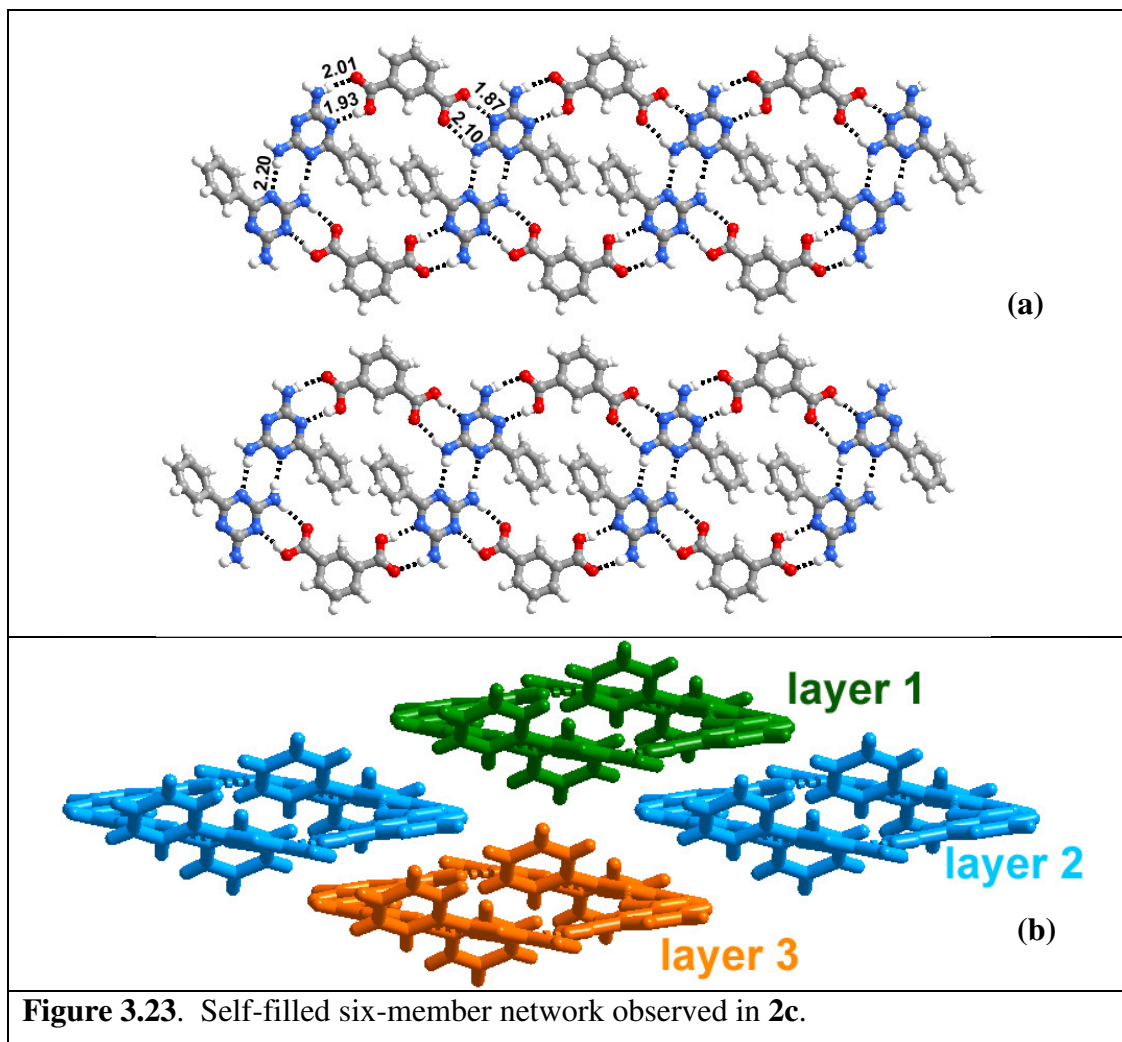


Figure 3.22. (a) ORTEP diagram observed in **2c** (b) Layer packing observed in **2c**.

Molecular complex **2c**, of 2,4-diamino-6-phenyl-1,3,5-triazine and isophthalic acid, obtained from methanol, as shown in Figure 3.22(a), has an asymmetric unit of 1:1 ratio of the co-crystallized ligands. In complex **2c** also, in three dimensional packing, stacked layers structure is observed, as represented in Figure 3.22(b).

Packing of molecules in **2c** has very close similarity with **1c** in the recognition features between the triazine and acid, with similar features observed in **1c** as it was noted between **1b** and **2b** also. A typical layer is an aggregation of columnar hexameric units. Within a hexameric unit, molecules of triazine, **2** are held together by N-H \cdots N hydrogen bonds (H \cdots N, 2.20 Å), as shown in Figure 3.23. Such adjacent dimers are held together by acid molecules by a pair-wise hydrogen bonds of O-H \cdots N (H \cdots N, 1.87, 1.93 Å) and N-H \cdots O (H \cdots O, 2.01, 2.10 Å), yielding an hexameric unit, which extends in one dimension as a columnar assembly (see Figure 3.23(a)). It is interesting to note that, both within the hexameric unit and through the arrangement of adjacent columnar units, appreciable void space is formed. But neither of the voids is available for any other guest species, like solvent of crystallization, as bulky phenyl moieties effectively filled the voids, by protruding into the hexameric cavities in three dimensional arrangement and also by bulging from the layers, which are staggered in three-dimensional arrangement (Figure 3.23(b)).



3.3.4 Molecular complex of 2,4-diamino-6-phenyl-1,3,5-triazine with terephthalic acid-**2d**

Molecular complex, **2d**, obtained between triazine, **2** and terephthalic acid has reactants in a 2:1 ratio. Detailed analysis of the recognition pattern shows that in the complex, **2d**, molecules of triazine, **2** aggregate, yielding infinite tapes, through N-H \cdots N hydrogen bonds (H \cdots N, 2.08, 2.32 Å). In two-dimensional arrangement, the tapes are held together by terephthalic acid molecules by a pair-wise hydrogen bonds, O-H \cdots N (H \cdots N, 1.78 Å) and N-H \cdots O (H \cdots O, 2.05 Å), as shown in Figure 3.24. Such an

arrangement, has, created void space of dimension of $15 \times 10 \text{ \AA}^2$. Interestingly, such void space is stabilized by four-fold interpenetration perhaps, due to the incommensuration between the dimensions of the void space and phenyl moieties. Indeed the phenyl moieties are flipping away from the void space as one could visualize in Figure 3.24. The exotic interpenetrated structure is shown in Figure 3.25. A close observation of the three dimensional structure of complex **2d** directs that, it may be possible that by increasing the spacer length between the tapes of triazine, **2**, either the phenyl moieties on **2** or additional guest species like solvent of crystallization, may effectively fill the void space rather than interpenetration.¹¹ Hence, the complexes of triazine, **2** with 1,3- and 1,4-phenylenediacetic acid (analogues of terephthalic acid) have been carried out.

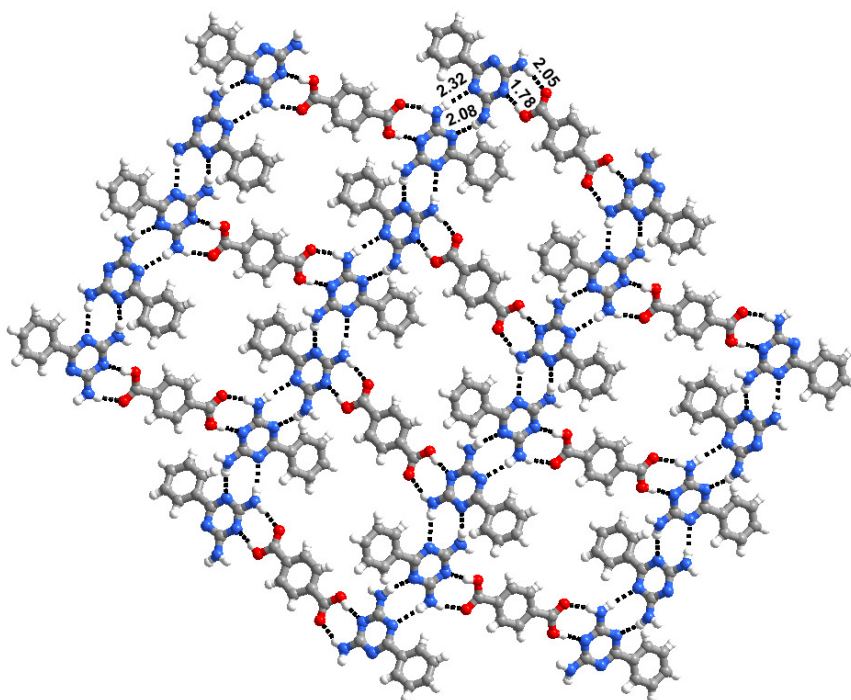


Figure 3.24. Eight member self-filled cyclic cavity of dimensions $15.2 \times 9.8 \text{ \AA}^2$, observed in the complex **2d**.

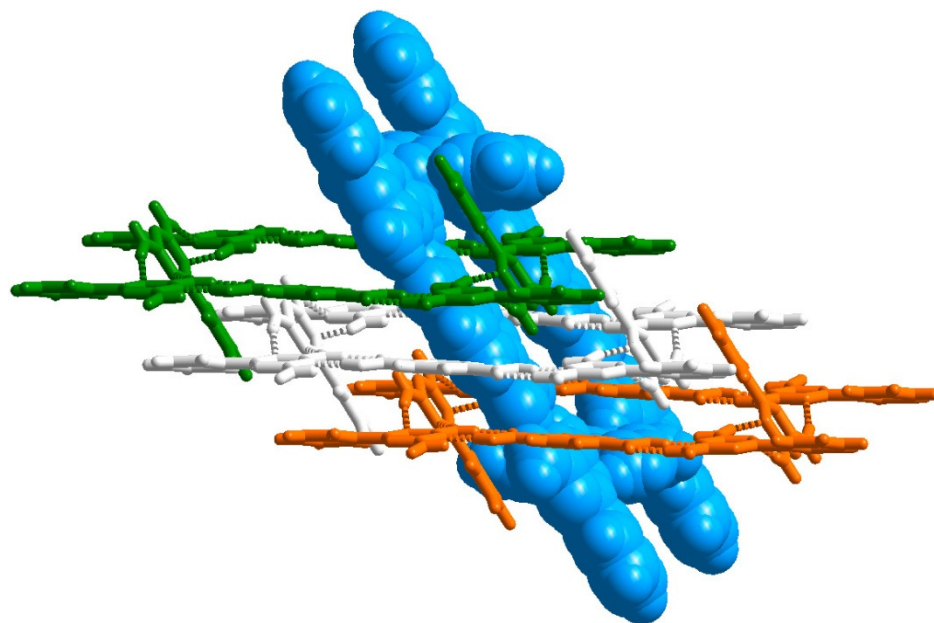


Figure 3.25. Four-fold interpenetration observed in the molecular complex **2d**.

3.3.5 Molecular adducts of 2,4-diamino-6-phenyl-1,3,5-triazine with 1,3-phenylenediacetic acid - **2e, and 1,4-phenylenediacetic acid-**2f****

Molecular complexes of **2e** and **2f**, obtained by co-crystallization of 2,4-diamino-6-phenyl-1,3,5-triazine, **2**, with 1,3-phenylenediacetic acid and 1,4-phenylenediacetic acid, respectively, are indeed, isostructural with a 2:1 composition of the constituents in the asymmetric units of the crystal lattices. In three dimensional arrangement, the molecules in both the complexes arrange as stacked layered, as shown in Figure 3.26(a), for the complex **2e**.

In fact, detailed analysis of a typical sheet shows that, the arrangement is quite similar to that noted in **2d** with the formation of infinite molecular tapes of triazine **2** through N-H \cdots N hydrogen bonds (**2e**, H \cdots N, 2.11 and 2.21; **2f**, 2.12 and 2.16 Å). The two-dimensional arrangement of molecules in the complexes **2e** and **2f** is shown in

Figures 3.26(b) and (c). The molecular tapes are further held together by the corresponding complementary acids, as the case may be, through O-H \cdots N and N-H \cdots O hydrogen bonds. While the H \cdots N and H \cdots O distances are 1.85 and 2.25 Å in **2e**, such distances are found to be 1.73 and 2.10 Å in **2f**. Such aggregation lead to the formation of voids with 14×10 Å² dimensions (see Figure 3.26), which is being filled by phenyl moieties. Thus anticipated, the void space is stabilized by phenyl moieties from the triazine molecules rather than undergoing interpenetration.

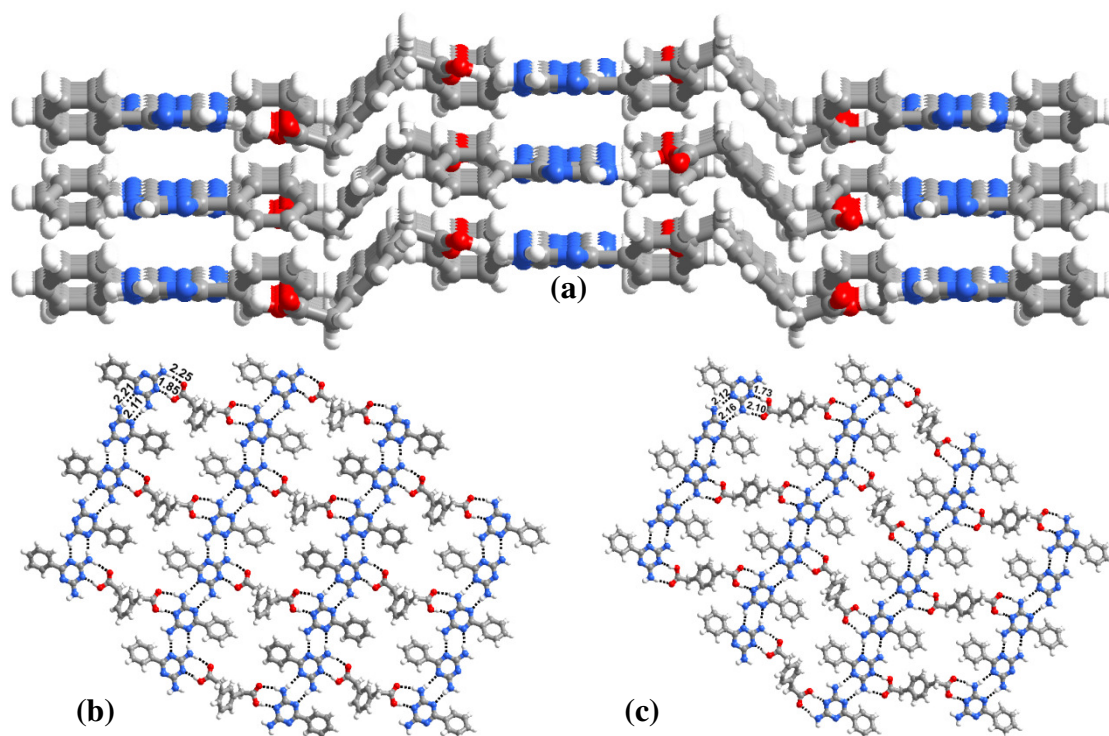
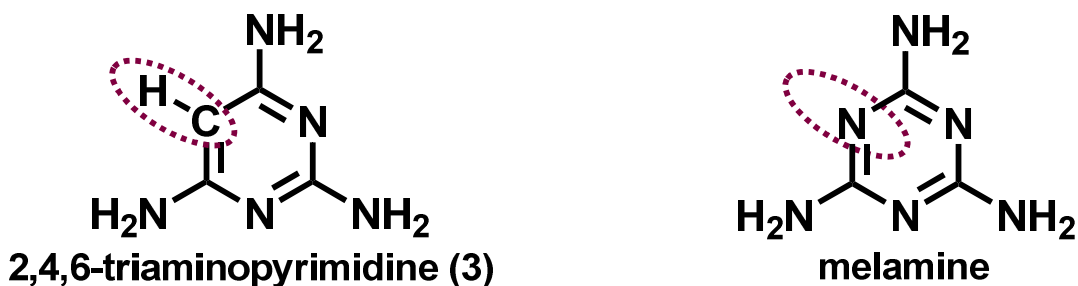


Figure 3.26. (a) Layered packing observed in the complex **2e**. (b) Eight member self-filled cavity of dimensions 13.9×9.7 Å² observed in the complex **2e**. (c) Eight member self-filled cyclic cavity of dimensions 14.0×9.7 Å² observed in the complex **2f**.

It may be understood from the structures **2a-2f** that bulky substituent (phenyl moiety) also gave very much similar structures as observed in **1a-1e** and also as

complexes of melamine, suggesting importance of hydrogen bonding sites on the substituent to alter the nature of architectures in the assemblies. Considering these views for further exploration, 2,4,6-triaminopyrimidine, (an analogue of melamine with the replacement of one of the hetero nitrogen atom by carbon, without any change in the hydrogen bonding sites on peripheral) has been co-crystallized with the carboxylic acids listed in Chart 1

3.4 Molecular Adducts of 2,4,6-Triaminopyrimidine with Various Aryl and Alkyl Carboxylic Acids.



Co-crystallization of 2,4,6-triaminopyrimidine, **3** with various carboxylic acids, listed in Chart 1, has been carried out, but good quality single crystals were obtained only with phthalic, terephthalic, 1,3 and 1,4-phenylenediacetic acids. The structures of these complexes are established by single crystal X-ray diffraction methods, as discussed below.

3.4.1 Molecular adduct of 2,4,6-triaminopyrimidine with phthalic acid-3b

Crystals of complex **3b** were obtained from a CH₃OH solution of **3** and phthalic acid. The structure determination reveals that the asymmetric unit consists of

1:1 ratio of **3** and phthalate, respectively, along with water molecules (see Figure 3.27(a)). Full crystallographic information is given in Table 3.1.

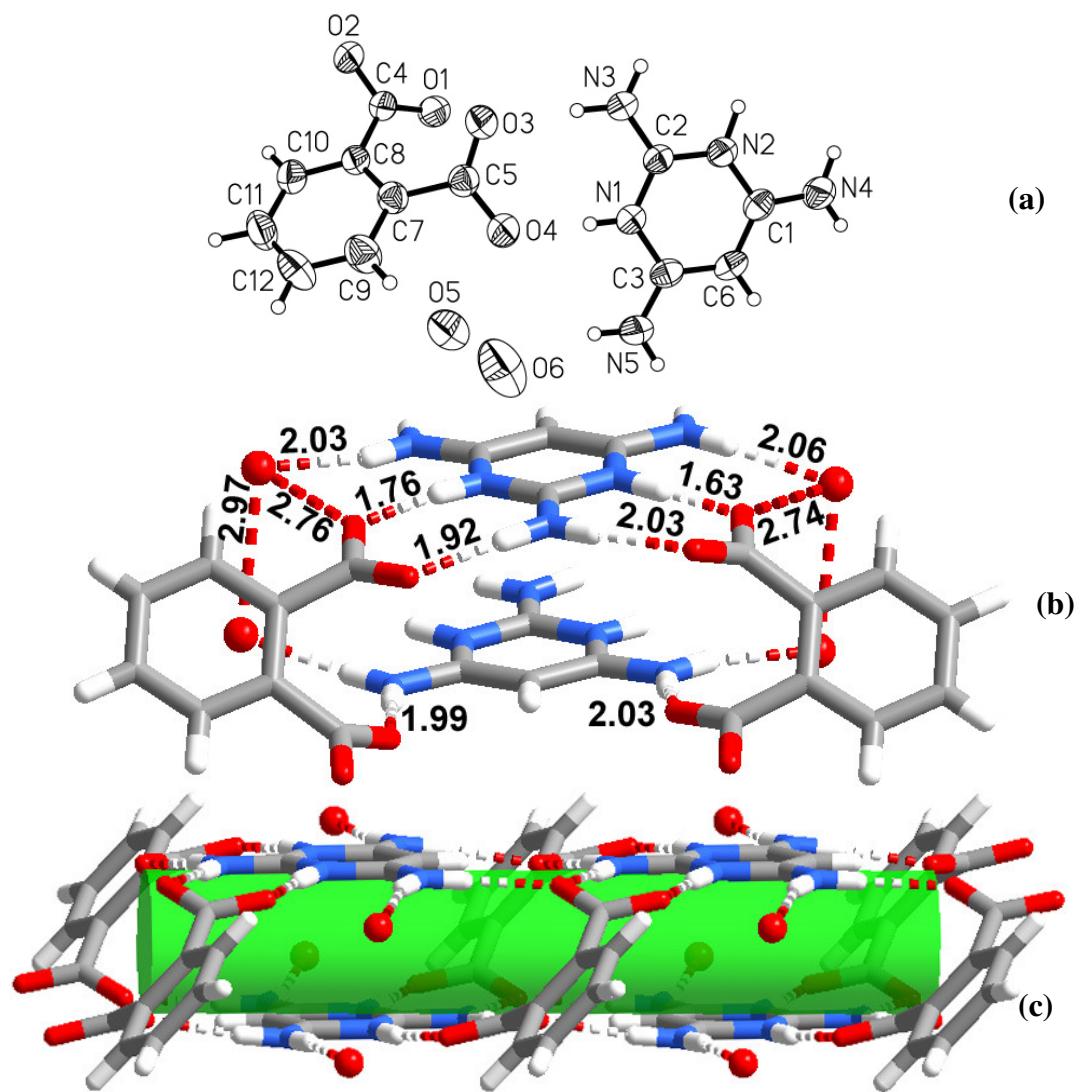


Figure 3.27. (a) Ortep diagram of the complex **1b**. (b) Recognition pattern observed in the complex **1b**. (c) Tubular network formed by the molecules of **1** and **b**.

In the complex, **3b**, proton transfer takes place from the molecules of phthalic acid to the molecules of **3**. Further, the molecules of **3** and phthalate ions recognize each other by a pair-wise $\text{N}^+\text{-H}\cdots\text{O}^-$ and $\text{N-H}\cdots\text{O}^-$ hydrogen bonds ($\text{H}\cdots\text{O}^-$, 1.63, 1.76 and 1.92, 2.03 Å) as well as single $\text{N-H}\cdots\text{O}^-$ hydrogen bond ($\text{H}\cdots\text{O}^-$, 1.99, 2.03 Å), as shown

in Figure 3.27(b), constituting a four member cyclic unit, which further constitutes, tubular type structure, as depicted in Figure 3.27(c).

3.4.2 Molecular adduct of 2,4,6-triaminopyrimidine with terephthalic acid-3d

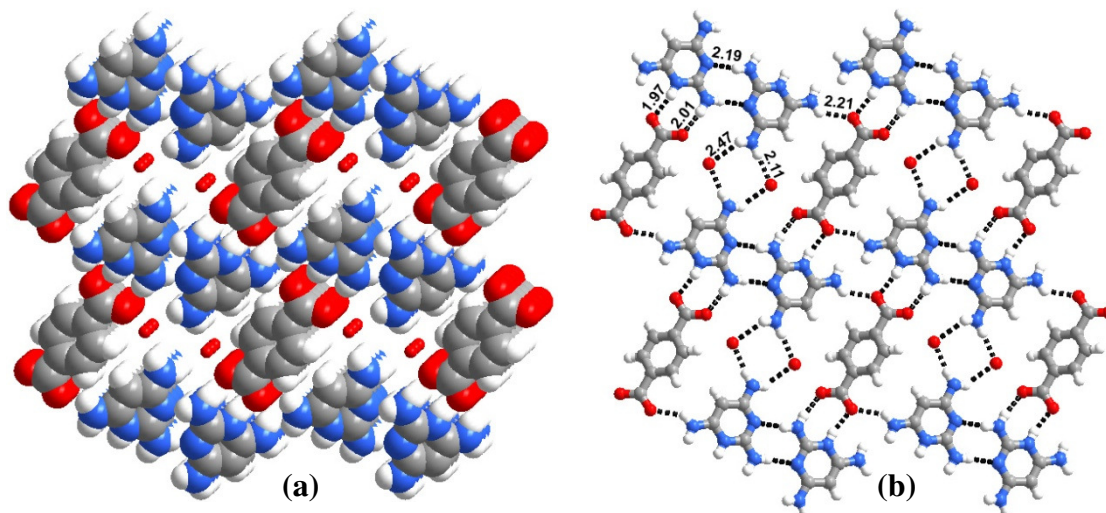


Figure 3.28. (a) Host-guest network observed in the complex **3d**. (b) Host-guest network observed in **3d**

Co-crystallization of **3** and terephthalic acid gave a complex **3d**, in a 2:1 ratio of the co-crystal constituents, along with water molecules. Structure determination parameters obtained from single crystal X-ray diffraction methods are given in Table 3.1. In three dimensional packing, molecules in the complex, **3d** form a host-guest network, with waters being in channels, as shown in Figure 3.28(a).

Detailed analysis of aggregation of molecules and nature of intermolecular interactions reveals that both the -COOH of terephthalic acid are deprotonated and protons are transferred to the aromatic nitrogen of **3**. Within two-dimensional arrangement, each terephthalate holds two molecules of **3** through $\text{N}^+\text{-H}\cdots\text{O}^-$ and $\text{N-H}\cdots\text{O}^-$ hydrogen bonds ($\text{H}\cdots\text{O}^-$, 1.97 and 2.01 Å), yielding a three-component entity.

Such adjacent supramolecular entities are held together by water molecules through N-H \cdots O hydrogen bonds (H \cdots O, 2.11, 2.47Å), yielding one-dimensional molecular tapes. Further, the adjacent molecular tapes are connected to each other by N-H \cdots N hydrogen bonds (H \cdots N, 2.19 Å), formed between the molecules of triazine, **3**. Stacking of these layers, in three dimensions, by translational symmetry, thus, reflected as if water molecules are like guests in the channels of 7 x 11 Å² dimensions (Figure 3.28 (a)).

3.4.3 Supramolecular adducts of 2,4,6-triaminopyrimidine with 1,3-phenylenediacetic acid-3e

Co-crystallization of **3** and 1,3-phenylenediacetic acid from methanol, a complex, **3e**, in 1:1 ratio, is obtained, as shown in Figure 3.29(a) and full crystallographic information is given in Table 3.1. In the complex **3e**, one of the –COOH groups on 1,3-phenylenediacetic acid undergoes deprotonation and in three-dimensional arrangement, the molecules form a ladder type structure, as shown in Figure 3.29(b), resembling the structure observed in the complex, **2e** (formed between the triazine, **2** and 1,3-phenylenediacetic acid). Thus, the molecules of 1,3-phenylenediacetic acid form the rods, while the triazine molecules constituting rungs.

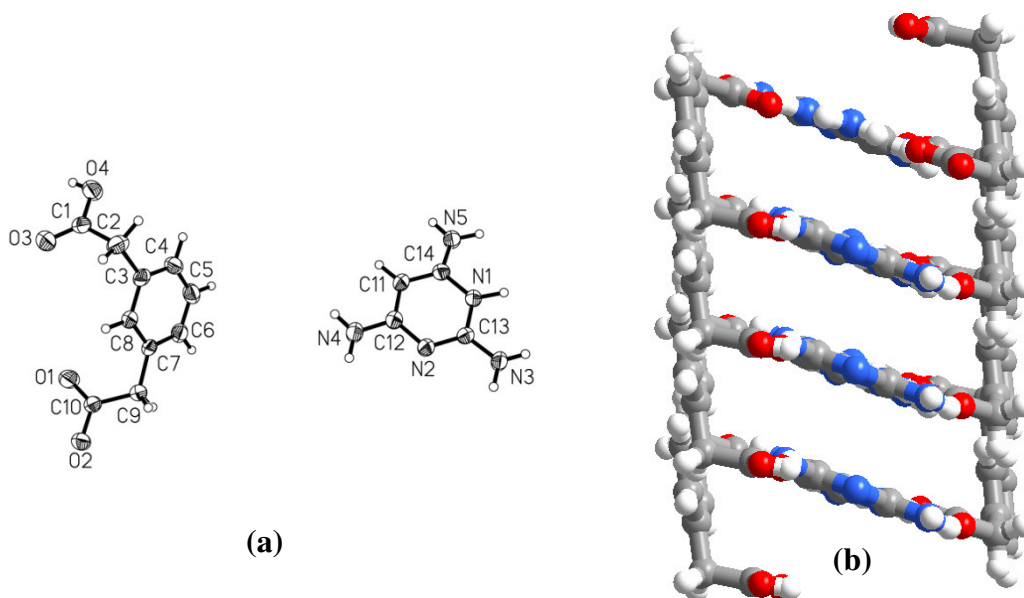
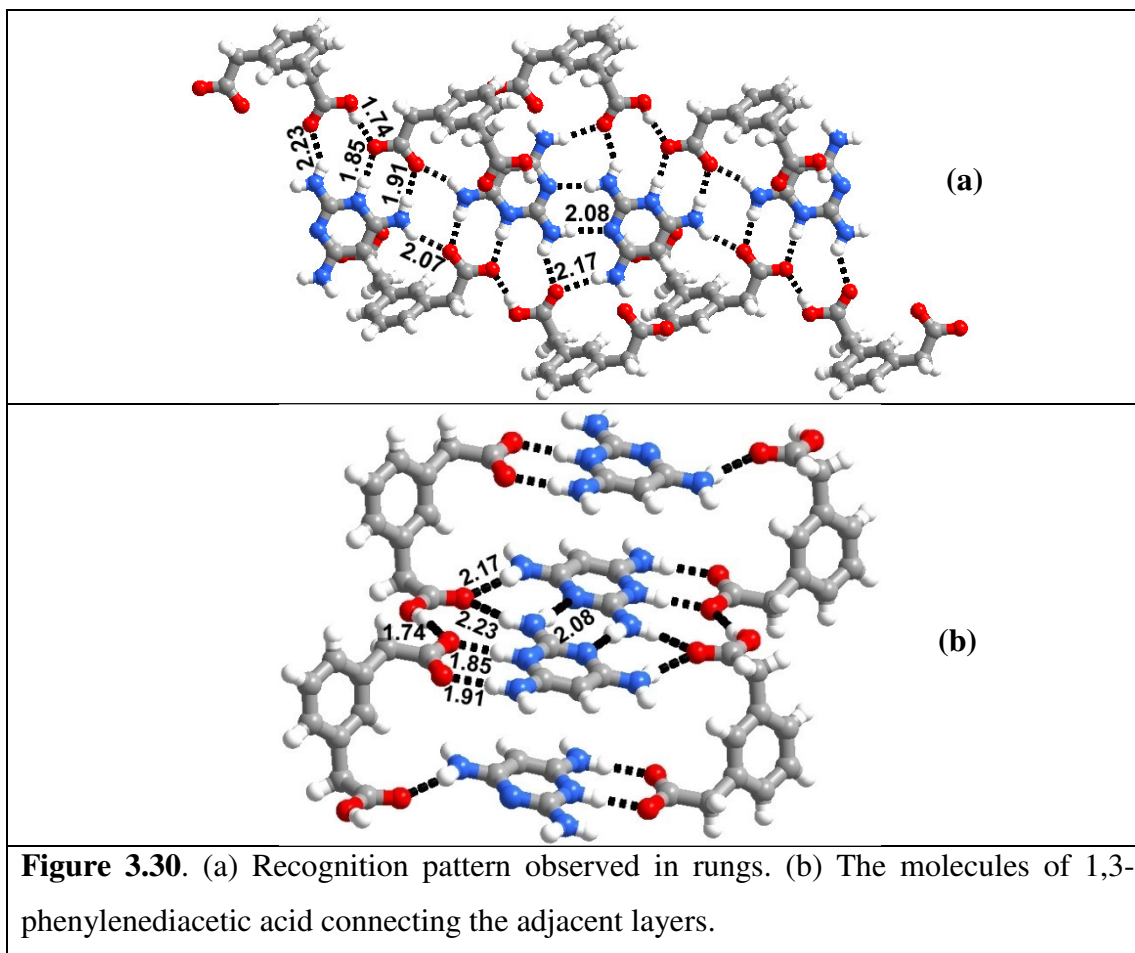


Figure 3.29. (a) ORTEP diagram of the complex **3e**. (b) Ladder packing observed in the complex **3e**.

Further, the aggregation of molecules in the complex **3e** is also almost similar to that observed in **2e**, as shown in Figure 3.30. Hence, it is noted that molecules of **3** are inserted between a pair of acid molecules, through a pair-wise $\text{N}^+\text{-H}\cdots\text{O}^-$ and $\text{N-H}\cdots\text{O}^-$ hydrogen bonds ($\text{H}\cdots\text{O}^-$, 1.85 and 1.91 Å) and single $\text{N-H}\cdots\text{O}$ ($\text{H}\cdots\text{O}$, 2.17, 2.23 Å) as well as $\text{N-H}\cdots\text{O}^-$ ($\text{H}\cdots\text{O}^-$, 2.07 Å) hydrogen bonds, yielding a four-member cyclic entity. The adjacent cyclic moieties are further held together by $\text{N-H}\cdots\text{N}$ hydrogen bonds ($\text{H}\cdots\text{N}$, 2.08 Å), formed between the molecules of **3**, as well as, by $\text{O-H}\cdots\text{O}^-$ hydrogen bonds ($\text{H}\cdots\text{O}^-$, 1.74 Å, Table 3.2), formed between the acid molecules, as shown in Figure 3.30.



3.4.4 Molecular adduct of 2,4,6-triaminopyrimidine with 1,4-phenylenediacetic acid-3f

Co-crystals of **3f**, obtained from methanol solution of **3** and 1,4-phenylenediacetic acid, have the reactants in a 1:1 ratio (Table 3.1), in its crystal lattice, as shown in Figure 3.31(a). In this complex, both the -COOH groups present on the acid molecules undergo deprotonation and transfer to the two hetero nitrogen atoms on **3**. In three dimensional arrangement, the molecules organize in the form of stacked zig-zag sheets, as shown in Figure 3.31(b).

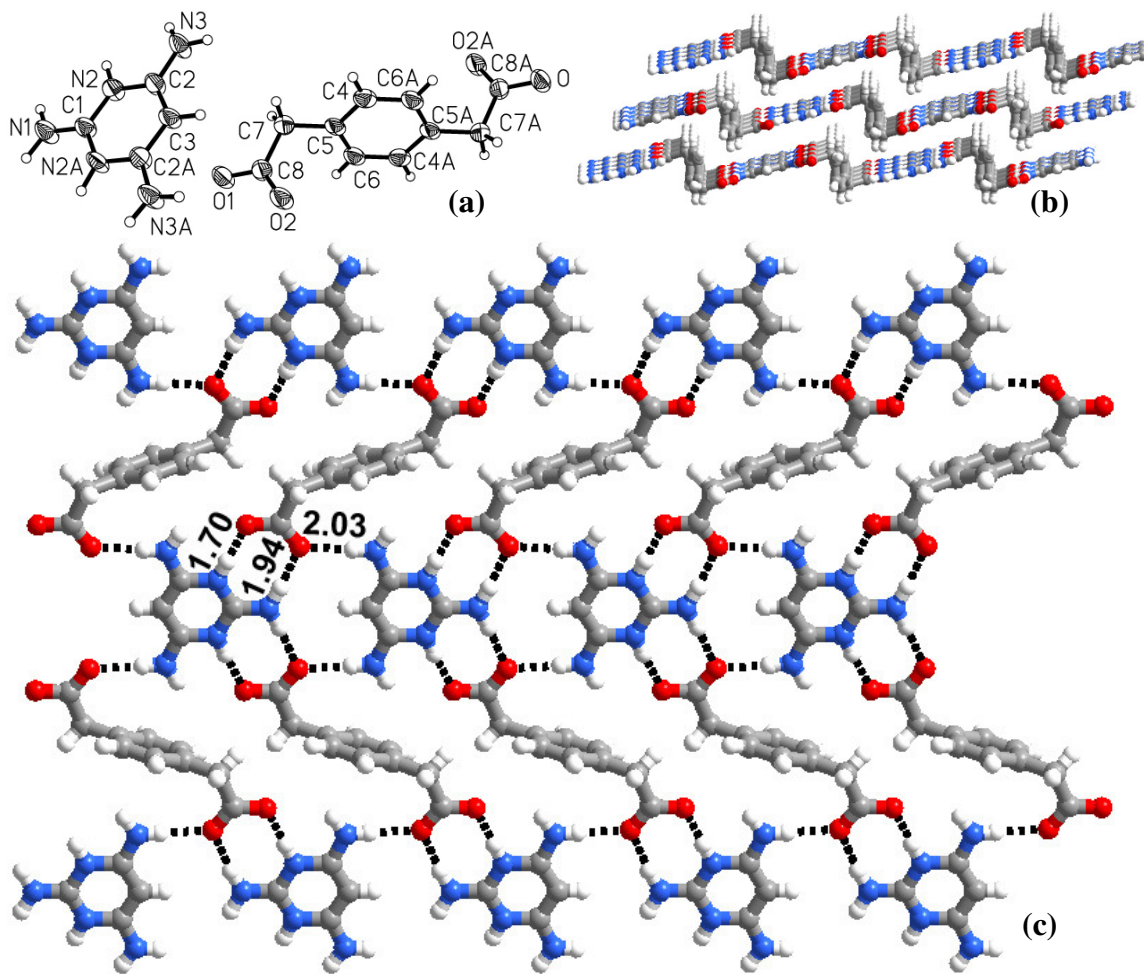


Figure 3.31. (a) ORTEP diagram of the complex **3f**. (b) Layered packing observed in the complex **3f**. (c) Sheet structure observed in the crystal structure of **3f**.

A typical sheet is due to the aggregation of molecular tapes by $\text{N-H}\cdots\text{O}^-$ ($\text{H}\cdots\text{O}^-$, 2.03 Å) hydrogen bonds. Such an arrangement is shown in Figure 3.31(c). However, within a molecular tape, the acid and the molecules of triazine are held together by $\text{N}^+-\text{H}\cdots\text{O}^-$, $\text{N-H}\cdots\text{O}^-$ hydrogen bonds ($\text{H}\cdots\text{O}^-$, 1.70 and 1.94 Å (see Figure 3.31(c)). Details of hydrogen bond characteristics are given in Table 3.2.

Thus, it may be realized from the structures of **3b**, **3d-3f** that, the recognition patterns between the acids and pyrimidine appears to have close relationship with that of the complexes formed by triazines. However, there is significant changes in the

ultimate supramolecular assemblies except in **3b**, perhaps being influenced by the ability of -NH_2 group against -CH_3 and phenyl towards forming hydrogen bonds.

3.5 Conclusion

In conclusion, molecular complexes of 2,4-diamino-6-methyl-1,3,5-triazine, 2,4-diamino-6-phenyl-1,3,5-triazine and 2,4,6-triaminopyrimidine with different aryl and arylalkyl carboxylic acids have been reported. Although not much correlation is observed within the co-crystals of specific triazine moieties (**1a-1e**, **2a-2f**), structures are appreciably shown close similarities formed by different triazines with the same acids (**1a** vs **1b** ; **1b** vs **2b** ; etc.). Indeed, 2,4,6-triaminopyrimidine assemblies also have shown similar recognition patterns as that of triazines but overall supramolecular assemblies shows some distinct differences, except in **3e**, perhaps facilitated by the presence of -NH_2 group, an effective hydrogen bonding directive functionality

3.6 Experimental Sections

3.6.1 Synthesis

All the chemicals, reagents and solvents were obtained from commercial suppliers and used without further purification. Spectroscopic-grade solvents were used in all co-crystallization studies. All co-crystals, **1a-1e**, **2a-2f**, **3b** and **3d-3f** were prepared by dissolving the respective reactants in a ratio of 1:1 in methanol and allowing the solvent to evaporate under ambient conditions. In all the cases, single crystals, suitable for X-ray diffraction analysis, were obtained over the period of 2-3 days.

General procedure for the synthesis of complexes, 1a-1e, 2a-2f, 3b and 3d-3f

In a typical preparation, 2,4-diamino-6-methyl-1,3,5-triazine (0.0625 g, 0.5 mmol) and benzoic acid (0.0610 g, 0.5 mmol) were dissolved in CH₃OH (20 mL) by gentle warming in a water bath. The resultant solution was evaporated under ambient conditions and with protection from external mechanical disturbances, and within 48 hours, good quality, colorless crystals of **1a** were obtained that were suitable for single-crystal X-ray diffraction studies.

3.6.2 Crystal structures determination

Good quality single crystals of **1a-1e**, **2a-2f**, **3b** and **3d-3f** were carefully selected with the aid of a polarized Leica microscope equipped with CCD camera, and glued to a glass fiber using an adhesive (cyanoacrylate). In all the cases, the crystals were smeared in the adhesive solution to prevent decay of crystals upon exposure to X-rays. The intensity data were collected on a Bruker single crystal X-ray diffractometer, equipped with an APEX detector, at temperature varying from 100-298 K, see table 3.1 Subsequently, the data were processed using Bruker suite of programmes (SAINT)¹² and the convergence was found to be satisfactory with good R_{int} parameters. The details of the data collection and crystallographic information are given in Table 3.1. The structure determination by direct methods and refinements by least-squares methods on F^2 were performed using SHELXTL-PLUS package. The processes were smooth without any complications. All non-hydrogen atoms were refined anisotropically. All the intermolecular interactions were computed using PLATON.¹³

Table 3.1. Crystallographic data the complexes **1a-1e**, **2a-2f**, **3b**, **3d**, **3e**, **3f**

	1a	1b	1c	1d	1e
Formula	2(C ₄ H ₇ N ₅): 2(C ₇ H ₆ O ₂): 1(H ₂ O)	1(C ₄ H ₈ N ₅): 1(C ₈ H ₅ O ₄)	1(C ₄ H ₈ N ₅): 1(C ₄ H ₇ N ₅): 1(C ₈ H ₅ O ₄) 1(CH ₄ O)	2(C ₄ H ₇ N ₅): 1(C ₈ H ₆ O ₄) 2(H ₂ O)	1(C ₄ H ₈ N ₅): 1(C ₁₀ H ₉ O ₄)
Formula Wt.	512.54	291.27	448.46	452.45	319.33
Crystal habit	Rectangular Blocks	Blocks	Rod Shaped	Blocks	Rod Shaped
Crystal color	Colorless	Colorless	Colorless	Colorless	Colorless
Crystal system	Triclinic	Monoclinic	Triclinic	Triclinic	Monoclinic
Space group	<i>P</i> $\bar{1}$	<i>P</i> 2 ₁ / <i>c</i>	<i>P</i> $\bar{1}$	<i>P</i> $\bar{1}$	<i>P</i> 2 ₁ / <i>c</i>
<i>a</i> (Å)	9.776(2)	7.204(2)	10.629(1)	6.756(3)	9.245(2)
<i>b</i> (Å)	11.519(2)	23.514(5)	10.662(1)	7.267(3)	26.479(5)
<i>c</i> (Å)	11.745(2)	8.109(2)	11.092(1)	10.564(4)	6.252(1)
α (deg)	104.48(1)	90.00	78.08(1)	94.70(1)	90.00
β (deg)	92.32(1)	106.87 (1)	72.08(1)	98.97(1)	107.10(1)
γ (deg)	90.55(1)	90.00	61.22(1)	91.55(1)	90.00
<i>V</i> (Å ³)	1279.3(4)	1314.5(6)	1045.7 (2)	510.2(4)	1462.8(5)
<i>Z</i>	2	4	2	1	4
<i>D</i> _{calc} (g cm ⁻³)	1.331	1.472	1.424	1.473	1.450
<i>T</i> (K)	298(2)	298(2)	273(2)	298(2)	298(2)
λ (Mo-K α)	0.71073	0.71073	0.71073	0.71073	0.71073
μ (mm ⁻¹)	0.098	0.114	0.109	0.116	0.109
2 θ range (deg)	50.58	50.48	50.48	50.64	50.48
Limiting indices	-11 \leq <i>h</i> \leq 11 -13 \leq <i>k</i> \leq 13 -14 \leq <i>l</i> \leq 14	-8 \leq <i>h</i> \leq 8 -28 \leq <i>k</i> \leq 27 -9 \leq <i>l</i> \leq 9	-12 \leq <i>h</i> \leq 12 -11 \leq <i>k</i> \leq 12 -13 \leq <i>l</i> \leq 13	-8 \leq <i>h</i> \leq 8 -8 \leq <i>k</i> \leq 8 -12 \leq <i>l</i> \leq 12	-11 \leq <i>h</i> \leq 10 -31 \leq <i>k</i> \leq 31 -7 \leq <i>l</i> \leq 7
<i>F</i> (000)	540	608	472	238	672
No. of Reflns. Measured	12230	9495	17861	5026	7302
No. Unique Reflns.	4602	2376	3745	1845	2629
No. of Reflns. used	3220	2060	2572	1574	1792
No. of Parameters	376	229	336	182	219
GOF on F ²	1.334	1.260	1.225	1.144	1.183
<i>R</i> ₁ [<i>I</i> > 2 σ (<i>I</i>)]	0.1123	0.0735	0.0512	0.0497	0.1065
<i>wR</i> ₂	0.2040	0.1470	0.1562	0.1202	0.2032
Final diff. Fourier map (e ⁻ ·Å ⁻³) max, min	0.233, -0.223	0.335, - 0.195	0.409, - 0.290	0.204, - 0.162	0.326, - 0.242

Table 3.1. Continued.....

	2a	2b	2c	2d	2e
Formula	1(C ₉ H ₉ N ₅): 1(C ₇ H ₆ O ₂):	1(C ₉ H ₁₀ N ₅): 1(C ₈ H ₅ O ₄)	1(C ₉ H ₉ N ₅): 1(C ₈ H ₆ O ₄)	2(C ₉ H ₉ N ₅): 1(C ₈ H ₆ O ₄)	2(C ₉ H ₉ N ₅): 1(C ₁₀ H ₁₀ O ₄)
Formula Wt.	309.33	353.34	353.34	540.55	568.60
Crystal habit	Blocks	Rod Shaped	Blocks	Rectangular Blocks	Blocks
Crystal color	Colorless	Colorless	Colorless	Colorless	Colorless
Crystal system	Monoclinic	Triclinic	Triclinic	Monoclinic	Orthorhombic
Space group	<i>Pc</i>	<i>P</i> $\bar{1}$	<i>P</i> $\bar{1}$	<i>C 2/c</i>	<i>Pbcn</i>
<i>a</i> (Å)	9.821(3)	7.162(2)	8.504(6)	29.943(1)	31.500(7)
<i>b</i> (Å)	7.135(2)	10.042(2)	10.199(7)	7.007(2)	12.412(3)
<i>c</i> (Å)	12.126(2)	12.835(3)	10.258(7)	12.152(4)	7.016(2)
α (deg)	90.00	68.27(1)	108.53(1)	90.00	90.00
β (deg)	116.60(2)	85.45(1)	91.79(1)	107.78(1)	90.00
γ (deg)	90.00	71.46(1)	92.96(1)	90.00	90.00
<i>V</i> (Å ³)	759.8(3)	812.2(3)	841.4(1)	2427.8(1)	2743.1(1)
<i>Z</i>	2	2	2	4	4
<i>D</i> _{calc} (g cm ⁻³)	1.352	1.445	1.395	1.479	1.377
<i>T</i> (K)	298(2)	273(2)	273(2)	100(2)	298(2)
λ (Mo-K α)	0.71073	0.71073	0.71073	0.71073	0.71073
μ (mm ⁻¹)	0.094	0.107	0.103	0.105	0.097
2 θ range (deg)	50.58	50.48	50.50	50.54	50.46
Limiting indices	-11 \leq h \leq 11 -8 \leq k \leq 8 -14 \leq l \leq 14	-8 \leq h \leq 8 -12 \leq k \leq 12 -8 \leq l \leq 15	-9 \leq h \leq 10 -7 \leq k \leq 12 -12 \leq l \leq 12	-35 \leq h \leq 35 -8 \leq k \leq 8 -14 \leq l \leq 14	-37 \leq h \leq 37 -14 \leq k \leq 14 -8 \leq l \leq 8
<i>F</i> (000)	324	368	368	1128	1192
No. of Reflns. Measured	7108	4143	4255	7497	18397
No. Unique Reflns.	2748	2883	2967	2210	2487
No. of Reflns. used	2498	1607	1693	1750	2109
No. of Parameters	210	265	259	206	225
GOF on F ²	1.576	1.012	0.973	2.037	1.106
<i>R</i> ₁ [<i>I</i> > 2 σ (<i>I</i>)]	0.0869	0.0639	0.0594	0.0871	0.0642
<i>wR</i> ₂	0.2169	0.1624	0.1387	0.2998	0.1617
Final diff. Fourier map (e ⁻ Å ⁻³) max, min	0.483, -0.330	0.265, -0.304	0.254, - 0.258	0.554, -0.361	0.420, -0.266

Table 3.1. Continued.....

	2f	3b	3d	3e	3f
Formula	2(C ₉ H ₉ N ₅): 1(C ₁₀ H ₁₀ O ₄)	1(C ₄ H ₉ N ₅): 1(C ₈ H ₄ O ₄): 2(H ₂ O)	2(C ₄ H ₈ N ₅): 1(C ₈ H ₄ O ₄): 2(H ₂ O)	1(C ₄ H ₈ N ₅): 1(C ₁₀ H ₉ O ₄)	1(C ₄ H ₉ N ₅): 1(C ₁₀ H ₈ O ₄)
Formula Wt.	568.60	327.31	452.45	319.33	319.33
Crystal habit	Blocks	Blocks	Needles	Rod-Shaped	Rectangular Blocks
Crystal color	Colorless	Colorless	Colorless	Yellow	Colorless
Crystal system	Orthorhombic	Triclinic	Triclinic	Triclinic	Monoclinic
Space group	<i>Pbca</i>	<i>P</i> $\bar{1}$	<i>P</i> $\bar{1}$	<i>P</i> $\bar{1}$	<i>C 2/c</i>
<i>a</i> (Å)	12.405(4)	7.682(3)	3.834(2)	7.307(5)	18.730(2)
<i>b</i> (Å)	6.948(2)	8.204(3)	10.399(4)	8.808(6)	7.975(9)
<i>c</i> (Å)	31.402(1)	13.272(5)	12.762(5)	12.830(9)	9.896(1)
α (deg)	90.00	91.31 (1)	90.90(1)	73.46(1)	90.00
β (deg)	90.00	94.85 (1)	91.95(1)	76.39(1)	96.54(2)
γ (deg)	90.00	117.13 (1)	94.52(1)	71.01(1)	90.00
<i>V</i> (Å ³)	2706.5(15)	740.0(5)	506.9(4)	739.2(9)	1469(3)
<i>Z</i>	4	2	1	2	4
<i>D</i> _{calc} (g cm ⁻³)	1.395	1.469	1.482	1.435	1.444
<i>T</i> (K)	298(2)	273(2)	273(2)	273(2)	298(2)
λ (Mo-K α)	0.71073	0.71073	0.71073	0.71073	0.71073
μ (mm ⁻¹)	0.098	0.119	0.116	0.108	0.109
2 θ range (deg)	50.58	50.50	50.48	50.46	50.46
Limiting indices	-14 ≤ <i>h</i> ≤ 14 -8 ≤ <i>k</i> ≤ 8 -37 ≤ <i>l</i> ≤ 37	-9 ≤ <i>h</i> ≤ 9 -9 ≤ <i>k</i> ≤ 9 -15 ≤ <i>l</i> ≤ 15	-4 ≤ <i>h</i> ≤ 3 -11 ≤ <i>k</i> ≤ 12 -15 ≤ <i>l</i> ≤ 15	-8 ≤ <i>h</i> ≤ 8 -10 ≤ <i>k</i> ≤ 10 -15 ≤ <i>l</i> ≤ 15	-22 ≤ <i>h</i> ≤ 20 -8 ≤ <i>k</i> ≤ 9 -8 ≤ <i>l</i> ≤ 11
<i>F</i> (000)	1192	344	238	336	672
No. of Reflns. Measured	18044	5294	2594	5387	3466
No. Unique Reflns.	2459	2618	1807	2644	1323
No. of Reflns. used	2152	2251	814	1825	579
No. of Parameters	234	256	161	274	106
GOF on <i>F</i> ²	1.292	1.076	0.992	1.043	0.989
<i>R</i> ₁ [<i>I</i> > 2 σ (<i>I</i>)]	0.0685	0.0515	0.0832	0.0448	0.0756
<i>wR</i> ₂	0.1856	0.1306	0.1817	0.1036	0.1459
Final diff. Fourier map (e ⁻ ·Å ⁻³) max, min	0.264, -0.389	0.307, - 0.282	0.506, -0.416	0.173, - 0.159	0.191, - 0.202

Table 3.2. Characteristic hydrogen bond distances (Å) and angles (°) of the various molecular complexes formed between aminopyrimidines and triazines with various aryl and aralkyl carboxylic acids (Chart 1).[#]

Hydrogen Bond, D-H...A	1a			1b			1c			1d			1e		
N-H...N	2.11	2.96	173	2.11	2.98	157	2.04	2.96	174	2.30	3.14	173	2.58	3.42	168
	2.12	2.98	177				2.16	3.02	179						
	2.16	3.01	168				2.17	3.04	173						
	2.17	3.03	173				2.22	3.00	174						
N-H...O	2.06	2.89	163	2.04	2.95	171	1.96	2.87	178	2.10	2.99	174	2.11	2.95	167
	2.07	2.92	171	2.06	2.90	147	2.18	2.95	143	2.12	3.03	169			
	2.30	2.99	137				2.46	3.35	166	2.13	2.96	160			
	2.30	3.10	155												
N-H...O ⁻				2.00	2.90	173	2.02	2.87	173				2.04	2.83	152
N ⁺ -H...O ⁻				1.71	2.66	172	1.72	2.58	173				2.19	2.95	147
													2.22	3.02	153
O-H...N	1.79	2.59	166				1.70	2.65	173	1.65	2.59	171			
	1.80	2.60	167							2.29	3.06	166			
O-H...O	1.94	2.87	168	1.57	2.39	178				2.05	2.82	154			
	2.01	2.82	164												
O-H...O ⁻							1.99	2.76	138				1.69	2.50	174
C-H...N													2.49	3.20	131
													2.52	3.48	173
C-H...O										2.59	3.22	123	2.79	3.54	143
C-H...O ⁻													2.23	3.11	152

[#] Three columns for each structure represent H...A, D...A distances and D-H...A angle, respectively for a typical hydrogen bond, being represented as D-H...A

Table 3.2. Continued.....

Hydrogen Bond, D-H...A	2a			2b			2c			2d			2e		
N-H...N	2.14	2.99	170	2.15	2.97	160	2.20	3.05	174	2.08	2.97	166	2.11	2.98	170
	2.31	3.16	172							2.32	3.18	174	2.21	3.06	169
N-H...O	2.03	2.88	167	2.09	2.77	136	2.01	2.86	173	2.05	2.90	168	2.25	3.08	162
	2.44	2.98	121	2.28	3.10	159	2.10	2.93	162	2.56	3.27	139	2.54	3.26	138
	2.59	3.25	134	2.59	3.24	133									
N-H...O ⁻				1.99	2.84	154									
N ⁺ -H...O ⁻				1.87	2.78	173									
O-H...N	1.79	2.61	173				1.87	2.69	171	1.78	2.59	170	1.85	2.65	166
							1.93	2.74	167						
O-H...O				1.59	2.40	167									
C-H...O							2.55	3.37	147						
C-H...O ⁻				2.34	3.19	151									

Table 3.2. Continued.....

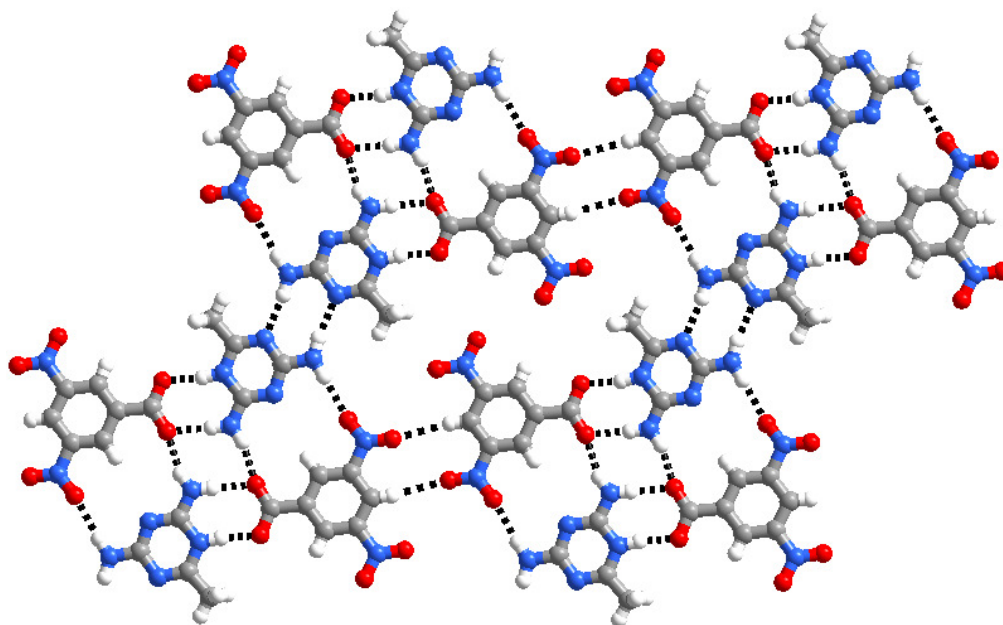
Hydrogen Bond, D-H...A	2f			3b			3d			3e			3f		
N-H...N	2.12	2.99	168				2.19	3.03	168	2.08	2.97	172			
	2.16	3.04	172				2.49	3.17	137						
N-H...O	2.10	2.98	175	2.03	2.89	165	2.11	2.97	168	2.17	3.04	163			
				2.06	2.94	164	2.47	3.13	145	2.23	2.93	136			
N-H...O ⁻				1.92	2.85	176	2.01	2.86	167	1.91	2.83	176	1.94	2.88	171
				1.99	2.86	179	2.21	2.91	138	2.07	2.89	155	2.03	2.89	178
				2.03	2.91	179									
				2.03	2.93	175									
N ⁺ -H...O ⁻				1.63	2.61	176	1.97	2.77	154	1.85	2.86	175	1.70	2.60	174
				1.76	2.61	173									
O-H...N	1.73	2.63	172												
O-H...O ⁻										1.74	2.55	168			
C-H...N										2.46	3.14	128			

3.7 References

- (1) (a) Sauriat-Dorizon, H.; Maris, T.; Wuest, J. D.; Enright, G. D. *J. Org. Chem.* **2003**, *68*, 240-246. (b) Le Fur, E.; Demers, E.; Maris, T.; Wuest, J. D. *Chem. Commun.* **2003**, *9*, 2966-2967. (c) Brunet, P.; Demers, E.; Maris, T.; Enright, G. D.; Wuest, J. D. *Angew. Chem. Int. Ed.* **2003**, *42*, 5303-5306. (d) Boils, D.; Perron, M. O.; Monchamp, F.; Duval, H.; Maris, T.; Wuest, J. D. *Macromolecules* **2004**, *37*, 7351-7357. (e) Fournier, J. H.; Maris, T.; Wuest, J. D. *J. Org. Chem.* **2004**, *69*, 1762-1775. (f) Demers, E.; Maris, T.; Wuest, J. D. *Cryst. Growth Des.* **2005**, *5*, 1227-1235. (g) Lalibert, D.; Maris, T.; Demers, E.; Helzy, F.; Arseneault, M.; Wuest, J. D. *Cryst. Growth Des.* **2005**, *5*, 1451-1456. (h) Malek, N.; Maris, T.; Simard, M.; Wuest, J. D. *J. Am. Chem. Soc.* **2005**, *127*, 5910-5916. (i) Lebel, O.; Maris, T.; Perron, M.; Demers, E.; Wuest, J. D. *J. Am. Chem. Soc.* **2006**, *128*, 10372-10373. (j) Maly, K. E.; Dauphin, C.; Wuest, J. D. *J. Mater. Chem.* **2006**, *16*, 4695-4700. (k) Maly, K. E.; Gagnon, E.; Maris, T.; Wuest, J. D. *J. Am. Chem. Soc.* **2007**, *129*, 4306-4322.
- (2) Perpetuo, G. J.; Janczak, J. *Acta Crystallogr.* **2005**, *E61*, o287-o289.
- (3) Janczak, J.; Perpetuo, G. J. *Acta Crystallogr.* **2001**, *C57*, 123-125.
- (4) Xiu-Lian, Z. *Chinese J. Struct. Chem.* **2008**, *27*, 117-122.
- (5) Zhang, J.; Kang, Y.; Wen, Y. H.; Li, Z. J.; Qin, Y. Y.; Yao, Y. G. *Acta Crystallogr.* **2004**, *E60*, o462-o463.
- (6) Zhang, X. L.; Chen, X. M. *Cryst. Growth Des.* **2005**, *5*, 617-622.

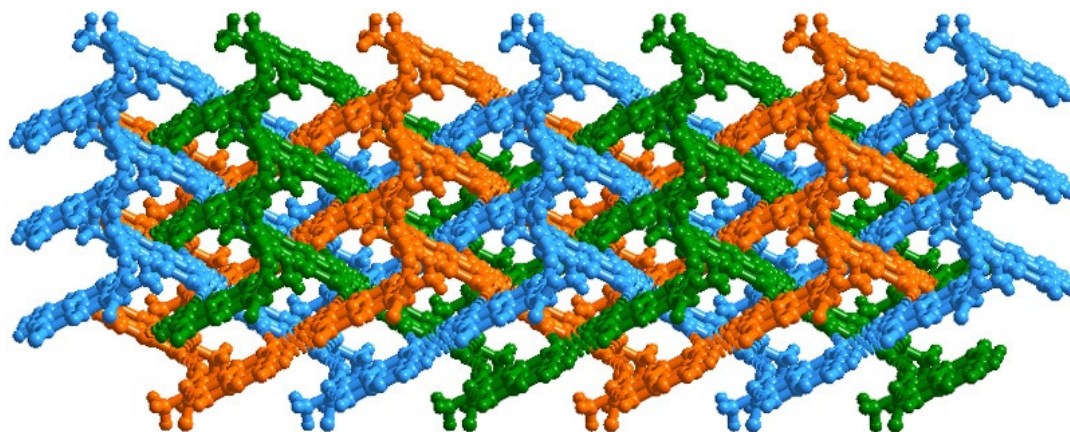
- (7) Karle, I.; Gilardi, R. D.; Rao, C.; Muraleedharan, K. M.; Ranganathan, S. J. *Chem. Crystallogr.* **2003**, *33*, 727-749.
- (8) Pedireddi, V. R.; Chatterjee, S.; Ranganathan, A.; Rao, C. N. R. *Tetrahedron* **1998**, *54*, 9457-9474.
- (9) (a) Zerkowski, J. A.; Seto, C. T.; Whitesides, G. M. *J. Am. Chem. Soc.* **1992**, *114*, 5473-5475. (b) Mathias, J. P.; Seto, C. T.; Simanek, E. E.; Whitesides, G. M. *J. Am. Chem. Soc.* **1994**, *116*, 1725-1736. (c) Ranganathan, A.; Pedireddi, V. R.; Rao, C. N. R. *J. Am. Chem. Soc.* **1999**, *121*, 1752-1753. (d) Mascal, M.; Hext, N. M.; Warmuth, R.; Moore, M. H.; Turkenburg, J. P. *Angew. Chem., Int. Ed.* **1996**, *35*, 2203-2206. (e) Whitesides, G. M.; Mathias, J. P.; Seto, C. T. *Science* **1991**, *254*, 1312-1319.
- (10) (a) Friščić, T.; MacGillivray, L. R. *Supramol. Chem.* **2005**, *17*, 47-51. (b) Gao, X.; Friščić, T.; MacGillivray, L. R. *Angew. Chem., Int. Ed.* **2004**, *43*, 232-236. (c) MacGillivray, L. R. *J. Org. Chem.* **2008**, *73*, 3311-3317. (d) MacGillivray, L. R.; Papaefstathiou, G. S.; Friščić, T.; Hamilton, T. D.; Buïar, D. K.; Chu, Q.; Varshney, D. B.; Georgiev, I. G. *Acc. Chem. Res.* **2008**, *41*, 280-291. (e) Varughese, S.; Pedireddi, V. R. *Chem. Eur. J.* **2006**, *12*, 1597-1609.
- (11) (a) Aitipamula, S.; Desiraju, G. R.; Jaskolski, M.; Nangia, A.; Thaimattam, R. *CrystEngComm* **2003**, *5*, 447-450. (b) Batten, S. R.; Robson, R. *Angew. Chem., Int. Ed.* **1998**, *37*, 1461-1494. (c) Chen, B. L.; Eddaoudi, M.; Hyde, S. T.; O'Keeffe, M.; Yaghi, O. M. *Science* **2001**, *291*, 1021-1023. (d) Friedrichs, O. D.; O'Keeffe, M.; Yaghi, O. M. *Solid State Sciences* **2003**, *5*, 73-78. (e) Guo, X.; Zhu, G.; Fang, Q.; Xue, M.; Tian, G.; Sun, J.; Li, X.; Qiu, S. *Inorg. Chem.* **2005**,

- 44, 3850-3855. (f) Kaye, S. S.; Dailly, A.; Yaghi, O. M.; Long, J. R. *J. Am. Chem. Soc.* **2007**, *129*, 14176-14177. (g) Mallinson, P. R.; Smith, G. T.; Wilson, C. C.; Grech, E.; Wozniak, K. *J. Am. Chem. Soc.* **2003**, *125*, 4259-4270. (h) Maly, K. E.; Gagnon, E.; Maris, T.; Wuest, J. D. *J. Am. Chem. Soc.* **2007**, *129*, 4306-4322. (i) Metrangolo, P.; Meyer, F.; Pilati, T.; Proserpio, D. M.; Resnati, G. *Chem. Eur. J.* **2007**, *13*, 5765-5772. (j) Reddy, D. S.; Dewa, T.; Endo, K.; Aoyama, Y. *Angew. Chem., Int. Ed.* **2000**, *39*, 4266-4268. (k) Sauriat-Dorizon, H.; Maris, T.; Wuest, J. D.; Enright, G. D. *J. Org. Chem.* **2003**, *68*, 240-246. (l) Batten, S. R.; Robson, R. *Angew. Chem., Int. Ed.* **1998**, *37*, 1461-1494. (m) Chae, H. K.; Kim, J.; Friedrichs, O. D.; O'Keefe, M.; Yaghi, O. M. *Angew. Chem., Int. Ed.* **2003**, *42*, 3907-3909.
- (12) (a) Siemens, SMART System, Siemens Analytical X-ray Instrument Inc., Madison, WI (USA), 1995; (b) G. M. Sheldrick, SADABS Siemens Area Detector Absorption Correction Program, University of Gottingen, Gottingen, Germany, 1994; (c) G. M. Sheldrick, SHELXTL-PLUS program for crystal structure solution and refinement, University of Gottingen, Gottingen, Germany.
- (13) A. L. Spek, PLATON, molecular geometry program, University of Utrecht, The Netherlands, 1995.



CHAPTER FOUR

SUPRAMOLECULAR ASSEMBLIES OF SOME DERIVATIVES OF TRIAZINES AND PYRIMIDINES WITH 3,5-DINITROBENZOIC ACID AND ITS DERIVATIVES



4.1 Introduction

Molecules possessing multiple functional groups of the same or different kind are interesting molecular building blocks in supramolecular synthesis. Systematic addition of functional groups to a molecule can change the dimensionality of the supramolecular networks, as illustrated by the supramolecular networks formed by successive addition of carboxylic acid functional group at various positions on benzene, (Figure 4.1(a)-(d)).

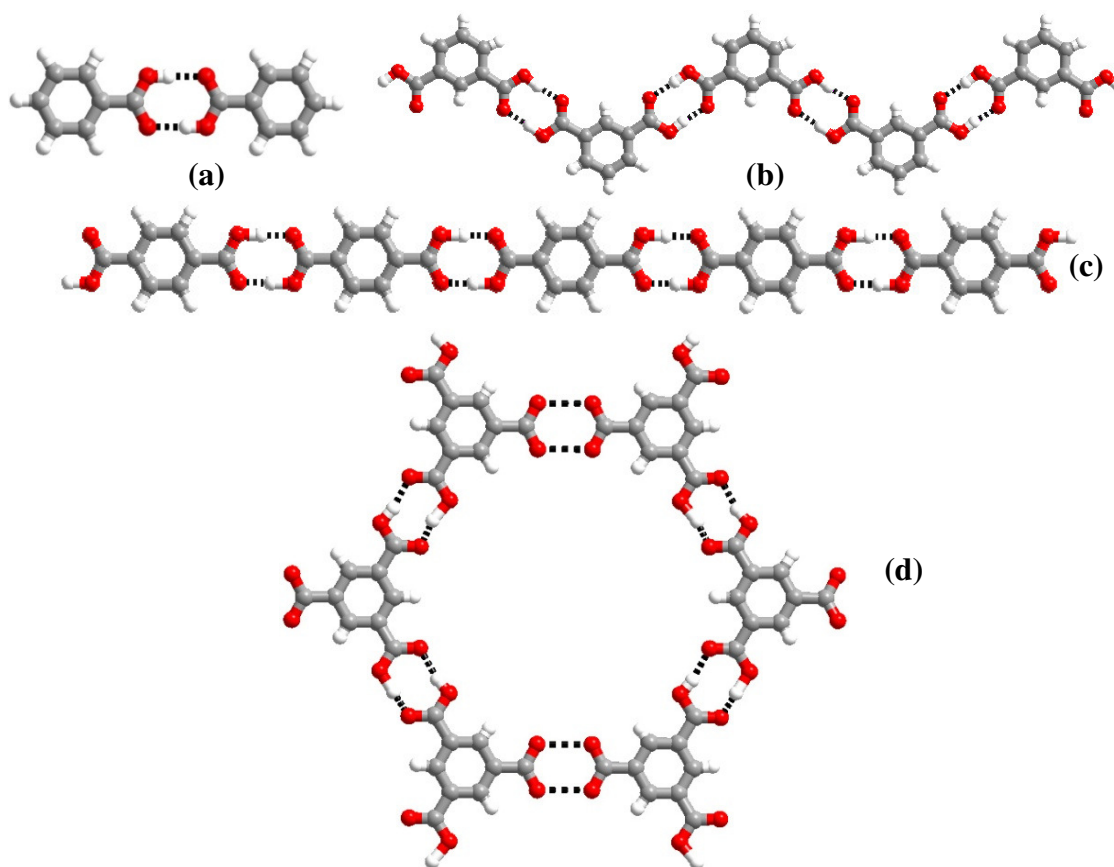


Figure 4.1. (a) Zero-dimensional dimers observed in benzoic acid (only one -COOH group). (b) and (c) Crinkled and linear tapes formed by isophthalic and terephthalic acid (two -COOH groups). (d) Six-member cyclic network formed by trimesic acid (three -COOH groups).

It is understood from Figure 4.1 that benzoic acid with a single –COOH group forms only zero-dimensional dimers¹, while isophthalic and terephthalic acids, with two –COOH groups, form crinkled² and linear tapes³ respectively. Trimesic acid, which contains three carboxylic acid groups, forms a two-dimensional six member cyclic network⁴.

Price and co-workers deduced the crystal structure of biphenyl-3,3',5,5'-tetracarboxylic acid, which is like an extended isophthalic acid, as a two-dimensional cyclic network with voids⁵ (Figure 4.2), resembling as if the tapes of isophthalic acid (see Figure 4.1(b)) are joined together, and illustrates the importance of appropriate placement of various functional groups for the formation of tailor made supramolecular assemblies⁶.

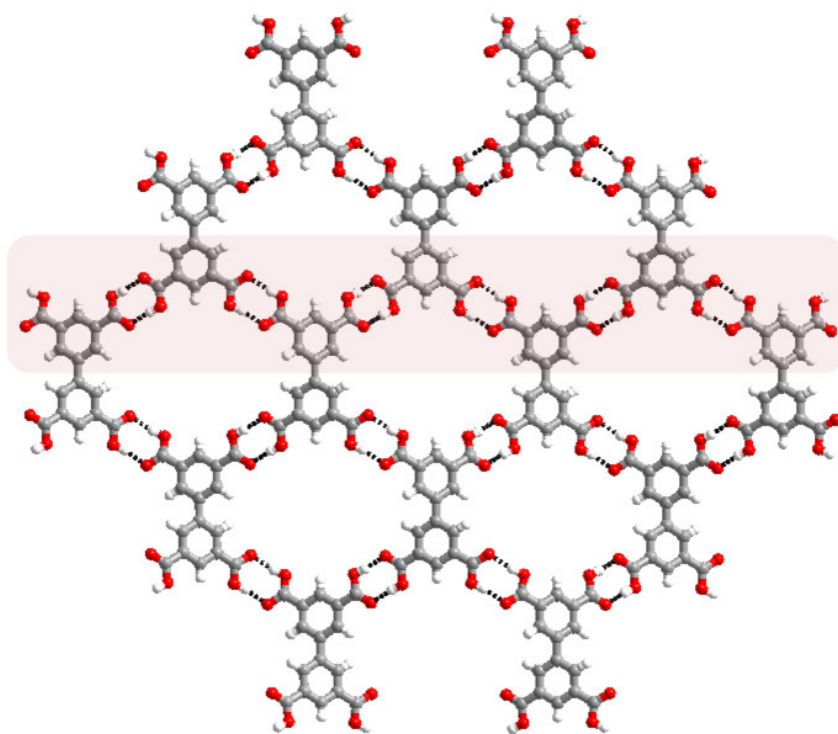


Figure 4.2. Biphenyl-3,3',5,5'-tetracarboxylic acid molecules interacting to form sheet structure, with voids.

Substitutions on molecules can change not only the dimensionality of the supramolecular network formed by it, but also change some physical properties of molecules, like pK_a , which can further influence the formation of a specific supramolecular network⁷. Thus, while a complex formed between 2-amino-4,6-dimethylpyrimidine and benzoic acid ($pK_a = 4.20$) is through neutral hydrogen bonds ($O-H\cdots N$ and $N-H\cdots O$)⁸, the complex formed by 2-amino-4,6-dimethylpyrimidine and 3,5-dinitrobenzene ($pK_a = 2.80$) is, however, ionic through $N^+-H\cdots O^-$ and $N-H\cdots O^-$ hydrogen bonds⁹, as shown in Figures 4.3(a) and (b). Generally the strength of an ionic hydrogen bond is more compared to neutral hydrogen bonds of the same kind.

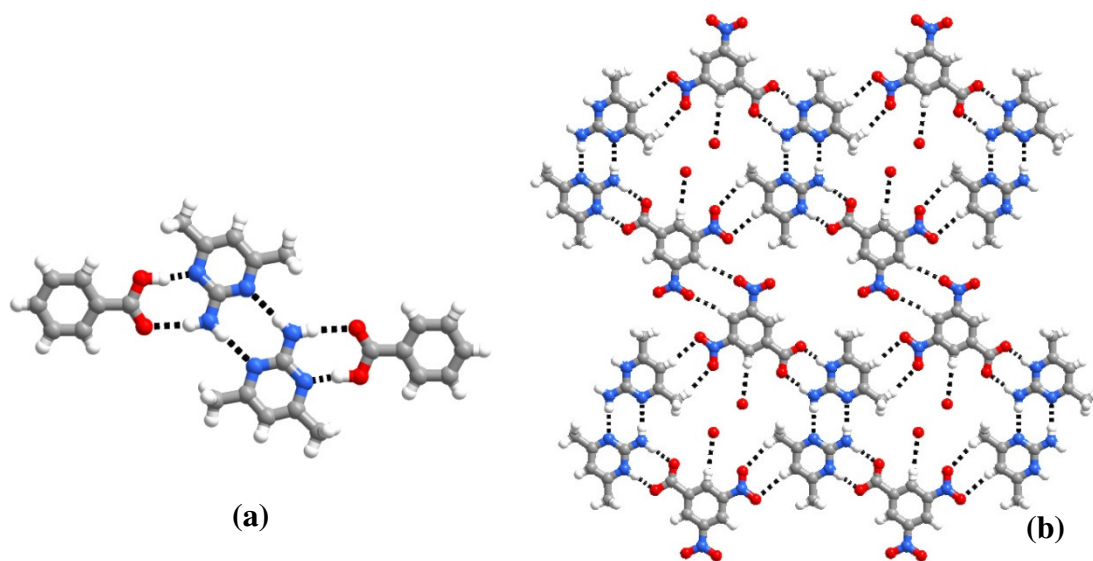


Figure 4.3. (a) Co-crystal formation observed between 2-amino-4,6-dimethylpyrimidine and benzoic acid (b) Molecular adduct of 2-amino-4,6-dimethylpyrimidine and 3,5-dinitrobenzoic acid.

Etter and co-workers used co-crystallization reactions to study competition between various functional groups and illustrated the hierarchy in the formation of hydrogen bonds between the various functional groups. According to this rule, in a

system with a multitude of hydrogen-bonding functionalities “the best hydrogen bond donors and best hydrogen bond acceptors will preferentially form hydrogen bonds to one another”¹⁰, as shown in Figure 4.4.

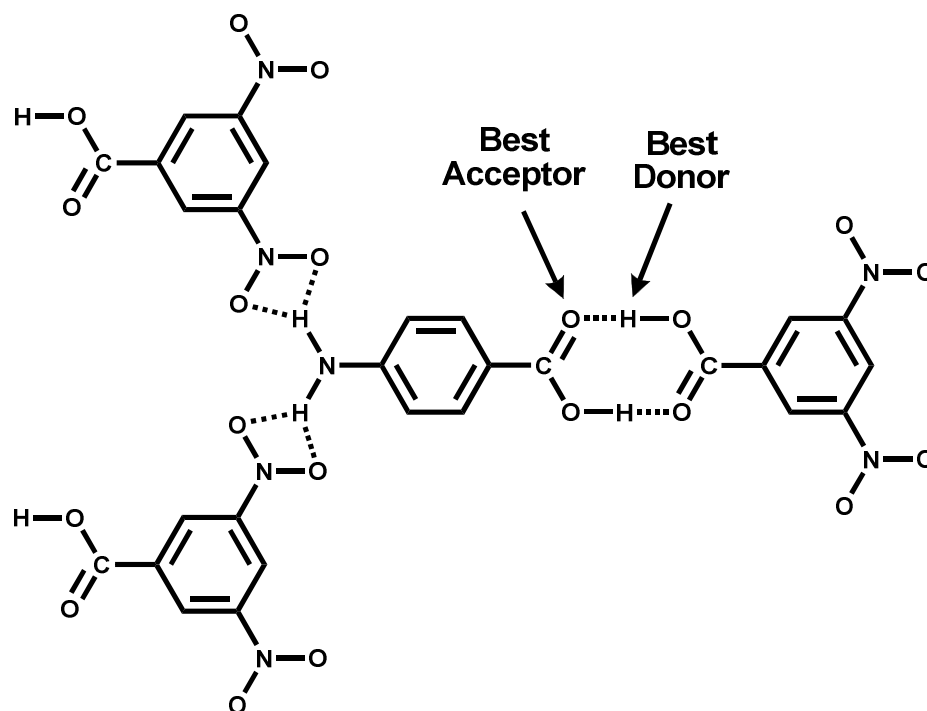
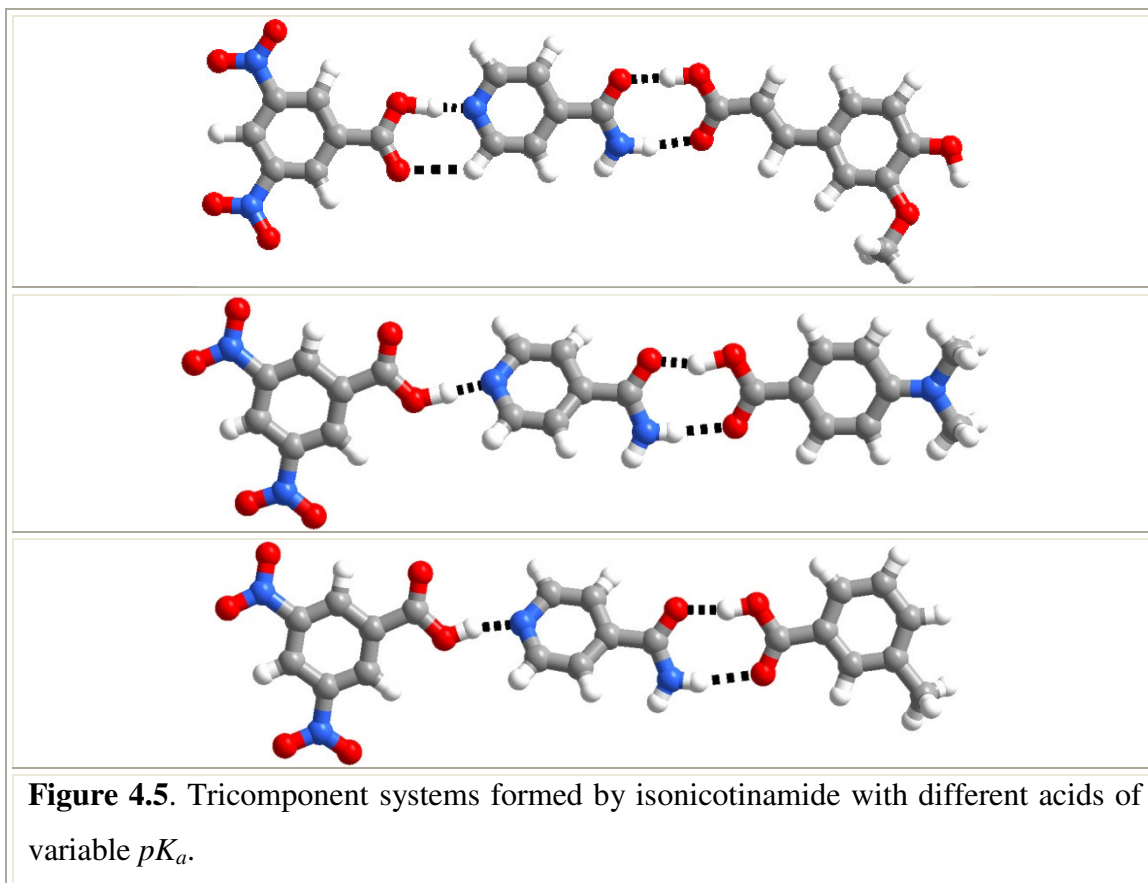


Figure 4.4. Interactions between best donor, acid hydrogen of carboxylic acid group of 3,5-dinitrobenzoic acid with best acceptor, carbonyl group of 4-aminobenzoic acid observed in a co-crystal between 3,5-dinitrobenzoic acid and 4-aminobenzoic acid.

Extrapolation of this rule suggests that the second-best donor will form a hydrogen bond to the second best acceptor. Aakerøy and co-workers made use of this concept for the formation of tri-component systems¹¹. They recognized isonicotinamide, having pyridyl nitrogen, as the best acceptor followed by carboxamide, for the formation of tri-component supramolecular assemblies. Thus co-crystallization of isonicotinamide with two different acid molecules of different pK_a , for example, 3,5-dinitrobenzoic acid ($pK_a=2.77$), in association with 4-hydroxy-3-

methoxybenzoic acid ($pK_a=4.45$), 3-methoxybenzoic acid ($pK_a=4.27$) or 4-*N,N'*-dimethylbenzoic acid ($pK_a=4.98$), demonstrated that higher pK_a acid preferentially interact with pyridyl nitrogen atom on isonicotinamide, while lower pK_a acid establish interaction with amide functionality,¹² as shown in Figure 4.5.



Considering the great variations in the ultimate supramolecular assemblies with more change of functional groups, as depicted above, for various carboxylic acid mediated assemblies, it was aimed to explore such features in triazines systems, in continuation of earlier endeavors described in the previous chapter. For this purpose, melamine and its derivatives have been chosen to co-crystallize with several carboxylic acids with different pK_a values, like 3,5-dinitrobenzoic acid and its

analogues derivatives, as illustrated in Chart 4.1. Co-crystals were analyzed by single crystal X-ray diffraction methods and the analysis of the structures is presented in the following sections.

4.2 Molecular complexes of melamine and its derivatives with 3,5-dinitrobenzoic acid and its derivatives

In this process we have noted that Bernstein and co-workers have reported that co-crystal structure of melamine and 3,5-dinitrobenzoic acid, as a salt with proton transfer from 3,5-dinitrobenzoic acid to the aromatic nitrogen of melamine.¹³ Thus, an adduct is formed primarily through strong $N^+-H^{\cdots}O^-$, $N-H^{\cdots}O^-$ charge assisted dimeric hydrogen bonds. Two adjacent hydrogen bonded dimers interact with each other by two $N-H^{\cdots}O^-$ hydrogen bonds, as shown in Figure 4.6(a), yielding ensembles of tetramers. Further, four such adjacent ensembles are held together by two different types of hydrogen bonded dimers comprising of either $N-H^{\cdots}N$ or $C-H^{\cdots}O$, and such an arrangement is shown in Figure 4.6 (b).

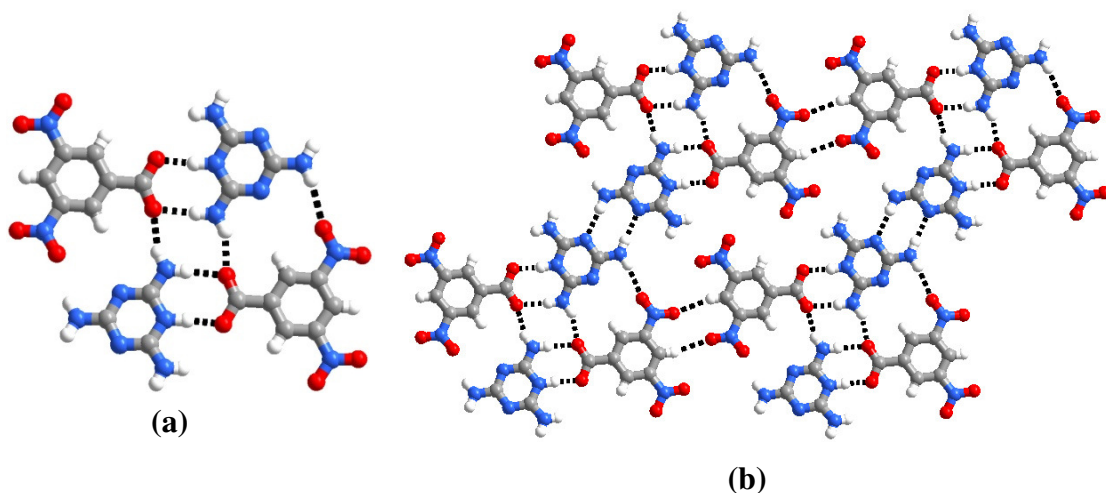
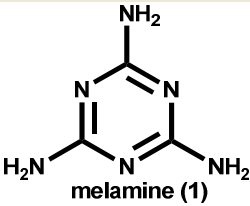
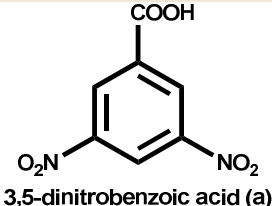
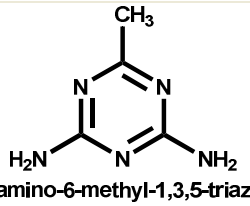
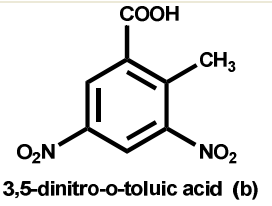
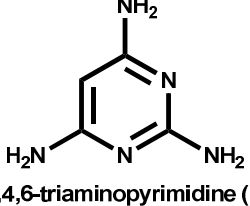
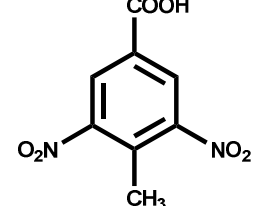


Figure 4.6. (a) Tetramers observed in the complex between melamine and 3,5-dinitrobenzoic acid (b) Adjacent four tetrameres interacting to form sheet structure.

The packing is quite intriguing with a large number of hydrogen bonds of various types simultaneous contribution towards the stabilization of the structure, analysis of the other co-crystals have been directed to evaluate the robustness of those patterns, especially the influence of pK_a of the constituent on the ultimate assembly. Hence, the complexes **1b**, **1c**, **2a-2c** and **3a-3c** have been analyzed as illustrated below.

Chart 4.1

Reactants		Reaction	Products and ratio
 <p>melamine (1)</p>	 <p>3,5-dinitrobenzoic acid (a)</p>	1 + a	1a (1:1) ¹³
		1 + b	1b.H₂O (1:1:1)
		1 + c	1c (1:1)
 <p>2,4-diamino-6-methyl-1,3,5-triazine (2)</p>	 <p>3,5-dinitro-o-toluic acid (b)</p>	2 + a	2a (1:1)
		2 + b	2b (1:1)
		2 + c	2c (1:1)
 <p>2,4,6-triaminopyrimidine (3)</p>	 <p>3,5-dinitro-p-toluic acid (c)</p>	3 + a	3a.CH₃OH (1:1:1)
		3 + b	3b (1:1)
		3 + c	3c

4.2.1 Molecular complex of melamine and 3,5-dinitro-*o*-toluic acid-**1b**

Crystals of complex **1b** were obtained from a methanol solution of melamine and 3,5-dinitro-*o*-toluic acid. The structure determination (Table 4.2) reveals that the asymmetric unit consists of 1:1 ratio of **1** and the acid, respectively, along with water molecules (see Figure 4.7 (a)). In this complex also the acid molecule is deprotonated and the proton goes to the aromatic nitrogen of melamine, as reported in **1a**.

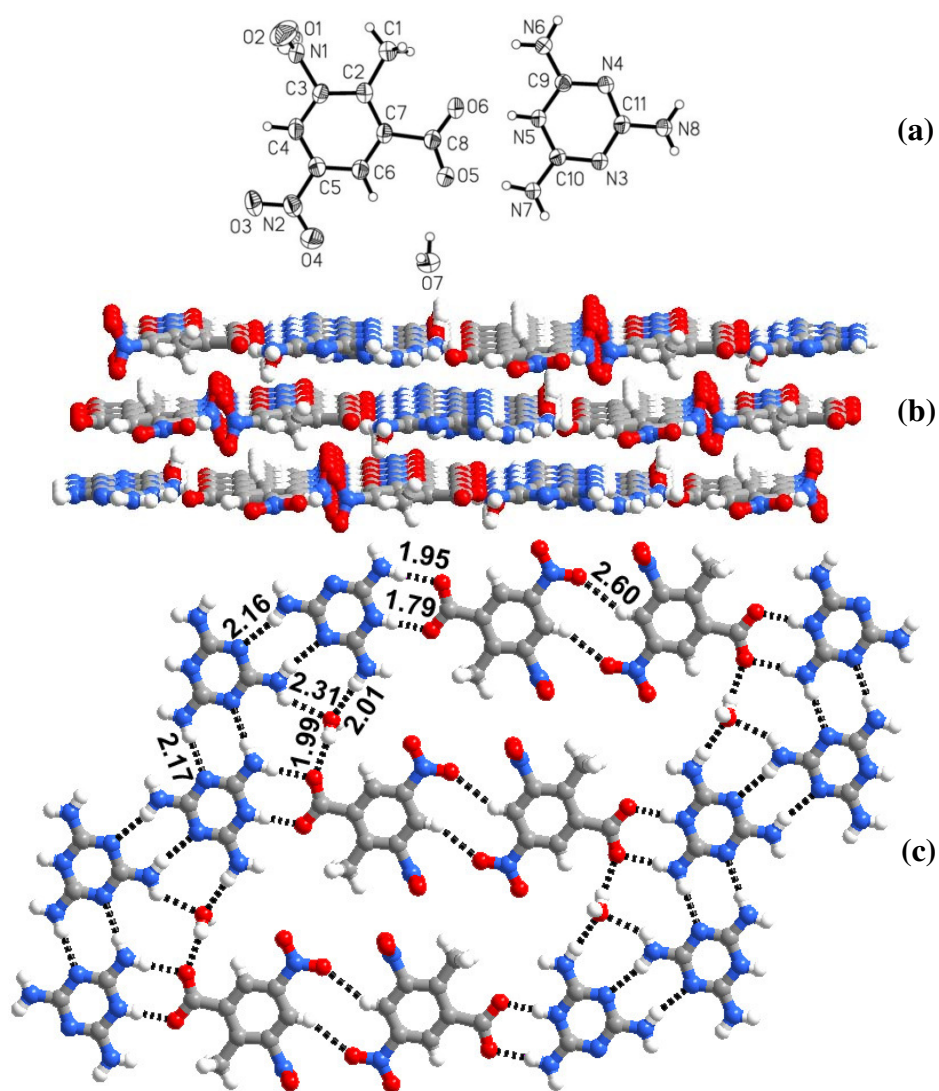


Figure 4.7. (a) ORTEP diagram of asymmetric unit observed in **1b** (b) layered packing observed in **1b** (c) Arrangement of molecules in a typical sheet structure.

In the complex **1b**, the three-dimensional arrangement is a layered structure, as shown in Figure 4.7(b). Interaction between **1** and the acid within a layer is quite intriguing with lot of deviations than observed in **1a**. In the complex **1b**, the molecular aggregation leads to the formation of a two-dimensional host-guest type assembly (Figure 4.7(c)), with very small voids, that are being filled by water molecules. The molecules of **1** and the acid interact with each other through a cyclic hydrogen bonding pattern consists of $N^+-H\cdots O^-$ ($H\cdots O$, 1.79 Å) and $N-H\cdots O^-$ ($H\cdots O^-$, 1.95 Å). Such six adjacent supramolecules are held together by dimers of $N-H\cdots N$ and $C-H\cdots O$ hydrogen bond dimers with $H\cdots N$ and $H\cdots O$ distances of 2.16, 2.17 and 2.60 Å respectively; yielding a cyclic network with small voids. In these voids water molecules are inserted, establishing interaction with the host network by $N-H\cdots O$ and $O-H\cdots O^-$ hydrogen bonds with both **1** and acid, as illustrated in Figure 4.7(c). Thus, tetrameric network obtained in **1a** is not present in **1b**, illustrating the significance of additional substituent $-CH_3$ group in perturbing the tetramer network observed in **1a**. However, it is interesting to note that a close look at Figure 4.6(a), the observed perturbation in **1b** is not expected on geometric consideration. Thus, the observed differences could be certainly accounted for the differences in the pK_a of the acids present in the complex **1a** and **1b**. Thus, further experiments by considering 3,5-dinitro-*p*-toluic acid, having different pK_a than the acids in **1a** and **1b**, have been carried out.

4.2.2 Molecular complex of melamine and 3,5-dinitro-*p*-toluic acid-1c

Complex **1c**, obtained by co-crystallizing melamine, **1** and 3,5-dinitro-*p*-toluic acid, from a methanol solution, has some similarities as well as distinct differences from the co-crystals of **1a** and **1b**. The structure determination (Table 4.2) reveals that the asymmetric unit consists of 1:1 ratio of **1** and the acid, (see Figure 4.8(a)). In **1c** also proton transfer has occurred, transferring from carboxylic acid functional group to the aromatic nitrogen of melamine, as observed in **1a** and **1b**. As in structures **1a** and **1b**, the co-crystallized ligands interact with each other primarily through strong charge assisted $\text{N}^+\text{-H}\cdots\text{O}^-$, $\text{N-H}\cdots\text{O}^-$ dimeric hydrogen bonds, with bond distances of 1.90 Å and 1.91 Å, respectively. Two such adjacent supramolecules interact with each other by two $\text{N-H}\cdots\text{O}^-$ and two $\text{N-H}\cdots\text{O}$ with the corresponding $\text{H}\cdots\text{O}^-$ and $\text{H}\cdots\text{O}$ distances being 2.05 Å and 2.30 Å yielding a tetrameric arrangement, as shown in Figure 4.8(b). In the further extended structure, the adjacent tetrameric ensembles are held together by $\text{N-H}\cdots\text{O}$ hydrogen bonds formed between $-\text{NO}_2$ and NH_2 groups, with $\text{H}\cdots\text{O}$ distance of 2.13 Å. Such two dimensional network structure, as shown in Figure 4.8(c), created huge cavity of dimension $18 \times 14 \text{ \AA}^2$, which is stabilized by 3-fold interpenetration¹⁴ as illustrated in Figure 4.9.

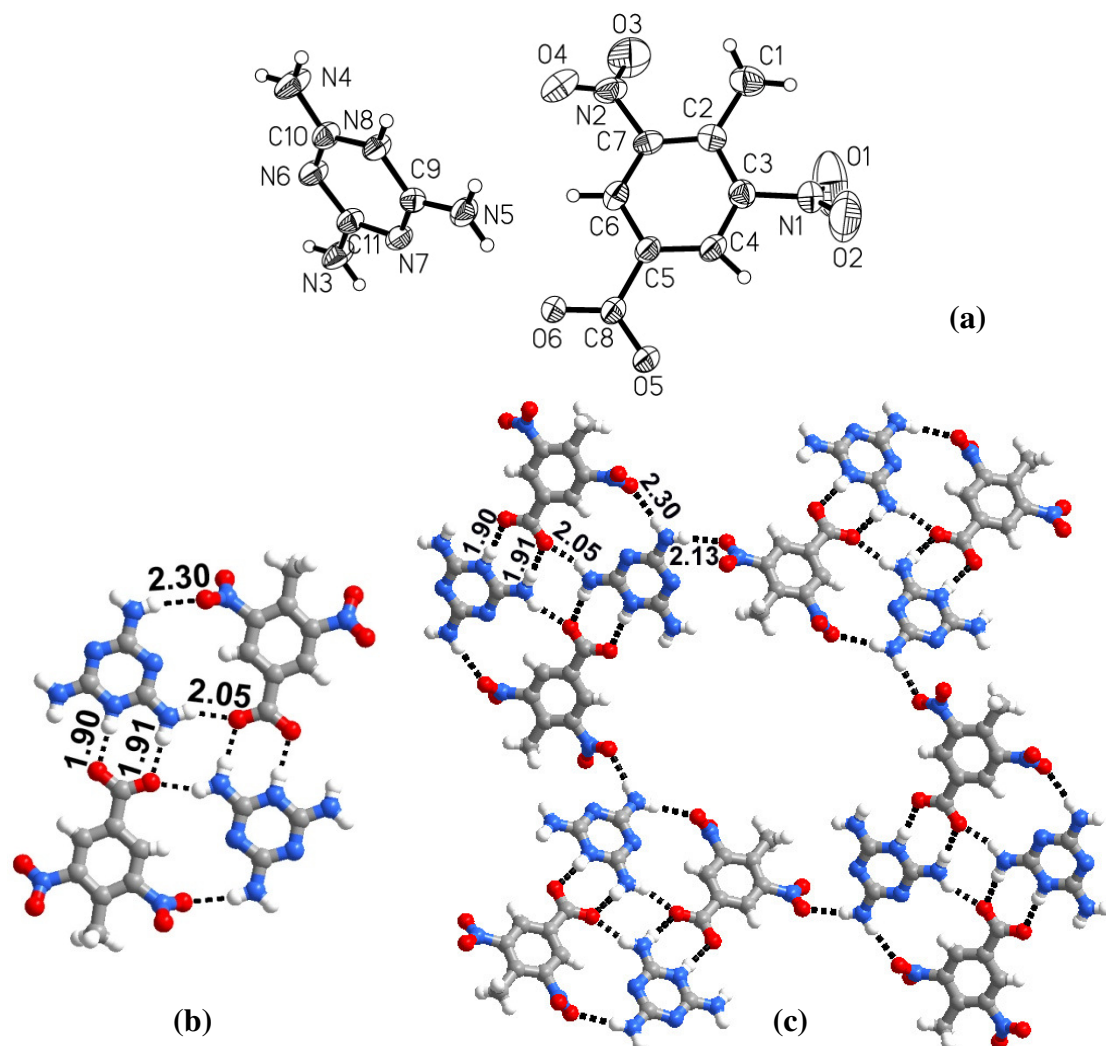


Figure 4.8. (a) ORTEP diagram of asymmetric unit observed in **1c** (b) Quartet formed by the interaction of two molecules each of **1** and **c**. (c) Four adjacent quartets interacting to form a void space of dimensions 18 × 14 Å².

Thus, either introducing a functional group, or altering the position, structural variations are realized, although **1a** and **1c** shown similar arrangements in the primary recognition pattern, especially yielding tetramer units. In these structures, as only the acid component is varied, it is appropriate to study the possible changes by varying substituents on heterocyclic compounds as well. Hence further studies are focused towards the structural elucidation of **2a-2c** and **3a-3c** obtained by co-crystallization of

2,4-diamino-6-methyl-1,3,5-triazine, **2** and 2,4,6-triaminopyrimidine, **3** with 3,5-dinitrobenzoic, 3,5-dinitro-*o*-toluic and 3,5-dinitro-*p*-toluic acids respectively.

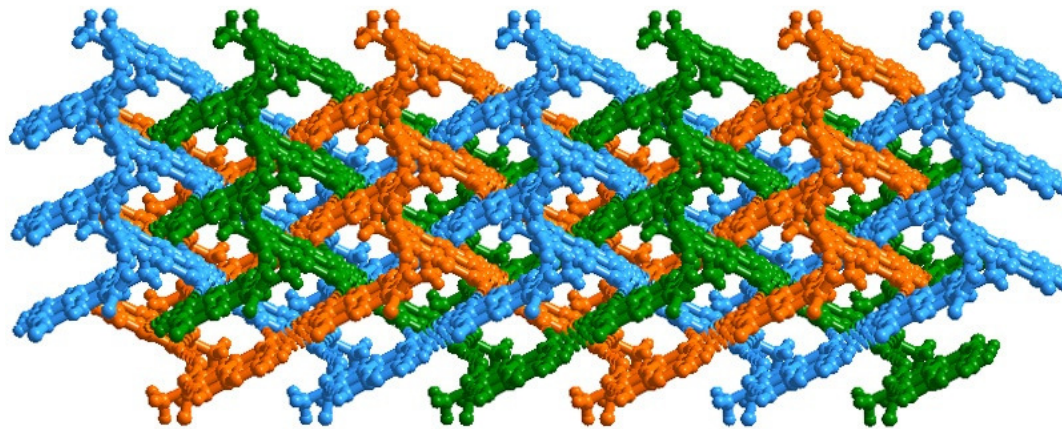


Figure 4.9. Three-fold interpenetration observed in **1c**.

4.2.3 Supramolecular assembly formed between 2,4-diamino-6-methyl-1,3,5-triazine and 3,5-dinitrobenzoic acid-2a

Co-crystallization of 2,4-diamino-6-methyl-1,3,5-triazine, **2** and 3,5-dinitrobenzoic acid from CH₃OH, resulted in the formation of a complex in a 1:1 ratio (Table 4.2). In the three-dimensional packing, the molecules are arranged in the form of stacked sheets, as shown in Figure 4.10.

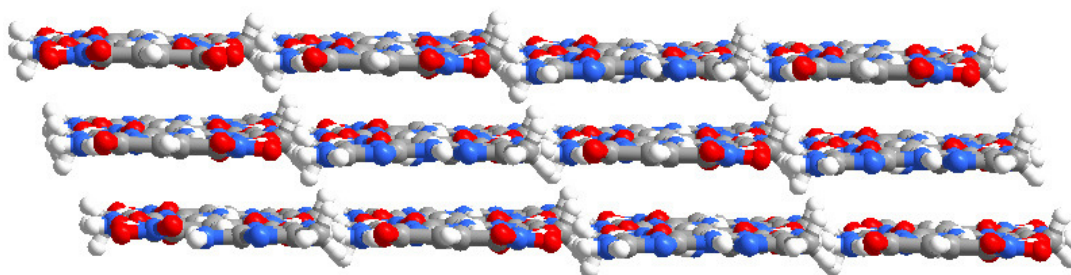


Figure 4.10. Packing arrangement in the form of stacked sheets observed in the crystal structure of **2a**.

In **2a** also the -COOH group of 3,5-dinitrobenzoic acid is deprotonated, as observed in **1a-1c** and the proton goes to the aromatic nitrogen of **2**, ortho with respect to methyl

group of 2,4-diamino-6-methyl-1,3,5-triazine. The molecules of **2** and the acid interact with each other primarily through $\text{N-H}^+\cdots\text{O}^-$ and $\text{N-H}\cdots\text{O}^-$ charge assisted hydrogen bonds, with the corresponding distances being 1.75 and 1.93 Å, respectively. Two such adjacent hydrogen bonded entities are held together by two $\text{N-H}\cdots\text{O}^-$ and $\text{N-H}\cdots\text{O}$ hydrogen bonds with the corresponding $\text{H}\cdots\text{O}^-$ and $\text{H}\cdots\text{O}$ distances being 1.98 and 2.16 Å, yielding a tetrameric assembly, as shown in Figure 4.11(a). In two dimensional arrangement, the tetramers are held together by two types of cyclic hydrogen bonds, found by either $\text{N-H}\cdots\text{N}$ or $\text{C-H}\cdots\text{O}$, with the corresponding $\text{H}\cdots\text{N}$ and $\text{H}\cdots\text{O}$ distances being 2.09 and 2.59 Å, respectively. Thus, the structure obtained in **2a** is identical with that of **1a** in all aspects and it is indeed quite intriguing and exciting to further proceed with co-crystals of **2b** and **2c** formed by **2** with 3,5-dinitro-*o*-toluic acid and 3,5-dinitro-*p*-toluic acid respectively for the comparison with **1b** and **1c**.

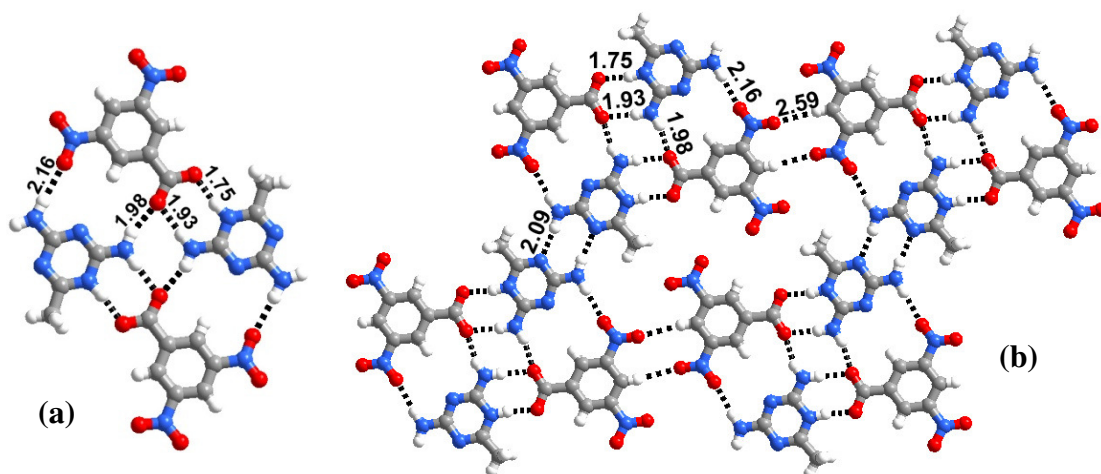


Figure 4.11. (a) Quartet observed in the crystal structure of complex, **2a** (b) Sheet structure formed by the interaction of four adjacent quartets.

4.2.4 Supramolecular assembly formed by 2,4-diamino-6-methyl-1,3,5-triazine with 3,5-dinitro-*o*-toluic acid-2b and 3,5-dinitro-*p*-toluic acid-2c

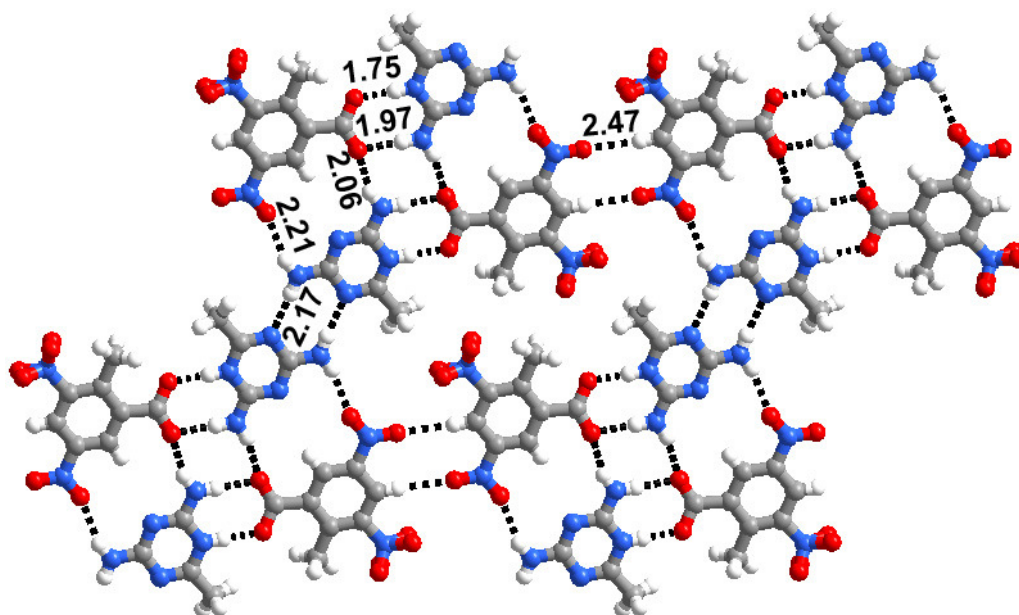


Figure 4.12. Formation of eight member cyclic network observed in **2b**.

In contrast to **1b** and **1c**, surprisingly the 1:1 complex, **2b** (Table 4.2) obtained between **2** and 3,5-dinitro-*o*-toluic acid, as well as 1:1 complex of **2c** obtained between **2** and 3,5-dinitro-*p*-toluic acid, from a methanol solution, are isostructural with the complexes **1a** and **2a**. Thus, carboxylic group of the acid is deprotonated in both **2b** and **2c**, as observed in **1a-1c** and **2a**. The molecules of **2** and the acid interact with each other through strong $\text{N-H}^+\cdots\text{O}^-$ and $\text{N-H}\cdots\text{O}^-$ dimeric hydrogen bonds. Further, the extended structures, as shown in Figures 4.12 and 4.13 are identical in all aspects, especially, formation of tetrameric units and clustering of such units. The hydrogen bond distances are annotated in Figure 4.12 and Figure 4.13 with complete details listed in Table 4.3.

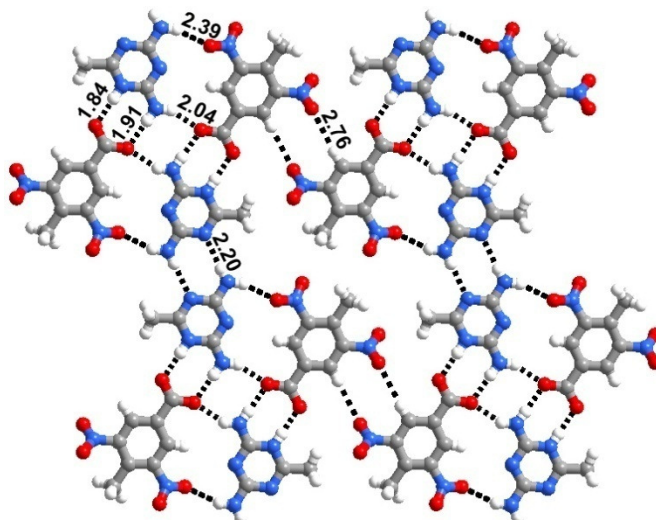


Figure 4.13. Eight member cyclic network, formed by the interaction of four adjacent quartets, observed in **2c**

4.2.5 Supramolecular structure of complex formed between 2,4,6-triaminopyrimidine and 3,5-dinitrobenzoic acid-**3a**:

On co-crystallizing 2,4,6-triaminopyrimidine, **3** with 3,5-dinitrobenzoic acid, from methanol, a host-guest complex, **3a**, is obtained.

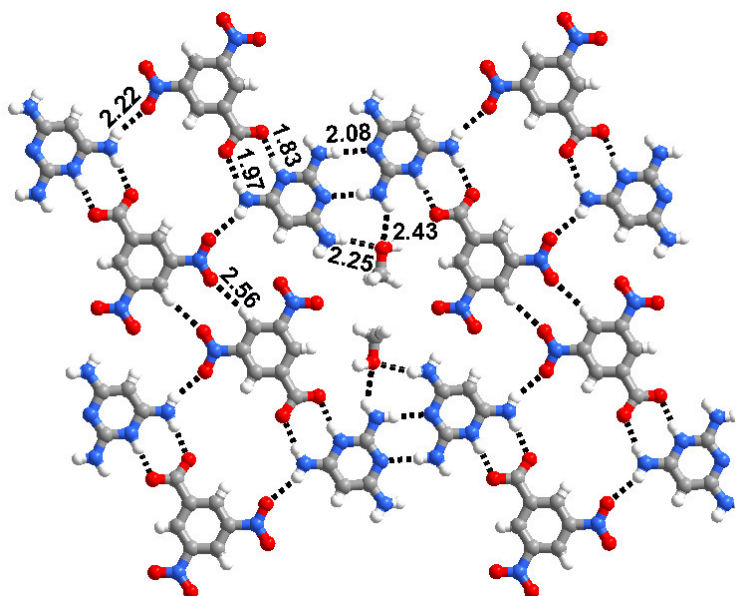


Figure 4.14. Host-guest complex observed in **3a**.

In this structure also the carboxylic group of the acid is deprotonated, as observed in all the other structures in this chapter, and the proton goes to one of the

aromatic nitrogen atom of **3**. Thus, the pyrimidine, **3** and the acid are held together by $\text{N}^+-\text{H}\cdots\text{O}^-$ and $\text{N}-\text{H}\cdots\text{O}^-$ hydrogen bonds, with the corresponding distances being 1.83 Å and 1.97 Å, respectively. Such aggregates are further held together by two single $\text{N}-\text{H}\cdots\text{O}$ hydrogen bonds ($\text{H}\cdots\text{O}$, 2.22 Å) yielding a tetramer as shown in Figure 4.14. As a result, the tetramer observed in this case is different than observed in **1a**, **1c** and **2a-2c**. However, in the extended structure, in two dimensions, four adjacent tetramers interact with each other by independent dimers of $\text{N}-\text{H}\cdots\text{N}$ and $\text{C}-\text{H}\cdots\text{O}$ hydrogen bonds ($\text{H}\cdots\text{N}$, 2.08 Å and $\text{H}\cdots\text{O}$ 2.56 Å, respectively), yielding cyclic network, with voids, occupied by two methanol molecules and establish interaction with host network by $\text{N}-\text{H}\cdots\text{O}$ hydrogen bonds with $\text{H}\cdots\text{O}$ distances 2.25 and 2.43 Å.

In fact, structure observed in **3a** has close relationship to that of **1b** discussed earlier for the complex formed between melamine and 3,5-dinitro-*o*-toluic acid, as far as the entire structure is taken into account.

4.2.6 Molecular complex between 2,4,6-triaminopyrimidine and 3,5-dinitro-*o*-toluic acid-3b

Molecular complex, **3b**, obtained between 2,4,6-triaminopyrimidine and **b** in 1:1 ratio (Table 4.2) also form sheet structure as observed in **1a-1c**, **2a-2c** and **3a**, and have lot of other similarities as well. Thus, the acid group of 3,5-dinitro-*o*-toluic acid is deprotonated. Pyrimidine, **3** and the acid **a** interact with each other through charge assisted $\text{N}^+-\text{H}\cdots\text{O}^-$, $\text{N}-\text{H}\cdots\text{O}^-$ hydrogen bonds, with the $\text{H}\cdots\text{O}^-$ distances being 1.80 Å and 1.96 Å, respectively. Two such adjacent entities are held together by two $\text{N}-\text{H}\cdots\text{O}$ hydrogen bonds constituting tetramers (see Figure 4.15(a)), exactly as observed in **3a**

and it is extended in two dimensional arrangement in the form of sheet, as shown in Figure 4.15(b). All the hydrogen bonds are annotated in Figure 4.15(b) and the complete details are listed in Table 4.3. However, further continuous attempts to obtain good-quality crystals of **3c**, between **3** and 3,5-diamino-*p*-toluic acid were not successful yet, although preliminary analysis indicates the similar unit cell parameters ($a = 9.402$, $b = 10.303$, $c = 10.730$, $\alpha = 62.05$, $\beta = 89.03$, $\gamma = 64.03$) as that of **3b**.

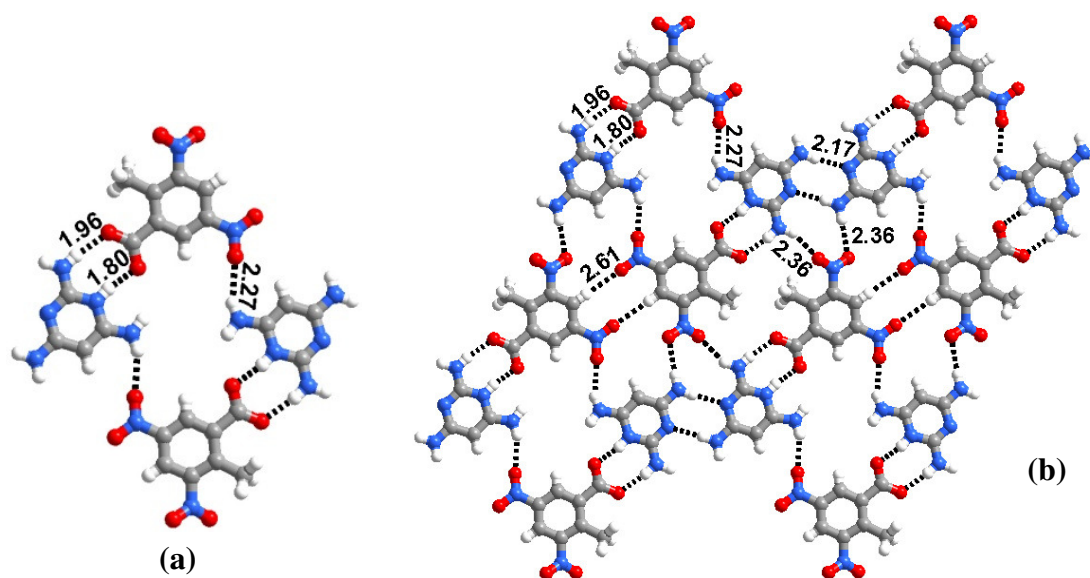


Figure 4.15. (a) Quartet formed by two molecules each of 2,4,6-triaminopyrimidine and 3,5-dinitro-*o*-toluic acid. (b) Sheet structure observed in **3b**.

4.3 Structural correlations of **1a-1c**, **2a-2c**, **3a** and **3b**

Although structures **1a-1c**, **2a-2c**, **3a** and **3b** are exotic, with maintaining the primary recognition patterns the same, despite varying the functional groups on both heterocyclic as well as acid compounds. However an important feature to note is some differences, especially either absence or variation in the formation of tetramer units in the structure of **1b**, **3a** and **3b** and ultimate structural integrity. As it was specified in the structural description, mere position and nature of substituents could not account

the observed differences. Under such circumstances taking the clue from the structural contribution of 2,4-diamino-6-methyl-1,3,5-triazine with various aliphatic carboxylic acids with respect to pK_a of the acids, similar approach has been put forward to understand the observed anomalies. However absolute value of pK_a of either acid or base did not provide any appreciable contribution. But, interestingly ΔpK_a (difference of pK_a listed in Table 4.1 in the ascending order of ΔpK_a base and acid in the co-crystal), has provided a meaningful contribution as described below.

Table 4.1. ΔpK_a of the various complexes in the ascending order.

Complex	pK_a of ligands		ΔpK_a
	Bases	Acids	
2c	4.63	2.95	1.68
2a	4.63	2.77	1.86
2b	4.63	2.41	2.22
1c	5.66	2.95	2.71
1a	5.66	2.77	2.89
1b	5.66	2.41	3.25
3c	6.80	2.95	3.85
3a	6.80	2.77	4.03
3b	6.80	2.41	4.39

Taken into account the order given in Table 4.1 it is apparent that structures of **1a,1c, 2a-2c** fall into a class with $\Delta pK_a < 3.0$. Thus, pK_a values at 3.0 appears to be a kind of demarcation for the classification of supramolecular structures with a nice correlation observed in Chapter 1 and 3. However, it is too premature generalize and certainly a lot of structural studies in this distinction is warranted to define the influence of pK_a , especially a borderline/cut-off limit for the preparation of tailor-made supramolecular architectures.

4.4 Conclusion

Structural description of **1a-1c**, **2a-2c**, **3a** and **3b** obtained from co-crystallization of melamine, 2,4-diamino-6-methyl-1,3,5-triazine and 2,4,6-triaminopyrimidine with 3,5-dinitrobenzoic acid, 3,5-dinitro-*o*-toluic acid, 3,5-dinitro-*p*-toluic acid, as described in detail in the previous sections. In the crystal structures of all the complexes(**1a-1c**, **2a-2c**,**3a-3b**), the carboxylic acid group of 3,5-dinitrobenzoic acid and its derivatives gets deprotonated and the acid molecules recognize the molecules of triazines or pyrimidine in their respective complexes, primarily by charge assisted N-H⁺...O⁻, N-H...O⁻ dimeric hydrogen bond. While formation of tetramers is observed in **1a**, **1c**, **2a-2c**, **3a** and **3b**, in **1b**, the structure is established through aggregation of binary entities. Structural contribution suggests that ΔpK_a of acid and base in the study has an influence on the formation of a specific supramolecular assembly.

4.5 Experimental sections

4.5.1 Synthesis

All the chemicals, reagents and solvents were obtained from commercial suppliers and used without further purification. Spectroscopic-grade solvents were used in all co-crystallization studies. All co-crystals, **1b**, **1c**, **2a-2c**, and **3a**, **3b** were prepared by dissolving the respective reactants in a ratio of 1:1 in methanol and allowing the solvent to evaporate under ambient conditions. In all the cases, single crystals, suitable for X-ray diffraction analysis, were obtained over the period of 3-5 days.

General procedure for the synthesis of complexes, 1b, 1c, 2a-2c, and 3a, 3b

In a typical preparation, 2,4-diamino-6-methyl-1,3,5-triazine (0.0625 g, 0.5 mmol) and 3,5-dinitrobenzoic acid (0.106 g, 0.5 mmol) were dissolved in CH₃OH (20 mL) by gentle warming in a water bath. The resultant solution was evaporated under ambient conditions and with protection from external mechanical disturbances, and within 48 hours, good quality, colorless crystals of **2a** were obtained that were suitable for single-crystal X-ray diffraction studies.

4.5.2 Crystal structures determination

Good quality single crystals of **1b**, **1c**, **2a-2c**, and **3a**, **3b**, were carefully selected with the aid of a polarized Leica microscope equipped with CCD camera, and glued to a glass fiber using an adhesive (cyanoacrylate). In all the cases, the crystals were smeared in the adhesive solution to prevent decay of crystals upon exposure to X-rays. The intensity data were collected on a Bruker single crystal X-ray diffractometer, equipped with an APEX detector, at temperature varying from 273 K to 298 K, see table 4.2. Subsequently, the data were processed using Bruker suite of programmes (SAINT)¹⁵ and the convergence was found to be satisfactory with good R_{int} parameters. The details of the data collection and crystallographic information are given in Table 4.2. The structure determination by direct methods and refinements by least-squares methods on F^2 were performed using SHELXTL-PLUS package. The processes were smooth without any complications. All non-hydrogen atoms were refined anisotropically. All the intermolecular interactions were computed using PLATON.¹⁶

Table 4.2. Crystallographic data for the molecular complexes **1b**, **1c**, **2a-2c**, **3a** and **3b**.

	1b	1c	2a	2b
Formula	(C ₈ H ₅ N ₂ O ₆): (C ₃ H ₇ N ₆):(H ₂ O)	(C ₈ H ₅ N ₂ O ₆): (C ₃ H ₇ N ₆):	(C ₇ H ₃ N ₂ O ₆): (C ₄ H ₈ N ₅)	(C ₈ H ₅ N ₂ O ₆): (C ₄ H ₈ N ₅)
Formula Wt.	370.30	352.29	337.27	351.29
Crystal habit	Rod-Shaped	Blocks	Blocks	Rectangular Blocks
Crystal color	Colorless	Colorless	Colorless	Yellow
Crystal system	Triclinic	Monoclinic	Triclinic	Triclinic
Space group	<i>P</i> $\bar{1}$	<i>P</i> 2 ₁ / <i>c</i>	<i>P</i> $\bar{1}$	<i>P</i> $\bar{1}$
<i>a</i> (Å)	6.851(1)	8.197(2)	8.540(5)	7.220(2)
<i>b</i> (Å)	9.651(2)	7.395(1)	9.034(5)	10.592(3)
<i>c</i> (Å)	12.355(2)	24.333(5)	10.655(6)	11.192(4)
α (deg)	100.01(1)	90.00	68.56(1)	65.67(2)
β (deg)	94.04(1)	91.85(1)	75.12(1)	76.53(2)
γ (deg)	103.07(1)	90.00	77.48(1)	79.48(2)
<i>V</i> (Å ³)	778.5(2)	1474.2(5)	732.6(7)	754.8(4)
<i>Z</i>	2	4	2	2
<i>D</i> _{calc} (g cm ⁻³)	1.580	1.587	1.529	1.546
<i>T</i> (K)	298(2)	298(2)	298(2)	298(2)
λ (Mo-K α)	0.71073	0.71073	0.71073	0.71073
μ (mm ⁻¹)	0.133	0.132	0.127	0.127
2 θ range (deg)	50.50	50.44	50.48	50.48
Limiting indices	-8 ≤ <i>h</i> ≤ 8 -11 ≤ <i>k</i> ≤ 11 -14 ≤ <i>l</i> ≤ 14	-9 ≤ <i>h</i> ≤ 9 -8 ≤ <i>k</i> ≤ 8 -29 ≤ <i>l</i> ≤ 18	-10 ≤ <i>h</i> ≤ 10 -10 ≤ <i>k</i> ≤ 10 -12 ≤ <i>l</i> ≤ 12	-8 ≤ <i>h</i> ≤ 8 -12 ≤ <i>k</i> ≤ 12 -13 ≤ <i>l</i> ≤ 13
<i>F</i> (000)	384	728	348	364
No. of Reflns. Measured	7600	7159	5271	9337
No. Unique Reflns.	2818	2653	2619	2720
No. of Reflns. used	2370	2329	1498	1526
No. of Parameters	291	232	234	248
GOF on F ²	1.128	2.052	1.124	1.137
<i>R</i> _{<i>I</i>} [<i>I</i> > 2 σ (<i>I</i>)]	0.0533	0.0969	0.0977	0.0586
<i>wR</i> ₂	0.1289	0.2787	0.1870	0.1536
Final diff. Fourier map (e ⁻ ·Å ⁻³) max, min	0.211, -0.227	1.254, -0.448	0.333, -0.231	0.409, -0.304

Table 4.2. Continued.....

	2c	3a	3b
Formula	(C ₈ H ₅ N ₂ O ₆): (C ₄ H ₈ N ₅)	(C ₇ H ₃ N ₂ O ₆): (C ₄ H ₈ N ₅): CH ₄ O	(C ₈ H ₅ N ₂ O ₆): (C ₄ H ₈ N ₅)
Formula Wt.	351.29	369.31	351.29
Crystal habit	Blocks	Blocks	Blocks
Crystal color	Yellow	Yellow	Orange
Crystal system	Triclinic	Triclinic	Triclinic
Space group	<i>P</i> $\bar{1}$	<i>P</i> $\bar{1}$	<i>P</i> $\bar{1}$
<i>a</i> (Å)	7.864(2)	7.701(2)	9.2240(10)
<i>b</i> (Å)	10.487(3)	9.835(2)	10.283(2)
<i>c</i> (Å)	10.635(3)	11.827(2)	10.389(2)
α (deg)	110.20(1)	66.31(1)	61.58(1)
β (deg)	101.12(1)	85.61(1)	89.55(1)
γ (deg)	105.50(1)	86.25(1)	63.62(1)
<i>V</i> (Å ³)	752.7(4)	817.3(3)	750.0(2)
<i>Z</i>	2	2	2
<i>D</i> _{calc} (g cm ⁻³)	1.550	1.501	1.556
<i>T</i> (K)	298(2)	273(2)	298(2)
λ (Mo-K α)	0.71073	0.71073	0.71073
μ (mm ⁻¹)	0.127	0.125	0.128
2 θ range (deg)	50.48	50.48	50.46
Limiting indices	-9 ≤ <i>h</i> ≤ 9 -12 ≤ <i>k</i> ≤ 12 -12 ≤ <i>l</i> ≤ 12	-9 ≤ <i>h</i> ≤ 9 -10 ≤ <i>k</i> ≤ 11 -14 ≤ <i>l</i> ≤ 13	-11 ≤ <i>h</i> ≤ 11 -12 ≤ <i>k</i> ≤ 12 -12 ≤ <i>l</i> ≤ 12
<i>F</i> (000)	364	384	364
No. of Reflns. Measured	19411	4124	7370
No. Unique Reflns.	2717	2886	2705
No. of Reflns. used	2071	2247	2268
No. of Parameters	252	287	231
GOF on F ²	1.083	1.042	1.030
<i>R</i> ₁ [I > 2 σ (I)]	0.0476	0.0515	0.0443
<i>wR</i> ₂	0.1322	0.1433	0.1232
Final diff. Fourier map (e ⁻ ·Å ⁻³) max, min	0.259, -0.193	0.271, -0.221	0.545, -0.168

Table 4.3. Characteristic hydrogen bond distances (Å) and angles (°) of the molecular complexes **1b**, **1c**, **2a-2c**, **3a** and **3b**[#].

	1b			1c			2a			2b		
N-H...N	2.16	3.02	168	2.36	3.03	135	2.09	3.00	167	2.17	3.02	171
	2.17	3.03	168									
N-H...O	2.01	2.91	176	2.13	2.99	174	2.16	3.06	175	2.21	3.02	159
	2.31	2.95	135	2.30	3.10	155						
N-H...O⁻	1.95	2.80	174	1.91	2.77	178	1.93	2.79	174	1.97	2.82	171
				2.03	2.88	169	1.98	2.80	161	2.06	2.88	159
				2.05	2.85	155						
N⁺-H...O⁻	1.79	2.63	179	1.90	2.76	176	1.75	2.68	171	1.75	2.61	176
O-H...O	1.99	2.79	168									
C-H...O	2.60	3.41	148	2.59	3.30	133	2.59	3.49	170	2.47	3.40	179

[#] Three columns for each structure represent H...A, D...A distances and D-H...A angle, respectively for a typical hydrogen bond, being represented as D-H...A

Table 4.3. Continued.....

	2c			3a			3b		
N-H⁺...N	2.20	3.00	178	2.08	2.97	178	2.17	3.01	166
N-H⁺...O	2.39	3.12	145	2.22	2.96	157	2.27	3.07	155
				2.25	3.05	162	2.36	3.10	144
				2.43	3.09	135	2.36	3.19	161
N-H⁺...O⁻	1.91	2.74	179	1.97	2.81	174	1.96	2.81	169
	2.04	2.81	151						
N⁺-H⁺...O⁻	1.84	2.70	179	1.83	2.71	175	1.80	2.65	168
O-H⁺...O				1.86	2.79	164			
C-H⁺...O	2.76	3.70	177	2.53	3.32	151	2.61	3.53	174
				2.56	3.47	157			

4.6 References

- (1) Bruno, G.; Randaccio, L. *Acta Crystallogr.* **1980**, *B36*, 1711-1712.
- (2) Derissen, J. *Acta Crystallogr.* **1974**, *B30*, 2764-2765.
- (3) Bailey, M.; Brown, C. J. *Acta Crystogr.* **1967**, *22*, 387-391.
- (4) Duchamp, D. J.; Marsh, R. E. *Acta Crystallogr.* **1969**, *B25*, 5-19.
- (5) Coles, S. J.; Holmes, R.; Hursthouse, M. B.; Price, D. J. *Acta Crystallogr.* **2002**, *E58*, o626-o628.
- (6) (a) Wang, X.; Simard, M.; Wuest, J. D. *J. Am. Chem. Soc.* **1994**, *116*, 12119-12120. (b) Wuest, J. D. *Chem. Commun.* **2005**, 5830-5837. (c) Desiraju, G. R. *Angew. Chem., Int. Ed.* **1995**, *34*, 2311-2327. (d) Ranganathan, A.; Pedireddi, V. R.; Rao, C. N. R. *J. Am. Chem. Soc.* **1999**, *121*, 1752-1753. (e) Whitesides, G. M.; Mathias, J. P.; Seto, C. T. *Science* **1991**, *254*, 1312-1319. (f) Bielejewska, A.; Marjo, C. E.; Prins, L. J.; Timmerman, P.; Jong, R. D.; Reinhoudt, D. N. *J. Am. Chem. Soc.* **2001**, *123*, 7518-7533. (g) Mascal, M.; Hext, N. M.; Warmuth, R.; Moore, M. H.; Yurkenburg, J. P. *Angew. Chem., Int. Ed.* **1996**, *35*, 2204-2206. (h) Ermer, O. *J. Am. Chem. Soc.* **1988**, *110*, 3747-3754. (i) Simard, M.; Su, D.; Wuest, J. D. *J. Am. Chem. Soc.* **1991**, *113*, 4696-4698. (j) Thalladi, V. R.; Goud, B. S.; Hoy, V. J.; Allen, F. H.; Howard, J. A. K.; Desiraju, G. R. *Chem. Commun.* **1996**, 401-402. (k) Allen, F. H. O.; Hoy, V. J.; Howard, J. A. K.; Thalladi, V. R.; Desiraju, G. R.; Wilson, C. C.; McIntyre, G. J. *J. Am. Chem. Soc.* **1997**, *119*, 3477-3480 (l) Meyer, E. A.; Castellano, R. K.; Diederich, F. *Angew. Chem., Int. Ed. Engl.* **2003**, *115*, 1244-1287. (m) Prins, L. J.; Reinhoudt, D. N.; Timmerman, P. *Angew. Chem., Int. Ed.* **2001**, *40*, 2382-2426.

- (7) (a) Bhogala, B. R.; Basavoju, S.; Nangia, A. *CrystEngComm* **2005**, *7*, 551-562.
(b) Vishweshwar, P.; Nangia, A.; Lynch, V. M. *J. Org. Chem.* **2002**, *67*, 556.
(c) Lynch, D. E. Jones, G. D. *Acta Crystallogr.* **2004**, *B60*, 748. (d) Johnson, S. L.; Rumon, K. A. *J. Phys. Chem.* **1965**, *69*, 74.
- (8) Goswami, S.; Jana, S.; Hazra, A.; Fun, H. -K.; Chantrapromma, S. *Supramol. Chem.* **2008**, *20*, 495.
- (9) Subahsni, A.; Muthiah, Lynch, D.E. *Acta Crystallogr.* **2008**, *E64*, o426.
- (10) Etter, M. C.; Frankenbach, G. M. *Chem. Mater.* **1989**, *1*, 10-12.
- (11) Aakeröy, C. B.; Desper, J.; Urbina, J. F. *Chem. Commun.* **2005**, 2820-2822. (b) Aakeröy, C. B.; Salmon, D. J. *CrystEngComm* **2005**, *7*, 439-448. (c) Aakeröy, C. B.; Beatty, A. M.; Helfrich, B. A.; Nieuwenhuyzen *Cryst. Growth Des.* **2003**, *3*, 159-165.
- (12) Aakeröy, C. B.; Beatty, A. M.; Helfrich, B. A. *Angew. Chem., Int. Ed.* **2001**, *40*, 3240-3242.
- (13) (a) Zhang, X. L.; Chen, X. M. *Cryst. Growth Des.* **2005**, *5*, 617-622. (b) Eppel, S.; Bernstein, J. *Cryst. Growth Des.* **2009**, *9*, 1683-1691.
- (14) (a) Batten, S. R.; Robson, R. *Angew. Chem., Int. Ed.* **1998**, *37*, 1461-1494. (b) Chae, H. K.; Kim, J.; Friedrichs, O. D.; O'Keefe, M.; Yaghi, O. M. *Angew. Chem., Int. Ed.* **2003**, *42*, 3907-3909. (c) Aitipamula, S.; Desiraju, G. R.; Jaskolski, M.; Nangia, A.; Thaimattam, R. *CrystEngComm* **2003**, *5*, 447-450. (d) Kaye, S. S.; Dailly, A.; Yaghi, O. M.; Long, J. R. *J. Am. Chem. Soc.* **2007**, *129*, 14176-14177 (e) Reddy, D. S.; Dewa, T.; Endo, K.; Aoyama, Y. *Angew. Chem., Int. Ed.* **2000**, *39*, 4266-4268. (f) Sauriat-Dorizon, H.; Maris, T.; Wuest,

- J. D.; Enright, G. D. *J. Org. Chem.* **2003**, *68*, 240-246. (g) Metrangolo, P.; Meyer, F.; Pilati, T.; Proserpio, D. M.; Resnati, G. *Chem. Eur. J.* **2007**, *13*, 5765-5772.
- (15) (a) Siemens, SMART System, Siemens Analytical X-ray Instrument Inc., Madison, WI (USA), 1995; (b) G. M. Sheldrick, SADABS Siemens Area Detector Absorption Correction Program, University of Gottingen, Gottingen, Germany, 1994; (c) G. M. Sheldrick, SHELXTL-PLUS program for crystal structure solution and refinement, University of Gottingen, Gottingen, Germany.
- (16) A. L. Spek, PLATON, molecular geometry program, University of Utrecht, The Netherlands, 1995.

Publications/Symposia/Awards

Publications

- 1) “pK_a-directed host-guest assemblies: Rational analysis of molecular adducts of 2,4-diamino-6-methyl-1,3,5-triazine with various aliphatic dicarboxylic acids”.
Amit Delori, Eringathodi Suresh, and V. R. Pedireddi *Chem. Eur. J.* **2008**, *14* (23), 6967-6977.
- 2) “Supramolecular assemblies of 2,4-diamino-6-phenyl-1,3,5-triazine with various aliphatic dicarboxylic acids: Ensembles with voids of self-filled to interpenetrating networks” **Amit Delori**, and V. R. Pedireddi (*Manuscript submitted*).
- 3) “Organic Ensembles With Voids, From Self Filled to Interpenetrating Networks: Molecular Adducts of 2,4-Diamino-6-phenyl-1,3,5-triazine With Various Aryl and Aralkyl Carboxylic Acids”. **Amit Delori**, and V. R. Pedireddi (*Manuscript submitted*).
- 4) “Molecular Complexes of 3,5-Dinitrobenzoic acid and its derivatives with various heterocyclic amines”. **Amit Delori**, and V. R. Pedireddi (*Manuscript under preparation*).
- 5) “Supramolecular Synthesis of Molecular Adducts of 2,4-Diamino-6-(2-fluorophenyl)-1,3,5-triazine with various aryl and aralkyl carboxylic acids”. **Amit Delori**, and V. R. Pedireddi (*Manuscript under preparation*).
- 6) “Molecular adducts of 2,4-Diamino-6-(4-methylphenyl)-1,3,5-triazine with various aryl and aralkyl carboxylic acids”. **Amit Delori**, and V. R. Pedireddi (*Manuscript under preparation*).

- 7) “Synthesis and analysis of some supramolecular complexes of 2,4-Diamino-6-methyl-1,3,5-triazine”. Amit Delori, and V. R. Pedireddi (*Manuscript under preparation*).
- 8) “Synthesis and analysis of some molecular adducts of 2,4,6-Triaminopyrimidine”. Amit Delori, and V. R. Pedireddi (*Manuscript under preparation*).

Symposia/invited talk etc.

- **Invited talk** for getting **Dr. Rajappa award** for the best research paper in organic chemistry with highest impact factor in 2008 at National Chemical Laboratory, Pune, India.
- **Invited talk** for getting **Keerti Sangoram endowment award** for the best research scholar of the year 2008 in Chemical Sciences at National Chemical Laboratory, Pune, India.
- **38th National Seminar on Crystallography**, held at University of Mysore, Mysore.
- XXI Congress of the **International Union of Crystallography** held at Osaka, Japan during 23rd-31st August, 2008.

Awards

- **Keerthi Sangoram Endowment Award** for the **best research scholar** in chemical sciences, from National Chemical Laboratory, Pune, India for the year, 2008.
- **Dr. Rajappa award** for the **best paper in organic chemistry** from National Chemical Laboratory, Pune, India, in the year 2008.
- **Best poster award** at the XXI Congress of the **International Union of Crystallography** held at Osaka, Japan on 23rd-31st August, 2008.